Phenotypical and Therapeutic Studies in Genetic Mouse Models for Inherited Neurotransmitter Disorders

Dissertation

zur

Erlangung der naturwissenschaftlichen Doktorwürde

(Dr. sc. nat.)

vorgelegt der

Mathematisch-naturwissenschaftlichen Fakultät

der

Universität Zürich

von

Germaine Florence Korner

von

Luzern

Promotionskomitee:

Prof. Dr. Beat Thöny

(Vorsitz und Leiter der Dissertation)

Prof. Dr. François Verrey

Prof. Dr. Isabelle Mansuy

ZÜRICH, 2015

The present study was performed from June 2010 until Mai 2014 in the Division of Metabolism at University Childrenôs Hospital Zurich under the supervision of Prof. Dr. Beat Thöny.

Publications represented in this study:

- Progressive catecholamine depletion and severely impaired motor control in a hypomorphic tyrosine hydroxylase knock-in (*Th*-ki) mouse

Germaine Korner, Daniela Noain, Ming Ying, Magnus Hole, Marte I. Flydal, Tanja Scherer, Gabriella Allegri, Anahita Rassi, Ralph Fingerhut, Damasia Becu-Villalobos, Samyuktha Pillai, Stephan Wüest, Daniel Konrad, Anna Lauber, Christian Baumann, Laurence Bindoff, Aurora Martinez and Beat Thöny

Manuscript is in preparation

- Abnormal body fat distribution and abdominal obesity in mouse mutant with mildly compromised tetrahydrobiopterin cofactor biosynthesis

Germaine Korner, Tanja Scherer, Dea Adamsen, Alexander Rebuffat, Anahita Rassi, Rossana Scavelli, Daigo Homma, Birgit Ledermann, Daniel Konrad, Hiroshi Ichinose, Christian Wolfrum, Marion Horsch, Birgit Rathkolb, Martin Klingenspor, Johannes Beckers, Eckhard Wolf, Valérie Gailus-Durner, Helmut Fuchs, Martin Hrabŋ de Angelis, Nenad Blau, Jan Rozman, and Beat Thöny

Manuscript under submission

Personal contributions to these projects and each chapter:

- Tyrosine hydroxylase deficiency (chapter 2): Designing and planning of the studies, breeding of the mice, genotyping, feeding solution preparation, feeding of mice, collecting of various mouse tissues, construction and generation of plasmid, application of virus, collection, analysis and validation of data, and preparation of the manuscript.

- Tetrahydrobiopterin deficiency (chapter 3): Designing and planning of the studies, breeding of the mice, genotyping, collecting of various mouse tissues, tissue lysate preparation, analysis of blood (L-Phe and L-Tyr), milk (biopterin and neopterin), brain and liver tissue (PTPS activity, biopterin and neopterin), establishing melking technique for mice, collection, analysis and validation of data, preparation of the manuscript.

- Phenylketonuria (chapter 4): Designing and planning of the studies, construction and generation of plasmids, virus production, collecting and analysing of blood (L-Phe and L-Tyr), collection, analysis and validation of data.

TABLE OF CONTENTS

ABBREVIATIONS 7

SUMMARY 12

ZUSAMMENFASSUNGé é 16

1. INTRODUCTION 20

1.1 TYROSINE HYDROXYLASE DEFICIENCY 21

1.1.1 DESEASE CHARACTERISTICS 21

1.1.2 DISEASE CAUSING GENE 22

1.1.3 DIAGNOSIS 23

1.1.4 MANAGEMENT AND TREATMENT APPROACHES 24

1.1.5 MOUSE MODELS 24

1.1.6 GENE THERAPEUTIC APPROACHES 25

1.2 TETRAHYDROBIOPTERIN DEFICIENCY 28

1.2.1 DESEASE CHARACTERISTICS 28

1.2.2 DISEASE CAUSING GENES 30

1.2.3 DIAGNOSIS 31

1.2.4 MANAGEMENT AND TREATMENT APPROACHES 33

1.2.5 MOUSE MODELS 33

1.2.5.1 GTPCH 33

1.2.5.2 PTPS 33

1.2.5.3 SR 34

1.2.5.4 PCD 35

1.2.6 GENE THERAPEUTIC APPROACHES 35

1.3 CLASSICAL PHENYLKETONURIA 36

1.3.1 DESEASE CHARACTERISTICS 36

1.3.2 DISEASE CAUSING GENE 37

1.3.3 DIAGNOSIS 37

1.3.4 MANAGEMENT AND TREATMENT APPROACHES 38

1.3.5 MOUSE MODELS 40

1.3.6 GENE THERAPEUTIC APPROACHES 41

1.3.6.1 Viral gene therapies 41

1.3.6.2 Non-viral gene therapies and minicircle technology 42

1.4 TOOLS FOR GENE TARGETING AND GENOME ENGENEERING TO GENERATE RECOMBINANT MICE 44

1.5 AIM OF STUDY 48

2. TYROSINE HYDROXYLASE KNOCK-IN (*TH*-KI) MOUSE MODEL WITH CATECHOLAMINE DEPLETION AND IMPAIRED MOTOR CONTROL: CHARACTERISATION AND TREATMENT STUDIES 50

2.1 MANUSCRIPT: PROGRESSIVE CATECHOLAMINE DEPLETION AND SEVERLY IMPAIRED MOTOR CONTROL IN A HYPOMORPHIC TYROSINE HYDROXYLASE KNOCK-IN (*TH*-KI) MOUSE 51

2.2 ORAL TREATMENT STUDY WITH BH_4 AND PHARMACOLOGICAL CHAPERONS IN *TH*-KI/KI MICE TO STABILZE THE MUTANT TH ENZYME AND INCREASE BRAIN CATECHOLAMINE LEVELS 86

2.2.1 ABSTRACT 86

2.2.2 INTRODUCTION 87

2.2.3 MATERIALS AND METHODS 89

2.2.3.1 Preparation of solutions 89

2.2.3.2 Gene (mRNA) Expression studies 89

2.2.4 RESULTS 90

2.2.4.1 Adult mice fed for 12 days with L-Dopa, BH_4 and pharmacological chaperons CIII/IV 90

2.2.4.2 Newborn mice fed for 3 weeks with pharmacological chaperon 94

2.2.5 DISCUSSION 97

2.3 INVESTIGATION OF A GENE THERAPEUTIC APPROACH TARGETING THE LIVER USING AAV TO RESTORE THE BRAIN CATECHOLAMINE IN *TH*-KI/KI MICE 100

2.3.1 ABSTRACT 100

2.3.2 INTRODUCTION 101

2.3.3 MATERIALS AND METHODS 102

2.3.3.1 Generation of AAV vector 102

2.3.3.2 Production of rAAV 102

2.3.3.3 Application of rAAV2/8 and carbidopa 102

2.3.3.4 Copy number assay 102

2.3.3.5 Gene (Th-mRNA) expression study 102

2.3.4 RESULTS 103

2.3.5 DISCUSSION 106

3. CHARACTERISATION OF MOUSE MODELS WITH MILDLY COMPROMISED BH_4 BIOSYNTHESIS: *PTS*-KI/KI AND *PTS*-KI/KO 1099

3.1 MANUSCRIPT: ABNORMAL BODY FAT DISTRIBUTION AND ABDOMINAL OBESITY IN MOUSE MUTANT WITH MIDLY COMPROMISED TETRAHYDROBIOPTERIN CO-FACTOR BIO-SYNTHESIS 110

3.2 CHALLENGING THE OBSERVATION OF ñUNAFFECTEDò AND ñAFFECTEDò *PTS*-KI/KO MICE FROM DIFFERENT BREEDING COMBINATIONS OF *PTS*-KI AND *PTS*-KO PARENTS 149

3.2.1 ABSTRACT 149

3.2.2 INTRODUCTION 150

3.2.3 RESULTS 153

3.2.3.1 Characterisation of newborn mice from different breeding combinations of *Pts*-ki/wt, *Pts*-ko/wt and *Pts*-ki/ki parents 153

3.2.3.2 Direct comparison of newborn *Pts*-ki/ko mice derived from different breeding combinations of *Pts*-ki/wt, *Pts*-ko/wt and *Pts*-ki/ki parents **156**
3.2.3.3 Breeding of ñaffectedò*Pts*-ki/ko mice: Comparison of 3-4 days old *Pts*-ki/ko mice derived from small and large litters **158**
3.2.4 DISCUSSION **161**

4. STUDY OF A MUSCLE-DIRECTED NON-VIRAL GENE THERAPEUTIC APPROACH FOR PKU AND ATTEMPT TO GENERATE A MOUSE MODEL EXPRESSING BH_4 IN MUSCLE **163**
4.1 EXPERIMENTAL STUDY ON A NON-VIRAL GENE THERAPY APPROACH BY INTRA-MUSCULAR EXPRESSION OF A COMPLETE PHENYLALANINE HYDROXYLATING SYSTEM **164**
4.1.1 ABSTRACT **164**
4.1.2 INTRODUCTION **165**
4.1.3 MATERIALS AND METHODS **168**
4.1.3.1 Vector plasmids **168**
4.1.3.2 Transfection of COS-1 cells with PP or MC vectors **168**
4.1.3.3 Enzyme activity assays *in vitro* **168**
4.1.3.4 Hydrodynamic limb vein injection of MC into *Pah*$^{enu2/2}$ mice **169**
4.1.3.5 Electroporation of MC into *Pah*$^{enu2/2}$ mice **169**
4.1.3.6 In vivo imaging system **169**
4.1.3.7 Blood L-Phe measurements **169**
4.1.4 RESULTS **170**
4.1.4.1 MC vectors and *in vitro* expression **170**
4.1.4.2 *In vivo* application of MCs by HLV injection **173**
4.1.4.3 *In vivo* application of MCs by electroporation **174**
4.1.5 DISCUSSION **177**
4.2 ATTEMPT TO GENERATE A PKU MOUSE MODEL SYNTHESISING BH_4 IN MUSCLE BY EXPRESSING THE *GCH*1 AND *PTS* GENES USING AAV **180**
4.2.1 ABSTRACT **180**
4.2.2 INTRODUCTION **181**
4.2.3 MATERIALS AND METHODS **183**
4.2.3.1 Viral vector plasmids **183**
4.2.3.2 rAAV production **183**
4.2.3.2.1 Transfection, purification and titer determination **183**
4.2.3.2.2 Enzyme activity **184**
4.2.3.2.3 Application of AAV vectors to *Pah*$^{enu2/2}$ mice **184**
4.2.3.3 In vivo imaging system **184**
4.2.4 RESULTS **185**
4.2.4.1 AAV vectors and *in vitro* expression **185**

4.2.4.2 *In vivo* evaluation of potential therapeutic efficacy of the separated rAAV2/1 triple-cystronic vector **186**

4.2.4.3 Evaluation of distribution and expression of PAH in muscle in combination with *Luc* **189**

4.2.5 DISCUSSION **191**

5. SUPPLEMTARY INORMATION **193**

5.1 CLONING OF PLASMIDS **193**

6. REVERENCES **195**

7. ACKNOWLEDGMENTS **211**

8. CURRICULUM VITAE **212**

ABBREVIATIONS

A, adenosine

aa, amino acids

AADC, aromatic L-amino acid decarboxylase

AAV, adeno-associated virus

Ala, alanine

AGMO, alkylglycerol monooxygenase

aPKU, atypical phenylketonuria

Arg, arginine

*att*B, bacterial attachment site (*E. coli*)

*att*L, left attachment site

*att*P, phage attachment site (Bacteriophage ə)

*att*R, right attachment site

BBB, blood brain barrier

BH_4, tetrahydrobiopterin

Bio, biopterin

bp, base pair

C, cytosine

°C, degree Celsius

CIII, compound III (chemical pharmachaperon)

CIV, compound IV (chemical pharmachaperon)

cDNA, complementary DNA

CMV, cytomegalovirus

CNS, central nervous system

crRNA, clustered regularly interspaced short palindromic repeats ribonucleic acid

CSF, cerebrospinal fluid

cPKU, classical phenylketonuria

CRISPR, clustered regularly interspaced short palindromic repeats

Cys, cystein

DA-/-, dopamine deficient mouse model

DCoH, dimerization cofactor of homeodomain protein hepatocyte nuclear factor

DDC, DOPA decarboxylase

Ddc, Dopa-responsive dystonia

DHPR, dihydropteridine reductase

DMSO, dimethylsulfoxid

DRD, Dopa-responsive dystonia

DRD1(a)-5, dopamine receptor D1-5

Drd, dopamine receptor gene

ENU, N-ethyl-N'-nitrosourea

ES, embryonic stem

FB, fibroblast

Fig., figure

G, guanine

g, gram

*GCH*1, guanosine triphosphate cyclohydrolase I gene

GH, growth hormone

Glu, glutamic acid

Gly, glycine

GTP, guanosine-5'-triphosphate

GTPCH, guanosine triphosphate cyclohydrolase I

h, hours

His, histidine

HLV, hydrodynamic limb vein

HNF, homeodomain protein hepatocyte nuclear factor

h*TH*, human tyrosine hydroxylase gene

HTV, hydrodynamic tail vein

HPA, hyperphenylalaninemia

HPLC, high performance liquid chromatography

HVA, homovanillic acid

IEM, Inborn errors of metabolism

IGF1, insulin-like growth factor 1

*Igf*1, insulin-like growth factor 1 gene

i.p., intraperitoneal

ITR, inverted terminal repeat

KanR, kanamycine resistance

kb, kilobase

kDa, kilodalton

LAT, L-type amino acid transporters

L-Dopa, L-dihydroxyphenylalanine
LNAA, large neutral amino acids
L-Phe, L-phenylalanine
L-Tyr, L-tyrosine
Luc, *firefly* l*uciferase*
Lys, lysine
MC, minicircle-based
mco, murine codon optimized
m*Gch*1, murine guanosine triphosphate cyclohydrolase 1 gene
m., musculus
MHPG, 3-methoxy-4-hydroxy-phenylethyleneglycol
mg, milligram
mg/kg, milligram per kilogram
mg/kg/d, milligram per kilogram per day
mg/ml, milligram per milliliter
mg/L, milligram per liter
min, minute(s)
MODY, maturity onset diabetes of the young
m*Pah*, murine phenylalanine hydroxylase gene
mPts, murine 6-pyruvoyl-tetrahydropterin synthase gene
mRNA, messanger ribonucleic acid
MS/MS, tandem mass spectrometry
m*Th*, murine tyrosine hydroxylase gene
N, no
n.a., not applicable
n.d., not detectable
NHEJ, non-homologous end joining
Neo, neopterin
NO, nitric oxide
NOS, nitric-oxide synthase
OH-BH_4, hydroxytetrahydrobiopterin
P, plasma
PAH, phenylalanine hydroxylase
PAL, phenylalanine ammonia lyase

PCBD, pterin-4a-carbinolamine dehydratase gene

PCD, pterin-4a-carbinolamine dehydratase

PD, Parkinson's disease

PEG, polyethylene glycol

PIL, pegylated immunoliposome

PKU, phenylketonuria

pmol, picomol

pmol/mg, picomol per milligram

pmol/min/mg, picomol per minute per milligram

PP, parental plasmid

Pr, promoter

Pri, primapterin

p/s, photons/second

PTPS, 6-pyruvoyl-tetrahydropterin synthase

PTS/*Pts*, 6-pyruvoyl-tetrahydropterin synthase gene

Pts-ki, 6-pyruvoyl-tetrahydropterin synthase gene knock-in

Pts-ki/ko, 6-pyruvoyl-tetrahydropterin synthase gene knock-in/knock-out

Pts-ko, 6-pyruvoyl-tetrahydropterin synthase gene knock-out

pUC ORI, bacterial origin of replication

q-BH2, quinone-dihydrobiopterin

QDPR, dihydropteridine reductase gene

rAAV, recombinant adeno-associated virus

rAAV2/1, recombinant adeno-associated virus pseudotyped with serotype 1 capsid

rAAV2/8, recombinant adeno-associated virus pseudotyped with serotype 8 capsid

ROS, reactive oxygen species

RBS, rep-binding site

sec, second(s)

Ser, serine

S/MAR, scaffold/matrix attachment region

SPR, sepiapterin reductase gene

SR, sepiapterin reductase

T, thymidine

TALE, transcription activator-like effector

TALEN, transcription activator-like effector nucleases

TfR, transferrin receptor

TH, tyrosine hydroxylase

THD, tyrosine hydroxylase deficiency

TK, thymidine kinase

TPH tryptophan hydroxylase

trcrRNA, *trans*-activating crRNA

Trp, tryptophan

Tyr, tyrosine

U, urine

µg, microgram

µl, microliter

εmol/L, micromole per liter

µU/mg, micro unit per milligram

Val, valine

vp, vector plasmid

WPRE, woodchuck hepatitis post-transcriptional regulatory element

Wt, wild-type

Y, yes

ZFN, zinc-finger nuclease

3-OMD, 3-O-methyldopa

4F2hc, 4F2 heavy chain

5-HIAA, 5-hydroxyindoleacetic acid

5-HTP, 5-OH-tryptophan

6-OHDA, 6-hydroxydopamine

SUMMARY

The present dissertation is based on characterization of mouse models for inborn errors of metabolic disorders concomitant with monoamine neurotransmitter deficiency and investigation of potential therapeutic approaches. Following an introduction (Chapter 1), this dissertation deals with the three metabolic diseases tyrosine hydroxylase deficiency (THD; chapter 2), tetrahydrobiopterin deficiency (BH_4 deficiency; chapter 3), and classical phenylketonuria (cPKU; chapter 4).

Chapter 2: Tyrosine hydroxylase knock-in (Th-ki) mouse model with catecholamine depletion and impaired motor control: Characterisation and treatment studies

Tyrosine hydroxylase (TH) is the rate-limiting enzyme in the synthesis of catecholamine neurotransmitters, hormones and a marker for dopaminergic neurons. Mutations in the *TH* gene are associated with the autosomal recessive neurometabolic disorder TH deficiency (THD), which manifests with phenotypes varying from infantile parkinsonism and L-Dopa-responsive dystonia to complex encephalopathy of perinatal onset. The most recurrent mutation in THD patients is TH-p.Arg233His (hTH1-p.Arg202His, isoform 1), which is mostly associated to a severe THD phenotype, often concomitant with non-responsiveness to L-Dopa treatment. While *Th* knock-out mice are not viable, homozygous *Th*-knock-in (*Th*-ki) mice expressing the Th-p.Arg203His mutation (equivalent to hTH1-p.Arg202His) showed normal survival and food intake but hypotension and moderate growth retardation. The mutant enzyme exhibited impaired inhibitory feedback and stabilizing dopamine binding, which lead to progressive disappearance of TH associated to gradual loss of catecholamines in the brain. Specially, unstable mutant TH was absent in striatum. Accordingly, mutant mice showed reduced motor coordination, ataxia and catalepsy with diurnal fluctuation, and non-responsiveness to L-Dopa treatment. This hypomorphic *Th*-ki mouse model with encephalopathy and impaired motor control thus provides understanding on molecular pathogenic mechanisms for THD, replicates the most severe form of the disease, and provides a platform for the evaluation of novel therapeutics (manuscript Korner et al., in preparation for submission).

In follow up-studies (not included in the above manuscript), *Th*-ki mice were studied for the effect of (oral) treatment with synthetic tetrahydrobiopterin (BH_4) cofactor and two pharmacological chaperones (compound III and IV). BH_4 and these pharmachaperone compounds were previously reported to stabilize mutant hTH-Arg202His *in vitro* and wild-type TH in mouse brains by increasing the amount of TH protein and its activity. However, in *Th*-ki mice, none of these compounds led to an improvement or normalization in brain catecholamine levels, TH activity, protein amount or behavioural changes.

In the final part, an alternative treatment approach was tested by ñ*in situ*ò biosynthesis of L-Dopa in the liver of *Th*-ki mice using an adeno-associated virus serotype 8 vector (rAAV2/8) expressing the wild-type *Th*-cDNA in liver. Theoretically, the hepatic synthesized L-Dopa should lead to an increase of brain catecholamines, which is potentially more effective then the treatment with L-Dopa, and might lead to the correction of motor dysfunction in the mutant mice. Although the wt TH was expressed in the liver of mutant mice, there was no effect on brain catecholamines or any improvements in motor function.

Chapter 3: Characterisation of mouse models with mildly compromised BH_4 biosynthesis: Pts-ki/ki and Pts-ki/ko

Tetrahydrobiopterin (BH_4) is an essential cofactor for the aromatic amino acid hydroxylases, alkylglycerol monooxygenase and nitric oxide synthases (NOS). Inborn errors of BH_4 metabolism lead to severe insufficiency of brain monoamine neurotransmitters while augmentation of BH_4 by supplementation or stimulation of its biosynthesis is thought to ameliorate endothelial NOS (eNOS) dysfunction, to protect from (cardio-) vascular disease and/or prevent obesity and development of the metabolic syndrome. We have previously reported that homozygous knock-out mice for the 6-pyruvolytetrahydropterin synthase (PTPS; *Pts*-ko/ko) mice with no BH_4 biosynthesis die after birth. We generated a *Pts*-knock-in (*Pts*-ki) allele expressing the murine PTPS-p.Arg15Cys with low residual activity (15% of wild-type *in vitro*) and investigated heterozygous (*Pts*-ki/wt), homozygous (*Pts*-ki/ki) and compound heterozygous (*Pts*-ki/ko) mutants. Mice were viable and, depending on the severity of the *Pts* alleles, exhibited up to 90% reduction of PTPS activity in liver and brain. Although neopterin was elevated in brain and liver, BH_4, blood L-phenylalanine and the brain monoamine neurotransmitters dopamine and serotonin were all unaffected.

Unexpectedly, *Pts*-ko/wt and *Pts*-ki/ki mice exhibited increased body weight and elevated intra-abdominal fat tissue. Comprehensive phenotyping of *Pts*-ki/ki mice revealed alterations in energy metabolism with higher fat content, lower lean mass, and increased blood glucose and cholesterol. Transcriptome analysis of liver indicated changes in glucose and lipid metabolism. Furthermore, differentially expressed genes associated with obesity, weight loss, hepatic steatosis and insulin sensitivity were consistent with the observed phenotypic alterations. Our study associates a novel single gene mutation with monogenic forms of obesity. We conclude that reduced PTPS and potentially BH_4-biosynthetic activity in mice leads to abnormal body fat distribution and abdominal obesity potentially through mildly elevated neopterin and/or compromised eNOS function (manuscript Korner et al., submitted).

In the additional work, not published in the context of the above observation, I challenged a claim by Dea Adamsen in her PhD thesis (University of Zurich, 2011). D. Adamsen described in her work that *Pts*-ki/ko had different phenotypes depending on the maternal genotype: ñaffectedò *Pts*-ki/ko newborns with *lethality* 3-4 days after birth and ñunaffectedò *Pts*-ki/ko offspring with *normal survival*. Furthermore, ñunaffectedò *Pts*-ki/ko mice had a similar phenotype like homozygous *Pts*-ki/ki mice. The definition of ñaffectedò mice included all hallmarks of lethal BH_4 deficiency with low biopterin and monoamine neurotransmitter levels, increased neopterin levels and hyperphenylalaninemia (HPA). D. Adamsen also claimed that the ñaffectedò mice only appear if the mother was homozygous for the knock-in mutation. Here we found that newborns (day 1) and 3-4 days old pups from different breeding combinations of *Pts*-ki/ki, *Pts*-ki/wt and *Pts*-ko/wt parents revealed that there were only minor deviations between *Pts*-ki/ko newborns from different breeding combination and that none of them showed the severe (ñaffectedò) phenotype.

Chapter 4: Study of a muscle-directed non-viral gene therapeutic approach for PKU and attempt to generate a mouse model expressing BH_4 in muscle

Deficiency of the hepatic phenylalanine hydroxylase (PAH), catalyzing the conversion from L-phenylalanine (L-Phe) to L-Tyr, is the cause for classical phenylketonuria (cPKU). Complete correction of cPKU in a mouse model was previously shown by muscle targeting using a recombinant rAAV vector expressing the complete phenylalanine hydroxylating system, i.e. coordinate expression of the *Pah* minigene

plus the two genes (cDNAs) guanosine triphosphate cyclohydrolase I (*Gch*1) and *Pts,* essential for BH_4-cofactor biosynthesis in muscle tissue. As an alternative to the (AAV) viral approach, the potential of such a triple-cistronic gene transfer using naked DNA/minicircle (MC) vectors to target skeletal muscle in PKU mice was investigated. Testing triple-cystronic gene vectors included a combination of various modifications such as codon-optimization, insertion of intronic sequences, and transcription or gene expression latency elements like the woodchuck hepatitis post-transcriptional regulatory element (WPRE) and the scaffold/matrix attachment region (S/MAR). Transgene expression from these vectors was validated under cell culture conditions before they were injected into PKU mice by hydrodynamic limb vein infusion or by electroporation. Although high concentrations of MCs were applied (up to 6.8 $x10^{14}$ vector particles), normalization of blood L-Phe levels in the treated PKU mice not yet be achieved with any of these vectors. Further efforts and optimization towards a non-viral gene transfer to muscle to treat cPKU is discussed in an additional chapter.

Zusammenfassung

Die vorliegende Dissertation behandelt die Charakterisierungen von Mausmodellen, welche angeborene Stoffwechselerkrankungen in der Monoamin-Neurotransmitter Synthese aufweisen, sowie die Untersuchung von möglichen therapeutischen Ansätzen. Nach einer Einführung (Kapitel 1) beschäftigt sich diese Dissertation mit den drei Stoffwechselerkrankungen Tyrosin-Hydroxylase-Mangel (Kapitel 2), Tetrahydrobiopterin-Mangel (Kapitel 3), und der klassischen Phenylketonurie (Kapitel 4).

Kapitel 2: Tyrosin-Hydroxylase Knock-in (Th-ki) Mausmodell mit progressivem Katecholamin-Abbau und eingeschränkter motorischer Kontrolle: Charakterisierung sowie mögliche Behandlungsansätze

Tyrosin-Hydroxylase (TH) ist das geschwindigkeitsbestimmende Enzym bei der Synthese von Katecholaminen-Neurotransmittern und Hormonen, und ein Marker für Dopaminerge-Neuronen. Mutationen im *TH*-Gen führen zu einem autosomal rezessiv vererbten TH-Mangel (THD), welche sich mit unterschiedlichen Phänotypen von infantilen Parkinsonismus und L-Dopa ansprechenden Dystonie bis hin zur komplexe Enzephalopathie mit perinatalem Auftreten manifestiert. Die häufigste Mutation bei THD Patienten ist die TH-p.Arg233His Mutation (hTH1-p.Arg202His, Isoform 1), welche meistens zu einem schweren Verlauf der Erkrankung führt, die nicht auf eine L-Dopa-Behandlung anspricht. Während *Th*-knock-out Mäuse nicht lebensfähig sind, waren die homozygoten *Th*-knock-in-Mäuse (*Th*-ki), welche die Th-p.Arg203His Mutation (entspricht hTH1-p.Arg202His) exprimieren, lebensfähig und wiesen eine normale Nahrungsaufnahme auf, jedoch zeigten sie Hypotonie und eine moderate Wachstumsverzögerung. *In vitro* Untersuchungen zeigten, dass das mutierte TH Enzym Dopamin nicht binden kann, was zu einer verminderten Protein-Stabilität und wahrscheinlich zum fortschreitenden Verschwinden der mutierten TH führte, und schliesslich den allmählichen Verlust der Katecholamine zur Folge hatte. Weitere Immunohistochemistrie-Analysen zeigten, dass die instabile TH Mutante im Striatum kaum vorhanden war. Dementsprechend zeigten die transgenen Mäuse eine verminderte Bewegungskoordination, Ataxie und Katalepsie mit tageszyklischen Schwankungen und sprachen nicht auf die L-Dopa-Behandlung an. Dieses hypomorphe *Th*-ki-Mausmodell mit Enzephalopathie und beeinträchtigter motorischer Steuerung bietet somit Einblicke zum Verständnis der molekularen Patho-

mechanismen für THD, repliziert die schwerste Form der Erkrankung und ermöglicht das Testen neuer Therapiemöglichkeiten (Manuskript Korner et al.).

In einer weiterführenden Studie (nicht im Manuskript enthalten), wurden *Th*-ki-Mäuse auf die Wirkung nach (oraler) Behandlung mit dem synthetischen Tetrahydrobiopterin (BH_4) Kofaktor und zwei pharmakologischen Chaperons untersucht (Chaperon III und IV). Bereits zuvor publizierte Studien zeigten, dass BH_4 und die Pharmachaperons die TH-Arg202His Mutante *in vitro* und die Wildtyp TH Enzyme in Mäusegehirnen stabilisierten, was zu Erhöhung der Menge von TH-Protein und seiner Aktivität im Hirn führte. In *Th*-ki Mäusen führte jedoch keine dieser Verbindungen zu einer Verbesserung bzw. Normalisierung der Gehirn Katecholamine, TH-Aktivität, Proteinmenge oder zu einer Verhaltensänderung.

Im letzten Teil dieser Arbeit wurde ein alternativer Behandlungsansatz getestet, welcher die "in situ" Biosynthese von L-Dopa in der Leber von *Th*-ki Mäusen durch die Behandlung eines Adeno-assoziierten Virus mit Serotyp 8 Vektors (rAAV2/8), welcher die wildtyp *Th*-cDNA in der Leber exprimiert, untersucht. Diese Behandlungsmethode ist möglicherweise effektiver als die Behandlung mit L-Dopa und theoretisch sollte das in der Leber synthetisierte L-Dopa zu einer Verbesserung der Katecholamine im Hirn führen. Dies bewirkt dann möglicherweise eine Korrektur der Bewegungsstörungen in den transgenen Mäusen. Obwohl die wildtyp TH in der Leber der transgenen Mäuse exprimiert war, ergaben sich weder Veränderungen der Katecholamine im Gehirn noch Verbesserungen in der Motorik.

Kapitel 3: Abnormale Körperfettverteilung und abdominale Adipositas in einer Maus-Mutante mit einer leicht beeinträchtigtem Tetrahydrobiopterin Kofaktor-Biosynthese

Tetrahydrobiopterin (BH_4) ist ein essentieller Kofaktor für die aromatischen Aminosäure-Hydroxylasen, die Alkylglycerinsulfate Monooxygenase und die Stickstoffmonoxid-Synthasen (NOS). Angeborene Fehler im BH_4 Metabolismus führen zu schwerer Monoamin-Neurotransmitter-Insuffizienz im Gehirn, während angenommen wird, dass die Augmentation von BH_4 durch Ergänzungen oder Stimulation der BH_4 Biosynthese die endotheliale NOS (eNOS) Dysfunktion verbessert, vor (Herz-) Gefäßerkrankungen schützt und/oder Fettleibigkeit und Entwicklung des metabolischen Syndroms verhindert. Es wurde bereits publiziert, dass homozygote knock-out-Mäuse für die 6-Pyruvoly-Tetrahydropterin Synthese

(PTPS; Pts-ko/ko), welche über keine BH_4-Biosynthese verfügen, kurz nach der Geburt sterben. Daher wurde das *Pts*-knock-in (*Pts*-ki) Allel generierten, welches die murine PTPS-p.Arg15Cys Mutation exprimiert die zu einer geringen PTPS Enzymaktivität führt (15% Aktivität *in vitro* im Vergleich zum Wildtypen) und heterozygote (*Pts*-ki/wt), homozygote (*Pts*-ki/ki) und komplex heterozygote (*Pts*-ki/ko) Mutanten wurden charakterisiert. Die transgenen Mäuse waren lebensfähig und zeigten, je nach Kombination der *Pts*-Allele, eine bis zu 90% Reduktion der PTPS Aktivität in Leber und Gehirn. Obwohl Neopterin im Gehirn und in der Leber erhöht war, zeigte sich das der BH_4 Level, das L-Phenylalanin im Blut und die Gehirn Monoamin-Neurotransmitter Dopamin und Serotonin unverändert waren. Überraschenderweise wiesen *Pts*-ko/wt und *Pts*-ki/ki Mäuse ein erhöhtes Körpergewicht und vermehrtes intra-abdominales Fettgewebe auf. Eine umfassende Phänotypisierung der *Pts*-ki/ki Mäusen zeigte Veränderungen im Energiestoffwechsel mit einem erhöhten Fettgehalt, einer geringeren Magermasse, und einem erhöhten Blutzucker- und Cholesterinspiegel. Die Transkriptom-Analyse der Leber deutete auf Veränderungen im Glukose- und Fettstoffwechsel hin. Darüber hinaus wurden differentiell exprimierte Gene gefunden, welche in Verbindung mit Übergewicht, Gewichtsverlust, Fettleber und Insulinempfindlichkeit stehen und die beobachteten phänotypischen Veränderungen der transgenen Tiere unterstützen. Unsere Studie verbindet eine neuartige Genmutation mit den monogenen Formen der Adipositas. Wir schliessen daraus, dass die reduzierte PTPS und die potentiell auch reduzierte BH_4-Biosynthese-Aktivität bei Mäusen zur abnormalen Körperfettverteilung und abdominaler Adipositas führt, welche möglicherweise durch das leicht erhöhte Neopterin und/oder durch die beeinträchtigte eNOS Funktion verursacht wird (Manuskript Korner et al.).

Ein weiteres Kapitel befasst sich mit der Validierung einer Beobachtung von Dea Adamsen aus ihrer Dissertation (Universität Zürich, 2011). D. Adamsen beschrieb in ihrer Arbeit, dass *Pts*-ki/ko verschiedene Phänotypen aufwiesen, welche angeblich vom Genotyp der Mutter abhängig ist: "betroffene" *Pts*-ki/ko Neugeborene, welche 3-4 Tage nach der Geburt verstarben und "nicht betroffene" *Pts*-ki/ko Nachkommen, welche sich normal entwickelten. "Nicht betroffene" *Pts*-ki/ko Mäuse zeigten einen ähnlichen Phänotypen wie die homozygoten *Pts*-ki/ki Mäuse. "Betroffene" Mäuse hatten alle Anzeichen des letalen BH_4-Mangels mit geringem Biopterin und Monoamin-Neurotransmittern, erhöhtem Neopterin und Hyperphenylalaninemia

(HPA). Ferner behauptete D. Adamsen, dass der "betroffenen" Mäuse Phänotyp nur auftrat, wenn die Mutter homozygot für die knock-in Mutation war. Es wurden Neugeborene (1 Tag alt) und 3-4 Tage alte Jungtiere aus verschiedenen Zuchtkombinationen von *Pts*-ki/ki, *Pts*-ki/wt und *Pts*-ko/wt Eltern untersucht. Dabei wurden lediglich geringe Abweichungen zwischen *Pts*-ki/ko Neugeborenen von unterschiedlichen Zuchtkombination gefunden und keines der Jungtiere zeigte die schweren ("betroffen") Phänotyp.

Kapitel 4: Eine Studie über Muskel-orientierten nicht-viralen Gentransfer zur Behandlung der klassischen PKU in der Maus und das Bestreben zur Generierung eines Mausmodells, welches BH_4 im Muskel exprimiert

Der Mangel des Leberenzymes Phenylalaninhydroxylase (PAH), dass für die Umwandlung von L-Phenylalanin (L-Phe) zu L-Tyr verantwortlich ist, stellt die Ursache für die klassische Phenylketonurie (cPKU) dar. Die vollständige Korrektur der cPKU wurde zuvor in einem Mausmodell durch muskelspezifische Behandlung unter Verwendung eines rekombinanten AAV-Vektors publiziert, welcher das komplette Phenylalaninhydroxylierungsystems exprimiert, d.h. mit einer koordinierten Expression der *Pah*-Minigens sowie die beiden Gene (cDNAs) Guanosintriphosphat Cyclohydrolase I (*Gch*1) und *Pts*, welche man für die BH_4-Kofaktor-Biosynthese im Muskelgewebe benötigt. Alternativ zum (AAV) viralen Ansatz sollte das Potential eines solchen triple-cistronischen Gentransfers unter Verwendung nackter DNA/Minicircle (MC) Vektoren zur Behandlung der Skelettmuskulatur von PKU-Mäusen untersucht werden. Die dafür getesteten triple-cistronischen Genvektoren verfügen über verschiedene Modifikationen wie Codon-Optimierung, Einfügen von intronischer Sequenz, Transkription oder Genexpression verstärkenden Elementen wie dem Woodchuck Hepatitis post-Transkriptionsregulationselement (WPRE) und der Scafold/Matrix-Attachment Region (S/MAR). Die Transgenexpression der Vektoren wurde unter Zellkulturbedingungen geprüft, bevor sie durch hydrodynamische Schenkel-Veneninfusion oder durch Elektroporation in die PKU-Mäuse appliziert wurden. Obwohl hohe Konzentrationen der MCs verabreicht wurden (bis zu 6,8 $x10^{14}$ Vektorpartikel), normalisierte sich die Blut L-Phe Konzentration in den behandelten PKU-Mäusen mit keinem der Vektoren.

Weitere Optimierungsmöglichkeiten für eine nicht-viralen Gentransfers für den Muskel zur Behandlung von cPKU wurden in einem weiteren Kapitel diskutiert.

1.

INTRODUCTION

CHAPTERS:

- 1.1 TYROSINE HYDROXYLASE DEFICIENCY
- 1.2 TETRAHYDROBIOPTERIN DEFICIENCY
- 1.3 CLASSICAL PHENYLKETONURIA
- 1.4 TOOLS FOR GENE TARGETING AND GENOME ENGENEERING TO GENERATE RECOMBINANT MICE
- 1.5 AIM OF STUDY

1.1 TYROSINE HYDROXYLASE DEFICIENCY

1.1.1 DESEASE CHARACTERISTICS

Tyrosine hydroxylase deficiency (THD: OMIM 605407), also called autosomal recessive Segawa syndrome, is an autosomal recessive disorder resulting from cerebral catecholamine deficiency (Szentivanyi et al., 2012). THD is a rare metabolic disease with approximately 70 reported cases (www.biopku.org/pnddb and personal communication with Jan Haavik, University of Bergen, Norway). Tyrosine hydroxylase (TH; EC 1.14.16.2) catalyzes the conversion of L-tyrosine (L-Tyr) to L-dihydroxyphenylalanine (L-Dopa), which is the rate-limiting step in the biosynthesis of the catecholamines dopamine, norepinephrine and epinephrine (see Fig. 1) (Goldstein et al., 2006, Willemsen et al., 2010).

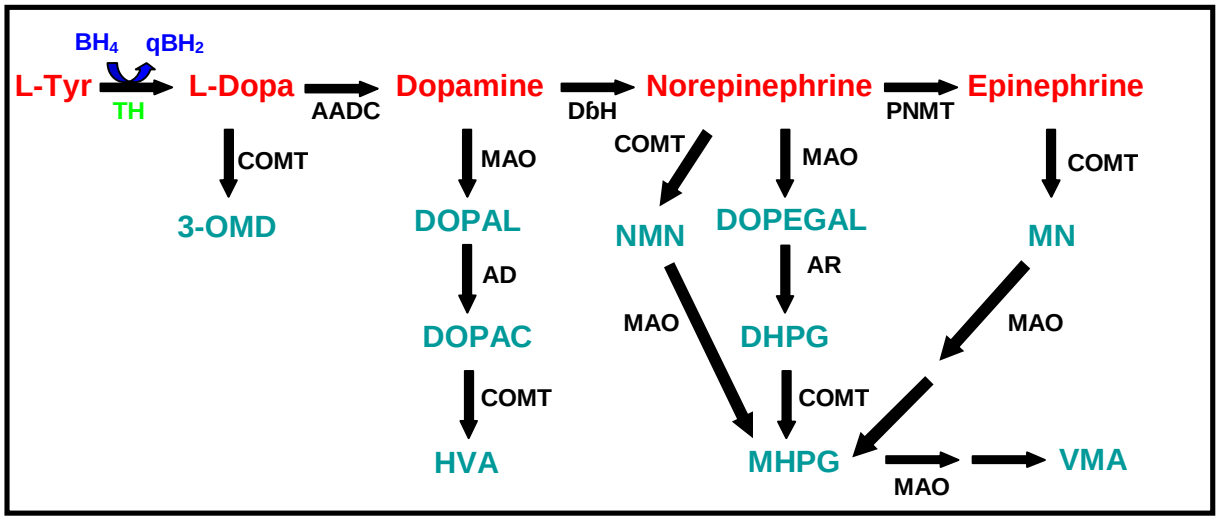

Figure 1: Chemical pathway of catecholamine synthesis and metabolism (Goldstein et al., 2006). AADC, L-amino acid decarboxylase; AD, aldehyde dehydrogenase; AR, aldehyde reductase; BH_4, tetrahydrobiopterin; COMT, catechol-*O*-methyltransferase; DβH, dopamine-β-hydroxylase; DHPG, 3,4-dihydroxyphenylglycol; DOPAC, dihydroxyphenylacetic acid; DOPAL, 3,4-dihydroxyphenyl-acetaldehyde; L-Dopa, L-dihydroxyphenylalanine; DOPEGAL, 3,4-dihydroxyphenylglycolaldehyde; HVA, homovanillic acid; L-Tyr, L-tyrosine; MAO, monoamine oxidase; MHPG, 3-methoxy-4-hydroxyphenylethyleneglycol; MN, metanephrine; NMN, normetanephrine; PNMT, phenyl-ethanolamine-N-methyltransferase; 3-OMD, 3-O-methyldopa; q-BH_2, dihydrobiopterin; TH, tyrosine hydroxylase; VMA, vanillylmandelic acid.

Dopamine, norepinephrine and epinephrine are involved in the regulation of motor coordination, behaviour, learning and memory, sleep-wake cycle regulation, endocrine and visceral functions and arousal in adults (Wevers et al., 1999). In 1971, the first report of THD described patients with an early onset, progressive L-Dopa-responsive dystonia (DRD) (Castaigne et al., 1971, Willemsen et al., 2010). In 2003, neonates with a more severe phenotype were described as progressive, L-Dopa-non-

responsive encephalopathy (Hoffmann et al., 2003). Therefore, THD is classed into two clinical phenotypes: type A (mild form) with an infantile progressive hypokinetic-rigid syndrome with dystonia and type B (severe from) with a neonatal complex encephalopathy (Szentivanyi et al., 2012). THD is a movement disorder with a very early onset: type B patients had an age onset within the first months of life, whereas most of the type A patients showed signs in the first year of life. Approximately 69% of all patients suffered from type A THD. Symptoms included unilateral or asymmetric limb dystonia, postural tremor, gait disorder or involuntary eye movements (Swoboda and Furukawa, 1993, Willemsen et al., 2010). Severity of dystonia may fluctuate during the day and is generally worse in the afternoon, but it can also fluctuate within days (Willemsen et al., 2010). Type B patients show infantile parkinsonism included developmental motor delay, truncal hypotonia, limb rigidity, hypokinesia, and neuropsychiatric features like attention deficit or impulsivity, learning disabilities, excessive anxiety, depression, or obsessive-compulsive symptoms (Swoboda and Furukawa, 1993, Furukawa, 2003, Hoffmann et al., 2003, Furukawa et al., 2004). Speech delay or difficulty with articulation can also occur. Autonomic dysfunction like constipation, reflux, poor feeding, temperature instability, hypoglycemia, and difficulty regulating blood pressure may be present (de Rijk-Van Andel et al., 2000, De Lonlay et al., 2000). More severely affected children have intellectual disability and hyperprolactinemia (dopamine is a prolactin-inhibiting factor) (Swoboda and Furukawa, 1993, Hyland, 1999). Another form is the progressive infantile encephalopathy in which children have persistent encephalopathy and motor disability (Swoboda and Furukawa, 1993, Hoffmann et al., 2003). Diurnal fluctuations of symptoms are present to a minor degree but are generally absent (Willemsen et al., 2010).

1.1.2 DISEASE CAUSING GENE

The only gene associated with THD is the human *TH* (h*TH*) gene encoding the hTH enzyme, which is the rate-limiting enzyme in catecholamine biosynthesis (Swoboda and Furukawa, 1993). The h*TH* gene lies on chromosome 11p15.5 and consists of 14 exons (13 exons in mice) spanning approximately 8.5 kb (Swoboda and Furukawa, 1993, Nagatsu, 1995, Wevers et al., 1999). In humans there are up to eleven types of mRNA produced through alternative splicing of which the most

important are h*TH* type 1ï 4 mRNAs encoding for the four TH isoenzymes with tissue-specific distribution (http://www.ensembl.org, Alterio et al., 1998). The hTH 1 variant (1491 bp; 497 amino acids) is the shortest encoding hTH isoform B, whereas hTH2ï 4 variants have inserts that lead to the expression of proteins containing 4, 27 and 31 (4 + 27) amino acids N-terminal to Ser31 in the hTH type 1 isoform. hTH type 4 (1584 bp; 528 amino acids) is the longest transcript encoding for the hTH isoform A (Swoboda and Furukawa, 1993, Gordon et al., 2009, Dunkley et al., 2004). The human brain (and adrenals) contains all four distinct isoforms of hTH, but the presence or relative amount of each isoform may differ among catecholaminergic cell populations and between catecholaminergic neurons and terminal fields (Lewis et al., 1993). hTH type 1 and hTH type 2 are the two major isoforms in the brain, comprising together approximately 90% of hTH in brain (Swoboda and Furukawa, 1993, Gordon et al., 2009, Dunkley et al., 2004). The native form of the hTH is a homotetramer, which consists of four identical subunits each with a molecular weight of approximately 60 kD (He, 1996). The amino acid sequence is highly conserved between species (Wevers et al., 1999). TH uses oxygene and tyrosine as substrates, and tetrahydrobiopterin (BH_4) as cofactor. More than 40 different mutations are described for h*TH* gene and patients carry homozygote or compound heterozygote mutations (Willemsen et al., 2010, Szentivanyi et al., 2012). Most mutations are single nucleotide substitutions, but single nucleotide deletions resulting in frame shift, protein truncation or mutations in the TH promoter were described (Swoboda and Furukawa, 1993, Nagatsu, 1995). The most prevalent mutation is the missense mutation c.698G>A/p.Arg233His (nomenclature refers to hTH type 4) associated with the severe form of THD (Willemsen et al., 2010).

1.1.3 DIAGNOSIS

The patterns of CSF neurotransmitter metabolites and pterins support the diagnosis of TH deficiency but only sequence analysis of the h*TH* gene to identify mutations can confirm THD (Swoboda and Furukawa, 1993). THD patients have normal biopterin, neopterin and 5-hydroxyindoleacetic acid (5-HIAA; metabolite of serotonin) levels but reduced homovanillic acid (HVA; metabolite of dopamine) and 3-methoxy-4-hydroxy-phenylethyleneglycol (MHPG; a metabolite of noradrenaline) levels in their CSF (Swoboda and Furukawa, 1993, Brautigam et al., 1998, Wevers et al., 1999). If

biopterin and neopterin are detected low, guanosine-5'-triphosphate (GTP) cyclohydrolase (GTPCH; EC 3.5.4.16)-deficient DRD associated with mutations in *GCH*1 should be considered since the clinical phenotypes of GTPCH-DRD and mild TH deficiency overlap significantly (Swoboda and Furukawa, 1993, Furukawa et al., 1996).

1.1.4 MANAGEMENT AND TREATMENT APPROACHES

In almost all patients with type A THD, successful treatment with L-Dopa leads to improvement of the neurological conditions, whereas in type B, L-Dopa treatment does not improve all signs equally, and it may take months before all effects of treatment can be noticed (Szentivanyi et al., 2012). Furthermore, hypersensitivity due to the L-Dopa treatment is an important management problem in many of type B patients and therefore, it is necessary to start with low L-Dopa dosages, which can be increased over periods of weeks or months. Carbidopa, which is a L-amino acid decarboxylase (AADC, EC. 4.1.1.28) inhibitor, has to be applied in addition to L-Dopa to prevent the peripheral metabolism of L-Dopa into dopamine (can not cross the BBB) (Hoffmann et al., 2003). While responsiveness to L-Dopa was absent or moderate in more than 80% of type B patients, it was good in proximally 84% of the type A patients (Willemsen et al., 2010). L-Dopa treated type A patients showed no evidence of progressive disease, and tolerate L-Dopa well during many years (Schiller et al., 2004). Compared to type A THD, prognoses of the outcome are worse for type B THD patients regarding their motor and cognitive functions (Willemsen et al., 2010).

1.1.5 MOUSE MODELS

In 1995, the disruption of the murine *Th* (m*Th*) gene (null mutation) in mouse embryonic stem (ES) cells by homologous recombination generated the *Th* (-/-) knock-out mouse model. *Th* (-/-) mice showed mid-gestational lethality of about 90% of mutant embryos between embryonic days 11.5 and 15.5, probably caused by cardiovascular failure. Administration of L-Dopa to pregnant females results in complete rescue of mutant mice *in utero*, but without further treatment the *Th* (-/-) mice died before weaning (Zhou et al., 1995). Heterozygous mice were apparently

normal showing less than 50% TH. Their catecholamine levels were decreased moderately in developing animals and maintained normal at adulthood, suggesting the presence of a regulatory mechanism for ensuring the proper catecholamine levels during animal development. To confirm that the mutant *Th* (-/-) phenotype observed derived from the disruption of the mouse m*Th* locus without effects on other chromosomal positions in the ES cell genome, the h*TH* transgene was introduced into the *Th* (-/-) homozygous mice, by crossing h*TH* transgenic mice carrying the h*TH* gene with the heterozygous *Th* (+/-) mice. The rescued mutants appeared normal showing recovered TH activity in the brain and restored catecholamine levels similar as wild-type mice. These results also indicated that the h*TH* transgene can replace the function of the m*TH* gene (Kobayashi et al., 1995).

Another THD mouse model has been created in 1995, which was unable to synthesize dopamine in dopaminergic neurons by inactivating the m*Th* gene then by restoring TH function in noradrenergic cells (DA-/- mice). These DA-/- mice were born at expected frequency but became hypoactive and hypophagic 3-4 weeks after birth and died without L-Dopa intervention. Continued administration of L-Dopa led to normal developed and the DA-/- mice became more active and consumed more food (Zhou and Palmiter, 1995). On the other hands, these mice showed hypersensitivity to dopamine 1 and 2 (D1 and D2) receptor agonists (Kim et al., 2000). The midbrain dopaminergic neurons, their projections, and most characteristics of their target neurons in the striatum appeared normal. These studies indicated that dopamine is essential for movement and feeding, but is not required for the development of neural circuits that control these behaviours (Zhou and Palmiter, 1995).

1.1.6 GENE THERAPEUTIC APPROACHES

None of the described THD mouse models were used to study gene therapeutic approaches so far. Patients with DRD (type A THD) have clinical similarities to Parkinson's disease (PD) patients. A consistent neurochemical abnormality in PD is the degeneration of dopaminergic neurons in substantia nigra, leading to a reduction of striatal dopamine levels. Since TH catalyses is the rate-limiting step in the biosynthesis of dopamine, the PD can be considered as a TH-deficiency syndrome of the striatum. Therefore, a treatment strategy for PD consists of L-Dopa, dopamine

agonists, inhibitors of dopamine metabolism, or brain grafts with cells expressing TH. A direct pathogenetic role of TH has also been suggested, as the enzyme is a source of reactive oxygen species (ROS) *in vitro* and a target for radical-mediated oxidative injury. Therefore, it is suggested that TH is involved in the pathogenesis of PD at several different levels, and is a promising candidate for developing new treatments of this disease (Haavik and Toska, 1998). Some of these approaches are described in this chapter.

There are several studies describing viral and non-viral gene therapeutic approaches using *TH* transgenes to treat symptoms in PD induced animal models. In this PD induced animal models (mainly in rats) the nigrostriatal dopaminergic pathway is lesioned using neurotoxin like 6-hydroxydopamine (6-OHDA). 6-OHDA is a catecholaminergic neurotoxin, which shares some structural similarities with dopamine and norepinephrine and exhibiting a high affinity for several catecholaminergic plasma membrane transporters such as the dopamine and norepinephrine transporters. 6-OHDA selectively destroys dopaminergic and noradrenergic neurons in the brain leading to the damage of the nigrostriatal dopaminergic pathway, generating experimental PD animal models used to test new medicines and treatments (Bove et al., 2005).

Already in 1994, a gene therapeutic approach to treat PD using partially denervated striatum of 6-OHDA lesioned rats treated with a defective herpes simplex virus type 1 vector expressing h*TH* transgene led to long-term recovery of striatal expression of mRNA, TH enzyme activity, extracellular dopamine concentration and behaviour (During et al., 1994). In the same year, another study showed successfully intracerebral gene transfer of an adenoviral vector expressing h*TH* in the rat model of PD (Horellou et al., 1994, Horellou et al., 1995). 1998 and 2000, studies with adeno-associated virus (AAV) vectors showed improved treatment of double or even triple gene therapy approaches by using h*TH* in combination with the human *DDC* gene (expresses AADC) and *GCH*1 gene (Fan et al., 1998, Shen et al., 2000). Already co-expression of TH and AADC, using two separate AAV vectors, resulted in more effective dopamine production and more remarkable behavioural recovery in 6-OHDA lesioned Parkinsonian rats, compared with the expression of TH alone (Fan et al., 1998). Not only levels of TH and AADC but also levels of BH_4 and GTPCH, which is

the rate-limiting enzymes for BH_4 biosynthesis, are reduced in Parkinsonian striatum. Triple transduction with AAV-TH, AAV-AADC, and AAV-GTPCH resulted in more dopamine production than double transduction with AAV-TH and AAV-AADC *in vitro* and *in vivo*, and improved the rotational behaviour of the rats more efficiently than double transduction. These results suggest that GTPCH, despite TH and AADC, is important for effective gene therapy for PD (Shen et al., 2000). These findings were further supported by a lentivirus study in 2002, showing that multicistronic lentiviral vector-mediated striatal gene transfer of TH, AADC and GTPCH induces sustained transgene expression, dopamine production, and functional improvement in a rat model of PD (Azzouz et al., 2002).

In 2003, it was described that intravenous non-viral gene therapy caused normalization of striatal TH and reversal of motor impairment in an experimental 6-OHDA rat model of PD (Zhang et al., 2003). In this approach, 6-OHDA treated rats with lesion in the striatum were intravenously injected with a TH expression plasmid which is encapsulated inside an 85-nm polyethylene glycol (PEG) chemical conjugated (pegylation) immunoliposome (PIL) that is targeted with the OX26 murine monoclonal antibody to the rat transferrin receptor (TfR). TfRMAb-PIL enters the brain via the transvascular route and enables the nanocontainer carrying the gene to undergo both receptor-mediated transcytosis across the BBB and receptor-mediated endocytosis into neurons behind the BBB by accessing the TfR. The measured TH enzyme activity was more then seven times higher and TH immunocytochemistry showed that the entire striatum was immunoreactive for TH after the intravenous gene therapy (Zhang et al., 2003). Further studies demonstrated that that ectopic gene expression is eliminated with the use of brain-specific gene promoters (Zhang et al., 2004).

Although there are several gene therapeutic approaches using *TH* gene transfer into brain, there are no clinical trails using TH transgenic vectors to treat PD so far.

1.2 TETRAHYDROBIOPTERIN DEFICIENCY

1.2.1 DESEASE CHARACTERISTICS

In 1958, the first description was presented of a cofactor required for the enzymatic conversion of L-phenylalanine (L-Phe) to L-Tyr by the phenylalanine hydroxylase (PAH; EC 1.14.16.1), which is nowadays known as BH_4 (Kaufman, 1958). BH_4 is *de novo* synthesized from GTP by the three enzymes GTPCH (EC 3.5.4.16), 6-pyruvoyl-tetrahydropterin synthase (PTPS, EC 4.6.1.10), and sepiapterin reductase (SR, EC 1.1.1.153) and can be regenerated by the pterin-4a-carbinolamine dehydratase (PCD; EC 4.2.1.96) and dihydropteridine reductase (DHPR, EC 1.6. 99.7) (Thöny et al., 2000, Thöny et al., 2000). Enzyme deficiencies in any of these genes have been reported to cause BH_4 deficiency (GTPCH: OMIM 233910; PTPS: OMIM 261640; SR: OMIM 612716; DHPR: OMIM 261630; PCD: OMIM 264070), also called atypical phenylketonuria (aPKU), in an autosomal recessive mode of inheritance (Shintaku, 2002, Thöny and Blau, 2006). The incidence of BH_4 deficiency is approximal one case per 1,000,000, responsible for 1-2% of all hyperphenylalanine (HPA) cases (Shintaku, 2002, Blau, 2008b, Blau et al., 2010). BH_4 is not only required to convert L-Phe to L-Tyr by PAH, but also by TH and tryptophan hydroxylase 1/2 (TPH1/2, EC 1.14.16.4) which synthesizes the monoamine neurotransmitter precursors L-Dopa and 5-OH-tryptophan (5-HTP), respectively. L-Dopa and 5-HTP are further converted into dopamine and serotonin by AADC, respectively. Furthermore, BH_4 is a cofactor for all three nitric-oxide synthases (NOSs; EC 1.14.13.39) for nitric oxide production, as well as for the alkylglycerol monooxygenase (AGMO, EC 1.14.16.5), which catalyzes the hydroxylation of alkylglycerols (Wei et al., 2003, Werner et al., 2003, Watschinger et al., 2010). Biosynthesis and regeneration of BH_4 including the metabolic defects are shown in Fig. 2.

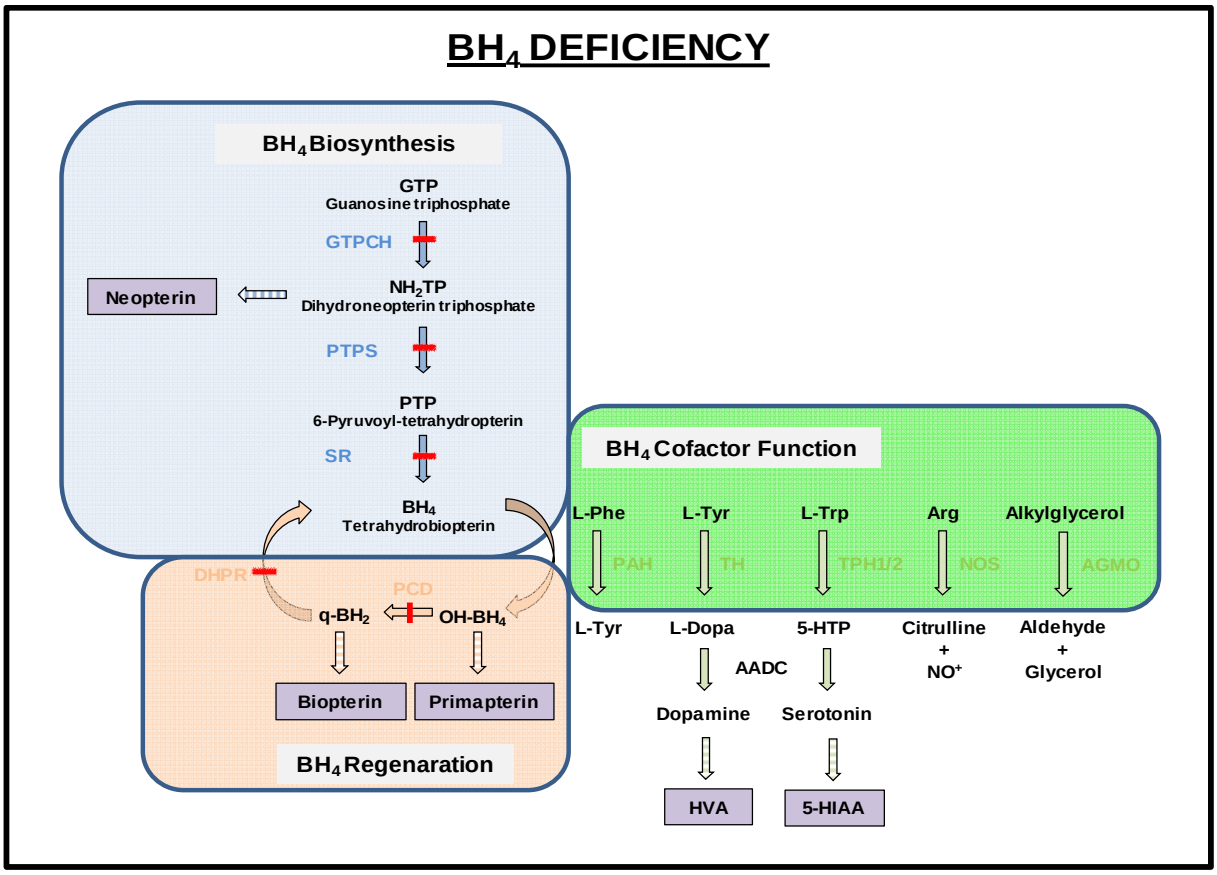

Figure 2: Biosynthesis and regeneration of BH_4 including metabolic defects; modified from (Blau, 2008b). GTPCH, guanosine triphosphate cyclohydrolase 1; PTPS, 6-pyruvoyl-tetrahydropterin synthase; SR, sepiapterin reductase; DHPR, dihydropterindine reductase; PCD, pterin-4a-carbinolamine dehydratase; PAH, phenylalanine hydroxylase; TH, tyrosine hydroxylase; TPH, tyrosine hydroxylase; NOS, nitric-oxide synthase; AGMO, alkylglycerol monooxygenase; AADC, aromatic L-amino acid decarboxylase; L-Phe, L-phenylalanine; L-Tyr, L-tyrosine; Arg, argimnine; NO, nitric oxide; HVA, homovanillic acid; L-Dopa, dihydroxyphenylalanine; 5-HTP, 5-hydroxytryptophan; BH_4, tetrahydrobiopterin; OH-BH_4, hydroxytetrahydrobiopterin; q-BH2, quinone-dihydrobiopterin.

Autosomal inherited deficiency in GTPCH, PTPS, PCD or DHPR is associated with a broad spectrum of phenotypes ranging from mild and peripheral, concerning only the peripheral hepatic L-Phe hydroxylating system, to severe and central, affecting all organs, including the central nervous system (CNS), and influencing mainly the L-Phe catabolism, and the brain neurotransmitters biosynthesis (Thöny and Blau, 2006, Blau, 2008b). Out of 250 BH_4 deficiency patients 58% revealed mutations in the *Pts* gene, encoding for the PTPS enzyme, followed by 35% affecting the DHPR enzyme and 3-4% have PCD or GTPCH deficiency (Blau, 2013). Patients with GTPCH, PTPS or DHPR deficiency have progressive mental and/or psychomotor retardation despite L-Phe diet, including symptoms such as hypotonia or hypertonia, temperature instability, seizures, microcephaly, and hypersalvation. PCD deficient patients are

reported despite having HPA, transient alterations in tone, and excretion of primapterin through the urine, with hypomagnesemia and renal magnesium wasting, and are at risk to develop diabetes with characteristics of maturity onset diabetes of the young (MODY) type 3 (Shih et al., 2001, Blau, 2008b, Ferre et al., 2014). MODY, renal malformations and hypomagnesemia are probably caused due to the relation of PCD as a dimerization cofactor for the transcription factor homeodomain protein hepatocyte nuclear factor (HNF). Mutations in the HNF genes have been shown to cause, renal malformations and hypomagnesemia and MODY, because HNF involved in glucose-stimulated insulin secretion, insulin synthesis, and ß-cell differentiation (Shih et al., 2001, Ferre et al., 2014).

Two disorders of BH_4 metabolism are present without HPA, the DRD (dominant form of Segawa syndrome) caused by a autosomal dominant mutation in the *GCH*1 gene, and sepiapterin reductase deficiency inherited in an autosomal recessive trait and thus can not be detected by the neonatal screening for PKU (Blau et al., 2001). Characteristic features of SR deficient patients is the progressive psychomotor retardation and similar signs as described for the other enzyme deficiencies, whereas DRD patients show in particular dystonia and parkinsonism symptoms (Blau, 2008b).

1.2.2 DISEASE CAUSING GENES

BH_4 deficiency is caused by affecting the three enzymes of biosyntheses and the two enzymes for recycling. An overview of the affected genes is shown in table 1 (Lang, 2009).

Table 1: Genetic causes of BH_4 deficiency [a].

Enzyme	EC No.	Subunit composition	AA[b] (MW)	Defective gene	Chromosome	No. of exon	Inheritance
GTPCH	3.5.3.16	Homodecamer	250 (37.9 kDa)	*GCH*1	14q22.1-q22.2	6	AR[c] or AD[d]
PTPS	4.6.1.10	Homohexamer	145 (16.4kDa)	*PTS*	11q22.3-q23.3	6	AR[c]
SR	4.2.1.96	Homodimer	261 (28.0kDa)	*SPR*	2p13.2	3	AR[c]
PCD	4.2.1.96	Homotetramer	103 (11.9kDa)	*PCBD*	10q22	4	AR[c]
DHPR	1.6.99.7	Homodimer	244 (25.8 kDa)	*QDPR*	4p15.3	7	AR[c]

[a]Modified (Lang, 2009); [b]amino acid; [c]autosomal recessive; [d]autosomal recessive.

There are more than 140 known mutations scattered over the entire *GCH*1 gene of which approximately 95% cause the dominant inherited DRD and only 5% autosomal recessive form of inheritable HPA. Compound heterozygous or homozygous mutations are spread over the entire genes for *PTS* with proximally 57 mutations, for

PCBD with 10 mutations, and for *QDPR* with approximately 39 mutations. There are 13 different mutant alleles in the *SPR* gene located in exons 2 or 3, in intron 2 and the 5ôUTR (Thöny and Blau, 2006).

1.2.3 DIAGNOSIS

BH_4 deficiency among newborns with HPA have to be rapidly diagnosed and distinguished from classical PKU (cPKU) because of the different treatments requirements to prevent irreversible neurological damage (Blau et al., 1992). Newborns with a positive Guthrie test (see chapter 1.3.3) with even mild HPA (>120 εmol/L) as well as children without HPA but with neurological symptoms should be screened for BH_4 deficiency (Blau, 2008b). The characteristic patterns of pterins excreted by the urine or found in blood serum lead to the identification of all four variants of BH_4 deficiency concomitant with HPA (GTPCH, PTPS, PCD and DHPR) (Blau, 1988, Blau et al., 1992, Shintaku, 2002, Blau, 2008b). Urine can be collected on a filter paper and pteridines can be measured by high performance liquid chromatography (HPLC) (Blau et al., 1992). DHPR enzyme activity can be measured in dried blood samples to recognize and confirm DHPR deficiency (Lenzi et al., 1989). For DRD and SR deficiency, neurotransmitter metabolites and pterines needed to be tested in the cerebrospinal fluid (CSF). Enzyme activity measurements in cytokine-stimulated or unstimulated fibroblasts are useful tools to determine GTPCH or PTPS, SR, DHPR and PCD deficiency, respectively (Bonafe et al., 2001, Blau, 2008b). Analysis of L-Phe and L-Tyr in blood before and after BH_4 challenge also discriminates between cPKU and the biopterin variants or helps to identify BH_4-responsive PAH deficiencies (Blau, 2008b). Screening policy for differential diagnosis of HPA (Fig. 3 A) and non-HPA (Fig. 3 B) variants is summarized in two diagnostic flowcharts in Fig. 3.

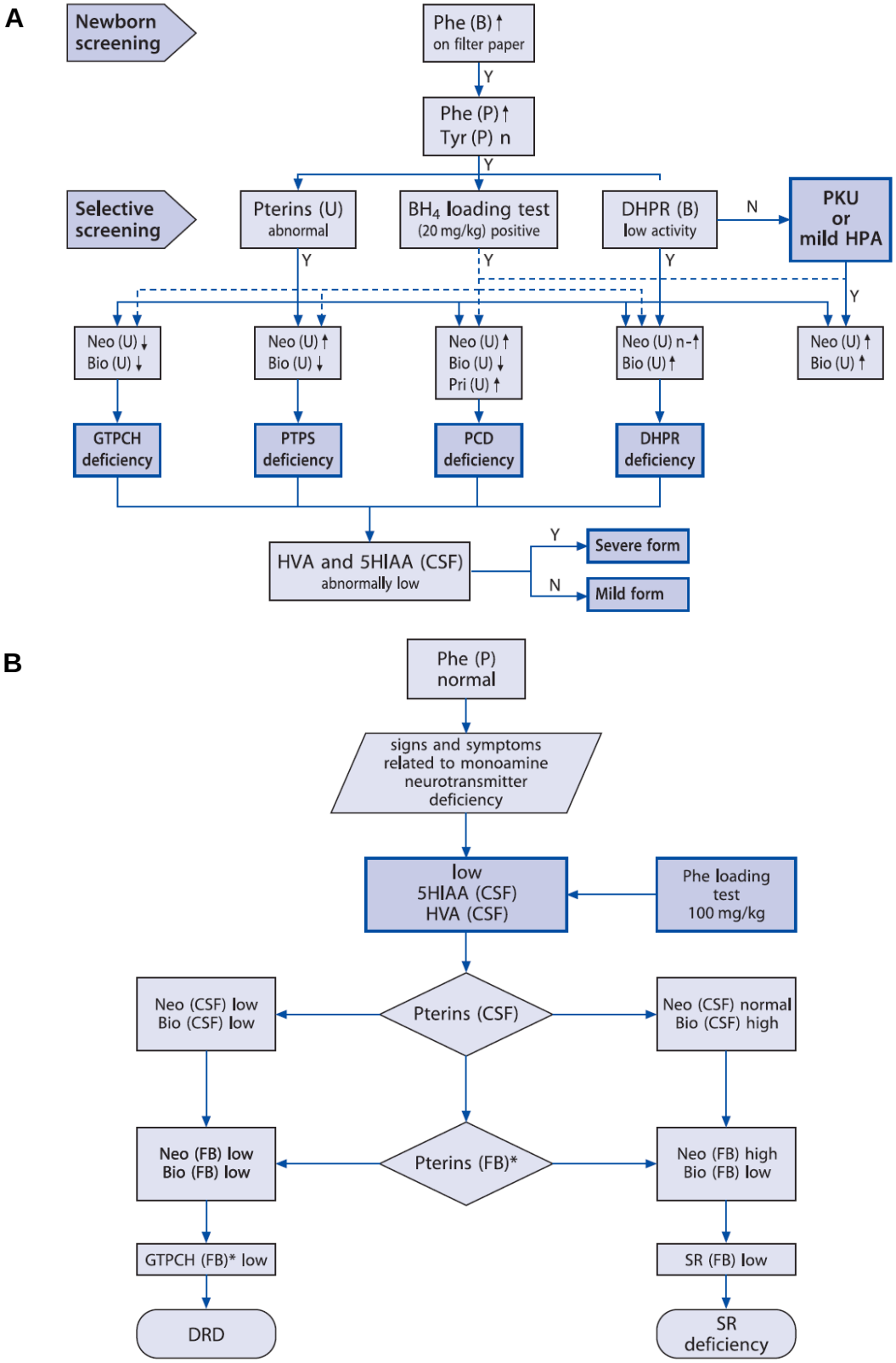

Figure 3: Diagnostic flowchart in differential diagnosis for HPA **(A)** and non-HPA **(B)** variants; modified version from (Blau, 2008b). GTPCH, guanosine triphosphate cyclohydrolase 1; PTPS, 6-pyruvoyl-tetrahydropterin synthase; SR, sepiapterin reductase; DHPR, dihydropterindine reductase; PCD, pterin-4a-carbinolamine dehydratase; DRD, Dopa-responsive dystonia; Phe, phenylalanine; Tyr, tyrosine; Neo, neopterin; Bio, biopterin; Pri, primapterin; CSF, cerebrospinal fluid; FB, fibroblasts; B, blood; U, urine; P, plasma; Y, yes; N, no. * Cytokines-induced cells.

1.2.4 MANAGEMENT AND TREATMENT APPROACHES

The treatment of BH_4 deficiencies depends on the enzyme deficiency and consists of BH_4 supplementation or diet to control blood L-Phe concentration, replacement therapy with monoamine neurotransmitters precursors L-Dopa and 5-HTP in combination with carbidopa because carbidopa prevents the conversion of L-Dopa and 5-HTP into dopamine and serotonin (can not cross BBB) in the periphery, respectively (Hoffmann et al., 2003). Supplementation of folinic acid has to be added in DHPR deficient patients (Shintaku, 2002, Blau, 2008b). An overview of each treatment is shown below:

- **GTPCH deficiency:** BH_4, L-Dopa, 5-HTP and carbidopa
- **PTPS deficiency:** BH_4, L-Dopa, 5-HTP and carbidopa
- **DHPR deficiency:** L-Dopa, 5-HTP, carbidopa, low L-Phe diet and folinic acid
- **PCD deficiency:** Evtl. low L-Phe diet, BH_4 and/or MODY treatment
- **SR deficiency:** BH_4, L-Dopa and carbidopa
- **DRD:** L-Dopa and carbidopa

1.2.5 MOUSE MODELS

1.2.5.1 GTPCH

The GTPCH deficient hph-1 mouse generated in 1988 by N-ethyl-N'-nitrosourea (ENU) mutagenesis is a model for the dominantly inherited GTPCH deficiency DRD. Homozygous mice showed low brain levels of BH_4, catecholamines, serotonin, together with low levels of TH protein within the striatum (Bode et al., 1988, Hyland et al., 2003).

1.2.5.2 PTPS

In the year 2001, a *Pts* knock-out (*Pts*-ko) mouse model was described that was unable to synthesize BH_4 due to the disruption of the *Pts* gene through homologous recombination. Homozygous mice showed a severe and central form of BH_4 deficiency with neonatal lethality (died within 48 hours). Analysis of brain lysate of homozygous mutant neonates revealed HPA and extremely low levels of biopterin, catecholamines and serotonin. Furthermore, the BH_4 depletion led also to the

impairment of the TH enzyme with reduced immunoreactivity in the nerve terminals (Sumi-Ichinose et al., 2001). Daily oral administration of BH_4 and neurotransmitter precursors led the survival of the *Pts*-ko/ko mice but the mice were sexual immature and showed dwarfism due to lowered insulin-like growth factor-1 (IGF-1) levels. Biochemical analysis revealed no HPA, almost normal brain serotonin levels, but reduced dopamine levels (3% of normal) (Elzaouk et al., 2003).

Since the *Pts*-ko/ko mouse model showed a very severe phenotype, a *Pts* knock-in (*Pts*-ki) mouse model was generated by homologous recombination introducing the missense mutation p.Arg15Cys in exon 1 (c.43 C>T; 15% of activity in comparison to wild-type), which is equivalent to the human *PTS*-p.Arg16Cys (c.46 C>T; 12% of activity in comparison to wild-type), by Rossana Scavelli (University of Zurich, 2006). Homozygous *Pts*-ki/ki mice showed a mild and peripheral phenotype with reduced PTPS activity, but normal biopterin and monoamine neurotransmitter levels in the CNS and no HPA. Neopterin levels were elevated in the liver but not in the brain (see chapter 3.1). To generate a more severe and central phenotype without newborn lethality, compound heterozygous *Pts* mice (*Pts*-ki/ko) were generated by breeding the p.Arg15Cys knock-in allele into the *Pts*-ko mouse strain. The first phenotypical analysis of these compound heterozygous *Pts*-ki/ko mice was performed by Dea Adamsen (University of Zurich, 2011). She reported that *Pts*-ki/ko mice from *Pts*-ki/ki mouse mothers showed two distinguishable phenotypes: the ñunaffectedò *Pts*-ki/ko mice with a slightly more severe BH_4 deficiency phenotype then *Pts*-ki/ki mice and the ñaffectedò *Pts*-ki/ko mice, which showed a severe and central form of BH_4 deficiency 3-4 days after birth causing their lethality. In detail, ñaffectedò *Pts*-ki/ko mice had low PTPS activity, reduce biopterin, increased neopterin, HPA, and reduced monoamine neurotransmitters and therefore, these mice reflected all hallmarks of severe PTPS deficiency.

1.2.5.3 SR

In 2006, a mouse model, which is deficient in the *Spr* (-/-) gene, display disturbed pterin profiles and diminished levels of dopamine, norepinephrine, and serotonin, exhibit PKU, dwarfism, and impaired body movement. Oral supplementation of BH_4 and neurotransmitter precursors completely rescued the dwarfism phenotype and restored the L-Phe metabolism (Yang et al., 2006).

1.2.5.4 PCD

PCD not only regenerates BH_4 but it is also a cofactor that regulates dimerization of the mammalian HNF-1Ŭ. Therefore PCD is also known as the dimerization cofactor of HNF (DCoH) (Mendel et al., 1991). In 2002, the *Dcoh*-null mouse model was generated displaying HPA and a predisposition to cataract formation. The HNF function was only slightly impaired in these Dcoh-null mice, suggesting that Dcoh activity was partially complemented by Dcoh2 (Bayle et al., 2002).

1.2.6 GENE THERAPEUTIC APPROACHES

So far, none of the existing mouse models for BH_4 deficiency were used to investigate gene therapeutic approaches.

1.3 CLASSICAL PHENYLKETONURIA

1.3.1 DESEASE CHARACTERISTICS

In 1934, the Norwegian biochemist and physician Ivar Asbjørn Følling was the first who described the inherited metabolic disorder phenylketonuria (PKU, OMIM 261600), also known as Følling's disease, by identifying affected individuals by the abnormal excretion of phenyl-pyruvic acid in their urine (Folling, 1938, Centerwall and Centerwall, 2000). The name PKU was actually given by Lionel Sharples Penrose in 1937, who described the autosomal recessive nature of PKU (Penrose, 1935). In 1953, George Jervis showed that the hepatic enzyme deficiency of PAH, catalyzing L-Phe to L-Tyr, was the responsible cause of PKU (Fig. 4) (Jervis, 1953). Hydroxylation by PAH needs the cofactor BH_4, in the presence of molecular O_2, to produces L-Tyr. Alternative metabolism of L-Phe by decarboxylation or transamination produces various metabolites, i.e. phenylpyruvic acid, phenylacetic acid and phenyllactic acid, which are excreted through the urine (Williams et al., 2008). The prevalence of PKU is one case per 10,000 Caucasian live births and therefore, it is the most prevalent disorder caused by an inborn error of amino acid metabolism (de Baulny et al., 2007, Blau et al., 2010). 98% of HPA cases result from mutations in the PAH enzyme, whereas the remaining cases are caused by biosynthesis defect of its cofactor BH_4 (aPKU) (de Baulny et al., 2007). The clinical phenotypes of HPA due to PAH deficiency are classified from classical PKU (cPKU, blood L-Phe > 1200 **ε**mol/L) to mild PKU (600ï 1200 **ε**mol/L) and mild HPA (120ï 600 **ε**mol/L) (Lagler et al., 2010). Untreated cPKU patients have systemic HPA concomitant with lowered levels of brain monoamine neurotransmitters leading to mental retardation and impairment, seizures, growth failure, microcephaly and hypopigmentation due to reduced L-Tyr levels needed for the production of melanin (Matalon and Michals, 1991, Blau et al., 2010).

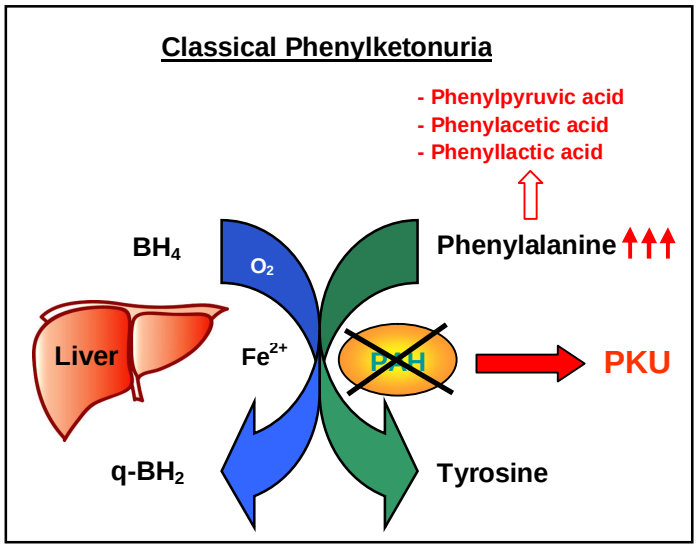

Figure 4: Schematic representation of cPKU.

The pathology underlying cognitive dysfunction in cPKU is unknown, although it is clear that the high L-Phe plasma concentrations influence the BBB transport of large neutral amino acids (LNAA) (van Spronsen et al., 2009). ñSystem Lò is a major nutrient transport system responsible for the transport of LNAA including four mammalian transmembrane proteins, the L-type amino acid transporters (LAT) 1-4 (Christensen, 1990, Yanagida et al., 2001). LAT1 and LAT2 (isoform of LAT1) are expressed in the brain and transport LNAA like L-Phe, L-Tyr for catecholamine synthesis or L-tryptophan for serotonin synthesis across the BBB (Segawa et al., 1999, Yanagida et al., 2001). The excess transport of L-Phe into the brain tissue seems to be the causative factor for PKU-related pathological symptoms (Yanagida et al., 2001, Bik-Multanowski and Pietrzyk, 2006).

1.3.2 DISEASE CAUSING GENE

The disease causing gene in cPKU is the iron- and BH_4-dependent monooxygenase PAH that catalyses the rate limiting step in the conversion of L-Phe to L-Tyr, which is the major degradation pathway for L-Phe. L-Phe catabolism and PAH activity is mainly associated with the liver. The human *PAH* gene lies on chromosome 12q23.2, where the gene comprises 13 exons extending over 171 kb of genomic DNA. The PAH enzyme exists as a mixture of tetramers and dimers; the monomer is 51.9 kDa in size and is comprised of 452 amino acids. There are more than 850 disease-causing mutations identified in patients with PKU or HPA caused by PAH deficiency usually with less then 1% of PAH activity (Flatmark and Stevens, 1999, Williams et al., 2008, Blau et al., 2010). Most mutations are missense mutations (62%), followed by small or large deletions (13%), splicing defects (11%), silent polymorphisms (6%), nonsense mutations (5%) and insertions (2%) (Williams et al., 2008). The most prevalent PAH mutation is the missense mutation c.1,222C>T/ p.Arg408Trp (Lee et al., 2008).

1.3.3 DIAGNOSIS

In 1963, Robert Guthrie described a mass screening test for newborns using dried blood spots for a bacterial inhibition assay test (Guthrie and Susi, 1963). The test uses the growth of the *Bacillus subtilis* bacteria strain on a specially prepared agar

plate containing B-2-thienylalanine, which inhibits the growth of the bacterium. L-Phe, phenylpyruvate, and/or phenyllactate, which are present in high amounts in the blood or urine of PKU patients, restore the growth of the bacterium which is an indicator for PKU (Guthrie and Susi, 1963, Blumenfeld et al., 1966). It was reported that with this Guthrie test one out of 25 PKU patients failed to be detected when screened at three days of age or less leading to ñfalse negativeò results (Blumenfeld et al., 1966). Nowadays, newborn blood testing for PKU is screened by using tandem mass spectrometry (MS/MS) (Banta-Wright and Steiner, 2004). Newborn screening for HPA, instituted in Switzerland in the sixties and practiced now throughout the Western world, has provided the opportunity to diagnose PKU in the neonate and to initiate therapy before the onset of severe and irreversible clinical manifestations (Bickel, 1987, Metzger et al., 2013). In addition, the oral BH_4 loading test (20 mg/kg), first described in 1999, can be used to identify BH_4-responsive PAH deficient patients, showing a positive response when the blood L-Phe decreases at least 30% during 48 h after the BH_4 challenge (Kure et al., 1999, Desviat et al., 2004, Burton et al., 2011, Anjema et al., 2013).

1.3.4 MANAGEMENT AND TREATMENT APPROACHES

In 1953 Horst Bickel described that dietary protein intake for PKU patients must be severely restricted to reduce L-Phe accumulation in their body by restricting or eliminating foods with high L-Phe content like for example meat, chicken, fish, eggs, nuts, cheese, vegetable and milk (Fig. 5) (Ievers-Landis et al., 2005, Blau et al., 2011, Camp et al., 2012). Starchy foods like potatoes, bread, pasta, and corn must be monitored (Bickel, 1987, Blau et al., 2010, Blau et al., 2011, Argyros, 2012, Camp et al., 2012). The sweetener aspartame, which is present in many diet foods and soft drinks, must also be avoided since aspartame consists of the two amino acids L-Phe and aspartic acid. Such an extreme protein restriction can only be

Figure 5: Schematic representation of foods allowed on the diet for PKU (http://depts. washington.edu/pku/about/ diet.html).

accomplished through the use of synthetic medical foods devoid of L-Phe, a lifelong unpalatable, rigid, and complicated diet. The supplementation of amino acids like L-Tyr and other necessary nutrients by pills, formulas, and specially formulated foods, are necessary for a normal development (Ievers-Landis et al., 2005, de Baulny et al., 2007, Argyros, 2012, Camp et al., 2012). Infants can be breastfed but the quantity must also be monitored. A low L-Phe diet should be initiated within the first days of life for newborns with elevated blood L-Phe levels above 600 **ε**mol/L and should be continued until teenage age to control blood L-Phe levels between 120 and 300 **ε**mol/L (de Baulny et al., 2007). Thereafter, a progressive and controlled relaxation of the diet is allowed, below 1200 **ε**mol/L in adulthood (Ievers-Landis et al., 2005, de Baulny et al., 2007). It is recommended for PKU women to control their blood L-Phe levels during pregnancy to avoid maternal HPA, which can cause microcephaly, mental retardation, and structural birth defects in the unborn (the so-called maternal PKU syndrome) (Matalon and Michals, 1991). Untreated PKU patients have systemic high level of L-Phe concomitant with lowered levels of the brain monoamine neurotransmitters, leading to mental retardation (Butler et al., 1981, de Baulny et al., 2007, Blau et al., 2011). Later on, it was examined that the long-term treatment with BH_4 (sapropterin dihydrochlorid; trade name: Kuvan), improves L-Phe tolerance mainly in mild HPA patients but also in some cPKU cases (Thöny et al., 2000, Hennermann et al., 2005, Blau, 2008a). Although the mechanism of action underlying this therapeutic effect is not entirely understood, it is thought that BH_4 reduces L-Phe serum levels by improving the folding conformation of certain types of mutant PAH enzyme resulting in increased L-Phe catabolism (Christ et al., 2013).

The most obvious treatment for cPKU would be the substitutions with PAH enzyme, but this treatment approach is challenging because PAH is inherently unstable, making large-scale isolation and purification extremely challenging. In addition its complex activity and cofactor requirement, plus its inherent protease sensitivity and potential immunogenicity in human lacking the functional enzyme further (Sarkissian and Gamez, 2005). To overcome this problems, truncated forms of PAH were generated showing increased stabilization and catalytic activity (Erlandsen et al., 2003, Sarkissian and Gamez, 2005). Furthermore, protection of PAH against immune response has been achieved by pegylation (Gamez et al., 2004, Sarkissian and Gamez, 2005). Nevertheless, the drawbacks of PAH as therapeutic drug are

debatable. An alternative to PAH is the substitution with the phenylalanine ammonia lyase (PAL, EC 4.3.1.5), a bacteria-derived enzyme involved in L-Phe degradation to *trans*-cinnamic acid and ammonia without a cofactor requirement (Sarkissian et al., 1999, Sarkissian and Gamez, 2005, Argyros, 2012). It is predicted that by PAL produced *trans*-cinnamic acid is harmless in humans and that the ammonia formed would be metabolically insignificant (Hoskins et al., 1980, Hoskins et al., 1984, Sarkissian and Gamez, 2005). Various formulations and mechanisms have been tested to avoid immune response and prevent protease inactivation and are currently investigated in clinical trials (PAL-001, NCT00634660) (Bourget and Chang, 1986, Chang and Prakash, 1998, Sarkissian et al., 1999, Argyros, 2012). Nevertheless, L-Phe levels have to be stringently monitored to prevent hypophenylalanemia since there is no regulatory system for PAL in humans in contrast to PAH which is activated by L-Phe and inhibited by tetrahydrobiopterin (BH_4) (Argyros, 2012, Fitzpatrick, 2012). Recently, it was described that aminoglycoside antibiotics induced read-through of nonsense PAH mutations *in vitro* led to partially restoration of enzymatic activity comparable to a missense mutation associated with mild PKU (Ho et al., 2013). Although nonsense read-through drugs are a potential form of treatment for PKU, the high needed dosage of aminoglycosides can not be used for clinical setting because of its toxicity (Ho et al., 2013).

1.3.5 MOUSE MODELS

Mutant cPKU mice exhibiting heritable HPA have been isolated after ENU mutagenesis of the germ line (McDonald et al., 1990, Shedlovsky et al., 1993). The first mouse mutant line, the *Pah*$^{enu1/1}$ mouse model (originally called PAH^{hph-5}) carried the mutation p.Val106Ala in exon 3 and showed a mild HPA phenotype and was BH_4 responsive, but failed to exhibit the biological effects associated with human cPKU. The *Pah*$^{enu2/2}$ mouse model harbouring the null mutation p.Phe263Ser in exon 7 resulted in nonfunctional PAH enzyme, exhibiting symptoms found in human cPKU patients like slow growth, microencephaly, hypopigementation, behaviour disturbances, seizures, epilepsy and maternal PKU (Shedlovsky et al., 1993, Cho and McDonald, 2001, Martynyuk et al., 2007, Argyros, 2012). In addition, the compound heterozygous mouse *Pah*$^{enu1/2}$ was generated bearing a mild and a severe mutation (p.Val106Ala/p.Phe363Ser) to study further the therapeutic efficacy of BH_4,

since the majority of BH_4 responsiveness patients (87%) with PAH deficiency are compound heterozygous carrying two different mutations with about 26% of the alleles being putative null-mutations (Lagler et al., 2010). The *Pah*$^{enu2/2}$ mouse model is the most used mouse model to test gene therapeutic approaches for cPKU (Shedlovsky et al., 1993, Fang et al., 1994, McDonald et al., 2002, Ding et al., 2006, Rebuffat et al., 2010, Thöny, 2010, Yagi et al., 2011).

1.3.6 GENE THERAPEUTIC APPROACHES

1.3.6.1 Viral gene therapies

It was reported that treated cPKU patients have more cognitive deficits, learning difficulties and emotional problems in comparison to the general population. Furthermore, adults with cPKU off the strict diet regime are at risk for new onset of neurological deficits (Waisbren and White, 2010). Also maternal HPA during pregnancy very frequently causes birth defects in the fetus. For this reason, gene therapy is an attractive, experimental and very promising approach to treat cPKU not at least because of the fact that 5-10% of normal enzymatic activity in the mouse liver is sufficient to restore normal serum L-Phe levels (Fang et al., 1994, Eisensmith and Woo, 1996, Templeton, 2005). In 1994, recombinant adenoviral vector containing the human PAH complementary DNA (cDNA) completely normalized the hyperphenylalaninemic phenotype of *Pah*$^{enu2/2}$ mice within 1 week of treatment, although this therapeutic effect did not persist due to neutralizing antibodies against the viral vectors (Fang et al., 1994, Nagasaki et al., 1999).

AAV is one of the most used viral vectors for transgene delivery because it is not pathogenic, induces a minimal immune response, infects dividing and non-dividing cells, and the transgene expression persists for long time in cells (Choi et al., 2014). In 2006, the liver-directed gene therapeutic approach using recombinant AAV2 (rAAV2) pseudotyped with serotype 8 capsid (rAAV2/8) expressing the m*Pah* in *Pah*$^{enu2/2}$ mouse liver stable corrected the serum L-Phe levels (Ding et al., 2006, Harding et al., 2006). Although these treatment therapies are very promising, the high amount of rAAV needed to treat the liver of cPKU patients is still challenging and harbours unknown risks like the development of hepatocellular carcinoma (Donsante et al., 2001, Bell et al., 2006, Donsante et al., 2007). Therefore, there is the need of

alternative treatable tissues, despite the fact that in cPKU there is no liver pathology making it not necessary to target the liver for treatment. In 2008, an alternative gene therapeutic approach for cPKU by targeting the limb muscles of *Pah*$^{enu2/2}$ mice with a rAAV2 pseudotype 1 (rAAV2/1) let to life-long treatment. The multicistronic vector used in this approach not only expressed m*Pah* but also the m*Gch*1 and m*Pts* genes, necessary to synthesis the essential metabolic cofactor BH_4, which is not occurring naturally in muscle tissue (Ding et al., 2008). Overall, the skeletal muscle as target for gene therapy has the advantages that it is easier accessible and it is a not essential, vital organ, which would facilitate the treatment. Furthermore, muscle cells have lower cell turnover time than liver cells, which positively influences the latency of gene therapeutic efficacy (Jang et al., 2011). Therefore, in 2010 the intramuscular injection of rAAV2 with the pseudotype 1, 2 or 8 expressing the m*Pah* gene let to effective clearance of serum L-Phe for up to 1 year in *Pah*$^{enu2/2}$ mice (Rebuffat et al., 2010). The long-term correction of HPA by rAAV-mediated gene transfer led also to recovery of altered behaviour in the PKU mice (Mochizuki et al., 2004).

1.3.6.2 Non-viral gene therapies and minicircle technology

Despite the success with AAV-based gene transfer in small and large animal disease models, AAV can trigger immunogenicity, inflammatory response, severe malignancy and eventually complete shutdown of transgene expression in humans. In this context, non-viral vectors for gene therapy have recently gained considerable momentum, and are becoming very attractive approaches to treat PKU. The first described studies of non-viral gene therapy in 2005/2007, using the phiBT1 bacteriophage integrase system, was retracted in 2010 (Chen and Woo, 2005, 2007, Woo, 2010). Recently in 2014, life-long treatment of PKU using minicircle-based (MC) naked-DNA vectors expressing the m*Pah* cDNA by targeting the liver in *Pah*$^{enu2/2}$ mice was achieved (Viecelli et al., 2014). Minicircles are circular episomal DNA vectors containing the expression cassettes devoid of any bacterial plasmid DNA (Kay et al., 2010). The MC producing parental plasmid (PP) contains the bacterial origin of replication (ORI), the antibiotic resistance gene for kanamycine (KanR), the endonuclease I-*Sce*I restriction site and an expression cassette containing the gene(s) of interest flanked by the recombination bacterial attachment site (*att*B) and the phage attachment site (*att*P). MCs are generated in the *E.coli*

strain ZYCY10P3S2T, which contains the L-arabinose inducible phage øC31 integrase gene and the endonuclease I-*Sce*I restriction gene. The induction of the ZYCY10P3S2T *E.coli* with L-arabinose leads to the production of the øC31 integrase and the I-*Sce*I endonuclease. The øC31-mediated intramolecular recombination between the *att*B and *att*P sites results in the formation of two circular DNA molecules, the MC containing the expression cassette, and one including the plasmid bacterial backbone (BB), which is digested by the I-*Sce*I endonuclease and finally degraded (Fig. 6). MC DNA can be isolated from the bacteria by routine plasmid purification procedures such as one-step affinity column revealing high and over 96% pure titers (Chen et al., 2005, Stenler et al., 2014). It is proposed that the MC technology offers an improved safety profile over viral vectors and has the potential successful gene therapy for heritable liver diseases (Viecelli et al., 2014).

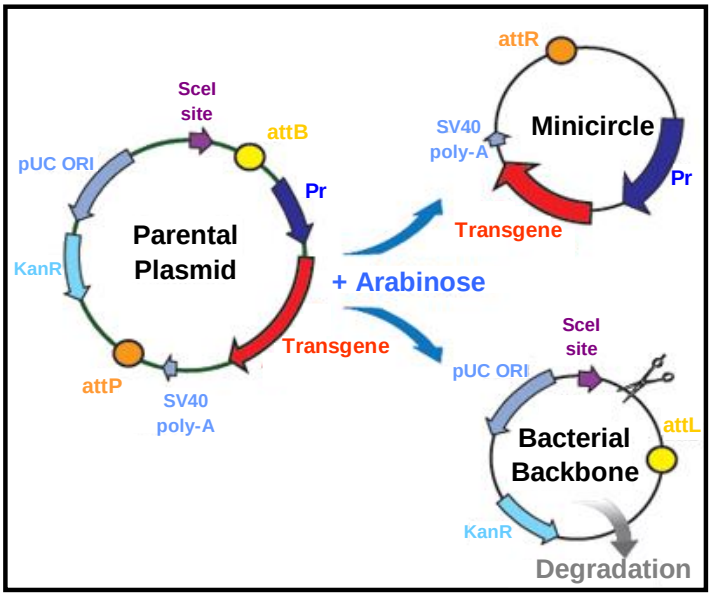

Figure 6: Schematic representation of MC production (Modified from http://www.biocat.com). Pr, promoter; *att*B, bacterial attachment site; *att*P, phage attachment site; *att*L, left attachment site; *att*R, right attachment site; pUC ORI, bacterial origin of replication; KanR, kanamycine resistance gene.

1.4 TOOLS FOR GENE TARGETING AND GENOME ENGENEERING TO GENERATE RECOMBINANT MICE

Transgenesis is applicable to a wide range of mammalian species, including mice, rats, rabbits, sheep, pigs, and cattles, resulting from an inheritable genetic modification induced by the artificial transfer of an exogenous DNA fragment (Hofker and Breuer, 1998, Houdebine, 2002). This chapter summarizes the most widely used strategies for generating transgenic mice.

Recombinant mice are appropriate animal models to investigate the genetic basis of human diseases and for obtaining insight into human physiology (Carlson and Largaespada, 2005). In 1974, Rudolf Jaenisch created the first genetically modified mouse by injecting SV40 DNA into mouse blastocysts, although the introduced DNA was not stably inherited (Jaenisch and Mintz, 1974). There are several different ways to produce transgenic mice. Generation of recombinant mice include chemical and insertional mutagenesis or gene-targeting methods (Cho et al., 2009, Wang et al., 2013). Chemical mutagens such as ENU are potent mutagens of the mouse germ-line producing random, single base-pair changes throughout the genome, and can produce a high frequency of mutant phenotypes (Carlson and Largaespada, 2005). The disadvantage of this method is that the random induced mutations require labor-intensive screening processes. Therefore, gene-targeting methods commonly are used to introduce mutations through homologous recombination in mouse ES cells. Traditionally, there are two main methods used to generate a transgenic mouse: pronuclear microinjection and the ES cell injection (Houdebine, 2002). In the pronuclear microinjection method, the DNA is directly injected into the pronuclei of a fertilized oocyte or zygote, which is then re-implanted into recipient foster mice (Fig. 7 A). It takes approximately a year from making the DNA construct for pronuclear injection to establishing a new transgenic mouse strain with some phenotypic characterization. The drawback of this method is that the DNA inserts at random positions in the host chromosome, which could lead to multiple copies of the transgene in the genome, insertion into in a coding sequence or disruption of regulatory sequences in the genome (Feng et al., 2004, Cho et al., 2009). In the ES injection method, DNA is introduced into ES cells derived from an early mouse embryo. The targeted DNA sequence contains the gene of interest, the neomycin resistant gene that inactivates the antibiotic neomycin to screen for positive cells, and the gene encoding for thymidine kinase (TK), an enzyme that

phosphorylates ganciclovir. The addition of ganciclovir in the growth medium eliminates cells that contain the *TK* gene due to random insertion of the transgene since non-functional phosphorylated ganciclovir inserts into freshly-replicating DNA leading to the cell death. Cells that pass the neomycin and the ganciclovir selection have the DNA integrated into the desired genomic site by homologous recombination (Capecchi, 2005) (Fig. 7 B). The neomycin selection marker (flanked by *FRT* or *LoxP* sites) can be removed from the transgene by using the site-specific recombination Flp/FRT- or Cre/loxP-system (Dymecki, 1996, Metzger and Chambon, 2001). Targeted ES cells are injected into mouse wild-type blastocysts that can contribute to the germline of chimeric animals, generating mice containing the targeted gene modification. Heterozygous mice need to be interbred to produce homozygous experimental animals (Cho et al., 2009) (Fig. 7 A). It is a costly and time consuming method limited to species with established ES cell lines (Wang et al., 2013).

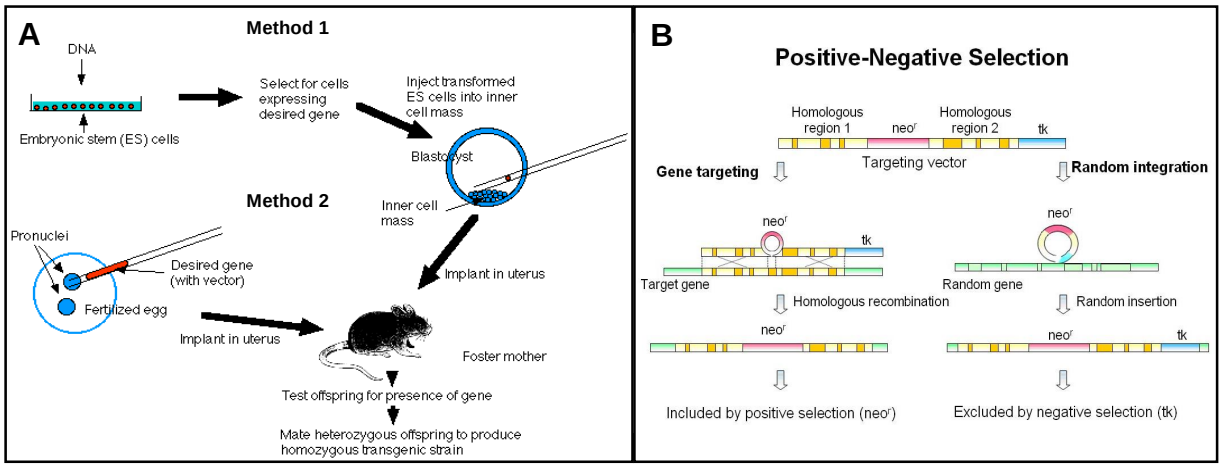

Figure 7: (**A)** Generation of transgenic mice. Method 1: Targeting of ES cells; method 2: Pronuclei injection (modified from http://users.rcn.com); **(B)** Positive-negative selection for targeted ES cells (modified from Tsai et al, 2007)

Alternative methods to generate transgenic mice include intracytoplasmic sperm injection, transfection of spermatozoa with exogenous DNA/DMSO complexes or retroviral-mediated approaches to make transgenesis easier in terms of time, expertise and equipment needed. The intracytoplasmic sperm injection, are used to introduce large genomic transgenes but the efficiency of transgenesis by pronuclear approach is relative low. The retroviral-mediated approaches, as another example, have the drawback to cause multiple chromosomal integration of the transgene (Ittner and Gotz, 2007).

New technology for more efficient and less time-consuming gene targeting in mice include zinc-finger nucleases (ZFNs, Fig. 8 A), transcription activator-like effector nucleases (TALENs, Fig. 8 B) or clustered regularly interspaced short palindromic repeats (CRISPRs, Fig. 8 C).

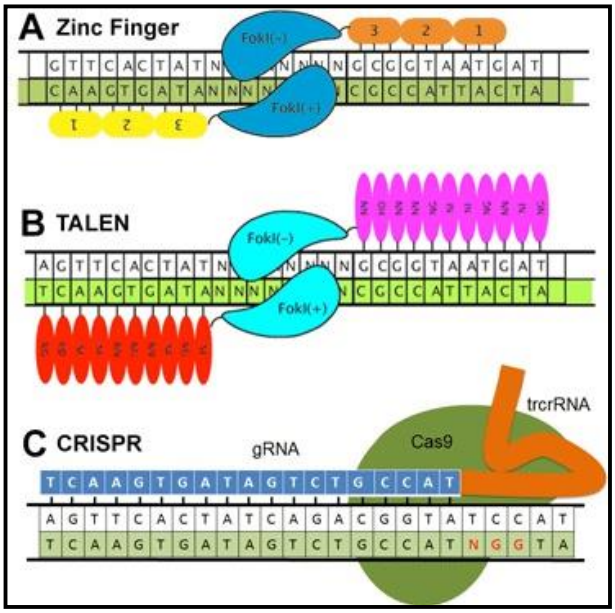

Figure 8: Schematic representation of new technology for gene targeting: **(A)** ZFN, **(B)** TALEN, **(C)** CRISPR (http://www.zhihu.com).

ZFNs are fusions of specific DNA-binding zinc finger proteins engineered to target desired DNA sequences and a nuclease domain, such as the DNA cleavage domain of a type II endonuclease of *Fok*I (Carbery et al., 2010). Donor plasmid DNA and respective ZFN mRNA were co-injected into the pronucleus of one-cell embryos (Cui et al., 2011). A pair of zinc finger proteins target specifically, and their nuclease domains dimerize to cleave the DNA, generating double strand breaks, leading to insertions or deletions via DNA repair by the error-prone non-homologous end joining (NHEJ) pathway or high-fidelity homologous recombination. ZFN technology has the advantages that the targeted gene disruption is highly efficient, faster (couple of months) and can be applied in various genetic backgrounds since it is ES cell independent. In addition, no exogenous sequences need to be introduced because antibiotic selection is not necessary (Carbery et al., 2010). Although the potential of ZFN genome modification is big, the method is technical limited on embryo-injection and culturing of primary cells, the design and assembly is labor-intensive and there is the limitation of available target sites (Carlson et al., 2012). Furthermore, decreased ZFN specificity could lead to cellular toxicity via off-target cleavage (Pinkert, 2014).

TALENs, are artificial sequence-specific endonucleases that contain *Xanthomonas* transcription activator-like effector (TALE) and a nuclease domain of *Fok*I restriction endonuclease. The DNA binding domain of TALE consists of a tandem repeat of 33ï 35 amino acid motifs in which there are two adjacent amino acid pairs called a repeat-variable diresidue that determines the binding specificity for single nucleotide. One repeat-variable diresidue recognizes one nucleotide. Using this code, a TALEN can be constructed with a DNA binding motif recognizing the desired nucleotide sequence. When two TALENs bind to the genome, the nuclease domain of *Fok*I dimerizes and generates a double-strand break. The lesion is frequently repaired via NHEJ resulting in the introduction of small insertion or deletion mutation (Kato et al., 2013). Most importantly, TALENs appear to be superior to ZFNs in terms of simple and straightforward design and assembly strategies, making TALENs manufacturing more effective, significantly cheaper and faster than for ZFNs (Carlson et al., 2012).

Recently, the type II bacterial CRISPR/Cas system has been demonstrated as an efficient gene-targeting technology with the potential for multiplexed genome editing generating transgenic mice in just weeks. Bacteria and archaea have evolved an RNA-based adaptive immune system that uses Cas9 (CRISPR-associated) proteins, CRISPR RNAs (crRNAs), and *trans*-activating crRNA (trcrRNA) to form a ribonucleoprotein complex, which targets and degrades foreign nucleic acids from invading viruses and plasmids. The Cas9 endonuclease from *Streptococcus pyogenes* type II CRISPR/Cas system can be programmed to produce sequence-specific double strand breaks by providing a synthetic ñguide RNAò (gRNA) containing a 20-base match to the genomic target. The CRISPR/Cas system drives both NHEJ-based gene disruption and homology directed repair-based precise gene editing to achieve highly efficient and simultaneous targeting of multiple genes in stem cells and mice which is not possible to achieve with the ZFN or TALEN methods. Furthermore, this new technique does not rely on engineering ES cells, but it introduces the genetic changes directly into the developing mouse embryos. Despite, the CRISPR/Cas system not only makes the production of transgenic mice faster and easier, but it should also theoretically work with other organisms whose ES cells are difficult to engineer and manipulate. The limitations of the CRISPR/Cas technology are limited target spaces for Cas9, the challenge of designing gRNAs, the need for more information about the potential off-target cleavage sites and the risk of unwanted mutation of the second allele through NHEJ (Wang et al., 2013).

1.5 AIM OF STUDY

Animal models for inborn errors of metabolism (IEM) are needed to study and further understand the disease causing pathogenic mechanism (Herschkowitz, 1982). Furthermore, animal models are useful to test new treatment approaches such as gene therapy. The aim of this study was the characterization of new mouse models for IEM and/or appropriate gene therapeutic approaches for three metabolic diseases, namely THD, PTPS deficiency (BH_4 deficiency) and cPKU (chapter 2, 3, and 4, respectively).

Chapter 2: A new knock-in mouse model expressing the recurrent mutation TH-p.Arg203His (equivalent to the hTH-p.Arg202His) to study the severe form of THD was generated. The main aim of this study was to conduct the biochemical and behaviourally characterization of this mouse model. Subsequently, these mice should be used to perform treatments experiments, including the standard application of L-Dopa/carbidopa, the TH cofactor BH_4, and pharmacological chaperons that have previously shown to stabilize wt-TH. Furthermore, a hepatic AAV based gene therapy study expressing the murine *Th*-cDNA should be examined.

Chapter 3: The first aim of this study was to perform the final characterization of the p.Arg15Cys knock-in mouse models with heterozygous *Pts*-ki/wt, homozygous *Pts*-ki/ki and compound heterozygous *Pts*-ki/ko mice, which were described with lowered PTPS activity and abnormal obese phenotype in the dissertation by D. Adamsen (University of Zurich, 2011). Furthermore, it should be investigated what conditions could lead to the appearance of ñaffectedò compound heterozygous *Pts*-ki/ko mice. Especially the two hypotheses by Dea Adamsen that differences in biopterin amounts in mother milk and/or that the ñmother effectò (*Pts*-ki/ki females) in combination with ñallelic effectò (homozygosity) led to these two diverse phenotypes. Therefore, newborn mice from different breeding combination of *Pts*-ki and *Pts*-ko parents and 3-4 days old pups from homozygous *Pts*-ki/ki mothers should be investigated for biochemical and phenotypical differences. With this gain of knowledge, ñaffectedò compound heterozygous *Pts*-ki/ko mice could be specifically bred and used to study hepatic viral and non-viral gene therapy approaches.

Chapter 4: The aim of this study was to achieve a non-viral-vector gene therapy using naked DNA/MC vectors to target skeletal muscle of PKU mice to correct cPKU. The transgenic mouse model (Tg/*Pah*^{enu2}) which expressed m*Pah* and m*Gch*1 in skeletal muscle, was unfortunately not anymore available for the present study (Ding et al., 2008), and the subsequent efforts failed for generating a similar transgenic PKU mouse which expresses m*Gch*1 and m*Pts* for BH_4 production in skeletal muscle. With such mouse models, non-viral muscle gene therapy would have been simplified by using a one-gene vector (expressing *Pah*), instead of a three-gene transfer. Since these mice were not available, non-viral muscle gene therapy should be established in the *Pah*$^{enu2/enu2}$ (ñPKUò) mouse requiring the coordinate expression of the three murine genes *Pah*, *Gch*1 and *Pts*. For naked DNA-vector gene delivery, MC vectors should be delivered by the hydrodynamic limb vein injection technique or by electroporation.

2.

TYROSINE HYDROXYLASE KNOCK-IN (*TH*-KI) MOUSE MODEL WITH CATECHOLAMINE DEPLETION AND IMPAIRED MOTOR CONTROL: CHARACTERISATION AND TREATMENT STUDIES

Chapters:

- 2.1 MANUSCRIPT: PROGRESSIVE CATECHOLAMINE DEPLETION AND SEVERLY IMPAIRED MOTOR CONTROL IN A HYPOMORPHIC TYROSINE HYDROXYLASE KNOCK-IN (*TH*-KI) MOUSE

- 2.2 ORAL TREATMENT STUDY WITH BH_4 AND PHARMACOLOGICAL CHAPERONS IN *TH*-KI/KI MICE TO STABILZE THE MUTANT TH ENZYME AND INCREASE BRAIN CATECHOLAMINE LEVELS

- 2.3 INVESTIGATION OF A GENE THERAPEUTIC APPROACH TARGETING THE LIVER USING AAV TO RESTORE THE BRAIN CATECHOLAMINE IN *TH*-KI/KI MICE

2.1 MANUSCRIPT: PROGRESSIVE CATECHOLAMINE DEPLETION AND SEVERLY IMPAIRED MOTOR CONTROL IN A HYPOMORPHIC TYROSINE HYDROXYLASE KNOCK-IN (*TH*-KI) MOUSE

Germaine Korner[1,2], Daniela Noain[3], Ming Ying[4], Magnus Hole[4], Marte I. Flydal[4], Tanja Scherer[1], Gabriella Allegri[1], Anahita Rassi[5], Ralph Fingerhut[1], Damasia Becu-Villalobos[6], Samyuktha Pillai[7], Stephan Wüest[8], Daniel Konrad[8], Anna Lauber[9], Christian Baumann[3], Laurence A. Bindoff[10,11], Aurora Martinez[4,*] and Beat Thöny[1,2,*]

[1] Division of Metabolism, Department of Pediatrics, University of Zürich, Zürich, Switzerland

[2] Affiliated with the Neuroscience Center Zurich (ZNZ) and Children's Research Centre (CRC), Zürich, Switzerland

[3] Department of Neurology, University Hospital of Zurich, Zürich, Switzerland

[4] Department of Biomedicine, University of Bergen, Bergen, Norway

[5] Division of Clinical Chemistry and Biochemistry, Department of Pediatrics, University of Zürich, Zürich, Switzerland

[6] Institute of Biology and Experimental Medicine, Buenos Aires, Argentina

[7] Institute of Physiology, University of Zurich, Zürich, Switzerland

[8] Division of Endocrinology, Department of Pediatrics, University of Zurich, Switzerland

[9] Department of Medicine, University of Fribourg, Fribourg, Switzerland

[10] Department of Clinical Medicine (K1), University of Bergen, Norway

[11] Department of Neurology, Haukeland University Hospital, Bergen, Norway

*Shared correspondence:

Dr. Aurora Martinez, Department of Biomedicine, University of Bergen, Jonas Lies vei 91, 5009 Bergen, Norway, Tel: +47 55586427, aurora.martinez@biomed.uib.no

Dr. Beat Thöny, Division of Metabolism, Department of Pediatrics, University of Zurich, Steinwiesstrasse 75, CH-8032 Zürich, Switzerland, Tel +41 44 2667622; beat.thony@kispi.uzh.ch

ABSTRACT

Tyrosine hydroxylase (TH) is the rate-limiting enzyme in the synthesis of catecholamine neurotransmitters and hormones and a marker for dopaminergic neurons. Mutations in the *TH* gene are associated with the autosomal recessive neurometabolic disorder TH deficiency (THD), which manifests with phenotypes varying from infantile parkinsonism and L-Dopa-responsive dystonia to complex encephalopathy of perinatal onset. The most recurrent mutation in THD patients is *TH*-p.R233H (h*TH*1-p.R202H, isoform 1), which is mostly associated to a severe THD phenotype, often concomitant with non-responsiveness to L-Dopa treatment. While *Th* knock-out mice are not viable, homozygous *Th*-knock-in mice expressing the *Th*-p.R203H mutation (equivalent to h*TH*1-p.R202H) showed normal survival and food intake but hypotension and moderate growth retardation. The mutant enzyme exhibited impaired inhibitory feedback and stabilizing dopamine binding, which lead to progressive disappearance of TH associated to gradual loss of central catecholamines. Notably, unstable mutant TH was absent in striatum. Accordingly, mutant mice showed reduced motor coordination, ataxia and catalepsy with diurnal fluctuation, and non-responsiveness to L-Dopa treatment. This hypomorphic *Th*-ki mouse model with encephalopathy and impaired motor control thus provides understanding on molecular pathogenic mechanisms for THD, replicates the most severe form of the disease, and provides a platform for the evaluation of novel therapeutics.

Key words: TH deficiency, infantile parkinsonism, *Th* knock-in mice, dopamine deficiency, catecholamine deficiency, L-Dopa treatment

INTRODUCTION

Tyrosine hydroxylase (TH; EC 1.14.16.2) is a homo-tetrameric enzyme that catalyzes the conversion of L-tyrosine (L-Tyr) to dihydroxyphenylalanine (L-Dopa) by using molecular oxygen as additional substrate and the cofactor (6*R*)-L-erythro-5,6,7,8-tetrahydrobiopterin (BH_4)[1,2]. This hydroxylation is the rate limiting step in the synthesis of the catecholamine neurotransmitters dopamine (DA), norepinephrine and epinephrine[2]. In the central nervous system (CNS), TH is expressed in dopaminergic neurons of the *substantia nigra*, ventral tegmental area, hypothalamus, and olfactory bulb, in noradrenergic neurons of the *locus coeruleus* and lateral tegmental system, and in the adrenergic neurons of the brain stem[3,4]. Outside the CNS, TH expression is also found in the adrenal medulla and in non-neuronal (renal, intestine, pancreatic and lymphoid) tissues. DA is distinctively involved in motor control, but also in cognition, memory and reward, and, as a precursor of norepinephrine and epinephrine, indirectly regulates attention and helps to maintain normal blood pressure, body temperature and blood sugar[5]. The single human *TH* gene undergoes alternative mRNA splicing generating four main isoforms (hTH1-hTH4), with variations in the length of the N-terminal, where hTH4 corresponds to the longest, full-length isoform (where notation of mutations in the gene are provided), and hTH1 to the shortest and most abundant one[6]. TH activity is tightly controlled by regulatory mechanisms at the transcriptional, translational and posttranslational levels[7]. The latter includes phosphorylation at several Ser/Thr residues at the N-terminal tail[8]. Notably, phosphorylation at Ser40 by cAMP dependent protein kinase A (PKA) activates TH by releasing the feed-back inhibition of catecholamines and decreasing the K_m for the cofactor BH_4[2]. Binding of the catecholamine end-products inactivates and stabilizes TH both *in vitro*[9,10] and *in vivo*[11]. Another short-term regulatory mechanism of TH of important biological significance is substrate inhibition, that allows steady synthesis of DA despite fluctuations in blood L-tyrosine[12].

TH deficiency (THD; OMIM *191290), also known as autosomal recessive Segawa syndrome, infantile parkinsonism, or L-Dopa-responsive dystonia (DRD; OMIM 605407), is a rare neurometabolic disorder associated with a phenotypic spectrum raging from a mild progressive limb dystonia, postural tremor or hypokinetic rigid syndrome that is responsive to L-Dopa (termed type A) to progressive and complex

neonatal or early-infancy onset encephalopathy with L-Dopa-unresponsive parkinsonism (termed type B)[13]. An accurate clinical diagnosis of THD must be based on central catecholamine deficiency reflected by low homovanillic acid (HVA) and 3-methoxy-4-hydroxyphenylethylene glycol (MHPG) in cerebrospinal fluid (CSF) from lumbar puncture, and by mutation analysis of the *TH* gene[14,15]. Peripheral (urinary) concentration of catecholamines, HVA and MHPG are non-informative most probably due to DA production by residual TH and tyrosinase activity in non-neuronal tissues (for a discussion see[13]). On the other hand, elevated serum prolactin may be used as a peripheral biomarker reflecting central neurotransmitter status[16], as the release of this hormone into the serum from the pituitary gland is under control of hypothalamic DA, which is the primary physiological inhibitor of prolactin secretion[17]. To date, approximately 70 patients have been reported with THD (www.biopku.org/pnddb)[13,18]: the most recurrent *TH* mutation accounting for ~30% of all mutant alleles, is c.698G>A/p.Arg233His in exon 6; NM_1999292.2 (corresponding to c.605G>A/p.Arg202His in hTH1). While this mutation can be associated with THD subtypes A or B[13,15] as a homozygous or compound heterozygous allele, about half of the patients with THD type B are homozygous for change p.R233H[13].

Parkinsonian syndromes or dystonias and related catecholamine deficiencies are closely associated with changes in the levels of TH activity and DA levels[14,19], and the motor features of Parkinsonôs disease reflect to the loss of striatal DA due to degeneration of dopaminergic neurons[20]. Various transgenic animal models aiming to mimic TH deficiency by inactivating the *Th* gene have been generated in the past[21-23], yet neither the complete *Th*-knock-out which was not viable, nor rescue mutants fully reproduced the clinical and pathological feature of THD, although did provide valuable insights into the importance of DA and the other catecholamines for mouse fetal development[21,22] and the functional interdependence of the adrenomedullary and adrenocortical systems[24].

In order to provide novel insights into catecholamine function and study the pathophysiological mechanisms responsible for the severe (type B) THD phenotype, we generated a constitutive mouse *Th*-knock-in mouse with p.Arg203His, equivalent to the human *TH*-p.R233H (h*TH*1-p.R202H). This mouse, here termed *Th*-ki mouse, was viable and presented with motor dysfunction due to a progressively reduced TH activity and gradual loss of catecholamine metabolites, including DA. The severe

phenotype was also characterized by non-responsiveness to L-Dopa treatment, as in most patients homozygous for the *TH*-p.R233H mutation. This novel hypomorphic mouse replicates the salient clinical features of human THD type B including motor and non-motor functions and diurnal fluctuation of symptoms, and represents therefore an ideal model for pathomechanistic studies. Immunohistochemistry, measurements in brain extracts and analysis with recombinant enzymes showed the direct loss of TH activity due to instability of the mutant TH which could not be stabilized by DA, highlighting the importance of feedback stabilizing inhibition by catecholamines to maintain TH levels.

MATERIALS, METHODS AND MOUSE HUSBANDRY

Generation of the *Th*-ki mouse allele

A C57Bl/6 mouse carrying a constitutive knock-in of the point mutation p.Arg203His in the *Th* gene was custom generated by TaconicArtemis (Cologne, Germany; NCBI gene ID 21823, transcript variant *Th*-1 NM_0093771.1; Ensembl gene ID ENSMUSG00000000214). Details on the targeting vector for electroporation, homologous recombination and selection in mouse embryonic stem cells (Art B6/3.6 background C57Bl/6 NTac) are given in Supplementary Figures 1A-C. Validation of correct and single targeting was done by Southern blot and PCR analyses (details can be supplied upon request). For elimination of the *NeoR* cassette, mice were crossed with a Flp-deleter strain (C57Bl/6-*Tg*(CAG-*Flpe*)1 Arte) for random integration of the CAGGS-Flpe transgene, and subsequently mice were crossed to homozygosity.

Genotyping of *Th*-ki mice

One primer set was used for testing for the presence of an additional 85 bp FRT sequence by fragment size analysis (primers ñForò4601_33: 5ôGAGCTCCCAGAATT GACAGC-3ô, ñRevò 4601_34: 5ôGATCACACTCCACCATATCAAGG-3ô) and one set for the presence of the R203H mutation via Sanger sequencing (primers 4602_35: 5ô TGTCAGAGTTGGATAAGTGTCACC-3ô and 4602_36: 5ôTGACAGCTAACCAGTCA CCTCC-3ô, see also Supplementary Figures 1B,C). Standard PCR conditions were used for DNA amplification.

Mouse husbandry and treatment studies

Animal experiments were performed in accordance with the guidelines and policies of the State Veterinary Office of Zurich and Swiss law on animal protection, the Swiss Federal Act on Animal Protection (1978), and the Swiss Animal Protection Ordinance (1981). Animal studies received approval from by the Cantonal Veterinary Office, Zurich, and the Cantonal Committee for Animal Experiments, Zurich, Switzerland. All mice are based on C57Bl/6-background. For treatment studies, 6 tablets containing L-Dopa (levodopa 100 mg) and the decarboxylase inhibitor carbidopa (25 mg) were purchased from Sinemet, diluted in 20 ml of ddH_20. For validation, the final concentration of L-Dopa was determined by HPLC[43]. Newborn *Th*-ki and wt control mice were fed daily *per os* with a solution containing 10 mg levodopa plus 2.5 mg

carbidopa per kg of body weight and per day for a time period of up to 3 weeks of age. Before termination, treated mice were tested for motor behaviour, and upon sacrifice biochemical analyses were performed. For mock control, *Th*-ki and wild-type mice were given ddH_2O in parallel.

Metabolic cage analysis

Locomotion, food and water intake, O_2 consumption and CO_2 production were determined for single housed mice (females at the age of 9 months) during a 24-h period in metabolic cages in an open-circuit indirect calorimetry system as previously described[44] (PhenoMaster, TSE Systems, Bad Homburg, Germany). After being adapted to single caging, mice were placed in cages closed with air-tight lids. Water bottles and food cups were placed on scales to measure water and food intake continuously. The measurements were saved on a computer in 20 min intervals and were used to calculate cumulative food and water intake. Activity data were measured using an infrared light-beam. To measure energy expenditure (EE) and respiratory exchange ratio (RER), ambient air was pumped through the cage via a flow controller. Air entering and leaving each cage was monitored for its O_2 and CO_2 concentration. The cages were connected to two analyzers measuring O_2/CO_2 concentration of each cage for a period of 2 min in 20 min intervals. EE and RER were calculated using the manufacturer's software based on the following equation: EE (kcal/h) = $(3.941\times VO_2+1.106\times VCO_2)/1000$; RER=$VCO_2/VO_2$.

Behavioural mouse testing

All experiments were carried out during the light-phase, between 10 am and 5 pm. Experiments were carried always at the same time of the day within the same group of animals, and all experimental batches were acclimated to the test room for at least 1-2 days before experiments.

Open field test[45]: Plexiglas activity boxes monitored by a video tracking system (Ethovision, Noldus) were used to assess total horizontal activity and mean velocity of locomotion. Animals were placed in a neutral position of the acrylic boxes (40 x 40 x 40 cm) and let to explore freely and undisturbed for 30 min. Boxes were carefully cleaned between tests to minimize odour cues in the arena.

Bar test[41]: Spontaneous catalepsy was determined in wt and *Th*-ki mice using the horizontal bar test in which the time of immobility was assessed. Five trials were

performed for each animal with a 180 sec cut-off each. For the analysis, the maximum time of immobility for each mouse over the five trials was considered.

Rotarod test[46]: Wt and *Th*-ki mice were individually placed in a neutral position on the immobile rotarod treadmill (UgoBasile, Milan, IT, USA). Immediately, the speed was increased to 16 revolutions per min (rpm) and each mouse was given a 10 min training session. During the training session mice were repositioned on the rod after each fall. Mice were tested 3 h later for 3 min at a fixed velocity of 16 rpm, and the latency to the first fall was recorded for each subject.

Gait analysis[47-49]: Both hind and fore paws of mice were inked with non-toxic blue and red ink, respectively. Animals were immediately placed at one end of a 30 cm acrylic alley, which floor was covered in white absorbent paper, and encouraged to walk to the opposite end. The paper was then removed and labelled with the animal ID number for further analysis. The stride length and width were manually measured and normalized to body weight (ñsizeò) of each mouse to obtain short-step and ataxia indexes, respectively.

Preparation of whole brain lysates from mice

Immediately after sacrifice, whole brains were resected and shock frozen in liquid nitrogen. Frozen brains were grinded to powder under liquid nitrogen; thereafter, all procedures were carried out at 4°C. Powdered brains were ñdissolvedò in 1 ml of homogenization buffer containing 50 mM Tris-HCl, pH 7.5, 100 mM KCl, 1 mM DTT, 0.2 mM PMSF (stock 10 mg/ml in isopropanol), 1 εM leupeptin (stock 5 mg/ml in H_2O) and 1 εM pepstatin (stock 1 mg/ml in methanol). A TissueLyser II (Qiagen; cat. no. 85300) was used for preparation of lysate following the manufacturer protocol.

Gene (mRNA) expression studies

Total RNA was extracted from powdered mouse brains by the QIAmp RNA Blood Mini Kit (Ref. 52304; Hombrechtikon, Switzerland) and cDNA was produced by the Promega reverse transcription system (Ref. nr. A3500; Dübendorf, Switzerland). Mouse *Th*, *Tph*1/2 and *Igf*-1-mRNA expression levels were performed using the commercially available ABI assays (Mm.00447546 for *Th* -mRNA; NCBI RefSeq NM_009377.1; Mm00493798_m1 for *Tph*1-mRNA, NCBI RefSeq NM_001136084.1; NM 009414.2; Mm00557717_m1 for *Tph*2-mRNA, NCBI RefSeq NM_173391.2; Mm00439560_m1 for *Igf*-1-mRNA, NCBI RefSeq NM_001111274.1). The murine glyceraldehyde-3-phosphate dehydrogenase (*Gapdh*) mRNA (ABI assay ID:

Mm99999915_g1; NCBI RefSeq NM_008084.2) was used to normalize the relative *Th* and *Tph*1/2 mRNA levels. Values were calculated as described in a published method[50].

Determination of protein, neopterin, biopterin and monoamine neurotransmitter metabolites

Protein concentration (in g/L) was determined by using the M-TP Mikroprotein kit from Beckman Coulter Synchron LX-System (Beckman Coulter Inc, Brea, CA; kit-no. 445860). Biopterin, neopterin and monoamine neurotransmitter metabolites were determined in brain tissue following published protocols[43,51].

Serum IGF-1, total thyroxine (tT4), thyroxine stimulating hormone (TSH) and prolactin

Serum IGF-1 was determined by radioimmunoassay (RIA) using a rat IGF-1 RIA kit (DSL-2900, Bühlmann Laboratories AG, Switzerland)[51], total thyroxine (tT4) from whole blood dried on filter paper was measured with the ñGSPTM Neonatal Thyroxine kitò from PerkinElmer (Life and Analytical Sciences, Turku, Finland), and prolactin were quantified using an ELISA kit for mouse and rat (GenWay Biotech, Inc., San Diego, CA) following to manufacturerôs instructions.

Measuring blood pressure in mice

A non-invasive computerized tail-cuff system for measuring systolic blood pressure in mice was applied as described[52].

Analytical methods for *in vitro* and *in vivo* characterization of (human) hTH1 and (mouse) mTH wt and mutant enzyme

Cloning of mouse mTh into pET-MBP-1a The pSL1180 vector containing mouse *Th* (*mTh*) cDNA was a generous gift from Prof. Hiro Ichinose (Tokyo Institute of Technology, Japan) and used as template DNA in a PCR with the following primers: 5ôGCTTCCATGgaCCCACCCCCAG-3ôand 5ôGCTTGGTACCTTAGCTAATGGCA-3ô This amplifies the *Th* gene with an *Nde*I site in the 5ôend and an *Acc*65I site after the stop codon. Restriction sites in the primers are underlined and lowercase letters indicate bases inserted to facilitate restriction (translates into an extra glycine in position 2). Cloning of human *TH*1 (*hTH*1) into pET-MBP-1a has been described previously. The *mTH* PCR-products and pET-MBP-1a/h*TH*1 were cut with *Nco*I and

*Acc*65I and purified before mixed in a ligation reaction to produce pET-MBP-1a/mTH. The correct pDNA was detected by colony PCR and verified by sequencing.

Mutagenesis of human and mouse TH, and expression and purification of the recombinant human and mouse TH-proteins The mutagenic primers 5ô CAGGTGTACCGCCAGCACAGG AAGCTGATTGCTGAG-3ô and 5ô GCGTATCGCCAGCATCGGAAGCTGATTGC-3ô(and their complements) were used to generate the pET-MBP-1a/hTH1-R202H and pET-MBP-1a/mTH-R203H mutants, respectively, using QuikChange mutagenesis (Stratagene). The mutated bases are underlined. Correct mutations were verified by sequencing. hTH1-wt, mTH-wt, hTH1-R202H and mTH-R203H were expressed as His-MBP-TH fusion proteins in *E. coli* strain BL21 using LB medium with induction by 1 mM IPTG, isolated on amylose resin and eluted with 10 mM maltose. Fusion proteins were cut for 1 hour at 4°C using TEV-protease at a TH:TEV ratio of 10:1. Tetrameric TH-proteins were isolated using size-exclusion chromatography on a HiLoad Superdex200 column (GE Healthcare), leaving the protein in 20 mM NaHepes pH 7, 200 mM NaCl. The proteins were homogeneous and contained correct N-terminal sequence (as seen by MS-spectroscopy; not shown).

Immunodetection Brain extracts were prepared by homogenization in 4 volumes of 50 mM Tris-HCl, pH 7.5, 100 mM KCl, 1 mM EDTA, 1 mM DTT, 200 μM PMSF and protease inhibitor cocktail (Roche). Extracts were clarified by centrifugation at 20,000g for 15 min at 4°C. Free amino acids and contaminants of low molecular weight were removed from the supernatants using Zeba desalting spin columns (Thermo Scientific), and then the supernatants were stored in liquid nitrogen prior to use. Protein concentration was measured with Direct Detect (Merck Millipore). Quantification of TH protein was performed by western blot analyses after SDS-PAGE (10% acrylamide) with 20 μg total protein in each lane, and transfer to nitrocellulose membrane and immunostaining using affinity-purified polyclonal rabbit anti-rat TH (Thermo Scientific) in a 1:1,000 dilution was used as the primary antibody. Secondary antibody was goat anti-rabbit IgG horseradish peroxidise conjugate (Bio-Rad) in a 1:2,000 dilution. The membrane was also immunostained with a polyclonal antibody against glycerolaldehyde 3-phosphate dehydrogenase (GAPDH; Abcam) as a loading control. Purified recombinant hTH1 (10 ng/lane) was used as standard for immunoquantification. Detection was performed by enhanced chemiluminescence

(ECL; Amersham), and immunoquantification in a Molecular Image using Image Lab 3.0.1 software (Bio-Rad).

Tyrosine hydroxylase activity assay TH activity in brain extracts was assayed at 30°C immediately following the preparation of the extracts (see above) as described[29], with the modifications reported[53] in using an incubation mixture containing 100 mM Hepes, pH 7.0, 50 μM L-[3,5-^{3}H]-tyrosine, 0.05 mg/ml catalyse, 20 μM ammonium iron (II) sulphate hexahydrate, and 100 μM 3-hydroxybenzyl hydrazine (NSD-1015, an inhibitor of L-aromatic amino acid decarboxylase). The enzyme was pre-incubated for 1 min in this mixture, and reaction started by addition of 500 μM BH4 and 5 mM DTT. The reaction was stopped after 30 min by addition of 1 ml of 7.5% activated charcoal suspension in 1 M HCl. After centrifugation at 10,000 g, the supernatant was counted in a scintillation counter. TH activity of the TH enzymes was assayed at 25°C, essentially as described[30], with certain modifications. The incubation mixture contained 40 mM NaHepes, pH 7.0, 0.1 mg/ml catalase, 10 μM ferrous ammonium sulphate and 50 μM L-Tyr. To this mixture the enzyme was added to a final concentration in the assay of 0.01 mg/mL (0.16 μM subunit, diluted in 0.1 mg/ml bovine serum albumin and 2 μM ferrous ammonium sulphate, in 20 mM NaHepes, pH 7.0, 200 mM NaCl). The reaction was started by adding 200 μM BH_4 (Schircks Laboratories) in 2 mM dithiothreitol (DTT), and stopped after 5 min, by adding an equal volume of 2% (v/v) acetic acid in ethanol. The enzyme was precipitated at -20°C for at least 30 min and the samples were centrifuged at 20,000 g for 14 min. L-Dopa was separated and measured by HPLC with fluorimetric detection (excitation at 274 nm and emission at 314 nm). The L-Tyr-concentration dependence was analyzed in the range 6.25 to 100 μM at a fixed concentration of BH_4 of 200 μM and 2 mM DTT. The BH_4-concentration dependence was analyzed in the range 16 to 1000 μM (and fixed DTT and L-Tyr concentrations of 2 mM and 25 μM, respectively). The results were analyzed using the enzyme kinetics function in SigmaPlot, where the K_m and V_{max} values, in the case of BH_4-dependency and the K_m and K_{si} for the substrate inhibition by L-Tyr were obtained using Michaelis-Menten and substrate-inhibition equations, respectively.

Differential scanning fluorimetry (DSF) DSF was used to measure the thermal stability of hTH1, mTH, hTH1-R202H and mTH-R203H, with and without DA. 0.9 μM hTH1 (subunit concentration) was incubated with 3X ferrous ammonium sulphate

(FAS) and 5X Sypro Orange before added to DA-containing wells of a 96 well-plate (Roche Applied Science). DA-concentrations used were 0.45 µM (0.5X), 0.9 µM (1X) and 1.8 µM (2X). A LightCycler 480 Real-Time PCR System (Roche Applied Science) was used to heat the plate from 25°C to 90°C at a heating rate of 2°C per minute. Thermal denaturation of TH was monitored by detecting the increase in Sypro Orange fluoresence (λ_{ex} = 465 nm, λ_{em} = 610 nm) upon its binding to exposed hydrophobic patches. The data was scaled to reflect fraction unfolded and midpoint denaturation (T_m). T_m-values were determined as maximal temperature in a first-derivative plot.

Limited proteolysis by trypsin The susceptibility of TH to limited proteolysis by trypsin was performed at 25°C, as described[54], with some modifications. hTH1 or hTH1-R202H (0.14 mg/ml) was incubated with TPCK-treated trypsin (Sigma) at a TH:trypsin ratio of 200:1 in 20 mM NaHepes, pH 7.4, 200 mM NaCl, in presence or absence of 50 µM DA. 1.5 µg/ml trypsin soybean inhibitor (Sigma) and SDS-buffer were added to stop the reaction and perform SDS-PAGE (10 %) at 180 V. The gels were stained with Coomassie Brilliant Blue and scanned using ChemiDoc XRS+ from BioRad. The raw volume of the bands was measured using the Image Lab 3.0.1 software.

The amino acid sequence of the bands obtained by limited proteolysis was analyzed by MS. Proteins in the excised bands were reduced, alkylated and in-gel trypsinized following standard procedure[55]. The proteolytic reaction was stopped by acidification with trifluoroacetic (TFA) acid. Peptides from in-gel digestions were extracted and prepared for LC (liquid chromatography)ï MS/MS (tandem MS) analysis. Samples were applied to micro-columns pre-equilibrated in 60% acetonitrile and 0.1% TFA, filtered and collected. After removal of acetonitrile by speed vacuum, the samples were injected into a nanoflow HPLC system online with positive electrospray ionization on Thermo Scientific Orbitrap Velos Pro hybrid ion trap-Orbitrap mass spectrometer. Collision-induced dissociation was the mode used for fragmentation. MS analysis was performed essentially as described by Berle et al. [56] with minor modifications. The MS and MS/MS raw data files were processed using Proteome Discoverer 1.4 software. The generic files were further processed using an in-house Mascot server (version 1.4.0.288) (Matrix Sciences) and searched against the Swissprot_HomoSapiens database, selecting for trypsination and allowing for 2

missed cleavages. Mascot was searched with a fragment mass tolerance of 0.6 Da and a parent ion tolerance of 10 ppm. Scaffold_4.0.5 (Proteome Software) was used with additional Search engine X! Tandem (version CYCLONE 2010.12.01.1) to validate MS/MS-based peptide and protein identifications.

Tissue Preparation and immunohistochemistry

Adult mice at the age of 6-7 months were anesthetized with sodium pentobarbital and perfused through the left cardiac ventricle with 10 ml of ice-cold 0.9% NaCl followed by 30 ml of ice-cold 4% paraformaldehyde in phosphate buffered saline (PBS, pH 7.4). Brains were immediately removed and post fixed in the same 4% formaldehyde solution overnight at 4°C and then cryoprotected in subsequent 10% and 30% sucrose in PBS solutions. Brains were stored at -80ºC until further use and eventually sectioned in 40 µm slices with a cryostat (Leica, CM3050 S). Cryosections were collected in cold potassium phosphate buffer (KPBS; 140 mM NaCl, 20 mM K_2HPO_4, pH 7.4), and used for free-floating immunohistochemistry. Sections were incubated for 1 h in 1% H_2O_2 in KPBS to inactivate endogenous peroxidases and then washed twice for 20 min with KPBS. A rabbit polyclonal anti-TH antiserum was used at a 1:1,000 dilution (Millipore, AB152). Sections were incubated with primary antibody over night at 4°C in a solution containing KPBS, 0.3% Triton X-100, and 2% normal goat serum. After washing twice for 20 min with KPBS, sections were incubated with a solution containing biotinylated goat anti rabbit IgG (1:400, VectorLaboratories, Burlingame, CA) diluted in KPBS/0.3% Triton X-100 for 2 h at room temperature followed by washing twice with KPBS for 20 min. Sections were then incubated with avidin/biotin complex (1:200, ABC Vectastain Elite Kit, Vector) for 1 h at room temperature. After washing for 20 min in KPBS, sections were equilibrated for 20 min in TBS buffer (150 mM NaCl, 50 mM Tris-HCl, pH 7.2ï 7.6). Finally, sections were exposed to a solution of 0.025% diaminobenzidine, 0.05% H_2O_2 in TBS buffer and monitored for colour development before stopping the reaction by rinsing in TBS buffer (for a reference see also[57]).

RESULTS

Th-ki/ki mice display moderate growth retardation and hypotension

A constitutive knock-in containing the *Th*-p.Arg203His was generated by homologous recombination in the C57BL/6 background and bred to homozygosity (see Supplementary Figure S1 and Table S1, and Methods for details). The *Th*-ki litter size was normal with an expected Mendelian ratio and an apparently normal phenotype initially. After weaning, however, *Th*-ki mice were found to exhibit a moderate and continuous growth retardation with 25-34% less body weight compared to their wild-type (wt) or heterozygous littermates (Figure 1A and B). That this was not due to feeding abnormalities was confirmed quantitatively by metabolic cage analyses showing normal food intake and respiratory quotient. Locomotor activity and energy expenditure were, however, slightly reduced (see Supplementary Figure S2). Follow up examinations of mutant mice revealed no constipation, and a quantitative analysis of the fat and total energy contents in feces also revealed no differences between wt and *Th*-ki, indicating that mutant mice had normal absorption and digestion (data not shown). IGF-1 gene expression was normal (in liver and brain tissues; not shown) as were IGF-1 serum levels in adult mice at the age of 12 weeks (Supplementary Figure S3C). In contrast, *Igf-1*-mRNA expression from whole brain extracts was significantly elevated at the age of 3 weeks (not shown), suggesting that the IGF system might be involved in growth as it has been suggested by others (see for instance[25]). We further detected elevation of the total thyroid hormone thyroxine (tT4) (Supplementary Figure S3A-B). *Th*-ki mice also manifested hypotension similar to patients with type B THD[26] and mice with norepinephrine and epinephrine deficiency[27], while we found normal levels of catecholamines in adrenals and heart of adult *Th*-ki mice (data not shown) which indicated central regulation for growth and hypotension. Normal catecholamine contents in peripheral tissues was also reported for heterozygous *Th*-knock-out mice with significant reduction of TH activity[22], similarly as we observed for the mutant TH-R203H (~50% of wt; see below).

Progressive loss of brain catecholamines in *Th*-ki mice

Prolactin release, which is under control of DA, is a peripheral biomarker for central DA deficiency[16,17], and we consistently observed elevated serum prolactin levels in mutant mice (Supplementary Figure S3D). Brain catecholamine and serotonin metabolites were measured in newborn (day 1), juvenile (3 weeks) and adult mice

(12 weeks and one year). HVA, the major biomarker in CSF for TH deficiency in patients, was low in *Th*-ki mice at all ages, whereas L-Dopa, DA, norepinephrine and MHPG were initially normal but fell continuously thereafter in mutant mice (Figure 2A-D). The serotonin pathway, which is typically not compromised in THD, remained unchanged and only at an advanced age, when mutant mice exhibited a striking loss of catecholamines, a reduction of the serotonin precursor 5-hydroxytryptophan (5-HTP) was observed. Other relevant brain parameters, such as serotonin, 5-hydroxyindoleacetic acid (5-HIAA) and biopterin (and neopterin) content remained unchanged at all ages (Figure 2 and Supplementary Figure S4).

Early motor dysfunction in THD mutant mice

A moderate reduction of motor activity was observed in mutant mice during metabolic cage analyses (see above). In order to explore the nature of this motor dysfunction, we performed a series of behavioral tests assessing catalepsy, motor coordination, amount and velocity of spontaneous locomotion, and gait characteristics at different ages. Motor defects were tested in juvenile (3 weeks old), young adult (11 weeks old) and one year old mutant male mice plus sex and age-matched wt controls (Figures 3A to F). In the bar test, *Th*-ki mice showed increased time of immobility compared to their controls, indicating catalepsy, a sign of rigidity and inability to initiate movements. In addition, when placed at the bar, *Th*-ki mice of all ages but particularly older adults presented an abnormal body posture and muscle twitching, suggesting the presence of a dystonic component. When the same *Th*-ki male mice were challenged with the rotarod, a significantly reduced latency to fall was observed, indicating impaired motor coordination. In the open field test, *Th*-ki mice showed significantly reduced levels of horizontal activity (amount and velocity of spontaneous locomotion), indicating a hypokinetic and bradykinetic phenotype. Next, we analyzed the characteristics of gait (normalized to body weight in order to compensate for the size difference between genotypes). Mutant mice had an increased stride width per body weight index compared to normal controls, suggestive of a significant ataxia in these animals. This was confirmed by a generalized disorganization of the gait, including dragging marks, changes in direction and freezing (data not shown). In contrast, *Th*-ki mice did not show abnormal step length, as can be observed by an unchanged stride length per body weight index compared to controls. In summary, while catecholamine deficiency was progressive, the severe motor dysfunction was

present from the first measurements at 3 weeks onwards, and its severity appeared independent of age.

Th-ki mutant mice exhibit diurnal fluctuation of motor deficits, a hallmark in patients with THD

THD in humans exhibits marked diurnal fluctuations of motor behaviour[13,28]. To determine whether the motor performance in mutant mice varied with time of the day, we performed the bar test at 8 a.m. and 8 p.m. and found that *Th*-ki mice performed significantly better after the rest period (at 8 p.m., note the inverted circadian rhythms of mice compared to humans) than after the activity period (at 8 a.m.); wt controls presented a stable performance at both times[13,28] (see Figure 4).

Gradual reduction of TH protein and activity in brain of *Th*-ki mice

Expression of *Th*-mRNA (but also *Tph*1 and 2 mRNAs) in the brain was similar in wt *Th*-ki mice at different ages (Supplementary Table S1). In contrast, quantification of TH protein content in whole brain extracts showed an increase in TH relative to total protein from newborn (1 day) to 3 weeks in normal mice, but not in *Th*-ki mice (Figure 5A,B). Wt mice maintained their TH content from 3 weeks to 1 year, whereas *Th*-ki mice presented a clear decrease of TH protein from 3 weeks of age (Figure 5A,B) and a progressive loss of TH protein relative to the normal content already from newborns, reaching a value as low as ~3% of normal content in 1 year old animals (Figure 5B, inset). The specific TH activity in brain extracts under standard conditions - measured by a sensitive radiochemical assay[29] - followed the same development as the protein content for the wt animals (Figure 5B). However, the activity in *Th*-ki brain extracts was below the sensitivity threshold and could not be determined accurately by any method tested, with HPLC and fluorimetric detection of L-Dopa[30] or by the radiochemical assay[29].

Immunohistochemistry studies support axonal transport of TH across the nigrostriatal projection

In order to assess TH expression and distribution, we performed TH-immunohistochemistry on coronal brain sections from perfused adult male *Th*-ki and wt mice (6-7 months old). We observed a similar expression pattern of TH in the *substantia nigra pars compacta* (SNpc) and *ventral tegmental* area (VTA) of *Th*-ki and control mice, possibly with only less dense stained projections in the mutant

tissue (Figure 5C) but similar number of cell bodies. However, the results observed in the *corpus striatum* revealed an almost complete lack of immunoreactive processes in this brain area, confirming that there is a strong reduction in the amount of TH protein (corpus striatum; Figure 5D). Other TH-expressing brain areas did not show differential results either (data not shown), suggesting that the most affected brain areas are most likely those targeted by projections from TH producing neurons.

The misfolding loss-of-function mutations hTH1-R202H and mTH-R203H are not stabilized by DA

In order to understand better the TH dysfunction in THD patients and in *Th*-ki mice, we studied the molecular and kinetic effects of the p.R202H and the p.R203H mutations on the human TH isoform 1 (hTH1) and the mouse (mTH) background using purified, recombinant hTH1-wt, mTH-wt, hTH1-R202H and mTH-R203H. First we analyzed the substrate and cofactor dependent activity of each enzyme (Figure 6A,B), and the steady state activity constants are summarized in Table 1. Compared with hTH1-wt, mTH-wt showed reduced specific activity, a similar $K_m(BH_4)$, slightly decreased $S_{0.5}$(L-Tyr) (higher substrate affinity for L-Tyr) and reduced substrate inhibition constant (K_{si}), in agreement with stronger substrate inhibition. The mutants hTH1-R202H and mTH-R203H showed decreased V_{max} and $K_m(BH_4)$ (higher affinity for the cofactor), indicating a clear but not severe kinetic deficiency in the mutants. Additionally, a destabilizing misfolding effect of the mutation was indicated by a 10-fold lower yield of purified recombinant mutant enzymes compared with their wt counterparts, and predicted by the FoldX algorithm[31], which estimated a destabilization of 9.96 kcal/mol (æææG) for the tetrameric structure of hTH (PDB 2XSN), including the catalytic and tetramerization domains. To corroborate that the mutation caused the destabilization, we performed differential scanning fluorimetry (DSF) analyses. This method was chosen due to the small amounts of protein required, since protein was limited for the mutants. The mutant enzymes presented reduced stability (2-3°C decreased midpoint denaturation (T_m)-values compared with the respective wt-forms; Figure 7A). However, reduced stability alone could not fully explain the selective and progressive loss of TH protein in the *Th*-ki mouse (Fig. 5). We hypothesized that this progressive loss of the mutant mTH-R203H protein was due to a defect in the stabilization by DA and other catecholamines. Stabilization is an important outcome of the regulation of TH by the catecholamine feedback

inhibitors, which in addition to inhibiting TH activity competitively versus the BH_4 cofactor, act as natural chaperone compounds[9,11]. *In vitro*, the stabilization is manifested by an increase in the T_m-values and a decrease in its susceptibility to proteolysis[10]. As expected, hTH1-wt and mTH-wt were stabilized by DA binding, increasing their T_m-values up to 3°C (Figure 7A,B). However, the mutants were not stabilized by DA (Fig. 7C,D). In addition, DA protected the wt enzymes, but not the mutants, from limited tryptic proteolysis (shown for hTH1 in Figure 7E-J).

Non-responsiveness of *Th*-ki/ki mice to L-Dopa treatment

We determined the effect of L-Dopa treatment on the motor outcome of juvenile *Th*-ki mice and controls. Catalepsy and motor coordination were investigated after daily L-Dopa (plus carbidopa) or vehicle treatment from birth to 3 weeks of age. No significant differences were found either in the bar test or rotarod performance in *Th*-ki mice given L-Dopa or vehicle (see Supplementary Figures S5A-B). Similar negative results were obtained from treating adult *Th*-ki mice over a period of 12 days (not shown). Nevertheless, monoamine neurotransmitter analysis in brain extracts of sacrificed mice showed significant *metabolite* improvement and all signs of L-Dopa treatment (Figure 8), although TH protein was certainly not increased (Fig. 8, inset).

DISCUSSION

This mouse model was generated to provide an experimental source for *in vivo* mechanistic studies of TH to investigate its deficiency both in terms of disease pathogenesis and the effect of mutations on enzyme function. In the longer term it is also hoped that it will provide a model for testing treatments aimed at improving diseases related to loss of dopamine. The model presents clinically robust: The *Th*-ki mouse appears normal at birth, but thereafter exhibits moderate thriving problems and develops motor features that include abnormal body posture and twitching, reduced motor coordination, ataxia and catalepsy, with clear diurnal variation as well as lowered blood pressure, all sings that were also reported for THD patients[13]. The biochemical abnormalities include an early and progressive decrease in brain DA or catecholamines to critically low levels, associated to a progressive loss of brain TH, hyperprolactinemia - a peripheral marker for DA deficiency and the reason for the strongly reduced fertility of *Th*-ki females (not shown) - and elevated thyroxine, also a characteristic of THD patients.

The importance of catecholamines for fetal development has been clearly demonstrated in earlier studies both with $Th^{-/-}$ and the dopamine ß-hydroxylase deficient $Dbh^{-/-}$ knock-out mice[21,22,32]. Both of these mice variants have a high pre- and perinatal mortality due to cardiovascular failure associated to the lack of norepinephrine. TH function and norepinephrine synthesis can be rescued in noradrenergic neurons of the $Th^{-/-}$ mice, which then become a specific DA-deficient mice which survive for a short period after birth without treatment[13,19]. However, DA-deficient mice present normal norepinephrine levels and are thus not good models for THD. A catecholamine-deficient mouse model with 50% survival is the aromatic amino acid decarboxylase (AADC) knock-out line, but these mice show also seriously reduced serotonin levels[33] and are therefore also not a model to investigate the pathogenic mechanisms of TH dysfunction.

Newborn *Th*-ki mice show normal values of catecholamines and other metabolites, except for a reduction in HVA. By 3 weeks of age, however, a drastic drop in brain norepinephrine is observed in *Th*-ki, and despite the crucial role of norepinephrine for mouse fetal development[32], the very low level of norepinephrine in *Th*-ki mice of ≥3 weeks does not affect survival. The drop in norepinephrine is initially not

accompanied by a significant decrease in DA pointing to compensatory mechanisms that maintain DA levels, e.g. by down regulation of its degradation. Indeed, it has been shown that DA but not norepinephrine levels are regulated by catechol *O*-methyltransferase (COMT), at least in the prefrontal cortex[34]. Furthermore, the large decrease in norepinephrine in *Th*-ki mice occurs at the time when TH protein substantially increases in normal mice[35], actually a 5-fold increase in TH was observed in *Th*-wt from newborn to 3 weeks, while TH was not increased in *Th*-ki (5 fold increase; see Fig. 5B) despite the fact that *Th*-mRNA levels are similar (Table S1). The stabilization of TH necessary to sustain the critical increase in TH protein is required for post-natal development of the dopaminergic system and proper transport and distribution of TH in the striatum. Both the level of BH_4 and catecholamines themselves have been implicated in this stabilization, which is impaired e.g. in the BH4-deficient mice[35,36]. In this work, we show that BH_4 levels are similar in *Th*-wt and knock-in mice but, pertinently, the mTH-R203H enzyme is not stabilized by DA (or norepinephrine; data not shown): this explains the lower accumulation of the mutant TH protein in the critical postnatal period, as well as its progressive decay until 1 year of age. Furthermore, in agreement with our immuno-histochemical results of TH expression in brain of adult *Th*-ki mice presented here, the absence of TH stabilization by catecholamines has been associated with defects in the postnatal pattern of striatal TH immuno-reactivity[36]. It is well known that motor control depends on the transmission of DA through the nigrostriatal pathway from the SNpc along the processes to the caudate-putamen. Given the observed motor deficits in the *Th-ki* mutant mice, and the lack of L-Dopa responsiveness, our data suggest that these animals may not have enough synaptic DA to activate DA receptors in the caudate-putamen and thus allow proper motor function.

One puzzling feature in the phenotype of the *Th*-ki and the patients with THD type B, especially for those with the mutation hTH1-R202H, is the non-responsiveness to L-Dopa, both when mice are treated from the first day of life or during the course of the disease. This was unexpected in view that DA levels increase considerably and NA reaches the levels in *Th*-wt mice (Figure 8). Other mice models with DA deficiency show a partial recovery of some of the dysfunctions, specially related with feeding problems, upon DA treatment, though the recovery of motor disturbances is not well achieved[37], which has been related to brain developmental deficiencies in the fetus

and in the perinatal period[35,37]. In the case of *Th*-ki, a critical factor for the lack of responsiveness is also the inability of the brain catecholamines to stabilizing the mutant TH protein. The defective striatal distribution of TH is in itself probably related to impaired transport of TH protein - and thus neurotransmission - despite an elevated level of total brain DOPA, DA and norepinephrine[36]. It is therefore still crucial to develop novel and non-L-Dopa-based therapeutic strategies for THD type B. In this respect the major finding and molecular explanation for this phenotype is the direct loss of mutant TH protein and activity, and emerging therapies based on protein stabilization, e.g. pharmacological chaperones, appear promising[38]. The diurnal fluctuation of motor deficits is definitively an important hallmark of our *Th*-ki mutant mouse and may also be exploited on the search for novel treatment strategies based on therestorative potential of either circadian regulation of TH activity and/or restorative properties of sleep.

A few unexpected characteristics of the *Th*-ki mutant mouse remains unexplained and need further attention. For instance the growth retardation in combination with normal food intake, normoglycemia (not shown) and reduced energy expenditure remains elusive. An interesting observation in this context is the *Igf-1* gene over-expression in brain and thus the potential involvement of IGF-1 in growth attenuation in DA-compromised *Th*-ki mice during the growth period. The IGF-1 system is known to be an important mediator of cell growth and differentiation[25] but a link to the DA system needs in depth investigations for understanding, as thus far, IGF-1 over-expression in brain was rather described to be involved in neuronal survival than growth reduction. Another explanation is that disruption of DA signaling has been associated to growth retard due to altered GHRH-somatostatin regulation of GH[39]. Moreover, it was previously reported that mice with selective DA-deficiency in dopaminergic neurons, but not in noradrenergic neurons, exhibited abnormal feeding behaviour including swallowing difficulties (aphagy)[23,37], symptoms we did not observe in the *Th*-ki mice. On the other hand, growth retardation in combination with normal food intake was found in total and neuron specific DA-receptor knock-out mice which are in agreement with reduced DA signaling[40,41]. The *Th*-ki mouse therefore may also provide a model to study the role of central catecholamines and the control of body growth and food intake.

In conclusion, there is a large spectrum of phenotypes in patients with THD, resulting from diverse deficiencies in absolute and relative DA and norepinephrine levels with different impact on systemic and motor function[42]. This variability would depend on the catalytic and conformational defect of the TH mutation and on particular effects on regulatory mechanisms for TH, notably those affecting TH protein stability. The homozygous *Th*-ki mice studied in this work presents severe motor deficiencies from a juvenile age onwards, and these abnormalities are not corrected by classical replacement treatment with L-Dopa. The mutant hTH1-R202H and mTH-R203H proteins are not stabilized by DA, leading to intracellular instability, progressive loss of TH activity and altered striatal distribution, aiding to interpret a biochemical and locomotor phenotype of *Th*-ki. In addition to contribute to the understanding of the biochemical pathogenesis of catecholamine deficiency this mouse model offers a useful platform for designing and evaluating new routes to disease therapies not only for THD, but also to complement and improve present therapeutic regimes for genetic and idiopathic dopaminergic deficiencies.

CONFLICT OF INTEREST

The authors declare no conflict of interest.

ACKNOWLEDGMENTS

This work was supported by grants from the Swiss National Science Foundation (#310000-112275; to DK), the Hartmann Müller Stiftung für wissenschaftliche Forschung der Universität Zürich (to BT), the Neuroscience Center Zurich (to BT), The Research Council of Norway (to AM), the Western Regional Health Authorities (to AM) and the K. G. Jebsen Foundation (to AM). We are grateful the Division of Clinical Chemistry and Biochemistry at the University Childrenõs Hospital Zürich for sharing technical equipment, and the Animal Facilities (BZL) of the University Hospital Zürich for animal maintenance and support.

FIGURES AND TABLES

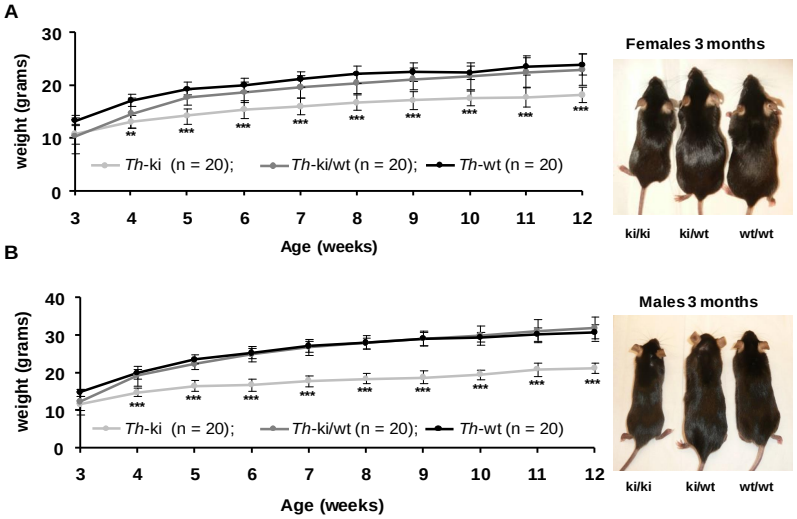

Figure 1. Sex-specific differences in body weight between wt and *Th*-ki mice. (**A**) Female and (**B**) male mice fed *ad libitum* with standard chow. Significant differences between *Th*-ki and wt combined with heterozygotes mice are indicated by **, p<0.01; ***, p<0.001 (Studentôs two tailed *t*-test).

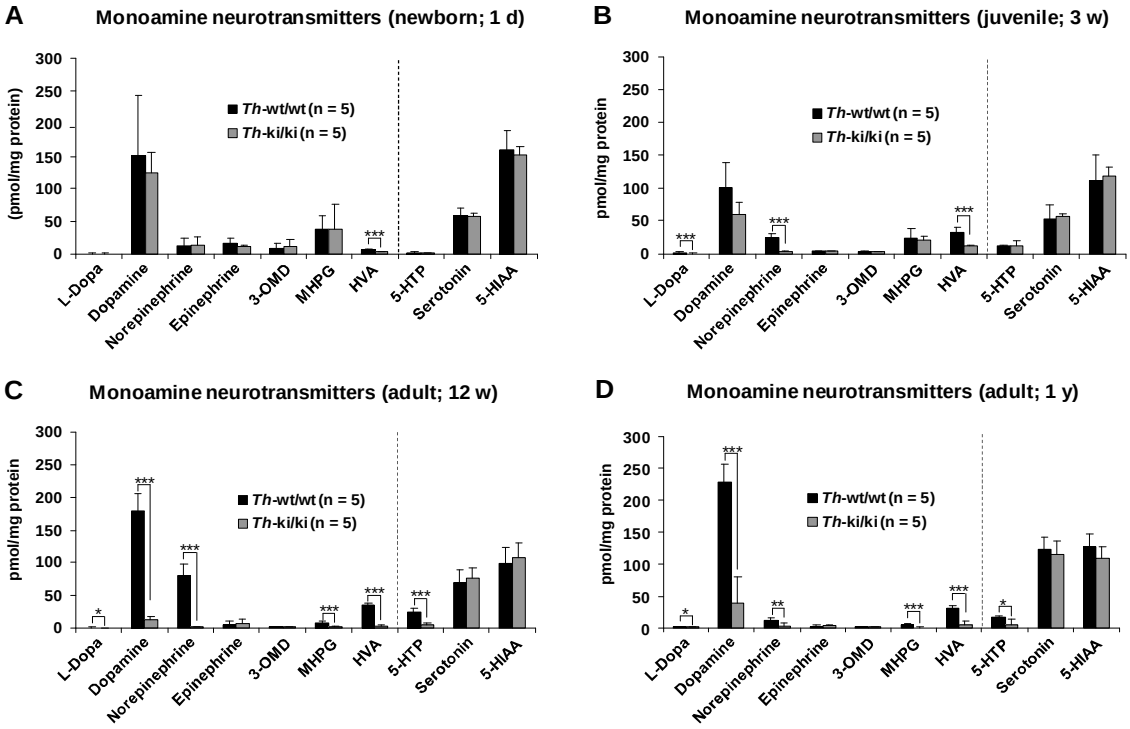

Figure 2. Progressive loss of brain monoamine neurotransmitter metabolites in *Th*-ki mice. (A) Newborn mice at the age of day 1, **(B)** juvenile mice at the age of 3 weeks, **(C)** adult mice at the age of 12 weeks, and **(D)** adult mice at the age of 1 year. *Th*-wt mice are shown in black and *Th*-ki in gray. Monoamine neurotransmitter metabolites are depicted in pmol/mg of total brain protein. Significant difference from the corresponding wt value is indicated by asterisks: *p<0.05, **p<0.01, ***p<0.001 (Studentôs two tailed *t*-test). 3-OMD, 3-*O*-methlydopa; MHPG, 3-methoxy-4-hydroxyphenylethylene glycol; HVA, homovanillic acid; 5-HTP, 5-hydroxytryptophane; 5-HIAA, 5-hydroxyindoleacetic acid. Significant difference from the corresponding wt value is indicated by asterisks: *, p<0.05; **, p<0.01; ***, p<0.001 (Studentôs two tailed *t*-test).

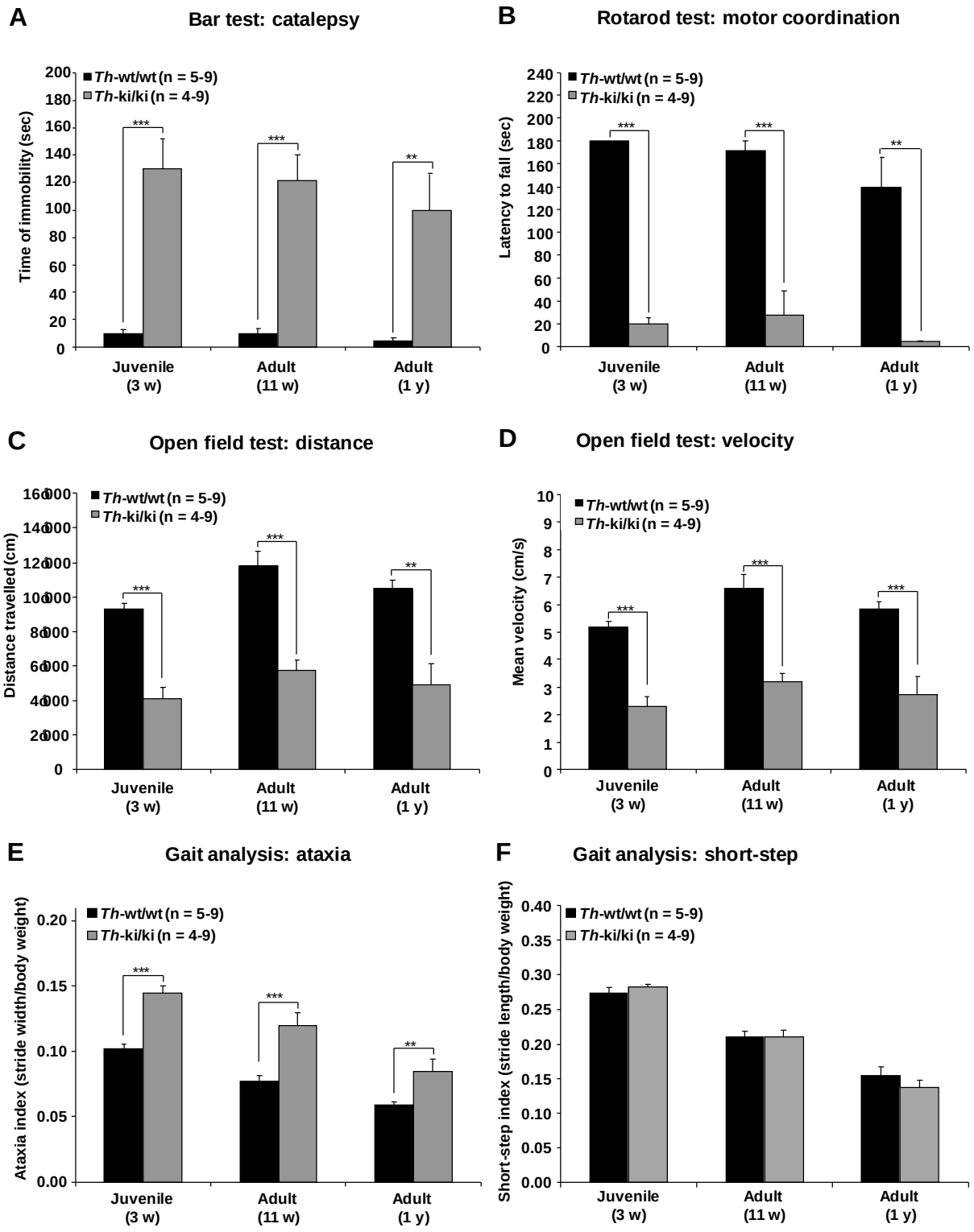

Figure 3. Behavioral analysis of *Th*-ki and wt (*Th*-wt) male mice at different ages. (A) Bar test for assessment of catalepsy (sec). **(B)** Rotarod test for determination of motor coordination (sec). **(C)** Total distance travelled (cm) in the open field test (cm). **(D)** Mean velocity (cm/s) of locomotion in the open field test **(E)** Gait analysis to test for ataxia (stride width normalized to body weight). **(F)** Gait analysis to test for short-step disorder (stride length normalized to body weight). *Th*-wt mice are shown in black and *Th*-ki in gray. Significant difference from the corresponding wt value is indicated by asterisks: **, p<0.01; ***, p<0.001 (Student's two tailed *t*-test or ANOVA for fluctuation bar test).

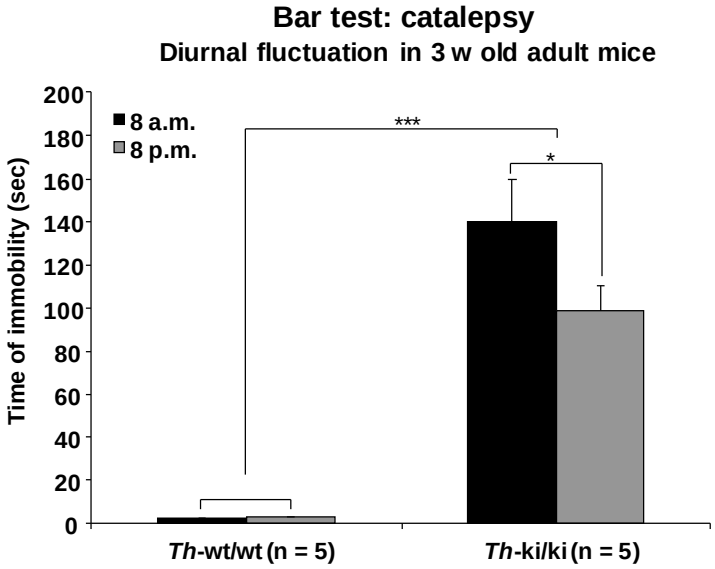

Figure 4. The bar test for catalepsy reveals diurnal fluctuation of motor deficits. Bar test performed at 8 a.m. and 8 p.m. to explore potential fluctuations in catalepsy severity (sec). *Th*-wt mice are shown in black and *Th*-ki in gray. While there was no difference for *Th*-wt mice performance at different day times, *Th*-ki mice exhibited a significant difference between morning and evening, indicated by the asterisk (*p<0.05; two ANOVA for fluctuation bar test). The difference between the two genotypes is repeated from Figure 3A (indicated by the three asterisks; ***, p<0.001 (Student's two tailed *t*-test).

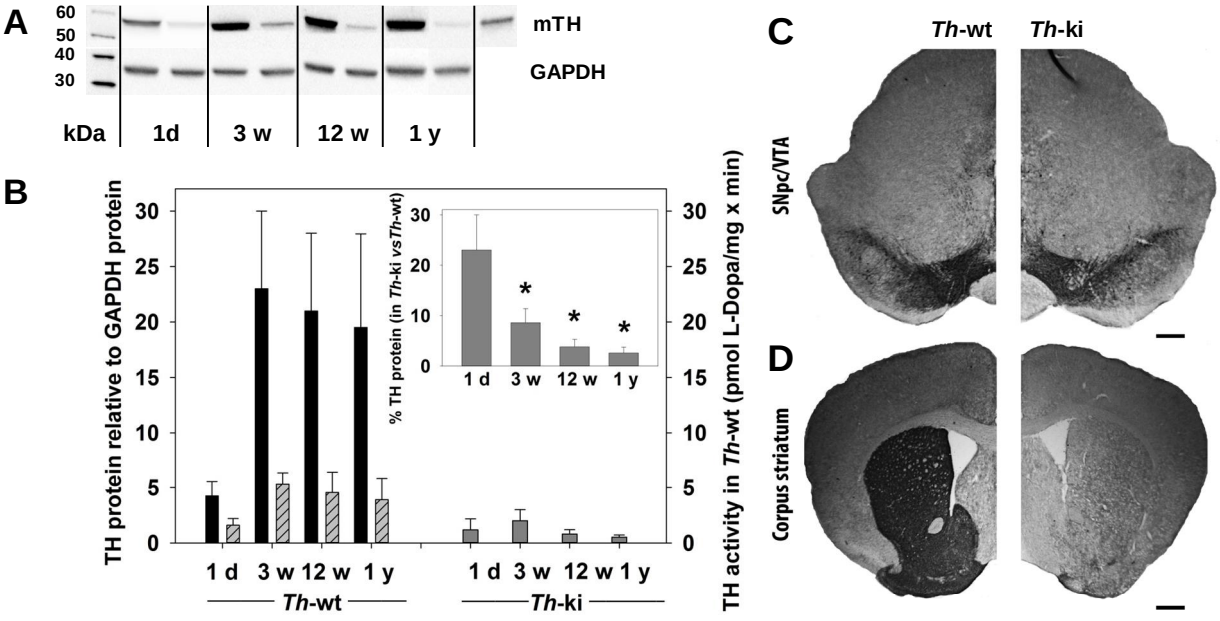

Figure 5. TH protein content in brain from wt (*Th*-wt) and *Th*-ki mice. (A) Representative immunoblots for brain extracts of mice of different age; kDa, standard; mTH, purified recombinant mouse TH. **(B)** TH protein content in brain extracts from wt (black bars) and *Th*-ki mice (grey bars) by density of the 59 kDa TH band relative to the intensity of the GAPDH band. The grey striped bars indicate enzyme activity for wt TH (scale for activity on the right). Inset: % of TH protein content in brain extracts of *Th*-ki vs. *Th*-wt. For both panels: newborn (1 d), 3 weeks (3 w), 12 weeks (12 w) and one year (1 y), in *Th*-wt (wt) and *Th*-ki (ki) mice. Asterisks: *, p<0.001 (Student's two tailed *t*-test).

(C-D) Immunohistochemical staining of TH in brain of *Th*-wt and *Th*-ki mutant mice, at the age of 6 months. **(C)** *Substantia nigra pars compacta* (SNpc) and ventral tegmental area (VTA) of *Th*-wt and *Th*-ki mice present a similar degree of neuronal staining indicating lack of neuro-degeneration, and (**D**) A striking lack of TH staining was observed in the *corpus striatum* in *Th*-ki mice compared to their controls, indicating that a reduced amount of TH protein is accumulated in these neuronal processes.

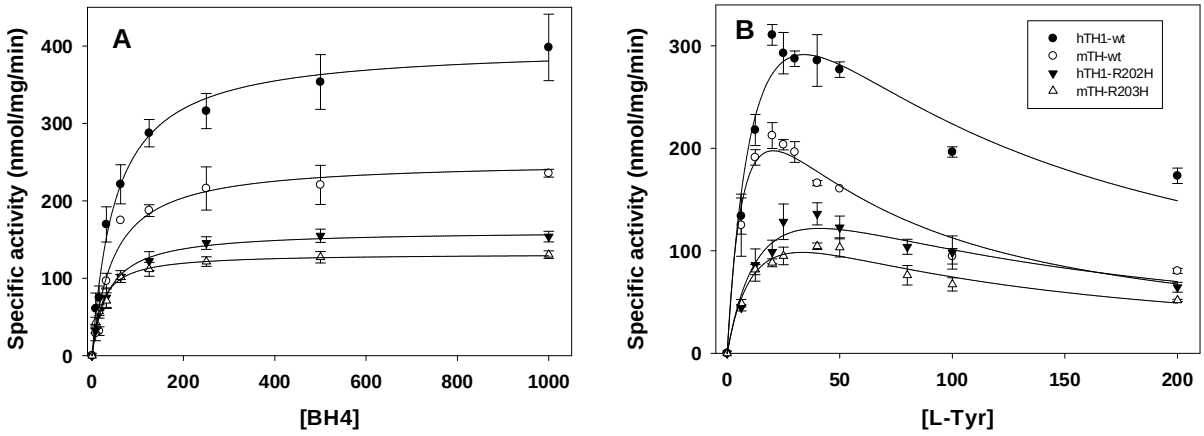

Figure 6. Steady-state kinetics characterization of recombinant purified human TH1 (hTH1) and mouse TH (mTH), and the respective mutants R202H and R203H. Specific activity of hTH1-wt (ŏ), mTH-wt (ʒ), hTH1-R202H (Ƹ) and mTH-R203 (△) measured **(A)** at different concentrations of the cofactor BH_4 (0ï 1000 μ M) at fixed L-tyrosine concentration (25 μ M), and **(B)** at different concentrations of the substrate (0ï 200 μ M) and fixed BH_4 concentration (200 μ M). Results are means ± S.D. for three different experiments.

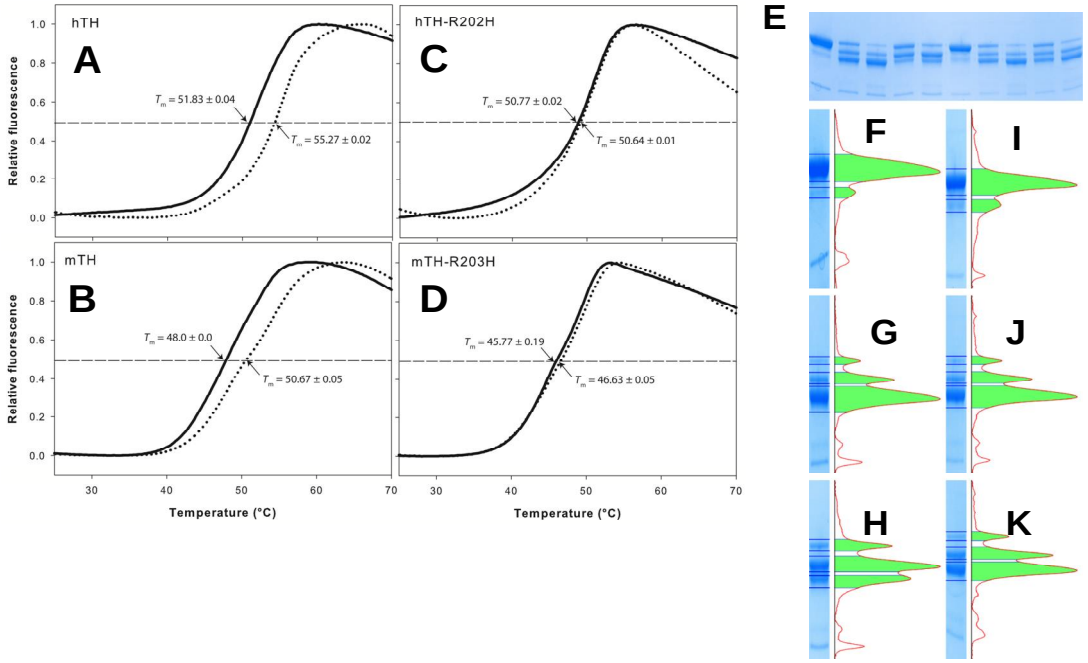

Figure 7. The stability of recombinant purified human TH1 (hTH1) and mouse TH (mTH) and the respective mutants R202H and R203H, and effect of DA. (A-D) Differential scanning fluorimetry profiles. Thermal denaturation profiles (fluorescence at 610 nm vs. temperature) for hTH1-wt **(A)**, mTH-wt **(B)**, hTH1-R202H **(C)** and mTH-R203 **(D)**, analyzed at a concentration of 0.9 µM subunit

without (solid black line) and with equimolar amount (0.9 µM) of DA (dotted line). The midpoint denaturation (T_m)-values, determined as maximal temperature in first-derivatives, are shown in the corresponding plots. **(E)** SDS-PAGE showing the tryptic digestion of hTH1-wt (lanes 1-5) and hTH1-R202H (lanes 6-10) in the absence (2,3,7,8) and the presence of 50 µM DA (4,5,9,10); 1 and 6 are the respective controls in the absence of trypsin. Conditions: 2.5 µM subunit hTH or hTH-R202H were incubated with trypsin for 30 s (2,4,7,9) or 60 s (3,5,8,10) at 25°C, at a TH:trypsin ratio of 200:1. The gels were stained with Coomassie Brilliant Blue and scanned. The raw volume of the bands was measured using the Image Lab 3.0.1 software and represented for lanes 1, 3, 5, 6, 8 and 10 in **F**, **G**, **H**, **I**, **J** and **K**, respectively. At the selected conditions, hTH1-wt, with an apparent molecular weight of 60 kDa, was converted by trypsin into two different truncated forms of 57 and 54 kDa. Both these truncated forms lack the N-terminal peptide MPTPDATTPQAKGFR, indicating that hTH1 undergo proteolysis at the N-terminal (analyses by MS spectroscopy; data not shown).

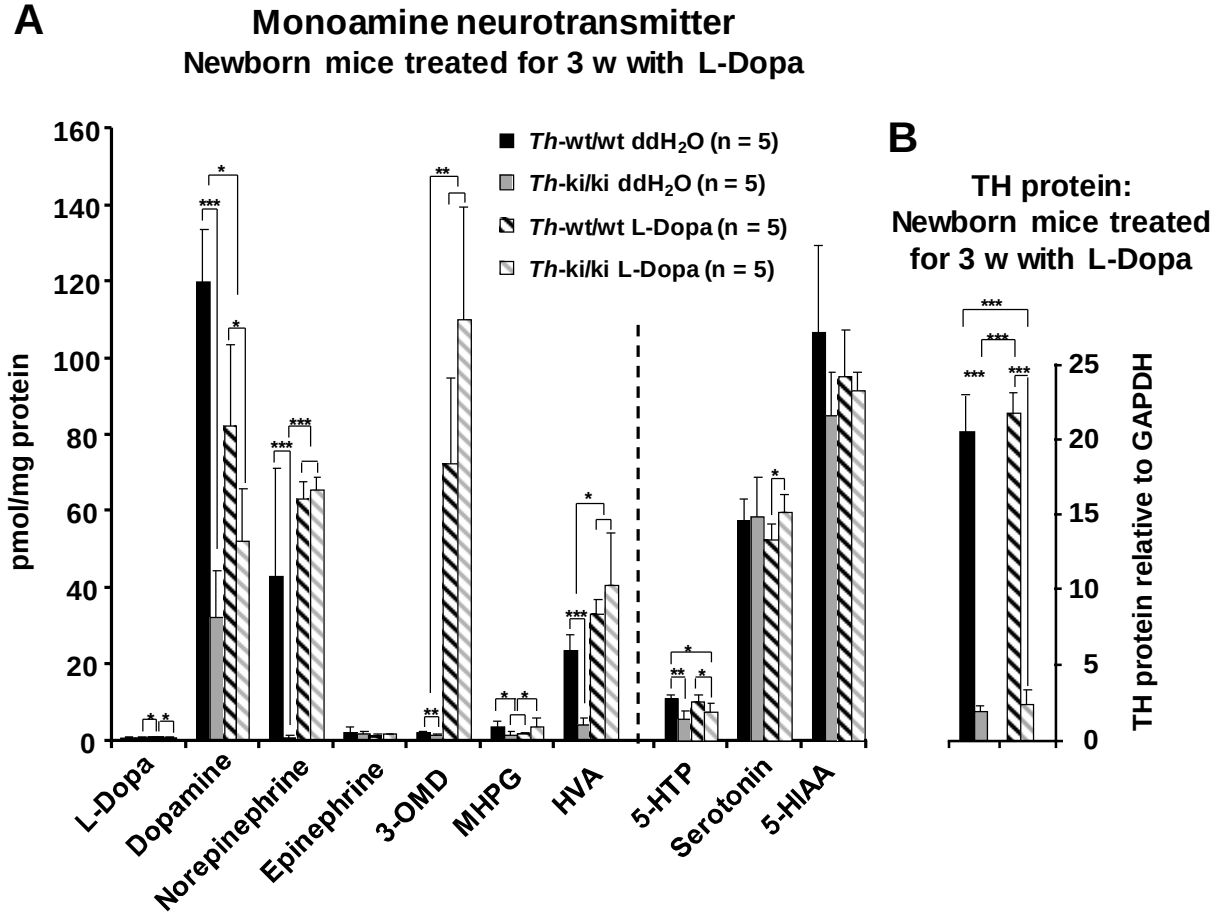

Figure 8. Outcome of L-Dopa treatment of *Th*-ki mice on brain monoamine neurotransmitter metabolites and TH protein. Mutant *Th*-ki and *Th*-wt mice were treated after birth for a period of 3 weeks with L-Dopa (10 mg/kg/d) plus carbidopa (2.5 mg/kg/d) or vehicle (controls). **(A)** Brain monoamine neurotransmitter metabolites are depicted in pmol/mg protein. **(B)** TH protein relative to GAPDH is shown for wt and mutant mice with or without L-Dopa treatment. In both A and B, significant difference from the corresponding wt value is indicated by asterisks: *, p<0.05; **, p<0.01; ***, p<0.001 (Student's two tailed *t*-test).

Table 1. Steady-state kinetics parameters for recombinant purified human TH1 (hTH1) and mouse TH (mTH), and the respective mutants R202H and R203H. See also Figure 2. Results are means ± S.D. for three different experiments.

Enzyme	_____ BH_4 _____		_____ L-Tyr _____		
	V_{max} (nmol of L-dopa/min×mg)	K_m (BH_4) (µM)	V_{max} (nmol of L-dopa/min×mg)	$S_{0.5}$ (L-Tyr) (µM)	K_{si}* (µM)
hTH1-wt	400 ± 11	50 ± 6	782 ± 41	22 ± 1	54 ± 5
mTH-wt	252 ± 14[1*]	47 ± 10	583 ± 46[1*]	15 ± 1[1*]	28 ± 4[1*]
hTH1-R202H	162 ± 3[1*]	34 ± 3[1*]	344 ± 50[1*]	28 ± 3	60 ± 9
mTH-R203H	132 ± 3[2*]	21 ± 2[2*]	280 ± 40[2*]	23 ± 5	49 ± 6[2*]

For BH_4 concentration dependency, data were fit to the Michaelis-Menten model and for L-Tyr concentration dependency to the substrate inhibition model.

K_{si}, substrate inhibition constant

[1]*, p< 0.5 with respect to corresponding values for hTH1-wt

[2]*, p< 0.5 with respect to corresponding values for mTH-wt

SUPPLEMENTARY FIGURES AND TABLES

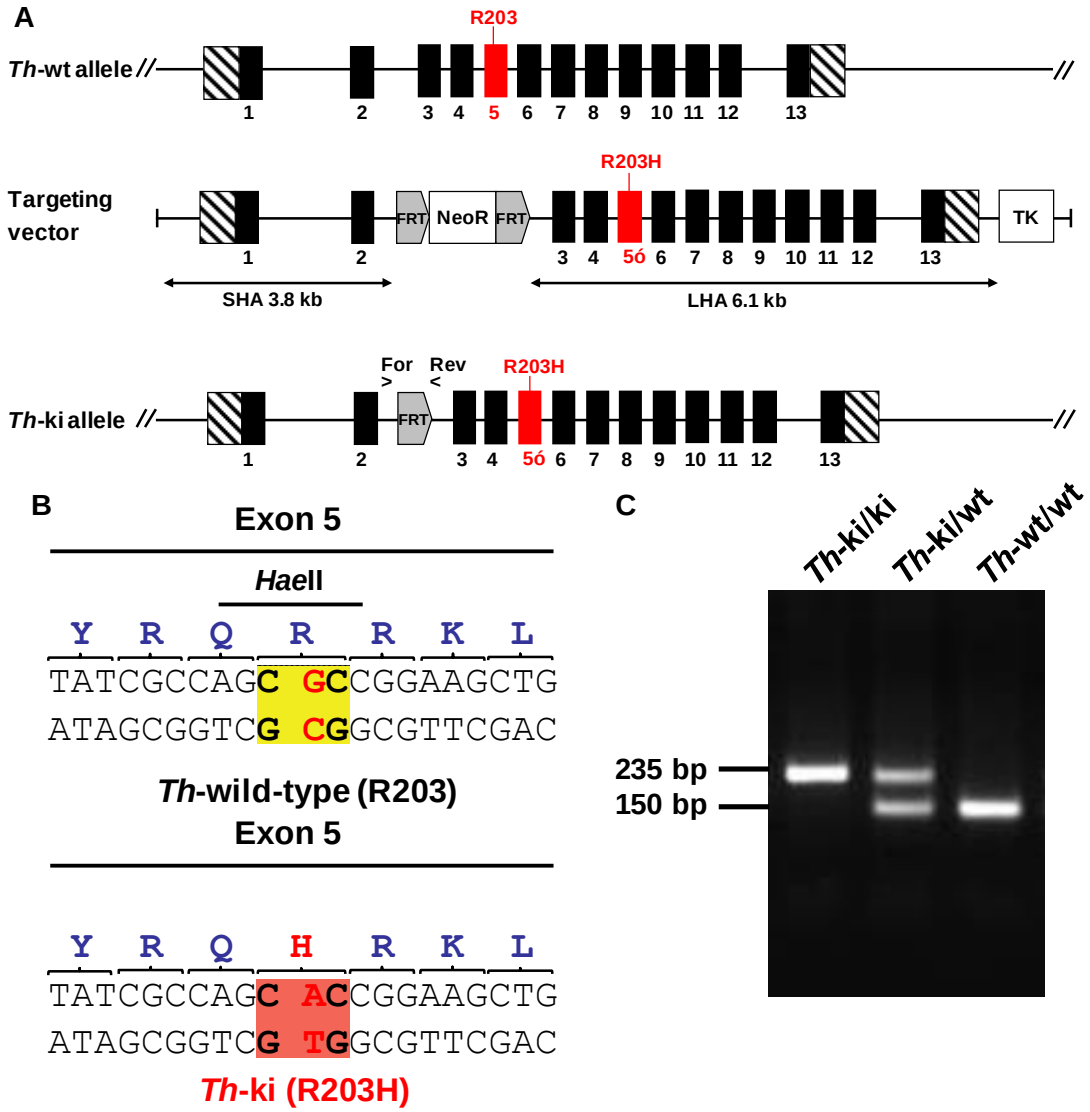

Suppl. Figure S1. Generation of the *Th*-ki mouse. (A) Schematic representation of the *Th*-ki mouse gene containing 13 exons with the *Th*-wt allele R203 in exon 5 (in red; the gene is not drawn to scale; NCBI gene ID 21823, transcript variant *Th*-1 NM_0093771.1; Ensembl gene ID ENSMUSG00000000214). The targeting vector contains a 3.8 kb short homology arm (SHA) and a 6.1 kb long homology arm (LHA), including the mouse R203H mutation in exon 5ô At the bottom, the targeted mutant *Th*-ki allele is shown with location of primers for PCR-genotyping (see below). For validation of correct recombination, Southern blot analyses were performed (see be supplied upon request). FRT, flippase recognition target site; NeoR, neomycin resistance gene for positive selection; TK, thymidine kinase gene for negative selection. **(B)** Details of the DNA sequence of exon 5 of the wt (left) and mutant (right) alleles. The wt sequence of the R203 codon overlaps with a *Hae*II endonuclease recognition site which is destroyed in the mutant allele R203H. **(C)** Conventional 2% agarose gel of representative PCR-genotyping for the *Th*-ki allele with a size difference of 85 bp due to the additional FRT site in the *Th*-ki allele which is in *cis* with the R203H mutation. Position of the primer pair is indicated in A (for more details see Materials and Methods).

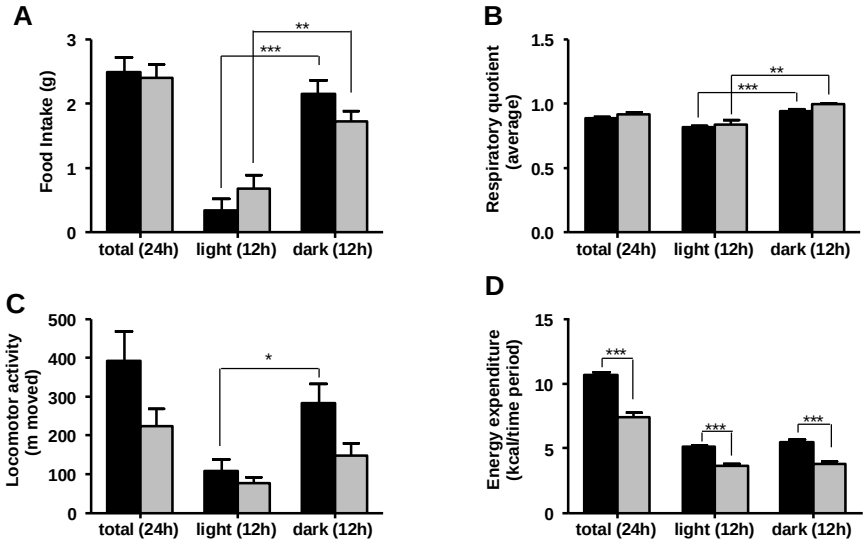

Suppl. Figure S2. Similar food intake and respiratory quotient but reduced energy expenditure in *Th*-ki compared to *Th*-wt mice. Food intake **(A)**, respiratory quotient **(B)**, locomotor activity **(C)** and energy expenditure **(D)** were determined in an open-circuit indirect calorimetry system equipped with an infrared light-beam and a feeding monitor system as described in Materials and Methods. After mice were adapted to single caging, data were obtained during a 24-h period in *Th*-wt (black bars) and *Th*-ki (gray bars) mice and results are depicted either over the whole 24-h period or separated into light and dark phase (n = 4-5). Error bars represent SEM. *, p<0.05; **, p<0.01; ***, p<0.001 (Student's *t*-test).

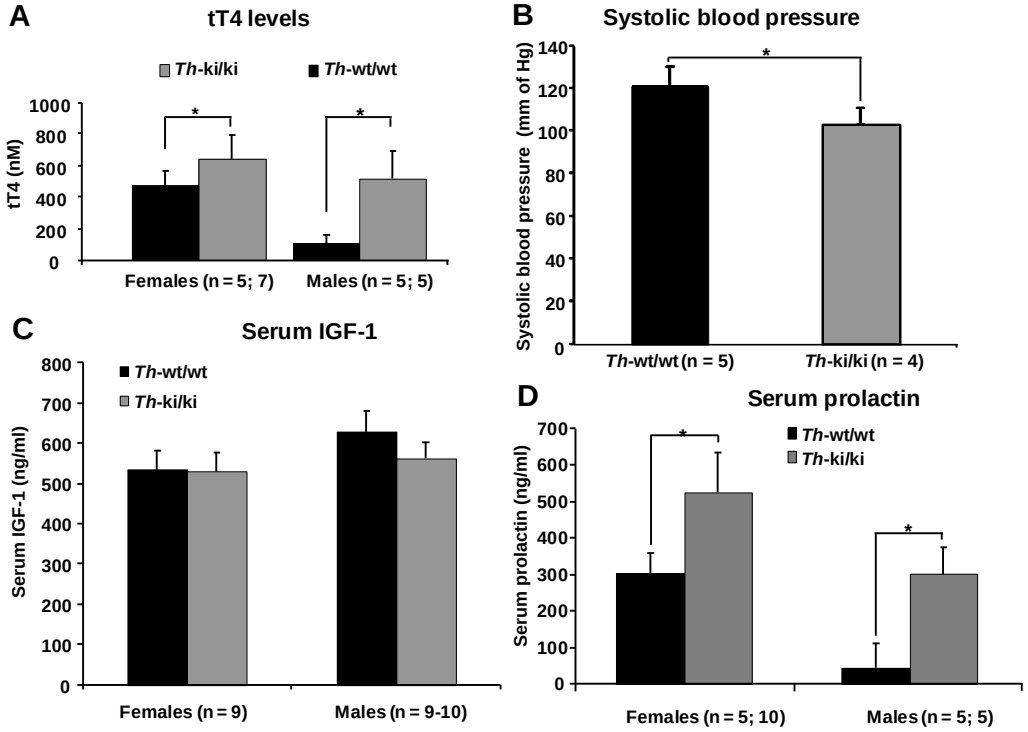

Suppl. Figure S3. Serum parameters including total thyroxine (tT4), IGF-1 and prolactin, as well blood pressure measurements in wt and *Th*-ki mice. **(A)** Serum total thyroxine (nM), **(B)** systolic blood pressure (mm of Hg), **(C)** serum IGF-1 (ng/ml), and **(D)** serum prolactin (ng/ml) in *Th*-wt and *Th*-ki mice. *Th*-wt are shown in black bars and *Th*-ki in grey bars; the number of mice per group is indicated. Significant difference is indicated by *, p<0.05 (Student's two tailed *t*-test).

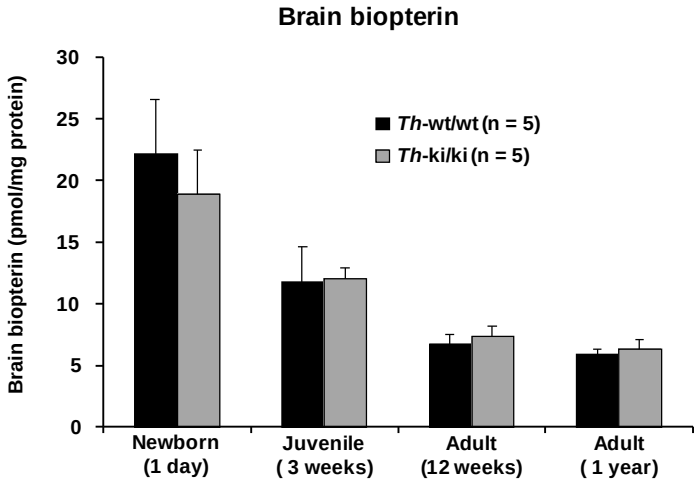

Suppl. Figure S4. Biopterin content in whole brain extracts (in pmol/mg of total protein) at different ages of *Th*-wt and *Th*-ki mice. See text for details.

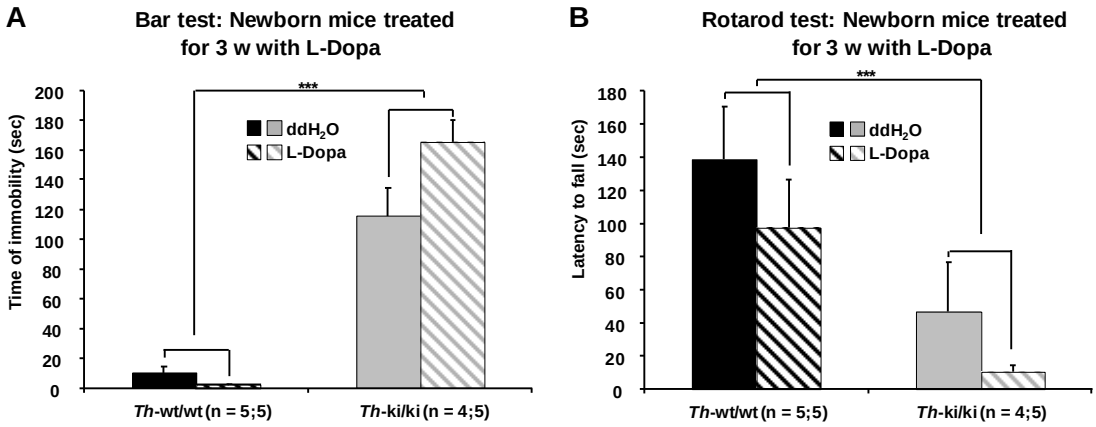

Suppl. Figure S5. Bar and rotarod tests in *Th*-wt and *Th*-ki mutant mice after treatment with L-Dopa. *Th*-ki and *Th*-wt mice were treated after birth for a period of 3 weeks with L-Dopa (10 mg/kg/d) plus carbidopa (2.5 mg/kg/d), or with vehicle. **(A)** Bar test to assess catalepsy, and **(B)** rotarod test to determine motor coordination. Treatment with ddH_20 (vehicle) or L-Dopa/carbidopa are shown in black or black-white stripes for *Th*-wt mice, and in gray or gray-white stripes for *Th*-ki. Significant differences from the corresponding wt values are indicated by asterisks: ***, p<0.001 (Student's two tailed *t*-test).

Supplementary Table S1: Gene expression of *Th* and *Tph*1/2 in brain of mice at different age

Genotype	Age	*Th*-mRNA[a]	*Tph*1-mRNA[a]	*Tph*2-mRNA[a]
Th-wt newborn	1 day	1.00 (0.65 - 1.55)	0.09 (0.03 - 0.23)	0.06 (0.01 - 0.31)
Th-ki newborn	1 day	1.06 (0.74 - 1.53)	0.06 (0.06 - 0.07)	0.08 (0.03 - 0.26)
Th-wt juvenile	3 weeks	1.48 (0.71 - 3.10)	0.03 (0.02 - 0.03)	0.14 (0.03 - 0.61)
Th-ki juvenile	3 weeks	1.62 (1.31 - 2.01)	0.03 (0.02 - 0.05)	0.07 (0.03 - 0.20)
Th-wt adult	12 weeks	1.46 (0.94 - 2.27)	0.04 (0.03 - 0.04)	0.05 (0.02 - 0.10)
Th-ki adult	12 weeks	1.96 (1.23 - 3.41)	0.03 (0.02 - 0.05)	0.03 (0.01 - 0.06)
Th-wt adult	1 year	1.60 (0.84 - 3.03)	0.04 (0.02 - 0.07)	0.03 (0.01 - 0.06)
Th-ki adult	1 year	1.46 (0.89 - 2.42)	0.04 (0.02 - 0.05)	0.01 (0.00 - 0.04)

[a] Normalized relative to *Gapdh*-mRNA (Livak and Schnittgen, *Methods 25*(4):402-408, 2001)

Th tyrosine hydroxylase; *Tph*1/2 tryptophan hydroxylases 1 and 2; *Gapdh*, glyceraldehyde 3-phosphate dehydrogenase

REFERNENCES

1. Roberts, K. M. & Fitzpatrick, P. F. Mechanisms of tryptophan and tyrosine hydroxylase. *IUBMB Life* **65**, 350-357, (2013).

2. Nagatsu, T., Levitt, M. & Udenfriend, S. Tyrosine hydroxylase. The initial step in norepinephrine biosynthesis. *J Biol Chem* **239**, 2910-2917 (1964).

3. Zigmond, R. E., Schwarzschild, M. A. & Rittenhouse, A. R. Acute regulation of tyrosine hydroxylase by nerve activity and by neurotransmitters via phosphorylation. *Annu Rev Neurosci* **12**, 415-461 (1989).

4. Bjorklund, A. & Dunnett, S. B. Dopamine neuron systems in the brain: an update. *Trends Neurosci* **30**, 194-202, (2007).

5. Eisenhofer, G., Kopin, I. J. & Goldstein, D. S. Catecholamine metabolism: a contemporary view with implications for physiology and medicine. *Pharmacol Rev* **56**, 331-349 (2004).

6. Nagatsu, T. Tyrosine hydroxylase: human isoforms, structure and regulation in physiology and pathology. *Essays Biochem* **30**, 15-35 (1995).

7. Kumer, S. C. & Vrana, K. E. Intricate regulation of tyrosine hydroxylase activity and gene expression. *J Neurochem* **67**, 443-462 (1996).

8. Daubner, S. C., Le, T. & Wang, S. Tyrosine hydroxylase and regulation of dopamine synthesis. *Arch Biochem Biophys* **508**, 1-12, (2011).

9. Okuno, S. & Fujisawa, H. Conversion of tyrosine hydroxylase to stable and inactive form by the end products. *J Neurochem* **57**, 53-60 (1991).

10. Martinez, A., Haavik, J., Flatmark, T., Arrondo, J. L. & Muga, A. Conformational properties and stability of tyrosine hydroxylase studied by infrared spectroscopy. Effect of iron/catecholamine binding and phosphorylation. *J Biol Chem* **271**, 19737-19742 (1996).

11. Sumi-Ichinose, C. *et al.* Catecholamines and serotonin are differently regulated by tetrahydrobiopterin. A study from 6-pyruvoyltetrahydropterin synthase knockout mice. *J Biol Chem* **276**, 41150-41160 (2001).

12. Reed, M. C., Lieb, A. & Nijhout, H. F. The biological significance of substrate inhibition: a mechanism with diverse functions. *Bioessays* **32**, 422-429, (2010).

13. Willemsen, M. A. *et al.* Tyrosine hydroxylase deficiency: a treatable disorder of brain catecholamine biosynthesis. *Brain* **133**, 1810-1822, (2010).

14. Kurian, M. A., Gissen, P., Smith, M., Heales, S., Jr. & Clayton, P. T. The monoamine neurotransmitter disorders: an expanding range of neurological syndromes. *Lancet Neurol* **10**, 721-733, (2011).

15. Haavik, J., Blau, N. & Thony, B. Mutations in human monoamine-related neurotransmitter pathway genes. *Hum Mutat* **29**, 891-902 (2008).

16. Aitkenhead, H. & Heales, S. J. Establishment of paediatric age-related reference intervals for serum prolactin to aid in the diagnosis of neurometabolic conditions affecting dopamine metabolism. *Ann Clin Biochem* **50**, 156-158, (2013).

17. Ben-Jonathan, N. Dopamine: a prolactin-inhibiting hormone. *Endocr Rev* **6**, 564-589, (1985).

18. Fossbakk, A., Kleppe, R., Knappskog, P. M., Martinez, A. & Haavik, J. Functional studies of tyrosine hydroxylase missense variants reveal distinct patterns of molecular defects in dopa-responsive dystonia. *Human mutation* **35**, 880-890, (2014).

19. Garcia-Cazorla, A. & Duarte, S. T. Parkinsonism and inborn errors of metabolism. *J Inherit Metab Dis* **37**, 627-642, (2014).

20. Obeso, J. A. *et al.* Missing pieces in the Parkinson's disease puzzle. *Nat Med* **16**, 653-661, (2010).

21. Zhou, Q. Y., Quaife, C. J. & Palmiter, R. D. Targeted disruption of the tyrosine hydroxylase gene reveals that catecholamines are required for mouse fetal development. *Nature* **374**, 640-643 (1995).

22. Kobayashi, K. *et al.* Targeted disruption of the tyrosine hydroxylase locus results in severe catecholamine depletion and perinatal lethality in mice. *J Biol Chem* **270**, 27235-27243 (1995).

23. Szczypka, M. S. *et al.* Feeding behavior in dopamine-deficient mice. *Proc Natl Acad Sci U S A* **96**, 12138-12143 (1999).

24. Bornstein, S. R. *et al.* Deletion of tyrosine hydroxylase gene reveals functional interdependence of adrenocortical and chromaffin cell system in vivo. *Proc Natl Acad Sci U S A* **97**, 14742-14747, (2000).

25. Delafontaine, P., Song, Y. H. & Li, Y. Expression, regulation, and function of IGF-1, IGF-1R, and IGF-1 binding proteins in blood vessels. *Arterioscler Thromb Vasc Biol* **24**, 435-444, (2004).

26. Grattan-Smith, P. J. *et al.* Tyrosine hydroxylase deficiency: clinical manifestations of catecholamine insufficiency in infancy. *Mov Disord* **17**, 354-359 (2002).

27. Swoap, S. J., Weinshenker, D., Palmiter, R. D. & Garber, G. Dbh(-/-) mice are hypotensive, have altered circadian rhythms, and have abnormal responses to dieting and stress. *Am J Physiol Regul Integr Comp Physiol* **286**, R108-113, (2004).

28. Haugarvoll, K. & Bindoff, L. A. A novel compound heterozygous tyrosine hydroxylase mutation (p.R441P) with complex phenotype. *J Parkinsons Dis* **1**, 119-122, (2011).

29. Reinhard, J. F., Jr., Smith, G. K. & Nichol, C. A. A rapid and sensitive assay for tyrosine-3-monooxygenase based upon the release of 3H2O and adsorption of [3H]-tyrosine by charcoal. *Life Sci* **39**, 2185-2189 (1986).

30. Haavik, J. & Flatmark, T. Rapid and sensitive assay of tyrosine 3-monooxygenase activity by high-performance liquid chromatography using the native fluorescence of DOPA. *Journal of chromatography* **198**, 511-515 (1980).

31. Schymkowitz, J. *et al.* The FoldX web server: an online force field. *Nucleic Acids Res* **33**, W382-388 (2005).

32. Thomas, S. A., Matsumoto, A. M. & Palmiter, R. D. Noradrenaline is essential for mouse fetal development. *Nature* **374**, 643-646 (1995).

33. Lee, N. C. *et al.* Regulation of the dopaminergic system in a murine model of aromatic L-amino acid decarboxylase deficiency. *Neurobiol Dis* **52**, 177-190, (2013).

34. Tunbridge, E. M., Harrison, P. J. & Weinberger, D. R. Catechol-o-methyltransferase, cognition, and psychosis: Val158Met and beyond. *Biol Psychiatry* **60**, 141-151, (2006).

35. Homma, D. *et al.* Partial biopterin deficiency disturbs postnatal development of the dopaminergic system in the brain. *J Biol Chem* **286**, 1445-1452, (2011).

36. Homma, D., Katoh, S., Tokuoka, H. & Ichinose, H. The role of tetrahydrobiopterin and catecholamines in the developmental regulation of tyrosine hydroxylase level in the brain. *J Neurochem* **126**, 70-81, (2013).

37. Zhou, Q. Y. & Palmiter, R. D. Dopamine-deficient mice are severely hypoactive, adipsic, and aphagic. *Cell* **83**, 1197-1209 (1995).

38. Calvo, A. C. *et al.* Effect of pharmacological chaperones on brain tyrosine hydroxylase and tryptophan hydroxylase 2. *J Neurochem* **114**, 853-863, (2010).

39. Diaz-Torga, G. *et al.* Disruption of the D2 dopamine receptor alters GH and IGF-I secretion and causes dwarfism in male mice. *Endocrinology* **143**, 1270-1279, (2002).

40. Baik, J. H. *et al.* Parkinsonian-like locomotor impairment in mice lacking dopamine D2 receptors. *Nature* **377**, 424-428, (1995).

41. Noain, D. *et al.* Central dopamine D2 receptors regulate growth-hormone-dependent body growth and pheromone signaling to conspecific males. *J Neurosci* **33**, 5834-5842, (2013).

42. Willemsen, M. A. *et al.* Tyrosine hydroxylase deficiency: a treatable disorder of brain catecholamine biosynthesis. *Brain* **133**, 1810-1822, (2010).

43. Blau, N. *et al.* Variant of dihydropteridine reductase deficiency without hyperphenylalaninaemia: effect of oral phenylalanine loading. *Journal of inherited metabolic disease* **22**, 216-220 (1999).

44. Wueest, S. *et al.* Fas (CD95) expression in myeloid cells promotes obesity-induced muscle insulin resistance. *EMBO Mol Med* **6**, 43-56, (2014).

45. Bello, E. P. *et al.* Cocaine supersensitivity and enhanced motivation for reward in mice lacking dopamine D2 autoreceptors. *Nat Neurosci* **14**, 1033-1038, (2011).

46. Avale, M. E. *et al.* The dopamine D4 receptor is essential for hyperactivity and impaired behavioral inhibition in a mouse model of attention deficit/hyperactivity disorder. *Mol Psychiatry* **9**, 718-726, (2004).

47. Kunkel-Bagden, E., Dai, H. N. & Bregman, B. S. Methods to assess the development and recovery of locomotor function after spinal cord injury in rats. *Exp Neurol* **119**, 153-164, (1993).

48. de Medinaceli, L., Freed, W. J. & Wyatt, R. J. An index of the functional condition of rat sciatic nerve based on measurements made from walking tracks. *Exp Neurol* **77**, 634-643 (1982).

49. Suresh Babu, R., Sunandhini, R. L., Sridevi, D., Periasamy, P. & Namasivayam, A. Locomotor behavior of bonnet monkeys after spinal contusion injury: footprint study. *Synapse* **66**, 509-521, (2012).

50. Livak, K. J. & Schmittgen, T. D. Analysis of relative gene expression data using real-time quantitative PCR and the 2(-Delta Delta C(T)) Method. *Methods* **25**, 402-408 (2001).

51. Elzaouk, L. *et al.* Dwarfism and low insulin-like growth factor-1 due to dopamine depletion in Pts-/- mice rescued by feeding neurotransmitter precursors and H4-biopterin. *The Journal of biological chemistry* **278**, 28303-28311 (2003).

52. Krege, J. H., Hodgin, J. B., Hagaman, J. R. & Smithies, O. A noninvasive computerized tail-cuff system for measuring blood pressure in mice. *Hypertension* **25**, 1111-1115 (1995).

53. Thöny, B. *et al.* Tetrahydrobiopterin shows chaperone activity for tyrosine hydroxylase. *J Neurochem* **106**, 672-681 (2008).

54. Flatmark, T. *et al.* Tyrosine hydroxylase binds tetrahydrobiopterin cofactor with negative cooperativity, as shown by kinetic analyses and surface plasmon resonance detection. *Eur J Biochem* **262**, 840-849 (1999).

55. Shevchenko, A., Tomas, H., Havlis, J., Olsen, J. V. & Mann, M. In-gel digestion for mass spectrometric characterization of proteins and proteomes. *Nature protocols* **1**, 2856-2860, (2006).

56. Berle, M. *et al.* Quantitative proteomics comparison of arachnoid cyst fluid and cerebrospinal fluid collected perioperatively from arachnoid cyst patients. *Fluids and barriers of the CNS* **10**, 17, doi:10.1186/2045-8118-10-17 (2013).

57. Gelman, D. M. *et al.* Transgenic mice engineered to target Cre/loxP-mediated DNA recombination into catecholaminergic neurons. *Genesis* **36**, 196-202, doi: (2003).

2.2 ORAL TREATMENT STUDY WITH BH_4 AND PHARMACOLOGICAL CHAPERON IN *TH*-KI/KI MICE TO STABILZE THE MUTANT TH ENZYME AND INCREASE BRAIN CATECHOLAMINE LEVELS

2.2.1 ABSTRACT

A comprehensive characterization of the novel constitutive *Th* knock-in (*Th*-ki) mouse model with progressive loss of brain TH and catecholamines, and severe motor dysfunction was presented in the previous chapter 2.1. This initial characterization included a treatment attempt with oral loading of newborn *Th*-ki/ki mice for three weeks with L-Dopa (10 mg/kg/d plus 2.5 mg/kg/d carbidopa), which resulted in normalization of brain catecholamines (except dopamine) but persistent motor deficits. Here we attempted to perform treatment with chemical pharmachaperons, the so called compounds III and IV (CIII and CIV) that were previously shown to stabilize mutant mTH-p.R203H in cell culture studies, and increased total TH activity in wild-type mouse brain (Calvo et al., 2010). Furthermore, treatment with BH_4-cofactor, which showed to stabilize TH in brain of wild-type mice, was included in the present loading study (Thöny et al., 2008). Young adult *Th*-ki/ki were treated by oral loading over a period of 12 days with CIII or CIV (each 5 mg/kg/d), with BH_4 (100 mg/kg/d) or with L-Dopa (10 mg/kg/d plus 2.5 mg/kg/d carbidopa). A follow-up study included treatment of newborn *Th*-ki/ki mice for 3 weeks with CIII (5 mg/kg/d). Mice were tested for motor function after treatment, and analyzed for *Th* gene expression and TH enzyme activity and protein amount, as well as monoamine neurotransmitter metabolites in whole brain extracts. Only treatment with L-Dopa/carbidopa led to partial normalization of brain catecholamines without changing the behavioral deficits, while treatment with CIII, CIV or BH_4 had no effect whatsoever. Unexpectedly, changes in gene expression in brain were observed in *Th*-ki/ki mice treated for 12 days with L-Dopa, BH_4, CIII or CIV, i.e. increase in *Tph*2 and decrease in the dopamine receptor genes *Drd*1a and *Drd*5. In addition, oral application of BH_4 reduced gene expression of the insulin growth factor-1 (*Igf*-1). In contrast, the 3 weeks CIII treatment only led to decreased *Drd*5 mRNA-expression level. Furthermore, 3 weeks mutant mice have increased *Igf*-1 expression independent form the treatment. These unprecedented observations in treated *Th*-ki/ki mice will be discussed also in the context of previously published results from similar treatment studies in wild-type mice.

2.2.2 INTRODUCTION

The homozygous *Th*-ki/ki mouse, expressing the *Th*-p.R203H mutation, is a model for the severe form of THD: Treatment with L-Dopa/carbidopa led to a remarkable improvement in their brain catecholamines, but it did not improve their motor coordination deficits (see chapter 2.1). Here we performed diverse treatment approaches to potentially not only correct their brain monoamine neurotransmitter deficit but to also improve their motor behavior. The *Th*-p.R203H mutation leads to highly instable mutant TH protein probably caused by the lack of stabilization by decreased levels of dopamine (see chapter 2.1). Several studies showed that chemical pharmachaperons, which are small molecules that can assist *in vivo* protein folding, enhances protein stabilization (Morello et al., 2000, Cohen and Kelly, 2003). Recently, it was shown that the pharmacological chaperon 3-amino-2-benzyl-7-nitro-4-(2-quinolyl)-1,2-dihydroisoquinolin-1 (termed compound III/CIII) and 5,6-dimethyl-3-(4-methyl-2-pyridinyl)-2-thioxo-2,3-dihydrothieno[2,3-d]pyrimidin-4(1H) (compound IV/ CIV) stabilized in wild-type mice the brain TH enzyme by increasing TH activity and amount of protein without affecting gene expression or monoamine neurotransmitter metabolites. This study was performed in wild-type mice treated for 12 days with 5 mg/kg/d CIII or CIV (Calvo et al., 2010). The fact that the gene expression and monoamine neurotransmitters were not raised in treated wild-type mice is probably due to the fact that dopamine is kept at a low level in ‚resting situations', because of the chemical toxicity of this neurotransmitter (Mosharov et al., 2009, Calvo et al., 2010). Furthermore, the addition of CIII stabilized the human *hTH*-p.R202H protein (equivalent to the mouse *Th*-p.R203H mutation) *in vitro* (Calvo et al., 2010).

In the here presented study, it was investigated whether the pharmacological chaperons CIII and CIV restore TH activity, protein levels, gene expression, monoamine neurotransmitters and/or motor function in *Th*-ki/ki mice. As described in a previous study, adult mice were orally fed with 5 mg/kg/d CIII or CIV (Calvo et al., 2010). BH_4, the cofactor of TH, also showed chaperon activity on TH. Therefore, BH_4 was also included in this oral feeding study with relative high oral dosage of 100 mg/kg/d, which allows to directly comparing between a natural and a synthetic chaperon effect (Thöny et al., 2008). In addition, adult mice were fed with 10/2.5 mg/kg/d L-Dopa/carbidopa, serving as positive control for changes in the catecholamines. It has to be considered that the 12 days treatment in adult mice

have possible less impact then a three weeks treatment started after birth. Therefore, newborn mice were also fed for 3 weeks with CIII, which is so far the most promising pharmacological chaperon candidate to stabilize and improve brain TH concomitant with potentially improving motor or behavior dysfunction.

Despite m*Th* gene expression, also m*Tph*1/2 gene expressions were investigated, although no alterations in wild-type mice were detected when treated for 12 days with the pharmacological chaperons (Calvo et al., 2010). TPH1 is mainly present in the pineal gland, the serotonergic neurons in the raphe nuclei that project in all brain areas, the enterochromaffin cells, and the myenteric neurons in the gut (Cote et al., 2003). TPH2 is predominantly found in the brainstem raphe nuclei (Walther and Bader, 2003, Patel et al., 2004).

In chapter 2.1 it was shown that there is a strong decrease of TH in the striatium of *Th*-ki/ki mice, but not in the substantia nigra pars compacta or in the ventrolaterale thalamus, probably due to reduced projection into the striatum. The dopamine receptor D1 (DRD1) is highly abundant in the striatum, and belongs to the D1-subtype of dopamine receptors, including also DRD5, and has a stimulatory effect on the cell. In addition, there is the D2-subtype including the DRD2, which is also highly abundant in the striatum, DRD3 and DRD4 receptors that have an inhibitory effect on the cell (Jaber et al., 1996). Therefore, it was investigated if there are alterations in the murine *Drd*1-5 (m*Drd*1-5) gene expressions and if the treatments with L-Dopa, BH_4, or CIII/IV alter gene expression since it was shown in dopamine-depleted rats that L-Dopa administration resulted in the stimulation of D1 and D2 receptor systems (Trugman et al., 1991).

Oral communication to Simon Heales indicated a possible increased AADC activity, encoded by the *Ddc* gene, in THD patients. Therefore, it was analyzed if the murine *Ddc* (m*Ddc*) gene expression is increased in *Th*-ki/ki mice and if L-Dopa, BH_4, or CIII/IV treatment has any altering effects on m*Ddc* gene expression.

Furthermore, *Th*-ki/ki mice have decreased body weight and size that is not caused by insulin-like growth factor-1 (IGF-1) deficiency (see chapter 2.1). Therefore, it was investigated further if murine *Igf*-1 gene (m*Igf*-1) expression is influenced in *Th*-ki/ki mouse brains when treated with L-Dopa, BH_4, or CIII/IV.

2.2.3 MATERIALS AND METHODS

In the following, additional methods are described that are not present in chapter 2.1 with the general description of the *Th*-ki mouse model (Korner et al, 2014, in preparation).

2.2.3.1 Preparation of solutions

BH_4 solution: 1.5 g ascorbic acid, 750 mg N-acetyl-L-cystein and 1.945 g BH_4 (Ref. no. 11.212, Schircks laboratories, Jona, Switzerland) were diluted in 15 ml degassed ddH_2O and aliquots were stored at -80°C until use. Biopterin concentration was determined by HPLC, and mice were orally fed with 100 mg/kg body weight per day by using a Gilson pipette (with yellow tips).

CIII or CIV solution: 400 mg dimethylsulfoxid (DMSO), 360 mg glucose and 20.05 mg of CIII or CIV were diluted in total 4 ml ddH_2O and aliquots were stored at -80°C until use. Mice were orally fed with 5 mg/kg body weight per day of CIII or CIV by using a Gilson pipette (with yellow tips).

As negative control, mice were fed with the equally amount of ddH_2O or DMSO/glucose solution.

2.2.3.2 Gene (mRNA) expression studies

Murine *Drd*1a-5*, Ddc*- and *Igf*-1-mRNA expression levels were performed using commercially available ABI assays (Mm.02620146 for m*Drd* 1a-mRNA, NCBI RefSeq NM_010076.2; Mm00438545_m1 for m*Drd2*-mRNA, NCBI RefSeq NM_010077.2; Mm00432887_m1 for m*Drd*3-mRNA, NCBI RefSeq NM_007877.1; Mm00432893_m1 for m*Drd*4-mRNA, NCBI RefSeq NM_007878.2; Mm00658653_s1 for m*Drd*5-mRNA, NCBI RefSeq NM_013503.1; Mm00516688_m1 for m*Ddc*-mRNA, NCBI RefSeq NM_001190448.1 and Mm00439560_m1 for m*Igf*-1-mRNA, NCBI RefSeq NM_001111274.1). The murine glyceraldehyde-3-phosphate dehydrogenase (*Gapdh*) mRNA (ABI assay ID: Mm99999915_g1; NCBI RefSeq NM_008084.2) was used to normalize the relative mRNA levels. Values were calculated as described in a published method (Livak and Schmittgen, 2001).

2.2.4 RESULTS

2.2.4.1 Adult mice fed for 12 days with L-Dopa, BH_4 and pharmacological chaperons CIII/IV

11 weeks old *Th*-ki/ki mice were fed for 12 days either with 10.0/2.5 mg/kg/d L-Dopa/carbidopa, or 100 mg/kg/d BH_4, or 5 mg/kg/d pharmacological chaperons CIII or CIV. As controls, age matched *Th*-ki/ki and *Th*-wt/wt animals were loaded with 3 ml/kg/d ddH_2O. It was expected that at least CIII would stabilize and thus increase the TH activity or protein amount since it was shown that CIII stabilizes the human TH mutant R202H *in vitro* and led to an increase in TH activity and protein amount in wild-type mice (Calvo et al., 2010). Unfortunately, brain TH activity was difficult to measure probably due to the large content of catecholamines found in the wild-type mouse brains, which seems to inhibit the TH activity. In our preliminary TH activity determination approach, only CIV treated mice had significantly reduced brain TH activity in comparisons to wild-type animals (Fig. 9 A). Unexpected, none of the oral feeding compounds led to the increase of brain TH protein (Fig. 9 B). Only treatment with L-Dopa/carbidopa led to the improvement of norepinephrine (63 % of wt), HVA (110% of wt) and 5-HTP (54% of wt), as well as a strong increase in 3-O-methyldopa (3-OMD, 16,068% of wt), which is the indicator for a successful L-Dopa/carbidopa treatment (Fig. 9 C). In comparison to the 3 weeks L-Dopa treatment of *Th*-ki/ki mice, which were treated after birth (see chapter 2.1), the 12 days L-Dopa treatment in adult *Th*-ki/ki mice led to less restoration of the brain monoamine neurotransmitters and metabolites (Fig. 9 C).

A **Brain TH activity: Adult mice fed for 12 days with L-Dopa, BH_4, CIII or CIV**

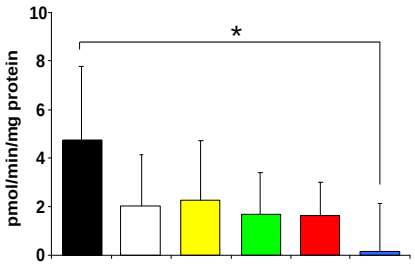

B **Brain TH protein: Adult mice fed for 12 days with L-Dopa, BH_4, CIII or CIV**

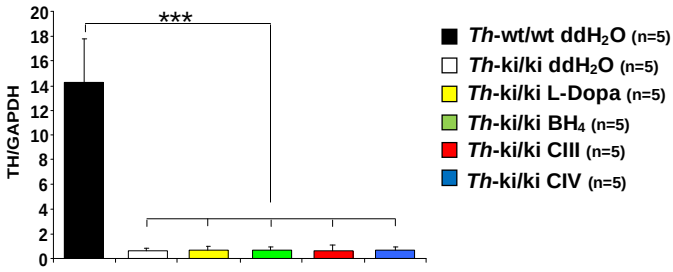

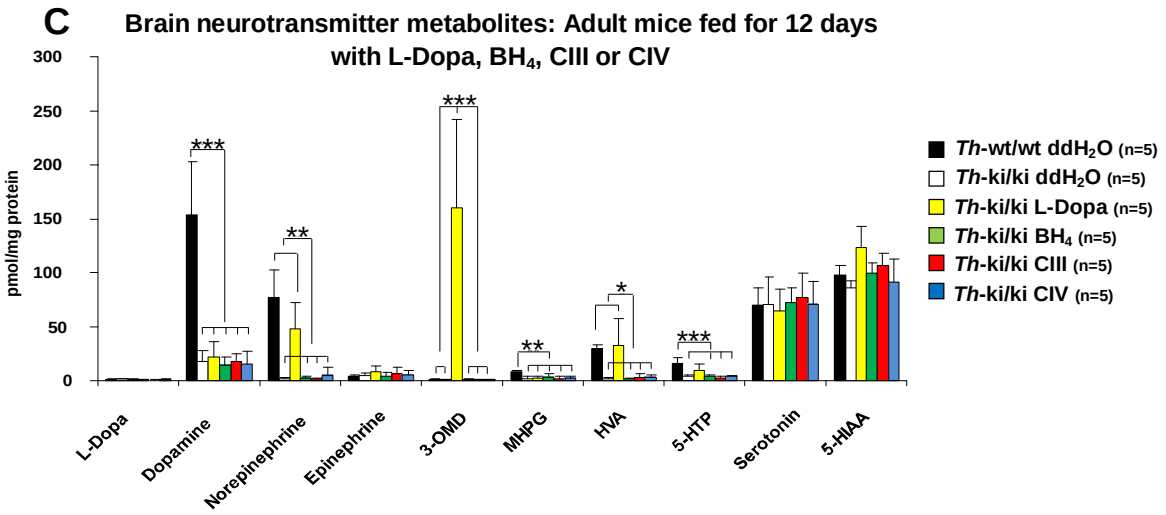

Figure 9: Biochemical analysis of brain tissue from adult mice fed for 12 days with 10.0/2.5 mg/kg/d L-Dopa/Carbidopa, 100 mg/kg/d BH_4, 5 mg/kg/d pharmacological chaperons CIII or CIV, or 3 ml/kg/d ddH_2O. **(A)** TH activity (pmol/min/mg protein). **(B)** TH protein (TH/GAPDH). **(C)** Monoamine neurotransmitters and metabolites (pmol/mg protein). *Th*-wt/wt treated with ddH_2O shown in black; *Th*-ki/ki treated with ddH_2O shown in white; *Th*-ki/ki treated with L-Dopa/carbodopa shown in yellow; *Th*-ki/ki treated with BH_4 shown in green; *Th*-ki/ki treated with CIII shown in red; *Th*-ki/ki treated with CIV shown in blue. Significant difference from the corresponding wild-type values is indicated by asterisks: * $p < 0.05$, ** $p < 0.01$, *** 0.001 (two-tailed Student's *t*-test).

The amount of biopterin in the brain was measured to confirm that the BH_4 crosses the BBB in BH_4 fed *Th*-ki/ki mice. Only *Th*-ki/ki mice fed with BH_4 had significantly more (1.5 times) BH_4 then wild-type control mice (Fig. 10). So far, there is no analytical method to detect pharmacological chaperon concentrations in brain or other tissues.

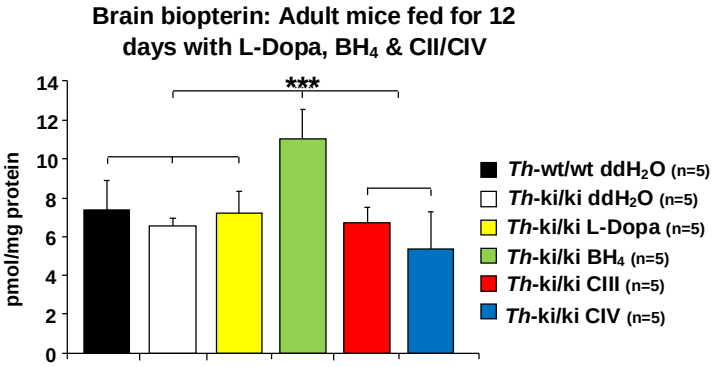

Figure 10: Biopterin measurements in brain of 12 days fed mice with 10.0/2.5 mg/kg/d L-Dopa/carbidopa, 100 mg/kg/d BH_4, or 5 mg/kg/d pharmacological chaperons CIII, CIV or 3 ml/kg/d ddH_2O (pmol/mg protein). *Th*-wt/wt treated with ddH_2O shown in black; *Th*-ki/ki treated with ddH_2O shown in white; *Th*-ki/ki treated with L-Dopa/carbodopa shown in yellow; *Th*-ki/ki fed with BH_4 shown in green; *Th*-ki/ki treated with CIII shown in red; *Th*-ki/ki treated with CIV shown in blue. Significant difference from the corresponding wild-type values is indicated by asterisks: *** $p < 0.001$ (two-tailed Student's *t*-test).

In the following, the influence of L-Dopa, BH_4, CIII or CIV on gene expression was analyzed. Despite testing the BH_4 cofactor depending genes m*Th*, m*Tph*1 and m*Tph*2, the m*Drd*1a (homolog to human Drd1), m*Drd*2-5, the m*Igf*-1 and m*Ddc* were analyzed in brain tissue. A summary of the gene expression is summarized in table 1.

Table 1: Gene expression (mRNA) in brain from *Th*-ki/ki and *Th*-wt/wt mice fed for 12 days with L-Dopa, BH_4, CIII and CIV.

Treatment	m*Th*-mRNA	m*Tph*1-mRNA	m*Tph2*-mRNA	m*Igf*-1-mRNA	m*Ddc*-mRNA
***Th*-ki/ki H_20** (n=5)	1.00 (0.58-1.74)	1.00 (0.70-1.43)	1.00 (0.40-2.51)	1.00 (0.89-1.13)	1.00 (0.66-1.52)
***Th*-wt/wt H_20** (n=5)	0.74 (0.48-1.16)	1.15 (0.93-1.42)	1.96 (0.95-4.08)	0.90 (0.81-0.99)	0.93 (0.61-1.41)
***Th*-ki/ki L-Dopa** (n=5)	1.48 (0.89-2.46)	1.63 (0.84-3.17)	2.39 (1.06-5.41)	0.97 (0.89-1.08)	1.31 (0.83-2.01)
***Th*-ki/ki BH_4** (n=5)	1.11 (0.64-1.93)	0.97 (0.83-1.13)	**3.74 (1.32-10.65)[a]**	**0.87 (0.82-0.92)[b]**	1.13 (0.66-1.93)
***Th*-ki/ki CIII** (n=5)	1.27 (0.82-1.96)	0.98 (0.89-1.09)	**6.36 (3.46-11.71)[c]**	0.88 (0.79-0.98)	1.43 (1.14-1.80)
***Th*-ki/ki CIV** (n=5)	1.36 (0.72-2.56)	1.35 (0.86-2.14)	**3.21 (1.11-9.28)[a]**	0.95 (0.83-1.08)	1.31 (0.79-2.19)

Treatment	m*Drd*1a-mRNA	m*Drd*2-mRNA	m*Drd*3-mRNA	m*Drd*4-mRNA	m*Drd*5-mRNA
***Th*-ki/ki H_20** (n=5)	1.00 (0.94-1.06)	1.00 (0.87-1.14)	1.00 (0.87-1.15)	1.00 (0.73-1.37)	1.00 (0.81-1.23)
***Th*-wt/wt H_20** (n=5)	0.89 (0.73-1.09)	0.81 (0.60-1.09)	0.84 (0.62-1.16)	1.25 (0.82-1.90)	1.10 (0.87-1.41)
***Th*-ki/ki L-Dopa** (n=5)	0.66(0.38-1.15)	1.11 (0.61-2.00)	0.94 (0.52-1.69)	0.86 (0.58-1.27)	**0.64 (0.41-1.00)[a]**
***Th*-ki/ki BH_4** (n=5)	**0.47 (0.35-0.62)[d]**	0.81 (0.61-1.08)	0.58 (0.31-1.11)	1.21 (0.89-1.66)	**0.60 (0.45-0.79)[c]**
***Th*-ki/ki CIII** (n=5)	**0.59 (0.41-0.86)[b]**	1.20 (0.80-1.81)	0.79 (0.37-1.72)	1.27 (0.82-1.96)	**0.53 (0.45-0.61)[d]**
***Th*-ki/ki CIV** (n=5)	**0.66 (0.55-0.79) [c]**	1.22 (0.99-1.51)	0.91 (0.64-1.30)	1.00 (0.65-1.55)	**0.48 (0.41-0.56)[d]**

Th-ki/ki fed with ddH_2O was set to 1. Significant difference from the corresponding *Th*-ki/ki control values: [a]$p < 0.1$, [b]$p < 0.05$, [c]$p < 0.01$, [d]$p < 0.001$ (two-tailed Student's *t*-test).

None of the oral treatments led to gene expression alteration of the m*Th*, m*Tph*1 and m*Ddc*. Contradictory to the published data, the BH_4, CIII and CIV treatment let to increased m*Tph*2 expression (Calvo et al., 2010). Furthermore, the BH_4, CIII, CIV and L-Dopa treatment led to decreased m*Drd*1a and/or m*Drd*5 gene expression whereas the m*Drd*2-4 were not altered. Generally, m*Igf*-1 gene expression is not different in *Th*-ki/ki mouse brains but the BH_4 treatment led to lower m*Igf*-1 gene expression.

To investigate if there is any improvement in motor function when treated with 10.0/2.5 mg/kg/d L-Dopa/carbidopa or 5 mg/kg/d CIII (BH_4 and CIV were not investigated), mice were tested for catalepsy by the bar test and their motor coordination by the rotarod test (Fig.11 A-D). *Th*-wt/wt and *Th*-ki/ki mice were fed at the age of 6 weeks with either L-Dopa or CIII. As control wild-type and *Th*-ki/ki mice were fed either with ddH_2O (L-Dopa control group) or DMSO/glucose solution (CIII control group).

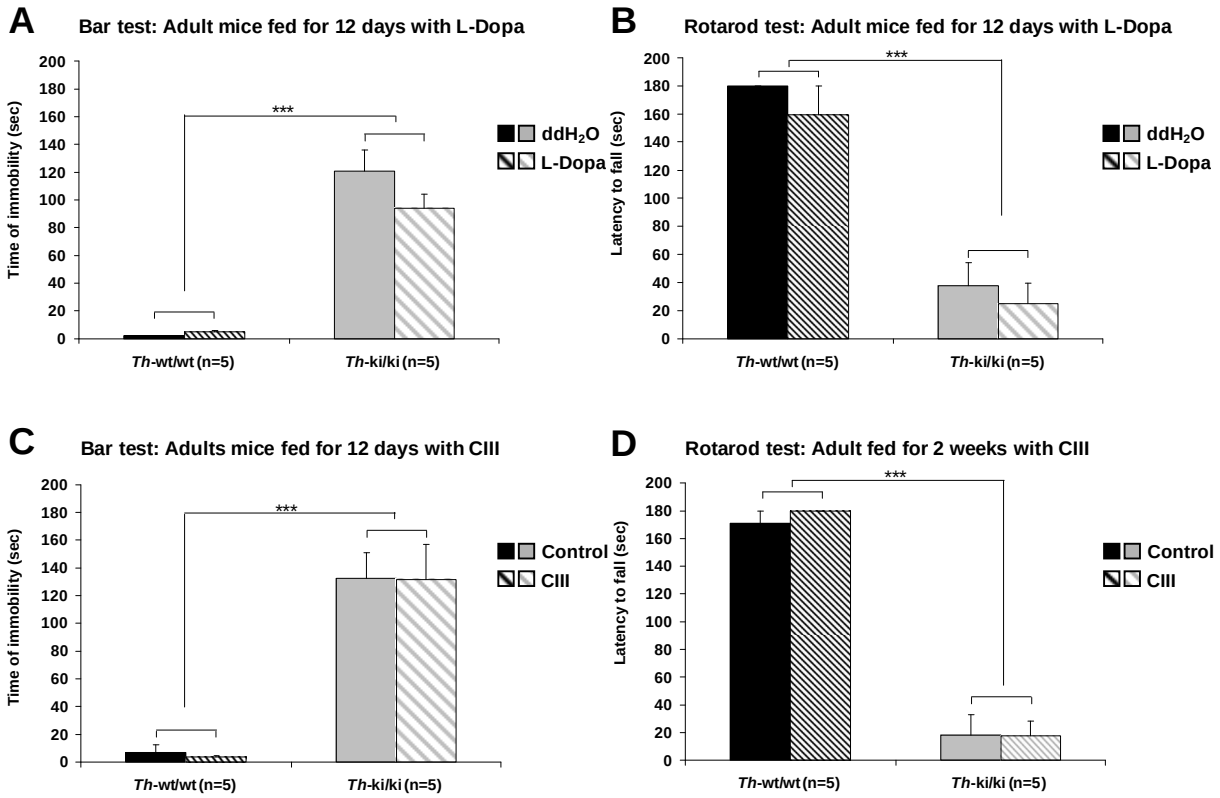

Figure 11: Catalepsy (bar test) and motor coordination (rotarod test) of adult mice fed for 12 days with 10.0/2.5 mg/kg/d L-Dopa or 3 ml/kg/d ddH_2O, and 5 mg/kg/d CIII or 1 ml/kg/d DMSO/glucose solution (control solution). **(A)** Bar test treated with L-Dopa or ddH_2O (sec). **(B)** Rotarod test treated with L-Dopa or ddH_2O (sec). **(C)** Bar test treated with CIII or control solution (sec). **(D)** Rotarod test treated with CIII or control solution (sec). *Th*-wt/wt treated with ddH_2O/control solution are shown in black; *Th*-wt/wt treated with L-Dopa/CIII are shown in black-white stripes; *Th*-ki/ki treated with ddH_2O/control solution are shown in gray; *Th*-ki/ki treated with L-Dopa/CIII are shown in gray-white stripes; ***p < 0.001 (two-tailed Student's *t*-test).

Neither the L-Dopa nor CIII treatment improved the catalepsy symptom or enhanced the motor coordination in *Th*-ki/ki mice. In comparison to the *Th*-ki/ki mice, wild-type mice showed significant better performances in both tests independent from the treatment.

In summary, only the L-Dopa treatment led to improvement in the brain monoamine neurotransmitters and none of the treatments had any positive effect on their motor function. Gene expression revealed alteration of m*Tph*2, m*Drd*1a/5 and/or m*Igf*-1 when treated with L-Dopa, BH_4, CIII or CIV.

2.2.4.2 Newborn mice fed for 3 weeks with the pharmacological chaperon CIII

As described in chapter 2.1, L-Dopa treatment over a period of 12 days of adult *Th*-ki/ki mice showed less improvement in brain monoamine neurotransmitters in comparison to newborn mice treated for a period of 3 weeks. Furthermore, treatment with CIII over a period of 12 days showed also no effect on brain catecholamines. Similarly as for the L-Dopa treatment, newborn *Th*-ki/ki mice were fed in a next step for 3 weeks with CIII, in order to exclude that treatment duration or age of mice diminish a potential positive therapeutic effect of CIII. Again difficulties in TH activity measurements led to none reliable results showing no difference in brain TH activity between *Th*-ki/ki and wild-type mice, independent from the treatment (Fig. 12 A). There was no increase of brain TH protein for *Th*-ki/ki or wild-type mice treated with CIII (Fig. 12 B). In addition, there was no improvement in brain monoamine neurotransmitters for *Th*-ki/ki or wild-type mice treated with CIII (Fig. 12 C).

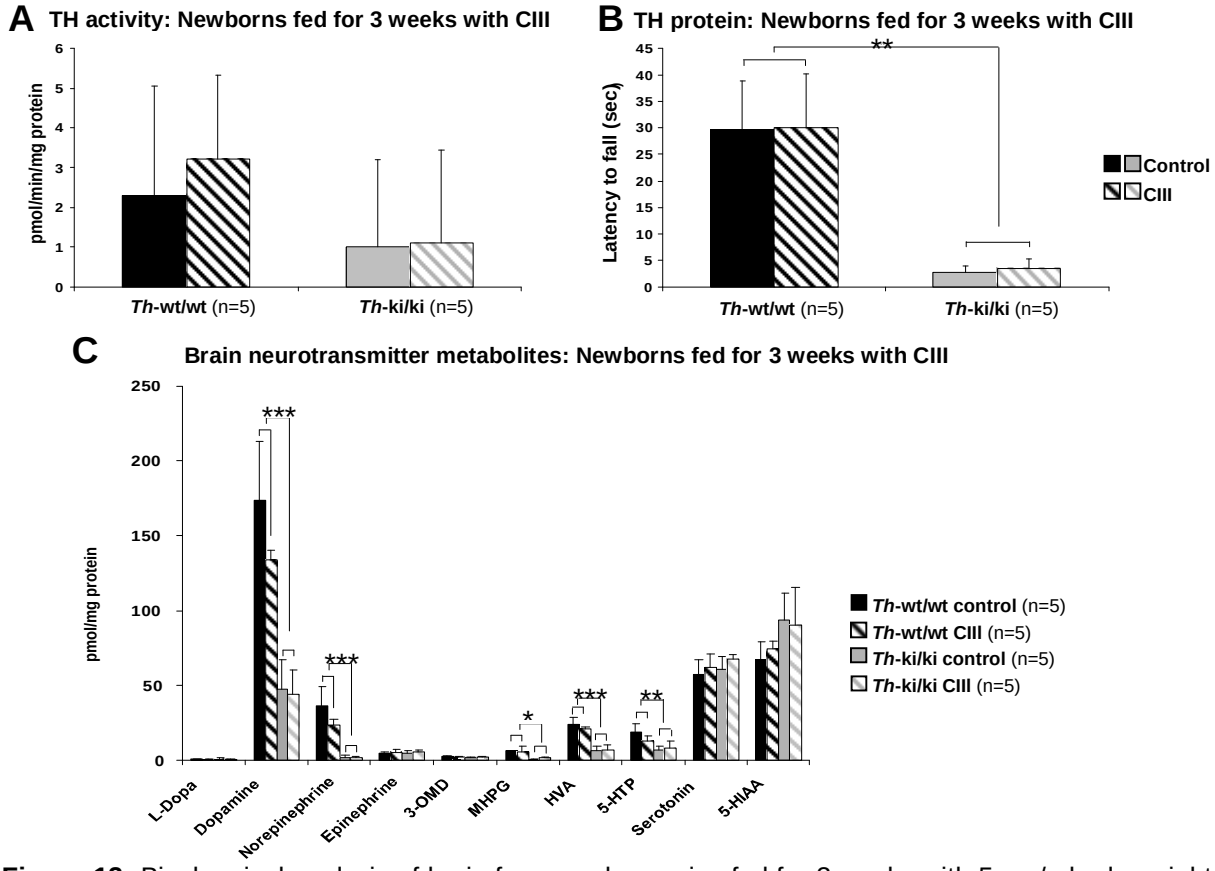

Figure 12: Biochemical analysis of brain from newborn mice fed for 3 weeks with 5 mg/g body weight of the pharmacological chaperons CIII. **(A)** TH activity (pmol/min/mg protein). **(B)** TH protein (TH/GAPDH). **(C)** Brain neurotransmitters (pmol/mg protein). *Th*-wt/wt mice treated with ddH_2O are shown in black; *Th*-wt/wt mice treated with CIII are shown in black-white striped; *Th*-ki/ki mice treated with ddH_2O are shown in gray; *Th*-ki/ki mice treated with CIII are shown in gray-white striped. Significant difference from the corresponding wild-type values is indicated by asterisks: * $p < 0.05$, ** $p < 0.01$, *** 0.001 (two-tailed Student's *t*-test).

Although, there was no significant improve in brain neurotransmitters the mice were tested for their catalepsy behavior and motor coordination (Fig. 13 A-B).

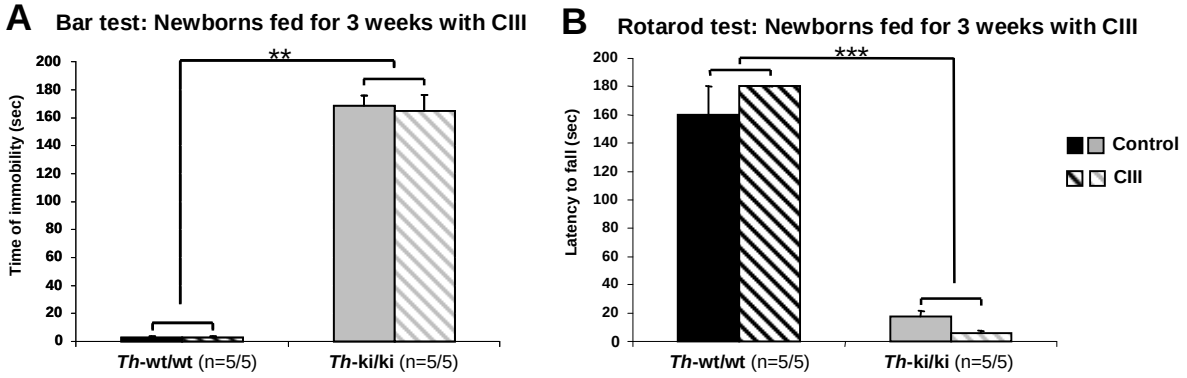

Figure 13: Catalepsy (bar test) and motor coordination (rotarod test) of newborn mice fed for 3 weeks with CIII. **(A)** Bar test (sec). **(B)** Rotarod test (sec). *Th*-wt/wt mice treated with control solution are shown in black; *Th*-wt/wt mice treated with CIII are shown in black-white stripes; *Th*-ki/ki mice treated with control solution are shown in gray; *Th*-ki/ki mice treated with CIII are shown in gray-white stripes; ***p < 0.001 (two-tailed Student's *t*-test).

The early and longer treatment with CIII did not lead to any improvement in the catalepsy symptom or the motor coordination in *Th*-ki/ki mice. In comparison to the *Th*-ki/ki mice, normal wild-type mice showed significant better performances in both tests independent from the treatment.

Adult mice fed for 12 days with CIII showed increased m*Thp*2 and decreased m*Drd*1a and m*Drd*5 mRNA-expression in the brain. Therefore, it was investigated if prolonged and earlier initiated CIII treatment in newborns would also lead to similar mRNA-expression alterations. Results are shown in table 2.

Table 2: Gene expression (mRNA) in brain from *Th*-ki/ki and wild-type mice fed for 3 weeks with CIII.

Treatment	m*Th*-mRNA	m*Tph*1-mRNA	m*Tph2*-mRNA	m*Igf*-1-mRNA
***Th*-ki/ki control** (n=5)	1.00 (0.46-2.16)	1.00 (0.70-1.42)	1.00 (0.49-2.03)	1.00 (0.82-1.22)
***Th*-ki/ki CIII** (n=5)	1.03 (0.54-1.96)	1.22 (0.92-1.63)	**0.14 (0.03-0.71)**[a]	1.04 (0.77-1.42)
***Th*-wt/wt control** (n=5)	1.34 (0.78-2.32)	**1.57 (1.32-1.85)**[b]	0.81 (0.24-2.70)	**0.71 (0.63-0.79)**[c]
***Th*-wt/wt CIII** (n=5)	0.94 (0.76-1.15)	1.23 (0.90-1.68)	**0.31 (0.13-0.76)**[a]	**0.75 (0.66-0.84)**[b]

Treatment	m*Drd*1a-mRNA	m*Drd*2-mRNA	m*Drd*3-mRNA	m*Drd*4-mRNA	m*Drd*5-mRNA
***Th*-ki/ki control** (n=5)	1.00 (0.77-1.31)	1.00 (0.62-1.62)	1.00 (0.78-1.28)	1.00 (0.74-1.36)	1.00 (0.82-1.22)
***Th*-ki/ki CIII** (n=5)	1.13 (0.76-1.68)	1.33 (0.82-2.18)	1.01 (074-1.38)	0.83 (0.56-1.22)	0.90 (0.58-1.41)
***Th*-wt/wt control** (n=5)	1.02 (0.69-1.52)	1.27 (0.74-2.20)	1.07 (0.41-2.79)	**0.52 (0.35-0.78)**[b]	1.26 (0.94-1.69)
***Th*-wt/wt CIII** (n=5)	1.03 (0.77-1.38)	1.51 (1.00-2.28)	1.06 (0.63-1.81)	1.05 (0.76-1.39)	**0.76 (0.58-0.98)**[a]

Th-ki/ki fed with control solution was set to 1. Significant difference from the corresponding *Th*-ki/ki control values: [a]p < 0.1, [b]p < 0.05, [c]p < 0.01, (two-tailed Student's *t*-test).

The prolonged CIII treatment did not alter the m*Th*-mRNA expression in the *Th*-ki/ki and wild-type mice. Surprisingly, the three weeks treated mice did not mirror the same mRNA-expression alterations seen in adult mice treated for 12 days. *Th*-ki/ki and wild-type mice fed for three weeks with CIII showed reduced m*Tph*2-mRNA expression levels whereas the 12 days treatment in adult *Th*-ki/ki mice showed increased m*Tph*2-mRNA expression. Furthermore, *Th*-wt/wt mice fed with CIII had significant increased m*Tph*1-mRNA expression. The prolonged CIII treatment did not alter the m*Drd*1a-3 mRNA-expression. Wild-type but not *Th*-ki/ki mice fed with CIII presented significant reduced m*Drd*5-mRNA expression levels as seen before in 12 days CIII treated adult *Th*-ki/ki mice. Furthermore, there is the indication that 3 weeks old *Th*-ki/ki mice might have higher *Drd*4-mRNA expression then corresponding wild-type animals. Unexpected, *Th*-ki/ki mice showed independent from the oral feeding increased m*Igf*-1 gene expression in comparison to wild-type mice. These results are contradictory to the results found in adult mice were brain m*Igf*-1 gene expression was not different from wild-type mice.

2.2.5 DISCUSSION

Overall, it was shown that the 12 days oral treatment with potential TH chaperons BH_4, or CIII/IV had no effect on brain m*Th* gene expression and translation, TH activity, monoamine neurotransmitter restoration or motor function in *Th*-ki/ki mice independent from their age or feeding duration. Only the L-Dopa/carbidopa treatment showed again some improvement in the catecholamines, although it was less efficient then the 3 weeks treatment started after birth. It is unknown, if a prolonged treatment in adult mice would lead to similar improvement or if the effect of L-Dopa is also age dependent. So far, it could have been validated that the additional applied BH_4 reached the mouse brain. Although BH_4 passed the BBB and thus reached the brain, there was no improvement in the catecholamines. Unfortunately there was no method available to quantify the amount of CIII or CIV in the brain to show that these compounds can cross the BBB reaching the TH. The *Th*-p.R203H mutation leads to highly destabilization of the TH protein. So far, it is unknown if a chaperon can stabilize this fragile mutant protein or if higher concentrations would improve the TH stability leading to more activity. It is highly likely that the mutant TH is too severe affected that stabilization would be possible.

No alterations in the brain m*Th*, m*Tph*1/2, m*Drd*1a-5, or m*Ddc* gene expression was found in *Th*-ki/ki mice in comparison to wild-type animals. Surprisingly, treatment with BH_4, CIII or CIV increased brain m*Tph*2 (321-636% of wt) gene expression in adult *Th*-ki/ki mice fed for 12 days but not in 3 weeks treated animals. Brain m*Tph*1-RNA expression was only significant increased in wild-type animals when fed for 3 weeks with CIII. The through CIII or IV altered m*Tph*1/2 gene expression stays in contrary to the published data about CIII/CIV, where no alteration in mTph1/2 gene expression was reported (Calvo et al., 2010). It was already described that supplementation of BH_4 leads to increased mTPH2 activity *in vitro* (Yang and Kaufman, 1994). Therefore, it would be interesting to measure mTPH2 activity in BH_4, CIII or CIV treated *Th*-ki/ki mice. Elevated expression of m*Tph*2 mRNA at the neuronal level was associated with increased anxiety-like behavior in mice and depressed suicides in humans (Hiroi et al., 2006, Bach-Mizrachi et al., 2008, Lowry et al., 2008). In contrast, polymorphisms in m*Tph*2 were associated with the attention-deficit hyperactivity disorder. So far, it has been reported that there are no side effects caused by long-term administration of BH_4 (Cerone et al., 2004, Hennermann et al., 2005). Still the

question arises if through BH_4, CIII or CIV treatment induced increased expression of m*Tph*2 would lead to an anxiety-like or depressive behavior in the *Th*-ki/ki mice.

L-Dopa, BH_4, CIII or CIV treatments led to decreased gene expression of brain m*Drd*1a (47-66% of wt), m*Drd*5 (48-64% of wt) and/or m*Igf*-1 (87% of wt) in 12 weeks old *Th*-ki/ki mice. It is unknown why the oral feeding of the substances led to this gene expression alterations. It was shown that D1A-/- mutant mice are growth retarded and die shortly after weaning unless their diet was supplemented with hydrated food, but they exhibit normal coordination and locomotion (Drago et al., 1994). In contrast, D5-/- mutant mice had a normal development but increased sympathetic tone and were hypertensive (Hollon et al., 2002). Further studies are needed to be done to elucidate the question if dopamine receptors are equally influenced in wild-type mice by the BH_4 or CIII/IV treatment as seen in *Th*-ki/ki mice.

The investigated m*Igf*-1 gene expression revealed that 3 weeks old *Th*-ki/ki mice seems to have increased m*Igf*-1 gene expression in comparison to wild-type mice, which was not the case in 12 weeks old *Th*-ki/ki mice, which also had normal serum IGF-1 levels (see chapter 2.1). The anabolic IGF-1 is synthesized in almost all tissues, dominantly in the liver which is the main contributor to serum IGF-1. IGF-1 is an important mediator for cell growth, differentiation, and transformation (Delafontaine et al., 2004). Studies with growth hormone (GH) depleted *Ghr*ī /ī mice showed that serum IGF-1 was as low as approximately 0.2% of the normal level. Therefore, serum IGF-1 levels are GH-dependent, excluding all tissues in which *Igf*-1 expression is GH-independent, such as the skeletal system, brain, lung, heart, spleen, testis, and uterus (Stratikopoulos et al., 2008). Therefore, the brain m*Igf*-1 gene expression does not influence serum IGF-1 levels. It was demonstrated that IGF-I plays has a highly distinctive pattern of gene expression during brain development and is essential for both fetal and postnatal CNS growth and development (Bondy, 1991, Netchine et al., 2009). *In vitro* and *in vivo* studies have demonstrated that IGF-1 stimulates mitosis in sympathetic neuroblasts, promotes embryonic neuronal survival and neurite outgrowth in cultured sensory, sympathetic, cortical, and motor neurons, induce oligodendrocyte differentiation, and is involved in dendritic maturation, synaptogenesis, and myelinization (Bondy, 1991). One of the many effects of IGF-1 in the CNS is promoting neuronal survival through activation of the PI3K/Akt pathway. It was shown that astrocyte-specific overexpression of IGF-1

protects hippocampal neurons and reduces behavioral deficits following traumatic brain injury in mice (Madathil et al., 2013). Transgenic mice that overexpress IGF-I exhibit marked brain overgrowth postnatally, whereas transgenic mice with ablated IGF-I gene expression have brain growth retardation (Calikoglu et al., 2001). Furthermore, studies of transgenic mice that overexpress IGF-I exclusively in the CNS, showed an increase in cerebellar granule cell number that appeared to be attributable predominantly to enhanced survival (Chrysis et al., 2001). It can be hypothesized that young *Th*-ki/ki mice might have overexpressed IGF-1 in brain to compensate the potential negative influence on brain development due to the TH deficiency. Further analysis of gene expression of unmature and developing mice should be done to further study *Igf*-1 expression in brain and peripheral tissues and IGF-I levels should be determined in the plasma. Furthermore, BH_4 treated *Th*-ki/ki mice had slightly compromised m*Igf*-1 gene expression (87% of wt). There are no studies describing any correlation of BH_4 on m*Igf*-1 gene expression, and therefore it is suggested to increase the cohort of mice to verify these results.

Overall, gene expression was not altered equally in two CIII treatment studies. Adult *Th*-ki/ki mice with 12 days treatment had more expression alterations in the investigated genes then juvenile mice fed for 3 weeks. It is highly likely that gene expression in the young mice cohort is more variable since the 3 weeks mice are still developing to become mature. Therefore, there are higher variations in the gene expressions, which may impede to find differences in small cohorts. It is also debatable if mRNA-expression is only short-term altered and stabilizes after time. Since it is not possible yet to measure the amount of CIII in the brain, it makes it more difficult to interpret the current data. More studies could be done to investigate further this phenomenon.

Still a huge challenge for the severe from of THD is in fact that although there is an improvement in brain monoamine neurotransmitters by L-Dopa/carbidopa treatment, there is no change in motor function probably due to prenatal developed lack of projection into the striatum, which plays an important role in planning and modulation of movement pathways (Voytek and Knight, 2010). Further oral treatment studies could investigate if projection into the striatum in *Th*-ki/ki mice increases and therefore, also their motor functions, when *Th*-ki/ki mice are already treated with L-Dopa/carbidopa, BH_4, or CIII/IV prenatal.

2.3 INVESTIGATION OF A GENE THERAPEUTIC APPROACH TARGETING THE LIVER USING AAV TO RESTORE THE BRAIN CATECHOLAMINE IN *TH*-KI/KI MICE

2.3.1 ABSTRACT

The standardized treatment of 10 mg/kg/d L-Dopa in combination with 25% carbidopa could restore the lowered brain monoamine neurotransmitter concentration in *Th*-ki/ki mice but it did not improve the motor behavior. In this chapter it was attempted to correct the altered motor function in *Th*-ki/ki mice by a different approach, i.e. hepatic rAAV2/8 gene transfer of the m*Th*-cDNA expressed from the (artificial) liver specific promoter P3. The transgenic TH enzyme, expressed from the rAAV2/8 transduced hepatic cells, was expected to lead to the conversion of L-Tyr to L-Dopa in the periphery, i.e. liver. To prevent peripheral degradation of L-Dopa, the AADC inhibitor carbidopa was added to the drinking water during an experimental period of three weeks. After this treatment, mice were investigated for their motor function by bar and rotarod tests showing no improvement. Whole brain monoamine neurotransmitters revealed no restoration. Evaluation of the vector copy number in the hepatic cells revealed efficient transduction of the rAAV2/8 and m*Th*-mRNA expression was confirmed. TH activity in brain was unchanged. The protein amount in liver and brain is still under investigation.

2.3.2 INTRODUCTION

The severe form of THD is difficult to treat and side effects can occur like dyskinesias, gastrointestinal side effects or hypersensitivity of the L-Dopa therapy as well as from other dopaminergic agonists (Furukawa, 2003, Hoffmann et al., 2003). *Th*-ki/ki mouse studies showed that oral application of L-Dopa for a limited period of 12 days or 3 weeks improved or normalized the brain catecholamines but did not corrected their motor function (described in chapter 2.1 and 2.2). As an alternative to oral loading, experimental gene therapy to potentially correct THD was attempted next then AAV mediated gene expression in brain is a widely used approach in preclinical studies (Fig. 14). 6-OHDA lesioned rats (PD model) applicated with AAV vectors expressing h*TH* in the brain had long-term recovery of striatal expression of mRNA, TH enzyme activity, extracellular dopamine concentration and behaviour (Chakrabarty et al., 2013, During et al., 1994). Although this approach was successful, the use of AAV as a vector for gene therapy to targeting the brain is quite invasive approach with unknown risks. Therefore, it was investigated whether targeting of the *Th*-ki/ki mouse liver with a rAAV2 serotype 8 vector expressing m*Th* from a liver-specific synthetic promoter P3, lead to the production of L-Dopa synthesis in the periphery (Fig. 14) (Viecelli et al., 2014). Analog to oral L-Dopa treatment for patients, carbidopa needs to be given in addition to prevent peripheral conversion, i.e. degradation to dopamine by the enzymatic reaction of AADC (Fig. 14). It is assumed that the in liver produced L-Dopa lead to the restoration of the brain catecholamines and the motor function in the *Th*-ki/ki mice.

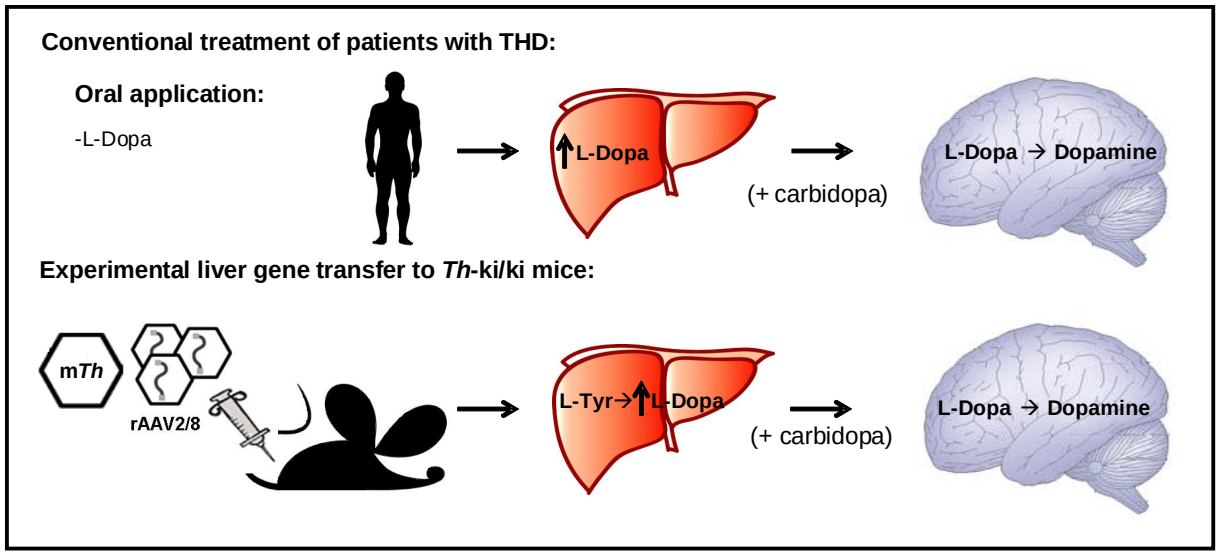

Figure 14: Schematic representation of viral gene therapeutic approach for *Th*-ki/ki mice. L-Tyr, L-tyrosine; m*Th*, tyrosine hydroxylase cDNA.

2.3.3 MATERIALS AND METHODS

In the following, additional methods are described that are not present in chapter 2.1 or 2.2 with the general description of the *Th*-ki mouse model (Korner et al, in preparation).

2.3.3.1 Generation of the AAV vector

The m*Th* cDNA (transcript ID: ENSMUST105929) was synthesized by GeneArt® Life technology (Regensburg, Germany). This synthesized m*Th* cDNA sequence was used to generate the viral vector AAV2-*Th*.

2.3.3.2 Production of rAAV

rAAV was produced in collaboration with Cary O. Harding and Shelley Winn from Oregon Health & Science University (Oregon, Portland, USA) (Grieger et al., 2006).

2.3.3.3 Application of rAAV2/8 and carbidopa

Three weeks old *Th*-ki/ki or wild-type mice were i.p. injected with 2 x 10^{12} vector particles (vp) AAV2/8-*Th* or saline using a U-100 insulin syringe with a 28G needle. One tablet of 25 mg carbidopa (Lodosyn®; ATON Pharma Inc., New York, USA) was diluted in 125 ml drinking water (200 mg/l) and applied to the mice *ad libitum*.

2.3.3.4 Copy number assay

The copy number per diploid genome was measured as described in the published methods (Lu et al., 2012, Viecelli et al., 2014). The primers used in the quantitative PCR analysis correspond to the WPRE and are published (Ding et al., 2006).

2.3.3.5 Gene (Th-mRNA) expression study

Mouse *Th*-mRNA expression levels were performed using commercially available ABI assay (Mm00447553_g1; NCBI RefSeq NM_009377.1). Values were calculated as described in chapter 2.1 or 2.2.

2.3.4 RESULTS

For the liver specific gene therapy for the *Th* deficient mice, the following AAV2 vector expressing m*Th* was generated (AAV2-*Th*), which is schematically represented in Fig. 15. The transgene cassette was expressed by the liver specific P3 promoter (minimal transthyretin promoter, TTR_{min}, coupled to a de novo designed hepatocyte-specific cis-regulatory module 8, HS-CRM 8) (Viecelli et al., 2014). The woodchuck hepatitis virus posttranscriptional regulatory element (WPRE) was added downstream of the m*Th* sequence to enhance the transgene transcription.

Figure 15: Schematic representation of the AAV2-*Th* vector. P3, minimal TTR_{min} coupled to a de novo designed HS-CRM 8; m*Th*, murine tyrosine hydroxylase cDNA; WPRE, woodchuck hepatitis virus posttranscriptional regulatory element; pA, poly A tail; I, inverted terminal repeats.

Th-ki/ki or wild-type mice were i.p. injected with either 2 x 10^{12} vp of the recombinant AAV2/8-*Th* (rAAV2/8-*Th*) or saline. Mice were kept for three weeks under 200 mg/l carbidopa in the drinking water *ad libitum*. Brain lysate was analyzed for their TH activity and brain monoamine neurotransmitters (Fig. 16 A-C). As expected, *Th*-ki/ki mice had significant lower TH activity in the brain than wild-type animals independent from the treatment (Fig. 16 A). In general, the rAAV-*Th* treated mice did not have higher TH activity in liver (Fig. 16 B). In contrast, saline treated *Th*-ki/ki mice had significant higher TH activity than the wild-type mice for unknown reasons (Fig. 16 B). There was no improvement in brain monoamine neurotransmitters in the rAAV2/8-*Th* injected *Th*-ki/ki mice although it seems that saline treated *Th*-ki/ki mice had significant lower 3-OMD levels in comparison to the other groups (Fig. 16 C). Alterations of 3-OMD in *Th*-ki/ki mice was not described yet.

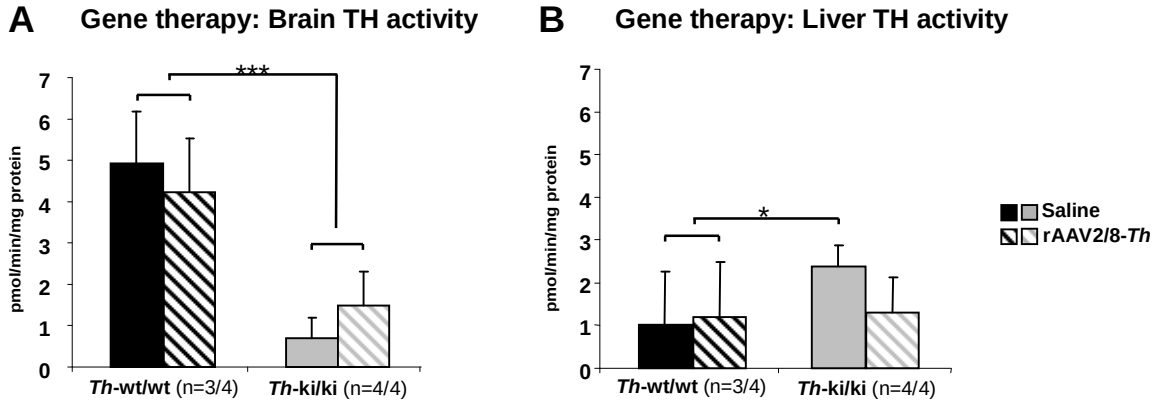

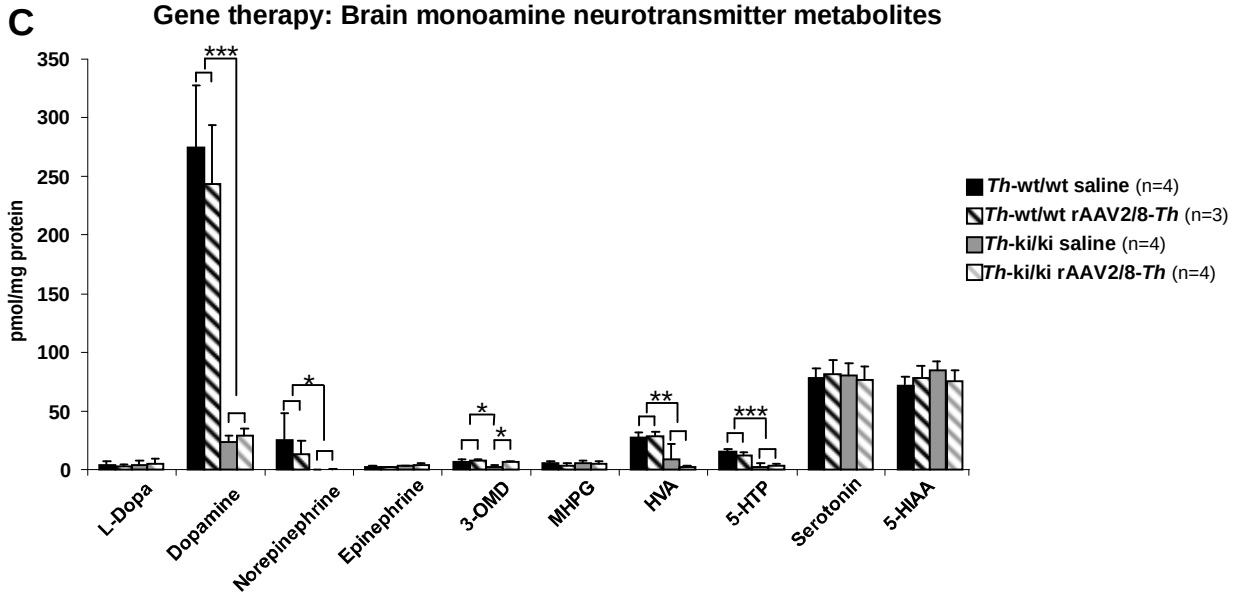

Figure 16: Biochemical analysis of rAAV2/8-*Th* or saline treated *Th*-ki/ki or *Th*-wt/wt mice. **(A)** Brain TH activity (pmol/min/mg protein). **(B)** Liver TH activity (pmol/min/mg protein). **(C)** Brain neurotransmitters (pmol/mg protein). *Th*-wt/wt mice injected with saline are represented in black; *Th*-wt/wt mice injected with rAAV2/8-*Th* are represented in black-white stripes; *Th*-ki/ki mice injected with saline are represented in gray; *Th*-ki/ki mice injected with rAAV2/8-*Th* are represented in gray-white stripes. Significant difference from the corresponding wild-type values is indicated by asterisks: * p < 0.05, ** p <0.01, *** 0.001 (two-tailed Studentôs *t*-test).

Gene therapy treated mice also showed no improvement in there motor behavior (Fig. 17 A-B).

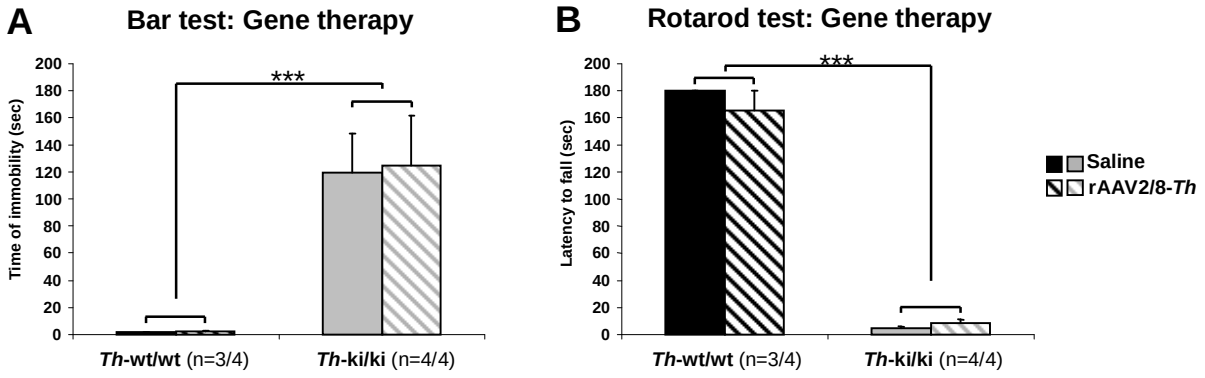

Figure 17: Catalepsy (bar test) and motor coordination (rotarod test) of gene therapy treated mice. **(A)** Bar test (sec). **(B)** Rotarod test (sec). *Th*-wt/wt mice injected with saline are represented in black; *Th*-wt/wt mice injected with AAV2/8-*Th* are represented in black-white stripes; *Th*-ki/ki mice injected with saline are represented in gray; *Th*-ki/ki mice injected with AAV2/8-*Th* are represented in gray-white stripes; ***p < 0.001 (two-tailed Studentôs *t*-test).

To determine if the AAV2/8-*Th* vector was present in the liver, the average number of vector genomes per diploid hepatocyte and the *Th*-mRNA expression in all liver cells was calculated (table 3) (Livak and Schmittgen, 2001, Lu et al., 2012, Viecelli et al., 2014).

Table 3: DNA copy number per diploid genome and m*Th*-mRNA transgene expression of rAAV2/8-*Th* treated mice.

Genotype	Treatment	DNA copy number/diploid genome	m*Th*-mRNA*
Th-wt/wt (n=4)	saline	n.a.	1.0 (0.8-1.3)
Th-wt/wt (n=3)	rAAV2/8-*Th*	6.8 ± 5.6	7,383.0 (2,635.0-20,685.0) [a]
Th-ki/ki (n=4)	saline	n.a.	1.1 (0.8-1.5)
Th-ki/ki (n=4)	rAAV2/8-*Th*	8.8 ± 2.8	24,902.5 (21,288.7-29,129.6)[a]

n.a., not applicable; * m*Th*-mRNA gene expression was normalized to *Gapdh* and *Th*-wt/wt treated with saline was set to 1. Significant difference from the corresponding wild-type values: [a]p< 0.001 (two-tailed Student's *t*-test).

Both, rAAV2/8-*Th* treated wild-type and *Th*-ki/ki mice had detectable amount of vector-DNA in the liver. There was no significant difference in the DNA copy number per diploid genome between AAV2/8-*Th* treated wild-type and *Th*-ki/ki mice. As shown in table 3, between 6-9 copies per hepatocyte were detected 21 days after rAAV2/8-*Th* injection. The liver m*Th*-mRNA gene expression analysis showed between 7,000-25,000 folds increase in m*Th*-mRNA expression in rAAV2/8-*Th* injected mice. *Th*-ki/ki mice treated with rAAV2/8-*Th* had significant higher liver m*Th*-mRNA expression then rAAV2/8-*Th* applicated wild-type mice ($p<0.05$). Furthermore, rAAV2/8-*Th* treated *Th*-ki/ki and *Th*-wt/wt mice had in average almost 57 ($p<0.001$) and 17 ($p<0.001$) times more m*Th*-mRNA expression (quantitative measurement), respectively, in comparison to m*Th*-mRNA expression levels found in untreated wild-type mouse brains.

2.3.5 DISCUSSION

The rAAV2/8-*Th* treated wild-type and *Th*-ki/ki mice showed significantly increased liver m*Th*-mRNA expression, which was between 17-57 times relative higher than m*Th* expression found in wild-type mouse brains. Changes in TH protein amount in liver still needed to be analyzed. Although m*Th* was very high expressed in the liver, there was no increase in the hepatic TH activity and therefore, there was no improve of brain monoamine neurotransmitter deficiency in *Th*-ki/ki mice. Higher viral dosages or different application methods could be tested. It was reported that intravenous virus application through the tail vein led to higher transgene expression in liver in comparison to i.p. injection (Dane et al., 2013). In the here presented study, the AAV-*Th* vector was delivered via i.p. injections, which might explain the relative low hepatic copy number of vector genomes. It is also possible that, although mRNA is expressed, the transcript was not translated into a protein sequence. Further analyses, including for instance Western blot, are necessary to rule out a potential translation problem and to proof that the lack of hepatic TH protein activity is responsible for the absence of increased brain L-DOPA following liver directed gene therapy. Low mRNA expression might be caused inefficient transport from the nucleus into the cytoplasm for translation. In this context, it has been shown that insertion of intronic sequence into a transgene cassette increases mRNA expression by supporting the delocalization of mRNA from the nucleus into the cytoplasm for translation (Buchman and Berg, 1988, Palmiter et al., 1991). Therefore, insert of an intron into the TH vector sequence might be beneficial to improve transgene expression. Furthermore, the *ad libitum* application method of adding carbidopa in the drinking water had the advantage that the mice receive carbidopa constantly but has the disadvantage that it was difficult to monitor their exact intake. It is also unknown how stable diluted carbidopa is over time. To avoid this unsteady administration of carbidopa, future rAAV gene therapeutic approaches should be directly applied to the brain. The successful delivery of rAAV into the mouse brain was described by either direct brain targeting of by peripheral injection through intracardiac administration route or by the intravenously by the superficial temporal vein (Rahim et al., 2011, Iwata et al., 2013, von Jonquieres et al., 2013). Furthermore, intravenously injection of rAAV2/9 into fetal mice *via* vitelline vessels to target the CNS was described (Rahim et al., 2011). The advantage of the intracardiac method is that the whole brain can be reached and not only restricted

brain areas (Iwata et al., 2013). The application method also depends on the age of the mice. Injections of neonates can be so far only performed by direct injection into the brain (Kim et al., 2013). Intracerebroventricular injection with rAAV2/1 on neonatal day P0 results in widespread CNS expression, whereas the biodistribution is limited if injected beyond neonatal day P1 (Chakrabarty et al., 2013). Also the choice of the AAV capsid serotype can influence the distribution if the rAAV in the brain: it was demonstrated that rAAV2/8 and 2/9 resulted in the most widespread biodistribution in the brain (Chakrabarty et al., 2013). In contrast, rAAV2/5 showed very limited brain transduction after neonatal injection (Passini et al., 2003). Furthermore, the biodistribution of most serotypes varying depending on the day of injection, like e.g. injection on neonatal day P0 resulted in mostly neuronal transduction, whereas administration between 24-84 hours postnatal resulted in more non-neuronal transduction (Chakrabarty et al., 2013). It was shown that a single rAAV2/1 intraventricular injection led to live long treatment in a ß-glucuronidase-deficient mouse model (mucopolysaccharidosis type VII) (Passini et al., 2003). Furthermore, it was described that rAAV2/8 achieved higher level of gene transfer to the central CNS upon intraventricular injection in neonatal mice compared to rAAV2/1 and rAAV2/2 (Broekman, 2005). Another application for targeted gene delivery is the *in vivo* electroporation of CNS, which can also be used to apply non-viral vectors (Saito, 2006, De Vry et al., 2010). Still AAV injection into the neonatal mouse brain accesses more regions of the brain including the cerebellum and brainstem that have been difficult to target by electroporation (Kim et al., 2013). Nevertheless, new AAV are described that have smaller and optimized AAV expression cassettes, which showed improved packaging capacity and transgene expression in neurons and would therefore, also increase rAAV efficacy (Choi et al., 2014). A phase 1 study of intrastriatal infusion of AAV encoding human AADC in subjects with PD was already tested (ClinicalTrials.gov, number: NCT00229736). Another phase 1 PD study showed the safety and tolerability of gene therapy with a rAAV expressing the glutamic acid decarboxylase (GAD) gene (ClinicalTrials.gov, number: NCT00195143). Multicistronic vector-mediated striatal gene transfer of TH, AADC, and GTPCH resulted in more effective dopamine production and more remarkable behavioural recovery in 6-OHDA lesioned Parkinsonian rats compared with the expression of TH alone (Fan et al., 1998). Furthermore, non-viral gene therapy of 6-OHDA lesioned Parkinsonian rats using a TH expression plasmid encapsulated inside a pegylated

immunoliposome led to increased TH enzyme activity and TH immunocytochemistry showed that the entire striatum was immunoreactive for TH after the intravenous gene therapy (Zhang et al., 2003).

Taken together, rAAV gene treatment by targeting the brain of neonatal *Th*-ki/ki mice would be a considerable approach to treat the monoamine neurotransmitter deficiency and the motor deficiency, and therefore, it would be a potential treatment for THD patients.

3.

CHARACTERISATION OF MOUSE MODELS WITH MILDY COMPROMISED BH_4 BIOSYTHESIS: *PTS*-KI/KI AND *PTS*-KI/KO

Chapters:

- 3.1 MANUSCRIPT: ABNORMAL BODY FAT DISTRIBUTION AND ABDOMINAL OBESITY IN MOUSE MUTANT WITH MIDLY COMPROMISED TETRAHYDROBIOPTERIN COFACTOR BIO-SYNTHESIS

- 3.2 CHALLENGING THE OBSERVATION OF ñUNAFFECTEDò AND ñAFFECTEDò *PTS*-KI/KO MICE FROM DIFFERENT BREEDING COMBINATIONS OF *PTS*-KI AND *PTS*-KO PARENTS

3.1 MANUSCRIPT: ABNORMAL BODY FAT DISTRIBUTION AND ABDOMINAL OBESITY IN MOUSE MUTANT WITH MIDLY COMPROMISED TETRAHYDROBIOPTERIN COFACTOR BIO-SYNTHESIS

Running title: Obesity in mice with compromised BH_4 biosynthesis

Germaine Korner[1,2,*], Tanja Scherer[1,2*], Dea Adamsen[1,2], Alexander Rebuffat[1], Anahita Rassi[3], Rossana Scavelli[1], Daigo Homma[4], Birgit Ledermann[5], Daniel Konrad[6], Hiroshi Ichinose[4], Christian Wolfrum[7], Marion Horsch[8], Birgit Rathkolb[8,9,13], Martin Klingenspor[10,11], Johannes Beckers[8,12,13], Eckhard Wolf[9], Valérie Gailus-Durner[8], Helmut Fuchs[8], Martin Hrabě de Angelis[8,12,13], Nenad Blau[1], Jan Rozman[8,10,13,], and Beat Thöny[1,2,**]**

[1] Division of Metabolism, University Childrenôs Hospital Zürich, Switzerland

[2] Affiliated with the Neuroscience Center Zurich (ZNZ), University of Zurich and ETH Zurich, Switzerland, and the Chidrenôs Research Center (CRC), Zürich, Switzerland

[3] Division of Clinical Chemistry and Biochemistry, University Childrenôs Hospital Zürich, Switzerland

[4] Department of Life Science, Graduate School of Bioscience and Biotechnology, Tokyo Institute of Technology, Yokohama, Japan

[5] Division of Animal Facility, University of Zurich, Switzerland; current address:

[6] Division of Pediatric Endocrinology and Diabetology, University Childrenôs Hospital Zürich, Switzerland

[7] Institute of Food Nutrition and Health, Swiss Federal Institute of Technology Zürich, Switzerland

[8] German Mouse Clinic, Institute of Experimental Genetics, Helmholtz Zentrum München, German Research Center for Environmental Health, Ingolstädter Landstrasse 1, 85764 Neuherberg, Germany

[9] Institute of Molecular Animal Breeding and Biotechnology, Gene Center, Ludwig-Maximilians-Universität München, Feodor-Lynen-Str. 25, 81377 Munich, Germany

[10] Molecular Nutritional Medicine, Else Kröner-Fresenius Center, Technische Universität München, Am Forum 8, 85354 Freising-Weihenstephan, Germany

[11] ZIEL ï Center for Nutrition and Food Sciences, Technische Universität München, D-85350 Freising, Germany

[12] Chair of Experimental Genetics, Center of Life and Food Sciences Weihenstephan, Technische Universität München, D-85354 Freising-Weihenstephan, Germany

[13] German Center for Diabetes Research (DZD), Ingolstädter Landstrasse 1, 85764 Neuherberg, Germany

* the first two authors have contributed equally

** Co-correspondence:
Dr. Beat Thöny, Division of Metabolism, University Childrenôs Hospital Zürich, Steinwiesstrasse 75, CH-8032 Zürich, Switzerland; tel: +41 44 266 76 22; fax: +41 44 266 71 69; e-mail: beat.thony@kispi.uzh.ch

Dr. Jan Rozman, Institute of Experimental Genetics, Helmholtz Zentrum München, German Research Center for Environmental Health (GmbH) Ingolstaedter Landstrasse 1, 85764 Neuherberg; tel: +49-89-3187-3807; fax: +49-89-3187-3500; e-mail jan.rozman@helmholtz-muenchen.de
Germany

ABSTRACT

OBJECTIVE: Tetrahydrobiopterin (BH_4) is an essential cofactor for the aromatic amino acid hydroxylases, alkylglycerol monooxygenase and nitric oxide synthases (NOS). Inborn errors of BH_4 metabolism lead to severe insufficiency of brain monoamine neurotransmitters while augmentation of BH_4 by supplementation or stimulation of its biosynthesis is thought to ameliorate endothelial NOS (eNOS) dysfunction, to protect from (cardio-) vascular disease and/or prevent obesity and development of the metabolic syndrome. We have previously reported that homozygous knock-out mice for the 6-pyruvolytetrahydropterin synthase (PTPS; *Pts*-ko/ko) mice with no BH_4 biosynthesis die after birth.

RESEARCH DESIGN: Here we generated a *Pts*-knock-in (*Pts*-ki) allele expressing the murine PTPS-p.Arg15Cys with low residual activity (15% of wild-type *in vitro*) and investigated heterozygous (*Pts*-ki/wt), homozygous (*Pts*-ki/ki) and compound heterozygous (*Pts*-ki/ko) mutants.

RESULTS: Mice were viable and, depending on the severity of the *Pts* alleles, exhibited up to 90% reduction of PTPS activity in liver and brain. Although (brain and liver) neopterin was significantly elevated, BH_4, blood L-phenylalanine and brain monoamine neurotransmitters dopamine were apparently unaffected. Yet, *Pts*-ko/wt and *Pts*-ki/ki mice exhibited increased body weight and elevated intra-abdominal fat tissue. Comprehensive phenotyping of *Pts*-ki/ki mice revealed alterations in energy metabolism, higher fat content, lower lean mass, and increased blood glucose and cholesterol. Transcriptome analysis indicated changes in glucose and lipid metabolism. Furthermore, differentially expressed genes associated with obesity, weight loss, hepatic steatosis and insulin sensitivity were consistent with the observed phenotypic alterations.

CONCLUSION: We conclude that reduced PTPS and potentially mildly compromised BH_4-biosynthetic activity in mice leads to abnormal body fat distribution and abdominal obesity. This study associates a novel single gene mutation with monogenic forms of obesity.

Key words: Tetrahydrobiopterin, endothelial dysfunction, eNOS/NOS3, neopterin, metabolic syndrome, monogenic obesity

INTRODUCTION

Tetrahydrobiopterin (BH_4) is synthesized *de novo* from guanosine triphosphate (GTP) by the three enzymes GTP cyclohydrolase I (GTPCH), 6-pyruvoyltetrahydropterin synthase (PTPS) and sepiapterin reductase (SR)[1]. BH_4 is an essential cofactor for the aromatic amino acid monooxygenases, i.e. the phenylalanine hydroxylase (PAH), the tyrosine hydroxylase (TH) and the two tryptophan hydroxylases (TPH1, TPH2). Besides providing L-tyrosine (L-Tyr) for protein and catecholamine biosynthesis, the major role of the hepatic PAH is the prevention from systemic L-phenylalanine (L-Phe) accumulation, which is toxic in the brain. TH and TPH1/2 are the key enzymes in the biosynthesis of L-3,4-dihydroxyphenylalanine (L-Dopa) and 5-hydroxy-L-tryptophan (5-HTP), respectively. BH_4 is also a cofactor for the three nitric-oxide synthases (NOS) isoenzymes neuronal NOS (nNOS/NOS1), cytokine-inducible NOS (iNOS/NOS2) and endothelial NOS (eNOS/NOS3) for nitric oxide production as well as for the alkylglycerol monooxygenase (AGMO) which catalyzes the hydroxylation of alkylglycerols or ether lipids[1].

BH_4 deficiency is a heterogeneous group of rare disorders associated with a spectrum of phenotypes ranging from mild, peripheral symptoms including hyperphenylalaninemia (HPA) due to lowered hepatic PAH activity to severe morbidity due to compromised monoamine neurotransmitter synthesis by dysfunction of TH and TPH in the brain[2]. Oral supplementation with BH_4 - in combination with neurotransmitter precursors - has been successfully employed to treat patients. Besides cofactor for the aromatic amino acid hydroxylases, BH_4 is an intracellular antioxidant and a key regulator of cellular redox signaling, and conditions of low BH_4 for NOS lead to NOS uncoupling and production of superoxide rather than NO[1, 3]. Since NO is required to maintain vascular function, limited bioavailability of the NOS cofactor BH_4 is associated not only to cell toxicity but also to vascular dysfunction[3]. Thus, perturbed homeostasis of BH_4 does not only lead to oxidative stress but is thought to be associated with pathogenesis of cardiovascular and neurodegenerative diseases.

Over the last years, numerous experiments with rodents or human patients were performed under conditions of increased BH_4 by augmentation of cofactor through pharmacological supplementation, stimulation of biosynthesis or protection from

oxidation, and they basically all confirmed correction of eNOS dysfunction to protect from (cardio-) vascular disease[4, 5]. Furthermore, the bioavailability of endothelial BH_4 for eNOS was found also to be important, besides probably many other dietary factors[6], for the control of glucose and lipid homeostasis[7, 8], and various experiments in animal models and patients suggest a role in, or progression to, type 2 diabetes mellitus (T2DM)[9-14]. Oral supplementation of BH_4 over several weeks in rats prevented endothelial dysfunction and restored adiponectin levels, a hormone secreted from adipose tissue and regulating glucose and fatty acid catabolism[15]. It was speculated based on such experiments with animals and in patients with T2DM that BH_4 might be a candidate for the treatment of the metabolic syndrome. Increase of abdominal obesity is known to contribute to insulin resistance and metabolic abnormality which is linked to development of T2DM and cardiovascular disease[16-18]. However, the underlying mechanisms for the relation between arterial hypertension, insulin resistance, and the metabolic syndrome are unclear[18].

Various transgenic animal models are available to study pathophysiology and disease mechanism of BH_4 cofactor deficiency[1]. We and others have reported on the perinatal lethal phenotype of a homozygous *Pts*-knock-out mouse (*Pts*-ko/ko)[19, 20]. This mouse mutant exhibited complete absence of PTPS biosynthesis activity accompanied by systemic HPA, severe brain monoamine neurotransmitter deficiency, IGF-1 depletion and dwarfism, while whole brain NOS activity was normal. Due to its severe morbidity and perinatal mortality, this mouse model turned out to be difficult for further and detailed studies on the natural history and development of pathophysiology for classical BH_4 deficiency. We thus aimed at generating a mouse model with a milder form of BH_4 deficiency. Here we report on the generation and characterization of a *Pts*-knock-in (*Pts*-ki) mouse with reduced PTPS activity and found in homozygous *Pts*-ki/ki and in heterozygous *Pts*-ko/wt mutant animals, both with severely compromised but residual PTPS activity, abnormal body fat distribution and abdominal obesity.

MATERIALS, METHODS AND ANIMAL HUSBANDRY

Pts gene targeting

A genomic clone containing the murine *Pts* gene was as described previously, isolated from a 129/Sv-ə- phage library[21]. For targeting vector (pMSY211) construction, a 1.3 kb fragment of the *Pts* gene spanning exon 1 was used as short arm of homology (see Supplementary Figure S1B). A phosphoglycerate kinase promoter (*Pgk*)-diphtheria toxin (DT) gene cassette, essential for the negative selection of the embryonic stem (ES) cells, was added 5ô to the short arm of homology. The long arm of homology was a 5.1 kb fragment containing exons 2, 3 and 4 of the *Pts* gene, and as a positive selective marker, the ñfloxedò *Pgk*-neomycin resistance gene (*neo*) cassette that was introduced between the short and the long arm of homology. After successful construction, the pMSY211 targeting vector was linearized and electoporated into ES cells derived from 129S6/SvEvTac strain. ES cell clones with correct homologous recombination were confirmed by nested PCR under standard amplification conditions with 40 cycles with primers MSY220: 5ô GCACCCCAAGGTAGCCAAGAATTTG-3ôand MSY221: 5ôTTCTTCGCCCACCCCG AAATTGATG-3ô, followed by 25 cycles with primers MSY226: 5ôACCGGGCTGGAG AACATCTGATAAG-3ô and MSY228: 5ôTCAGCAGCCTCTGTTCCACATACAC-3ô For further confirmation of correctly targeted ES cell clones, Southern blot analysis was performed (not shown). One correctly targeted ES cell clone was chosen for blastocyst injection. Blastocyst injection (FVB/N host embryos) led to generation of one 50% chimeric male that, when sexually mature, was mated with FVB females. The chimera revealed germline transmission resulting in the generation of heterozygous *Pts*-R15C knock-in (*Pts*-ki) targeted mice. Correct genotype was confirmed on genomic DNA from tail or ear biopsies by *Pts*-ki or *Pts*-ko genotyping PCR (for genotyping, see Supplementary Fig. S1C and S1D plus supplementary information).

Mouse husbandry

Animal experiments were carried out in accordance with the guidelines and policies of the State Veterinary Office of Zurich and Swiss law on animal protection, the Swiss Federal Act on Animal Protection (1978), and the Swiss Animal Protection Ordinance (1981). Animal studies presented here received approval from by the Cantonal Veterinary Office, Zurich, and the Cantonal Committee for Animal Experiments,

Zurich, Switzerland. All mice, including the wild-type controls, are based on C57/Bl6-background. The high fat diet was from Research Diets D12331 (with 58% kcal% fat w/sucrose Surwit Diet) for up to 10 weeks of feeding mice *ad libitium*. At the GMC mice were maintained in IVC cages with water and standard mouse chow (Altromin 1314, Altromin, Lage, Germany) according to the GMC housing conditions and German laws. All tests performed at the GMC were approved by the responsible authority of the district government of Upper Bavaria, Germany.

Preparation of mouse tissues

Mice were sacrificed, and brains and livers were removed and snap-frozen in liquid nitrogen. Whole mice brains and livers were ground down to powder. To each sample, 500 µl of homogenization buffer (50 mM Tris-HCl, pH 7.5, 100 mMKCl/1 mM EDTA, 1 mM DTT in H_2O, 0.2mM PMSF in isopropanol (10 mg/ml), 1 εM leupeptin in H2O (5 mg/ml) and 1 εM pepstatin in methanol (1 mg/ml)) was added. The TissueLyserII (Qiagen; cat. no. 85300) was used for lysate extraction. A 5 mm stainless steel bead (Qiagen; cat. no. 69989) was added to each sample. The samples were placed into the tissue lyser adapters and were shake at a frequency of 20/s for 90 sec. The lysate was clarified by centrifugation at 13,000 rpm for 20 min and supernatant was used for lysate measurements.

Determination of brain neurotransmitter metabolites, and neopterin and biopterin in mouse tissues and body fluids

Biopterin, neopterin in liver and brain, and monoamine neurotransmitter metabolites in brain were determined according to a published method[19]. For pterin measurements in mouse mother milk, milk was collected according to a published method[22]. After birth, pups were removed from the mothers. Six hours later, mothers were anesthetized by isoflurane, followed by a inter peritoneal injection of 2 U of oxytocin (Sigma-Aldrich, Buchs, Switzerland), and, after 1 min, mice were milked[23]. The few micro liters of collected milk was immediately diluted in ddH_2O and stored at -80°C before determination of pterins.

Determination of L-Phe and L-Tyr concentration in whole blood samples

Before blood collection, adult mice were starved between 4-6 hours to avoid fluctuation in plasma amino acid levels. Blood was collected from tail veins and directly spotted onto Guthrie cards. Concentrations of L-Phe and L-Tyr were

measured by electrospray ionization tandem mass spectrometry as described (ESI-MS/MS) [24].

Determination of PTPS enzyme activity

PTPS activity of mouse brain and liver lysates was determined according to a described method with minor modifications[19]. In a first step, an incubation mixture of 60 µl/sample was prepared, containing 22.6 µl of 100 mM Tris-HCl buffer pH7.4, 5.5 µl of 200 mM $MgCl_2$, 5.5 µl of 20 mM NADP, 5.5 µl of 20 mM NADPH, 13.2 µl of 0.6 mM NH_2P_3 and 2.3 µl of 0.39 U/ml SR. Contrary to our previously published method, no DHPR was added to the mixture (as we found that PTPS enzyme activity showed no significant differences in the presence or absence of DHPR; unpublished observation). To 60 µl of incubation mixture, either 50 µl of brain lysate or 25 µl liver lysate plus 25 µl homogenization buffer was added. The final volume of 110 □l containing liver or brain extracts were incubated at 37°C in the dark for 30 min (liver) or 1 hour (brain). For the ñblank reactionò, 50 µl of 100 mM Tris-HCl buffer pH 7.4 were added to 60 µl of incubation mixture and incubated for 30 min (liver) or 1 hour (brain) at 37°C in the dark. For ñblanks with no incubationò, 60 µl of 100 mM Tris-HCl buffer pH 7.4 were added to 50 µl of brain lysate or 25 µl of liver lysate plus 25 µl of homogenization buffer. To stop the reactions, 33 µl of 30% trichloroacetic acid were added to all samples, including blanks, followed by 10 min incubation at 4°C. Samples were centrifuged at 13,000 rpm for 5 min. The pellets were discarded, and 20 µl of a 1% iodine solution (0.1 g I_2 and 0.2 g KI in 10 ml 1M HCl) was added to a supernatant of 100 µl, followed by incubation at room temperature in the dark for one hour. Finally, 30 µl of 1% w/v ascorbic acid solution was added before samples were centrifuged in AmiconR Ultra-0.5 Centrifugal Filter (Millipore, cat. no: UFC501096) for 10 min at 13,000 rpm. The total amount of biopterin was detected by reversed-phase high-performance liquid chromatography (HPLC). PTPS activity was expressed in ε U/mg of total protein. Total protein was determined by using an M-TP Mikroprotein kit from Beckman Coulter Synchron LX-System (Beckman Coulter Inc, Brea, CA; kit-no. 445860).

Quantification of mRNA expression

RNA was extracted from mouse tissue (liver and brain) by the Qiagen DNeasy blood and tissue kit (Ref. 69504; Hombrechtikon, Switzerland) and cDNA was made by the Promega reverse transcription system (Ref. nr. A3500; Dübendorf, Switzerland).

Mouse *Pts*, e*Nos*/*Nos3* adiponectin and *Il6* mRNA expression levels were quantified using commercially available ABI assays (Mm.35856 for *Pts* mRNA, NCBI RefSeq NM_011220.2; Mm00435217_m1 for *eNos*/*Nos*3 mRNA, NCBI RefSeq NM_008713.4; Mm00456425-m1 for adiponectin mRNA, NCBI RefSeq NM_009605.4; Mm59064-m1 for IL6 mRNA, NCBI RefSeq NM_031168.1). The murine glyceraldehyde-3-phosphate dehydrogenase (*Gapdh*) mRNA (ABI assay ID: Mm99999915_g1; NCBI RefSeq NM_008084.2) was used to normalize relative *Pts*, adiponectin and IL-6 mRNA levels. Values were calculated as described in a published method[25].

Determination of various metabolic parameters

Abdominal fat was resected from mice followed by determination of its weight. Triglyceride in liver and plasma, cholesterol in plasma, and HDL in plasma was measured according to standard methods in our routine Clinical Chemistry unit in a Beckman Coulter UniCel® DxC 600 (Nyon, Switzerland) following the manufacturers procedures[26]. For determining ñfasted glucoseò, mice underwent overnight food withdrawal.

Western blot

PTPS protein was analyzed from liver extracts by Western blot. Protein-extracts (100 mg/ml) were blotted onto a nuPAGE® 4-12% Bis-Tris Gel (Life technologies, Zug Switzerland) incubated with the affinity-purified anti-human PTPS polyclonal antibody SZ28 (1:200 diluted)[27], followed by incubation with a secondary antibody, Anti-Rabbit IgG, Horseradish Peroxidase-Linked whole antibody Na-934V (1:100000 diluted; GE Healthcare, Glattbrugg, Switzerland), and visualization with the Amersham™ ECL™ Western Blotting Detection Reagents (GE Healthcare, Glattbrugg, Switzerland). Blots were striped with Restore Western Blot Stripping Buffer (Fisher Scientific AG, Wohlen, Switzerland) before staining with ß-actin where blots were incubated with the primary monoclonal anti-ß-actin antibody clone AC-74 produced in mouse (diluted 1:100000; Sigma-Aldrich, Buchs, Switzerland), followed by incubation with the secondary antibody, ECL™ anti-mouse IgG horseradish peroxidase-linked whole antibody NA931V produced in sheep (diluted 1:100000; GE Healthcare, Glattbrugg, Switzerland). The bands were acquired using Gel Logic 6000 PRO system (Bio Carestream Health, Centre ñLes Tuilleresñ, Switzerland) and the band intensity was

quantified by the Carestream Molecular Imaging Software, Version 5.0 (Carestream Health).

For Western analysis of TH, brain tissues were homogenized with 50 mM sodium-phosphate buffer (pH 7.4) containing 100 mM NaCl, 1 mM dithiothreitol, 2 ɛg/ml leupeptin, 1 ɛg/ml pepstatin and 0.5 mM phenylmethylsulfonyl fluoride. The homogenates were subjected to 12% SDS-polyacrylamide gel electrophoresis, blotted onto apolyvinylidenedifluoride membrane (Bio-Rad, Hercules, CA), blocked with 5% skim milk, incubated with anti-TH antibody (1:5000; AB152, Millipore, Billerica, MA), or anti-ß-actin antibody (1:30000; A5441, Sigma-Aldrich, St. Louis, MO) and then incubated with horseradish peroxidase-conjugated anti-rabbit IgG (NA9310, GE Healthcare, Pittsburgh, PA) or anti-mouse IgG (NA9340, GE Healthcare). The immunoreactivity was detected using Immobilon Western Chemiluminescent HRPSubstrate (Millipore).

Systemic phenotype analysis by the German Mouse Clinic

Comprehensive phenotypical and behavioral characterization of *Pts*-ki/ki mice was done in collaboration with the German Mouse Clinic (GMC) in Munich, Germany[28, 29]. Over a period of 10 weeks a total of 78 mice (20 *Pts*-ki/ki males, 20 *Pts*-ki/ki females, 20 wild-type males and 18 wild-type females) were subdivided into two pipelines and subjected to the various non-invasive tests including measurements of approximately 550 parameters within 14 different areas. The body composition was analyzed by non-invasive qNMR (Bruker MiniSpec LF50, Bruker, Ettlingen, Germany). Food uptake, energy expenditure and metabolic fuel utilization were assessed by indirect calorimetry (SM-MARS 8 Channel Metabolic System, Sable Systems Ltd., Las Vegas, USA). Parameters were monitored over 21 hours beginning 5 hours prior to lights-off (6 p.m. CET) and ended 4 hours after lights-on the next morning. Data were recorded every 10 min resulting in 126 data points for oxygen consumption (VO_2), carbon dioxide production (VCO_2), respiratory exchange ratio ($RER=VCO_2/VO_2$), cumulative physical activity, and total food uptake. Lipid and carbohydrate oxidation rates were calculated from gas exchange data[30]. Blood samples for clinical chemistry analyses were collected in Li-heparin coated tubes after overnight food withdrawal and from *ad libitum* fed mice. Plasma samples were analyzed using an AU400 autoanalyzer (Olympus, Germany) and adapted reagent kits provided by Beckman-Coulter, Wako Chemicals GmbH or Randox according to GMC standard

procedures[31]. Immunoglobulins in blood serum were detected by immunology and allergy screening.

Transcriptome analysis

Total RNA of brain and liver from of 17 weeks old male animals (*Pts-ki/ki* n = 4, wild-type n = 4) was extracted according a standardized protocol (RNAeasy mini kit, Qiagen). For gene expression profiling Illumina Mouse Ref8 v2.0 Expression BeadChips were performed as previously described[32, 33] Illumina Genomestudio 2011.1 was applied for data normalization (cubic spline) and background corrections. Statistical analysis[32, 34, 35] identified differential gene expression between mutant and wild-type tissues comparing single mutant values with the mean of four wild-types (FDR < 10% in combination with mean fold change > 1.9). Overrepresented functional annotations within the data set were provided as GO terms of the category ôDisease and Function Annotationsô (Ingenuity Pathway Analysis, IPA). Expression data were available at the public repository database GEO[36] (GSE55148).

GSE55148 for reviewers only: http://www.ncbi.nlm.nih.gov/geo/query/acc.cgi?token=srinessoffuxfcn&acc=GSE55148

RESULTS

Generation of a *Pts* knock-in mouse (*Pts*-ki)

To generate a viable mouse model for BH_4 deficiency, we chose to knock-in a single point mutation in the murine *Pts* gene, c.43C>T leading to mPTPS-p.Arg15Cys. This mutation corresponds to the human mutation *PTS*-c.46C>T/hPTPS-p.Arg16Cys which was found in a patient with a mild phenotype with lowered BH_4 biosynthesis in peripheral organs but normal BH_4 and neurotransmitter levels in the CNS (Supplementary Fig. S1A)[27, 37]. Expression studies of recombinant hPTPS-p.Arg16Cys and mPTPS-p.Arg15Cys in COS-1 cells revealed enzyme activity of 12% and 15%, respectively, compared to wild-type PTPS (not shown). Details for the targeting vector construct and strategy for knocking-in the mPTPS-p.Arg15Cys allele (*Pts*-ki), including mouse genotyping, are described in the section of materials and methods and are depicted in Supplementary Figures S1B - S1D.

Homozygous *Pts*-ki/ki mice exhibit lowered PTPS activity and elevated neopterin, but normal plasma L-Phe and tissue BH_4

Upon breeding *Pts*-ki mice to homozygosity, we found the expected Mendelian ratio for a recessive allele with ~25% *Pts*-ki/ki mice, and no behavioral or visible abnormalities compared to their wild-type littermates. In the following, we bred all possible viable *Pts* genotypes, excluding homozygous knock-outs which are perinatal lethal and analyzed 10-12 weeks old adults for their PTPS expression and activity, pterin content in different organs, L-Phe and L-Tyr in blood, and for monoamine neurotransmitter biosynthesis in the brain.

First, we quantified *Pts* gene expression in liver and brain, and found normal mRNA expression in *Pts*-ki/wt and *Pts*-ki/ki mice, and, as expected a roughly 50% reduction of gene expression in mice with one *Pts*-ko null allele (Table 1). We also quantified PTPS protein expression in liver and found a roughly 50% reduction in mice with one null (ko) allele compared to wild-type and *Pts*-ki/wt mice. An exception was the somewhat unprecedented elevation of PTPS expression in *Pts*-ki/ki mice, which might be due to a compensatory action due to low PTPS activity. Unfortunately, we could not quantify the PTPS protein in whole brain extracts, as expression levels were below detection limit.

Next, we determined PTPS enzyme activity in liver and brain. As depicted in Fig. 1A, PTPS activity was only slightly but not significantly reduced in liver and brain of *Pts*-

ki/wt and in brain of *Pts*-ko/wt compared to wild-type mice while *Pts*-ki/ki, *Pts*-ko/wt and *Pts*-ki/ko mice showed a strong reduction of activity in brain and/or liver. Taken together, progressive reduction of PTPS activity in mice with different *Pts* alleles is as follows: ko/wt > ki/ki > ki/ko > ko/ko (for *Pts*-ko/ko see[19]).

Systemic accumulation of neopterin, the oxidized and dephosphorylated substrate of the PTPS enzyme, is one of the diagnostic hallmarks of PTPS deficiency[1]. In accordance with the observation of lowered PTPS activity, we found slightly elevated neopterin in *Pts*-ki/ki mice at least in liver (but not in brain), but significantly elevated neopterin in liver and brain of *Pts*-ki/ko mice (Fig. 1B). In contrast, biopterin levels in liver, brain and mother milk did not differ in the different *Pts* backgrounds at least in our adult mice (Fig. 1C). From previous studies with *Pts*-ko/wt mice, we observed a roughly 50% reduction of BH_4 in the liver of newborns which was compensated later during development[19, 38]. Mother milk was analyzed because the mammary gland was reported to be the tissue with probably the highest concentration of biopterin biosynthesis, and a potential reduction of biopterin in milk might have an effect on the development of offsprings[39, 40]. There was no difference in mouse mother milk between *Pts*-wt/wt, *Pts*-ki/wt, *Pts*-ko/wt and *Pts*-ki/ki (Fig. 1D). Furthermore, we found no indication for (systemic) elevation of L-Phe or L-Tyr analyzed in peripheral blood (Fig. 1E). Plasma L-Phe remained also unchanged when *Pts*-ki/ki mice were exposed to high levels of L-Phe (300 mg/l) for 5 days in the drinking water (not shown).

Brain monoamine neurotransmitter levels and TH expression are not altered in *Pts* mice with lowered PTPS activity

Similarly to BH_4, monoamine neurotransmitter metabolites in the brain of adult mutant mice did also not differ in the different *Pts* backgrounds (Fig. 1F). Nevertheless, at least compound heterozygous *Pts*-ki/ko and homozygous *Pts*-ki/ki mice were severely compromised regarding PTPS activity as we found elevated neopterin (Figs. 2A and B). We thus further analyzed brain TH expression in these mice because TH expression and/or stability were reported to be reduced under conditions of BH_4 and/or PAH deficiency[20, 41, 42]. However, we found no difference in TH expression in adult brains between *Pts*-ki/ko mice compared to their *Pts*-wt/wt, *Pts*-ki/wt and *Pts*-ko/wt controls (Supplementary Fig. S2). In conclusion, we found no neurological abnormalities in our homozygous *Pts*-ki/ki or compound heterozygous *Pts*-ki/ko mice regarding the brain TH expression and/or monoamine neurotransmitter biosynthesis.

Heterozygous *Pts* mutant mice exhibit abnormal body weight and intra-abdominal fat content

Since *Pts*-ko/wt mutant synthesized potentially less BH_4 as we found a ~50% reduction at least after birth but compensation at later ages [19, 38], we initially hypothesized that these animals might be prone to cofactor limitation under for instance acute hyperglycemia. Yet, in standard oral glucose tolerance loading tests we could not see any difference in glucose clearance between groups of wild-type and *Pts*-ko/wt mice (not shown). At the same time, we found that *Pts*-ko/wt mice tend to have a slightly higher relative increase in body weight and in intra-abdominal fat than their wild-type litter mates. This phenomenon seemed to be more pronounced in male mice than in females, and we therefore limited the following analyses to male mutants. By serendipity, we further observed in the same male mice during autopsies an increase in intra-abdominal fat content. A representative quantification of such an early observation is summarized in Table 2: upon feeding limited number of male mice (n = 4) over a period of several weeks with high fat diet (58 kcal% fat with sucrose compared to normal diet with 11 kcal% fat with corn starch), we saw a two-fold increase in intra-abdominal adipose tissue compartments in *Pts*-ko/wt mice compared to an only 1.6-fold increase in wild-type control mice. For these first observations, we decided to dissect and weigh the sum of epididymal (or perigonadal) fat tissues, termed óintra-abdominal fatô, as a marker for fat increase. An *in vivo* determination of whole-body fat in mice using time-domain magnetic resonance analysis (TD-NMR) was only performed later to confirm these observations in *Pts*-ki/ki mouse mutants (see below). Next we extended our studies with male *Pts*-ko/wt male mice by further analyzing various metabolic parameters in a larger cohort of mice fed with high fat diet (see Supplementary Table S1). This study corroborated the previously observed increase in intra-abdominal fat in *Pts*-ko/wt mice ($p < 0.05$), while metabolic, inflammatory and oxidative stress parameters were either unchanged or only slightly and statistically not significantly increased in *Pts*-ko/wt mice compared to wild-type controls. As shown in Supplementary Table S1, these parameters included triglycerides in liver and plasma, plasma cholesterol and HDL, blood glucose, and adiponectin and *Il6* gene expression in fat tissue. The observation of body weight increase in mildly compromised *Pts* males, i.e. *Pts*-ko/wt compared to wt, was also seen in a parallel study including *Pts*-ki/ki males (see Table 3). Here we found differences in body weight (but not in plasma glucose) when mice

were kept over several weeks under standard chow *or* under high fat diet. From these observations we concluded that a lowered PTPS activity that is not necessarily connected to detectable reductions of BH_4 in tissues such as liver or brain is a potential risk factor for weight increase with a tendency for abdominal obesity at least in male mice. For further analysis, we undertook a comprehensive and standardized analysis towards a potential metabolic phenotype with our *Pts*-ki/ki mutant mice.

Comprehensive phenotyping of *Pts*-ki/ki mice revealed a reduced body mass with higher fat content and lower lean mass, and an increase in fasting plasma glucose, plasma cholesterol and triglycerides

Pts-ki/ki mice were systematically characterized in the primary screen of the German Mouse Clinic[43, 44]. 78 mice (40 mutants and 38 wild-type littermates) were analyzed in the screens dysmorphology, behavior, neurology, eye, nociception, energy metabolism, clinical chemistry, immunology, allergy steroid metabolism, cardiovascular function, lung function, and pathology. In addition, liver and brain tissue samples were used for microarray based analysis of differential gene expression. *Pts*-ki/ki mice showed phenotypic alterations indicating a mild metabolic phenotype. Despite a slight reduction in body mass in 13 weeks old mutants compared to wild-type controls, fat mass was increased especially in male mutants whereas lean mass was reduced (Fig. 2A-C and Table 4). The monitoring of daily energy expenditure and substrate utilization by indirect calorimetry in male control and mutant mice revealed no differences between genotypes (see Supplementary Table S2). Clinical chemistry analyses of plasma samples revealed for both sexes a mild increase of fasting glucose levels in *Pts*-ki/ki mice and significantly higher cholesterol and triglyceride concentrations in plasma of *ad libitum* fed mutant mice as compared to corresponding controls. Additionally, alkaline phosphatase activity in plasma of mutant mice was slightly increased compared to controls, pointing towards a potential liver dysfunction (Supplementary Table S3). The remaining parameters analyzed did not show significant genotype-related differences.

Brain and liver transcriptome profiles of *Pts*-ki/ki mice

To potentially identify differential gene regulation in *Pts*-ki/ki mice with reduced PTPS enzyme activity and elevated neopterin in brain and liver, transcriptome profiles of these organs were performed (see Supplementary Tables S4 for liver and S5 for brain). Slightly increased expression levels of *Pts* were detected in both organs

comparing *Pts*-ki/ki with *Pts*-wild-type mice (fold change: brain 1.45 ± 0.48; liver 1.66 ± 0.33) which is similar to what we found by RT-qPCR (see Table 1) and which might be a compensatory effect due to reduced PTPS enzyme activity. Statistical analysis revealed 36 significantly regulated genes in brain and 347 in liver of *Pts*-ki/ki mice (see Suppl. Table S4 and S5). An overlap of 22 differentially down-regulated genes was found between the analyzed organs: *Alg*, *Atm*, *Cd14*, *Cd207*, *Ch25h*, *Hp*, *Hspb1*, *Lcn2*, *Lrg1*, *Mkks*, *Ms4a6d*, *Miacr1*, *Osmr*, *Retnlg*, *S100a8*, *S100a9*, *Serpina3f*, *Serpina3g*, *Socs3*, *Srpr*, *Tmem25*, and *Zfp235*. Several of these common genes were associated with cytokine activity (*Mkks, Osmr, Serpina3f, Serpina3g*, and *Socs3*), immune processes (*Atm, Cd14, Cd207, Lrg2, S100a8* and *Tmem25*) and metabolism (*Ch25h, Lcn2, Osmr, S100a8* and *Socs3*). Further overlap was detected among the over-represented functional annotations of the regulated genes: proliferation and differentiation of cells, cell death, leukocyte migration and vascular disease (Supplementary Table S6) which might be an indication for inflammatory processes. Exclusively, genes annotated with glucose (e.g. *Cxcl14, Dusp1, Fabp5, Myd88, Nnmt, Nos3, Pilrb, Ptpn1, Retnlb, Serpina3, Stat3, Timp1, Tlr2, Vcam1, Xbp1*) and lipid metabolism (e.g. *Abcb1b, Adora1, Adrb2, Apoa4, Atf3, Cebpb, Fabp5, Fas, Lbp, Lcn2, Lgals3, Ptpn1, Saa1, Stat3, Xbp1*), protein synthesis (e.g. *Arntl, Bag3, Casp4, Gdf9, Hdc, Hmox1, Lgmn, Mkks, Mt1e, Mt1h, Myd88, Rcan1, S100a9, Sgms1, Slc39a14, Thbd, Tlr2*), obesity (e.g. *Adora1, Adrb2, Atf3, Cebpb, Fabp5, Gas6, Hhex, Icam1, Lbp, Mfsd2a, Mkks, Mt1e, Mt1h, Ppargc1b, Socs3, Stat3*), weight loss (e.g. *Adh7, Apcs, Arntl, Atf3, Bag3, Cdkn1a, Ikbke, Mt1e, Mt1h, Nfkb2, Tlr2, Tpmt*), hepatic steatosis (e.g. *Adora1, Atf4, Cyp4a11,, Fabp5, Igfbp1, Il18, Il1b, Lbp, Mfsd2a, Retnlb, Ripk2, Stat3, Steap4, Tlr2*) and insulin sensitivity (e.g. *Arntl, Cebpb, Ptpn1, Socs3, Spp1, Stat3, Tgm2, Tlr2, Xbp1*) were over-represented in liver. These gene ontology (GO) terms might be of particular interest with regard to reduced body mass and elevated blood glucose and cholesterol levels in *Pts*-ki/ki mice. It has to be emphasized that we found reduced gene expression levels for *Nos3* only in hepatic transcriptome profiling analysis which would give evidence towards a mildly compromised eNOS/NOS3 function, whereas a ñvalidationò by RT-qPCR did not necessarily confirm this in the various *Pts*-mice tested (see Supplementary Table S7). The potential association between the reduced BH_4-biosynthetic activity, abnormal body fat distribution and abdominal obesity, and the reduced gene expression levels of e*Nos*/*Nos3* found in liver will be discussed below.

DISCUSSION

The here presented *Pts*-ki mouse was initially thought to represent a hypomorphic model that mimics human BH_4 deficiency due to severely reduced PTPS activity which, if untreated, may be lethal in patients but *not* at birth as it is observed in *Pts*-ko/ko mice. We found that a reduction of up to 90% of PTPS activity (in *Pts*-ki/ko mice) does *not* lead to systemic hyperphenylalaninemia concomitant with brain monoamine neurotransmitter abnormality. Unexpectedly, such mice turned out to exhibit compromised or limited cofactor availability without classical sings of BH_4 deficiency but rather with abnormal body fat distribution and abdominal obesity. An indirect measure of BH_4 limitation due to low PTPS activity is the elevated neopterin that is clearly detectable in liver and less striking in brain in at least *Pts*-ki/ko mice. As described in the introduction, it was found that conditions of increased BH_4 may protect from cardiovascular diseases, endothelial dysfunction and potentially also from progression to T2DM through endothelial BH_4 for eNOS (for references see Introduction). Yet, whereas the role of increased BH_4 in abdominal obesity or the metabolic syndrome has been investigated, the opposite condition i.e. *decreased* BH_4 ï but not classical BH_4 deficiency ï in these processes has not been studied to our knowledge under *in vivo* conditions. By serendipity, we found in our first mouse model with potentially limited BH_4, i.e. in the heterozygous *Pts*-ko/wt mice, abnormal fat distribution which was later confirmed also in homozygous *Pts*-ki/ki mice.

A following up study by a comprehensive and standard systemic and phenotype analysis of *Pts*-ki/ki mice revealed slight alterations in energy metabolism with higher fat content, lower lean mass, and mildly increased fasting blood glucose as well as cholesterol and triglyceride levels in these mutant animals. Transcriptome analysis of liver indicated changes in glucose and lipid metabolism, including genes such as *Adora1, Adrb2, Apoa, Atf3, Atf4, Cebpb, Cxcl14, Dusp1, F13a1, Fabp5, Map3k14, Nos3, Ppargc1a, Rgs16, Socs3, Stat3, Steap4* and *Zc3h12a.* Furthermore, several of the differentially regulated genes in liver are associated with obesity, weight loss, hepatic steatosis and insulin sensitivity, which are consistent with the phenotypic alterations found in *Pts*-ki/ki mice. Genes as *Adrb2*, *Apoa4*, *Adora*, *Atm* and *Ripk2* play roles in lipid accumulation in liver and hepatosteatosis. Deficiency of *Ripk2*, also down-regulated in our study, exacerbates hepatosteatosis[45]. However, *Adrb2* and *Atm*, recently linked with activation of fatty liver-induced steatoapoptosis and

fibrosis[46, 47], were down-regulated in liver of *Pts*-ki/ki mice. Additionally, over-expression of *Apoa4* and *Adora*, both genes associated with reduction of lipid accumulation[48, 49], give evidence for protection of liver dysfunction. Several genes associated with insulin sensitivity showed decreased expression in *Pts*-ki/ki mutants. While *Atf3* has antidiabetic effects[50], *Tgm2* null mice were glucose intolerant[51] and *Fabp5* was described to modulate systemic glucose metabolism and insulin sensitivity[52]. Reduced body mass correlated also to the down-regulation of genes annotated with obesity, e.g. the adipocyte specific transcription factor *Cebpb*[53], *Dusp1*, expressed in visceral adipose tissue of several obese man[54] and *Nik*, a gene that protect against hyperglycemia and glucose intolerance in obese mice[55].

A potential direct link between reduced BH_4 biosynthetic activity to abnormal body fat distribution and abdominal obesity can potentially be through a mildly compromised eNOS/NOS3 function as suggested at least by the hepatic transcriptome profiling analysis with reduced expression of e*Nos*/*Nos3* in liver. It was reported that increased NO signaling inhibits insulin induced gluconeogenesis in hepatocytes[56], therefore reduced NO signaling might increase hepatic gluconeogenesis and fasting glucose levels. Furthermore, expression and stability of e*NOS*-mRNA are influenced by many epigenetic and external factors that could also account for differences seen in the degree of reduction in gene expression[57]. Since we have not found yet a molecular mechanism, we can only speculate about an influence of potential BH_4-cofactor limitation in e.g. endothelial tissues that is propagated in the organism through a (mildly) compromised eNOS/NOS3. An alternative link between the mildly reduced biopterin biosynthesis and the observed obesity could be accumulation of the by-product neopterin which was detectable at least in liver tissue from *Pts*-ki/ko and *Pts*-ki/ki mice while Pts-ko/wt mice had only an insignificant neopterin increase after birth[19]. Neopterin was proposed to reflect oxidative stress induced by immune system activation in general, and was found to be elevated in patients with inflammation and atherosclerosis[58]. Recently, neopterin was also shown to negatively effect expression of various transporters involved in cellular cholesterol efflux and foam cell formation and thus to have an aggravating effect on atherosclerosis[59]. Clearly, more studies are required to confirm a connection to eNOS/NOS3 and/or neopterin. Nevertheless, our study associates a single gene mutation with monogenic forms of obesity, a well know phenomenon related to the so-called leptin-

melanocortin pathway, that regulates energy balance and food intake, and, if compromised, may lead to obesity (for an review see[60]). In conclusion, a reduction in BH_4-biosynthetic activity caused by a single heterozygous gene mutation leads in mice to abnormal body fat distribution and abdominal obesity. Whether such an effect is also visible in humans that are carriers of a mutation in the *PTS* gene (or in other BH_4-cofactor metabolizing genes) need to be verified by additional studies.

CONFLICT OF INTEREST

The authors declare no conflict of interest.

ACKNOWLEDGEMENTS

We thank the Division of Clinical Chemistry and Biochemistry of the University Childrenôs Hospital for determination of L-Phe from dried blood spots and routine clinical chemistry parameters, the animal facilities of the university hospital for cooperativity, and F. H. Sennhauser for continuous support. We thank Ann-Elisabeth Schwarz, Anke Bettenbrock and Elfi Holupirek for expert technical assistance. We are grateful for financial support by the ZNZ PhD program of the University of Zurich, the Swiss National Science Foundation, the Hartmann Müller Stiftung and Stiftung für wissenschaftliche Forschung University of Zürich (Baumgarten Stiftung) and the Novartis ñStiftung für medizinisch-biologische Forschungò. GMC researchers were funded by the German Federal Ministry of Education and Research Infrafrontier grant (01KX1012) and by the German Diabetes Research Center (DZD e.V.), and JB by the Helmholtz Alliance ICEMED.

FIGURES AND TABLES

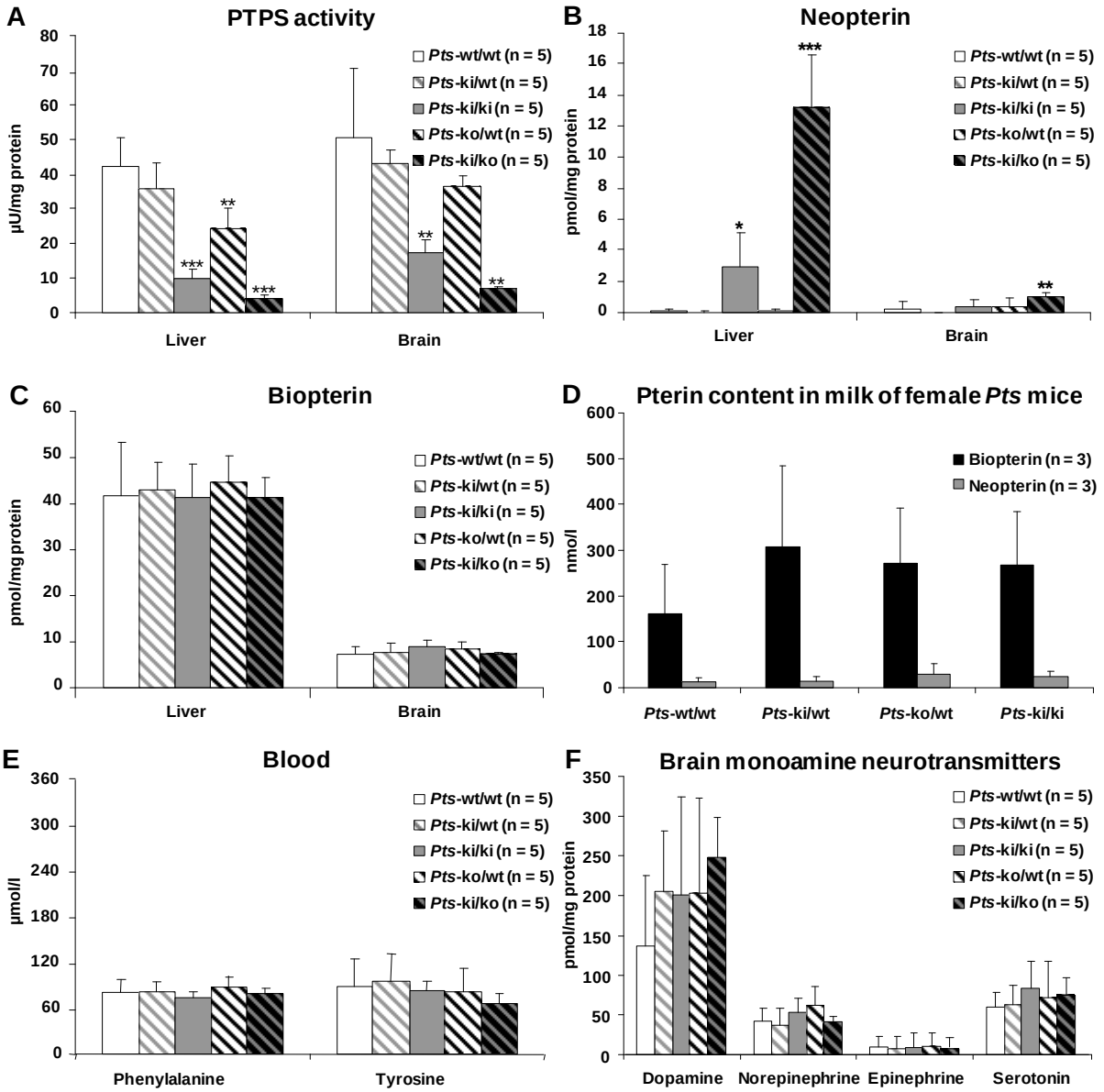

Figure 1. Biochemical analysis of blood, milk, liver and brain tissues from mice carrying the various *Pts* alleles *Pts*-wt/wt, *Pts*-ki/wt, *Pts*-ki/ki, *Pts*-ko/wt and *Pts*-ki/ko. (**A**) PTPS enzyme activity (µU/mg protein) in liver and brain, (**B**) neopterin (pmol/mg protein) in liver and brain, (**C**) biopterin (pmol/mg protein) in liver and brain, (**D**) biopterin and neopterin in mother milk (nmol/l), (**E**) blood L-Phe and L-Tyr concentrations (µmol/l), and (**F**) brain monoamine neurotransmitter metabolites dopamine, norepinephrine, epinephrine and serotonin (pmol/mg protein). Five10-12 weeks old mice were in every group (3 mice in **D**). Genotypes are indicated by bar color: *Pts*-wt/wt (white), *Pts*-ki/wt (gray-white striped), *Pts*-ki/ki (gray), *Pts*-ko/wt (black & white striped) and *Pts*-ki/ko (gray & black striped). Significant difference from the corresponding wild-type value is indicated by asterisks: *, $p < 0.05$; **, $p < 0.01$; ***, 0.001 (Student's two tailed *t*-test).

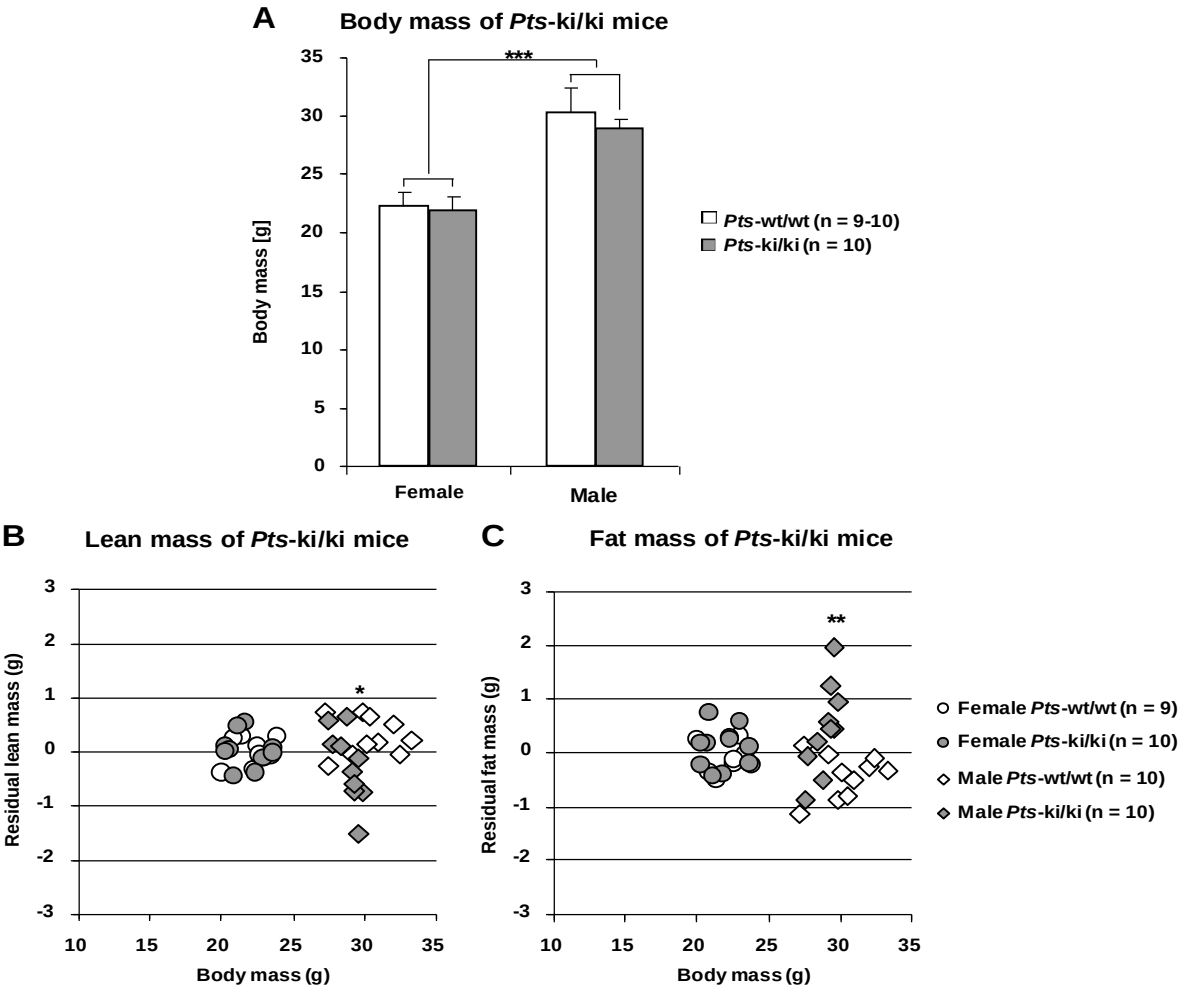

Figure 2. Body composition analysis by non-invasive NMR. (A) Body mass (in g). (**B**) Non-invasive NMR scans to determine the lean mass (in g), and (**C**) fat mass (in g). Open circles, *Pts*-wt/wt females (n = 9); grey circles, *Pts*-ki/ki females (n = 10); open squares, *Pts*-wt/wt males (n = 10); grey squares, *Pts*-ki/ki males (n = 10). Significant difference from the corresponding wild-type value is indicated by asterisks: *, $p < 0.05$; **, $p < 0.01$; ***, 0.001 (Student's two tailed *t*-test).

Table 1: *Pts*-gene expression and PTPS protein in liver and brain.

Genotype	Liver	Brain	Liver
	***Pts*-mRNA**[a]	***Pts*-mRNA**[a]	**PTPS protein** (PTPS/ß-Actin)
***Pts*-wt/wt (n=5)**	1.00 (0.75-1.33)	1.00 (0.89-1.13)	0.12 ± 0.03
***Pts*-ki/wt (n=5)**	1.27 (0.93-1.73)	1.12 (1.01-1.24)	0.18 ± 0.03
***Pts*-ki/ki (n=5)**	1.15 (0.97-1.39)	1.21 (1.09-1.35)[d]	0.28 ± 0.07[d]
***Pts*-ko/wt (n=5)**	0.55 (0.45-0.68)[c]	0.51 (0.45-0.58)[b]	0.06 ± 0.04
***Pts*-ki/ko (n=5)**	0.46 (0.40-0.53)[b]	0.64 (0.57-0.72)[b]	0.04 ± 0.02[d]

[a] Normalized relative to *GAPDH* mRNA; [b]$p < 0.001$; [c]$p < 0.01$; [d]$p < 0.05$ with value of *Pts*-wt/wt mice (Student's two tailed *t*-test), GAPDH, glyceraldehyde 3-phosphate dehydrogenase; PTPS, 6-pyruvoyltetrahydropterin synthase.

Table 2: Body weight and intra-abdominal fat tissue in male *Pts*-ko/wt versus *Pts*-wt/wt mice fed with standard chow or high fat diet (*ad libitum*).

Mouse (males; n = 4)	Diet	Body weight in g (increase in %)		Intra-abdominal fat in mg (increase in %)	
***Pts*-wt/wt**	**standard chow**	**4.7 ± 0.9**	**(100%)**	**342.5 ± 142.7**	**(100%)**
***Pts*-wt/wt**	**high fat**	**11.2 ± 2.2**	**(238%)**	**542.3 ± 170.1**	**(158%)**
***Pts*-ko/wt**	**standard chow**	**3.6 ± 1.2**	**(100%)**	**421.3 ± 121.2**	**(100%)**
***Pts*-ko/wt**	**high fat**	**10.0 ± 1.2**	**(275%)**	**845.5 ± 169.7**	**(201%)**

Table 3: Body weight increase in various *Pts* mutant mice.

Body weight increase in *Pts*-mutant mice, i.e. heterozygous *Pts*-ko/wt and homozygous *Pts*-ki/ki, after 10 weeks feeding with standard chow or high fat diet (ad libitum).

	Standard chow: Difference in body weight (grams)		High Fat diet: Difference in body weight (grams)		High fat diet: Blood glucose (mM)	
	4 weeks	10 weeks	4 weeks	10 weeks	4 weeks	10 weeks
***Pts*-wt/wt** (n = 10)	0.86	2.59	3.93	7.84	6.23	6.04
***Pts*-ko/wt** (n = 10)	3.49 [a]	6.17 [a]	4.61	10.62[c]	6.01	6.45
***Pts*-ki/ki** (n = 10)	2.43[b]	5.35[b]	9.42[a]	16.28[a]	6.46	6.22

[a]$p < 0.001$; [b]$p < 0.01$; [c]$p < 0.1$ with value of *Pts*-wt/wt mice

Table 4: Body composition analysis of *Pts*-ki/ki mice by qNMR (g, mean ± sd).

Statistics: body mass was analyzed by 2-WAY ANOVA for genotype, sex, and genotype x sex interaction. Fat mass and lean mass were analyzed by linear regression modeling for genotype, sex, and genotype x sex interaction (body mass as covariate). Superscripts at p-value of main effect of genotype indicate significance level of the genotype x sex interaction. Genotype effects were tested separately within males and females only when a significant genotype x sex interaction could be detected. Further explanations: n/a not analyzed; n.s. not significant, * $p \leq 0.05$, ** $p \leq 0.01$.

	Female *Pts*-wt/wt	Female *Pts*-ki/ki	Male *Pts*-wt/wt	Male *Pts*-ki/ki	Main effect genotype (superscript genotype x sex interaction)	within females	within males
	(n = 9)	(n = 10)	(n = 10)	(n = 10)	*p*-values		
Body mass (g)	22.3 ± 1.2	21.8 ± 1.3	30.4 ± 2.0	29.0 ± 0.8	0.0176[n.s.]	n/a	n/a
Fat mass (g)	5.4 ± 0.4	5.5 ± 0.5	6.4 ± 0.4	7.2 ± 0.9	0.5791[**]	0.3700	0.0035
Lean mass (g)	13.6 ± 0.8	13.4 ± 0.8	19.7 ± 1.5	18.2 ± 0.5	0.7468[*]	0.7197	0.0214

SUPPLENETARY FIGURES AND TABLES

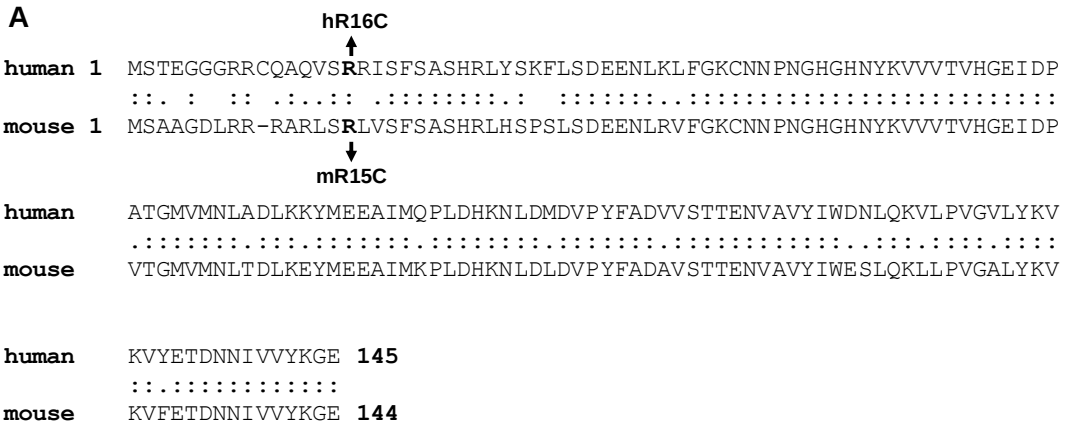

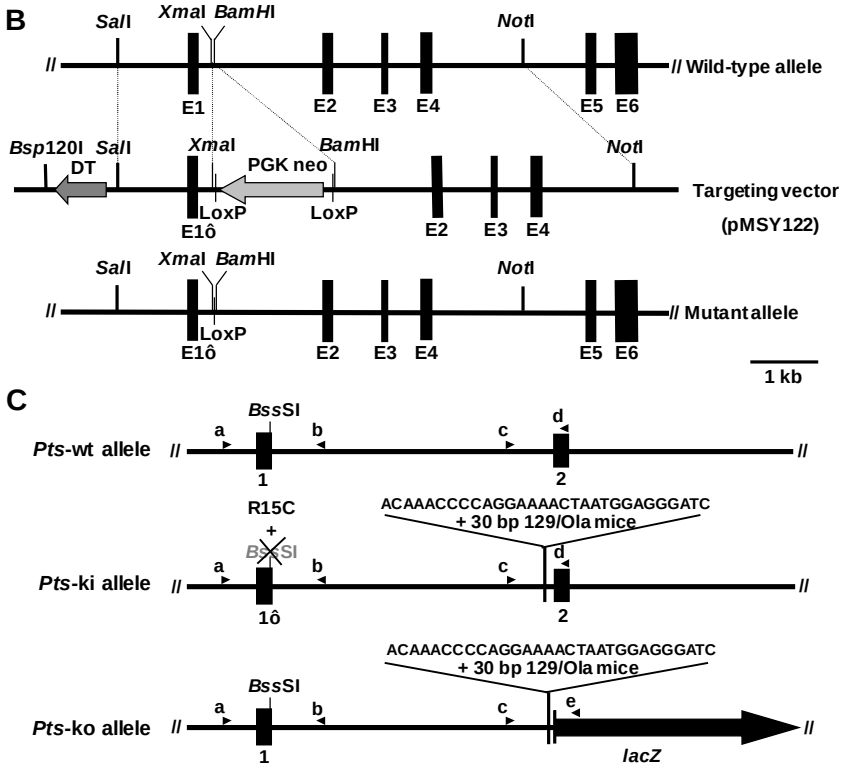

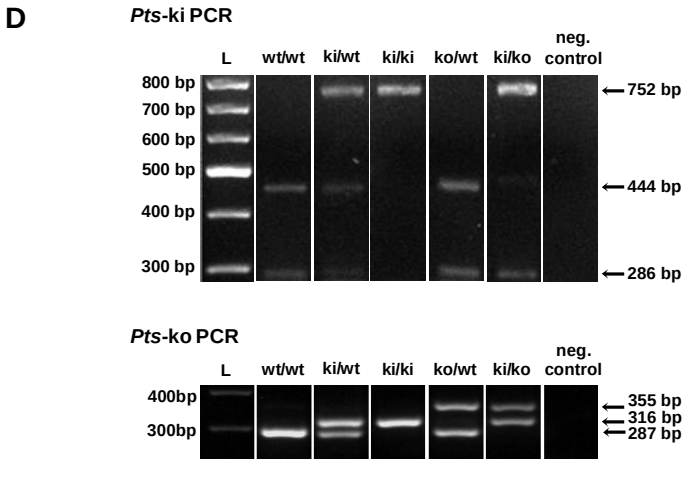

Supplementary Figure S1. Generation of the murine *Pts*-ki allele. **(A)** Primary amino acid sequence alignment of human and mouse PTPS, which share 82.1% sequence identity. The human mutation *PTS*-p.Arg16Cys (hR16C) and the corresponding mouse mutation *Pts*-p.Arg15Cys (mR15C), both located in exon 1, are marked with arrows. **(B)** Schematic representation of genomic structure of the murine *Pts* wild-type allele (top), the targeting vector pMSY211 including the mR15C mutation (E1), the p.L16L mutation to destroy the *Bss*SI restriction site, a *Pgk*-DT-gene-cassette (DT) for negative selection, and a ñfloxedò *Pgk*-neo-gene-cassette (PGK neo) for positive selection (middle), and the resulting targeted mutant allele (bottom). **(C)** Schematic representation of the genotyping concepts for the *Pts*-wt, *Pts*-ki and *Pts*-ko alleles with genomic DNA and the primer pairs a/b (*Pts*-ki PCR) and c/d/e (*Pts*-ko PCR). *Pts*-ki PCR: primers a and b are located upstream and downstream from exon 1 (E1), respectively. They generate a 730 bp for the wild-type/knock-out alleles and a 751 bp PCR fragment for the knock-in allele (due to additional targeting vector sequence; see **C**). Digestion with restriction enzyme *Bss*SI, 3 bp downstream of the mR15C-c.43C>T mutation, leads to a 444 bp and a 286 bp fragment for the wild-type/knock-out PCR products. The PCR fragment derived from the *Pts*-ki allele can not be digested with *Bss*SI because the silent p.L16L/c.48C>G mutation destroys the *Bss*S1-recognition site. The *Pts*-wt and the *Pts*-ko alleles can not be distinguished by the *Pts*-ki genotyping using primer pair a/b. *Pts*-ko PCR: genotyping according to our previously published method[19]. Primer c is upstream of exon 2 (E2), primer d is specific for exon 2 and primer e is specific for the *lacZ* gene. The primer pair c/d results in a wild-type fragment of 287 bp and a knock-in fragment of 316 bp whereas primer pair c/e generates mutant fragment of 355 bp (due to the difference in the *Pts*-intron 1 sequence between the 129/Ola and C57BL/6J mice strains; see **C**). **(D)** Conventional 2% agarose gel representative PCR-genotyping for the *Pts*-ki allele (top; after *Bss*SI digestion) and *Pts*-ko allele (bottom).

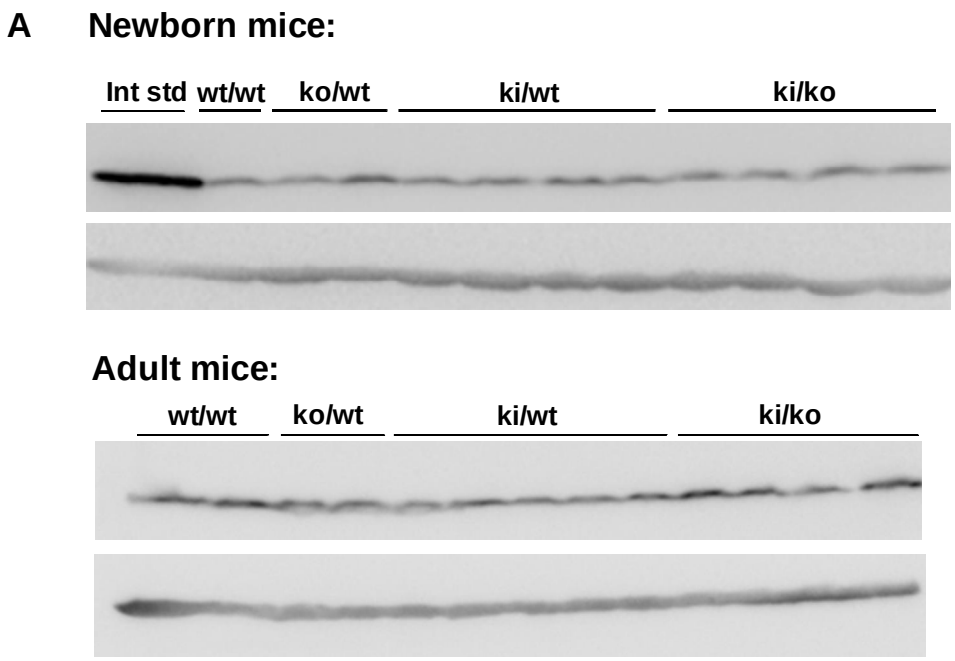

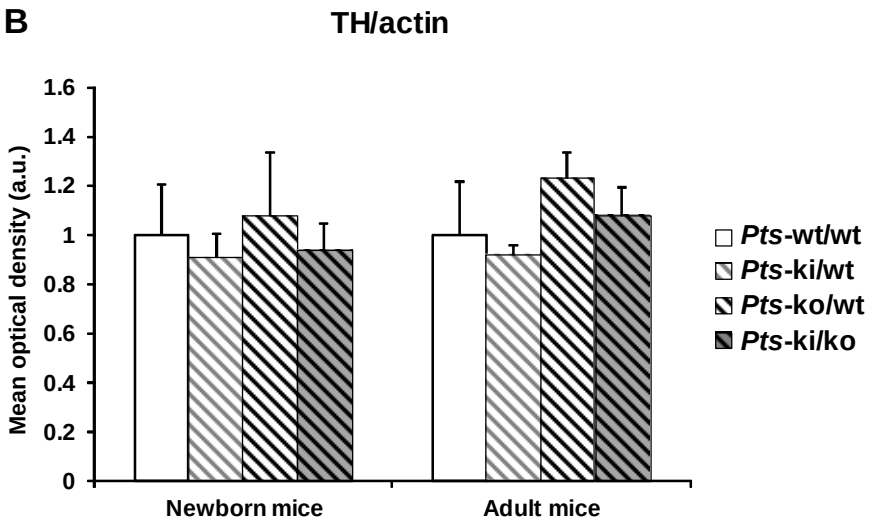

Supplementary Figure S2. TH protein expression in brain of *Pts*-ki/ko mice. Western blot analysis and densitometric quantification of TH in brains from (**A**) newborn mice (n = 3 *Pts*-wt/wt, 5 *Pts*-ko/wt, 24 *Pts*-ki/wt, and 19 *Pts*-ki/ko) and (**B**) young adult animals (n = 3 *Pts*-wt/wt, 7 *Pts*-ko/wt, 12 *Pts*-ki/wt, and 13 *Pts*-ki/ko). For details see also Materials and Methods.

Supplementary Table S1: Metabolic parameters in male *Pts*-ko/wt versus *Pts*-wt mice.

Parameter	***Pts*-ko/wt** (n = 10-15)	***Pts*-wt/wt** (n = 10-14)	**p-value**
Body weight (g)	28.0 ± 2.2	28.0 ± 1.3	0.956
Intra-abdominal fat (mg)	817 ± 244	652 ± 181	0.049*
Total Biopterin (pmol/mg protein)	92.6 ± 8.2	93.2 ± 9.6	0.889
PTPS activity in liver (µU/mg protein)	13.7 ± 1.2	28.6 ± 6.7	2.218 x 10e-6**
Triglycerides in liver (µmol/mg protein)	0.07 ± 0.02	0.05 ± 0.03	0.330
Plasma cholesterol (mmol/L)	3.30 ± 0.28	2.95 ± 0.71	0.302
Plasma triglycerides (mmol/L)	0.96 ± 0.20	0.85 ± 0.45	0.612
Plasma HDL (mmol/L)	3.52 ± 0.46	2.92 ± 1.06	0.251
Adiponectin in fat tissue (RT-qPCR gene expression in % of *Gapdh*)	62.6 ± 17.1	72.5 ± 19.4	0.229
IL-6 in fat tissue (RT-qPCR gene expression in % of *Gapdh*)	38.3 ± 18.8	42.9 ± 27.5	0.667

* $p < 0.05$; ** $p < 0.000005$

Supplementary Table S2: Indirect calorimetry of *Pts*-ki/ki male mice.

Parameter	Male		p-values	
	***Pts*-wt/wt**	***Pts*-ki/ki**		
	(n=7)	(n=7)	Genotype	Body mass
Body mass (g)	30.1 ± 1.8	28.6 ± 0.8	0.071	n/a
Body temperature (°C)	36.00 ± 0.4	36.30 ± 0.3	0.134	n/a
Food intake (g)	5.2 ± 0.5	6.7 ± 3.5	0.556	0.514
Mean VO_2 (ml h^{-1})	95.6 ± 5.1	89.2 ± 3.1	0.105	0.058
Min VO_2 (ml h^{-1})	55.4 ± 5.1	53.3 ± 4.4	0.761	0.045
Max VO_2 (ml h^{-1})	144.2 ± 10.3	137.4 ± 9.4	0.838	0.051
Mean RER (VCO_2/VO_2)	0.89 ± 0.02	0.89 ± 0.03	0.822	n/a
Lipid oxidation (g/min)	0.00027 ± 0.00006	0.00024 ± 0.00006	0.3818	n/a
Carbohydrate oxidation (g/min)	0.00142 ± 0.00012	0.00136 ± 0.00017	0.4212	n/a
Mean activity (counts)	0.081 ± 0.07	0.070 ± 0.06	0.749	n/a

Statistics: body mass, body temperature, mean RER, mean activity, lipid oxidation, carbohydrate oxidation: 1-WAY ANOVA (genotype); mean, min and max VO_2, food intake: linear regression model (genotype, body mass as covariate); mean ± sd.

Supplementary Table S3. Plasma clinical chemistry of *Pts*-ki/ki mice and *Pts*-wt/wt controls.

	Female *Pts*-wt/wt	Female *Pts*-ki/ki	Male *Pts*-wt/wt	Male *Pts*-ki/ki	p-values		
	(n = 9)	(n = 10)	(n = 10)	(n = 10)	genotype	sex	genotype x sex
Fasting Glucose [mmol/l]	7.84 ± 1.35	8.92 ± 1.94	9.23 ± 2.11	11.02 ± 2.23	0.028	0.009	0.578
Fasting Cholesterol [mmol/l]	2.117 ± 0.386	2.216 ± 0.431	2.6 ± 0.345	2.879 ± 0.321	0.122	< 0.001	0.457
Fasting HDL-cholesterol [mmol/l]	1.609 ± 0.351	1.7 ± 0.363	2.027 ± 0.263	2.259 ± 0.257	0.114	< 0.001	0.483
Fasting non-HDL Cholesterol [mmol/l]	0.507 ± 0.05	0.516 ± 0.086	0.573 ± 0.092	0.62 ± 0.084	0.292	0.002	0.465
Fasting Triglycerides [mmol/l]	0.813 ± 0.211	0.901 ± 0.156	0.971 ± 0.125	1.062 ± 0.297	0.186	0.022	0.979
Fasting NEFA [mmol/l]	0.99 ± 0.26	0.85 ± 0.27	0.72 ± 0.13	0.64 ± 0.13	0.106	0.001	0.686
Sodium [mmol/l]	144.89 ± 2.3	142 ± 4.3	146.4 ± 2.8	148.4 ± 2.1	0.648	< 0.001	0.016
Potassium [mmol/l]	3.76 ± 0.2	3.98 ± 0.5	3.92 ± 0.3	3.8 ± 0.3	0.644	0.945	0.133
Chloride [mmol/l]	111.07 ± 1.9	107.6 ± 3.1	108.96 ± 2.7	111.16 ± 1.8	0.426	0.362	0.001
Total protein [g/l]	48.22 ± 1.9	47.8 ± 2	50 ± 1.6	49.6 ± 2.6	0.539	0.011	0.987
Albumin [g/l]	28 ± 1.4	27.8 ± 1.5	28.6 ± 1.3	27.4 ± 1.6	0.148	0.834	0.298
Creatinine [µmol/l]	8.86 ± 0.7	8.19 ± 0.9	7.05 ± 1.1	6.97 ± 0.8	0.176	< 0.001	0.295
Urea [mmol/l]	10.62 ± 1.9	11.67 ± 1.7	12.03 ± 1.7	11.75 ± 2.1	0.521	0.215	0.274
Cholesterol [mmol/l]	1.8 ± 0.3	2.27 ± 0.3	2.78 ± 0.5	3.01 ± 0.8	0.038	< 0.001	0.459
Triglycerides [mmol/l]	1.07 ± 0.3	1.56 ± 0.4	2.23 ± 0.6	2.7 ± 1	0.028	< 0.001	0.983
ALAT/GPT [U/l]	26.44 ± 7.3	21.8 ± 6.1	37.6 ± 35.2	33.4 ± 22.9	0.531	0.112	0.975
ASAT/GOT [U/l]	59.33 ± 13.6	72.4 ± 29.9	49.8 ± 21	57.4 ± 19	0.15	0.089	0.699
alpha-Amylase [U/l]	734.86 ± 60.1	845.01 ± 333.1	907.93 ± 187.6	821.71 ± 163.6	0.862	0.28	0.159
Glucose [mmol/l]	12.35 ± 2.2	11.09 ± 1.7	10.97 ± 1.4	11.87 ± 1.8	0.753	0.604	0.066
Lactate-dehydrogenase [U/l]	220.77 ± 59.8	226.58 ± 61.4	211.31 ± 89.4	201.28 ± 51.7	0.923	0.426	0.716
Calcium [mmol/l]	2.24 ± 0.1	2.21 ± 0.1	2.29 ± 0.1	2.28 ± 0.1	0.405	0.011	0.458
Inorganic phosphate [mmol/l]	1.27 ± 0.2	1.16 ± 0.2	1.6 ± 0.4	1.52 ± 0.3	0.348	0.001	0.893
Iron [µmol/l]	24.26 ± 1.9	24.8 ± 4.1	21.57 ± 2.2	19.84 ± 2.7	0.524	< 0.001	0.225
Alkaline phosphatase [U/l]	138.89 ± 17.9	144.6 ± 15.4	83 ± 9.4	96 ± 16.5	0.061	< 0.001	0.456

Supplementary Table S4: Heat map liver.

mean linear fold change	Pts-ki/ki A B C D	Gene ID	Gene name
2.3		Cyp2a21-ps	cytochrome P450, family 2, subfamily a, polypeptide 21, pseudogene
2.2		Abcg8	ATP-binding cassette, sub-family G, member 8
2.3		Gm5820	
2.2		Pcsk4	proprotein convertase subtilisin/kexin type 4
2.3		Vldlr	very low density lipoprotein receptor
2.2		Ctsa	cathepsin A
2.1		Ppnr	per-pentamer repeat gene
2.3		Adora1	adenosine A1 receptor
2.2		Pcsk4	proprotein convertase subtilisin/kexin type 4
2.4		Gsta2	glutathione S-transferase, alpha 2 (Yc2)
2.3		Spata2l	spermatogenesis associated 2-like
2.3		Fam13a	family with sequence similarity 13, member A
2.3		Il18	interleukin 18
2.2		Cpsf4l	cleavage and polyadenylation specific factor 4-like
2.4		Cyp2a21-ps	cytochrome P450, family 2, subfamily a, polypeptide 21, pseudogene
2.3		Mycl1	v-myc myelocytomatosis viral oncogene homolog 1
2.3		Slco1a4	solute carrier organic anion transporter family, member 1a4
2.4		Upp2	uridine phosphorylase 2
2.3		Ces1e	carboxylesterase 1E
2.3		Asic5	acid-sensing (proton-gated) ion channel family member 5
2.3		Zfp280d	zinc finger protein 280D
2.5		Upp2	uridine phosphorylase 2
2.5		Upp2	uridine phosphorylase 2
2.5		Hhex	hematopoietically expressed homeobox
2.9		Cyp2a21-ps	cytochrome P450, family 2, subfamily a, polypeptide 21, pseudogene
2.5		Rfx4	regulatory factor X, 4
2.6		Pcsk4	proprotein convertase subtilisin/kexin type 4
2.5		D930015E06Rik	
2.9		Cyp2a21-ps	cytochrome P450, family 2, subfamily a, polypeptide 21, pseudogene
2.6		Fbxo21	F-box protein 21
3.1		Hamp2	hepcidin antimicrobial peptide 2
3.1		Acot3	acyl-CoA thioesterase 3
2.6		Mfsd2a	major facilitator superfamily domain containing 2A
2.7		9830163H01Rik	
3.0		Cyp4a10	cytochrome P450, family 4, subfamily a, polypeptide 10
2.9		Mfsd7c	major facilitator superfamily domain containing 7C
2.8		Fxyd6	FXYD domain-containing ion transport regulator 6
3.2		Slc17a8	solute carrier family 17, member 8
3.1		Apoa4	apolipoprotein A-IV
3.0		9130409I23Rik	
3.2		Sorl1	sortilin-related receptor, LDLR class A repeats-containing
3.4		Dbp	D site albumin promoter binding protein
3.4		Ppargc1b	peroxisome proliferative activated receptor, gamma, coactivator 1 beta
5.0		Cyp4a14	cytochrome P450, family 4, subfamily a, polypeptide 14
5.8		Krt23	keratin 23
12.3		Ctse	cathepsin E
8.8		Rgs16	regulator of G-protein signaling 16
-230.6		Lcn2	lipocalin 2
-86.8		Saa3	serum amyloid A 3
-53.9		Saa1	serum amyloid A 1
-79.0		Tmem25	transmembrane protein 25
-31.2		Tlr2	toll-like receptor 2
-32.9		Saa1	serum amyloid A 1
-21.1		Mt2	metallothionein 2
-22.0		Orm2	orosomucoid 2
-19.5		Cdkn1a	cyclin-dependent kinase inhibitor 1A (P21)
-24.5		Scara5	scavenger receptor class A, member 5
-18.0		Cd14	CD14 antigen
-19.1		Cxcl1	chemokine (C-X-C motif) ligand 1
-14.7		Il22	interleukin 22
-16.1		Prtn3	proteinase 3
-24.9		Nnmt	nicotinamide N-methyltransferase

-11.8	Steap4	STEAP family member 4
-13.2	Il1rn	interleukin 1 receptor antagonist
-10.8	Cpne8	copine VIII
-8.6	Apcs	serum amyloid P-component
-17.6	Nnmt	nicotinamide N-methyltransferase
-6.8	Fam211a	family with sequence similarity 211, member A
-7.7	Moxd1	monooxygenase, DBH-like 1
-6.7	Fam211a	family with sequence similarity 211, member A
-7.8	S100a8	S100 calcium binding protein A8 (calgranulin A)
-6.9	Cpne8	copine VIII
-8.0	Cxcl14	chemokine (C-X-C motif) ligand 14
-5.9	Plscr1	phospholipid scramblase 1
-5.9	Bcl3	B cell leukemia/lymphoma 3
-8.0	Socs3	suppressor of cytokine signaling 3
-5.6	Icam1	intercellular adhesion molecule 1
-5.8	Slc10a6	solute carrier family 10, member 6
-5.5	Cyb561	cytochrome b-561
-5.3	Plscr1	phospholipid scramblase 1
-5.4	Slc41a2	solute carrier family 41, member 2
-4.9	S100a9	S100 calcium binding protein A9 (calgranulin B)
-4.9	Syt11	synaptotagmin XI
-4.6	Cdkn1a	cyclin-dependent kinase inhibitor 1A (P21)
-4.8	Cldn14	claudin 14
-4.6	Snx10	sorting nexin 10
-4.6	Mpg	N-methylpurine-DNA glycosylase
-4.4	Tubb6	tubulin, beta 6 class V
-4.4	Fgl1	fibrinogen-like protein 1
-4.3	Dusp8	dual specificity phosphatase 8
-4.4	Nrg4	neuregulin 4
-4.6	Fabp5	fatty acid binding protein 5, epidermal
-5.8	Mt1	metallothionein 1
-3.8	Cyp21a1	cytochrome P450, family 21, subfamily a, polypeptide 1
-4.1	Cxcl14	chemokine (C-X-C motif) ligand 14
-4.0	Rpsa	ribosomal protein SA
-4.1	Moxd1	monooxygenase, DBH-like 1
-3.8	Sybu	syntabulin (syntaxin-interacting)
-4.2	Egr1	early growth response 1
-4.2	Gm8000	
-3.6	Slc10a6	solute carrier family 10, member 6
-3.6	Osmr	oncostatin M receptor
-3.6	Syne4	spectrin repeat containing, nuclear envelope family member 4
-7.1	Gadd45g	growth arrest and DNA-damage-inducible 45 gamma
-3.5	Rcan1	regulator of calcineurin 1
-3.6	Crybb3	crystallin, beta B3
-3.5	Ripk2	receptor (TNFRSF)-interacting serine-threonine kinase 2
-3.7	Isyna1	myo-inositol 1-phosphate synthase A1
-3.5	Gm11582	
-3.7	Acnat1	acyl-coenzyme A amino acid N-acyltransferase 1
-3.6	Slc37a2	solute carrier family 37, member 2
-4.0	Srpr	signal recognition particle receptor ('docking protein')
-3.7	Cdkn1a	cyclin-dependent kinase inhibitor 1A (P21)
-3.5	Zc3h13	zinc finger CCCH type containing 13
-6.3	Gadd45g	growth arrest and DNA-damage-inducible 45 gamma
-3.6	Creld2	cysteine-rich with EGF-like domains 2
-3.3	Tnfrsf8	tumor necrosis factor receptor superfamily, member 8
-3.3	Igfbp1	insulin-like growth factor binding protein 1
-3.4	Dpep1	dipeptidase 1
-3.4	Stk19	serine/threonine kinase 19
-3.4	Creld2	cysteine-rich with EGF-like domains 2
-3.2	Serpina3n	serine (or cysteine) peptidase inhibitor, clade A, member 3N
-3.4	Nxpe2	neurexophilin and PC-esterase domain family, member 2
-3.4	Tubb2a-ps2	tubulin, beta 2a, pseudogene 2
-3.3	Hsph1	heat shock 105kDa/110kDa protein 1
-3.3	Gbp8	guanylate-binding protein 8
-3.3	Fndc3b	fibronectin type III domain containing 3B
-3.1	Nfil3	nuclear factor, interleukin 3, regulated
-3.1	A330021E22Rik	

-3.1		4933426M11Rik	
-3.2		Gm527	
-3.2		Creb3l2	cAMP responsive element binding protein 3-like 2
-3.2		Ifi47	interferon gamma inducible protein 47
-3.2		Thbd	thrombomodulin
-3.1		Dnajc12	DnaJ (Hsp40) homolog, subfamily C, member 12
-2.9		Fas	Fas (TNF receptor superfamily member 6)
-3.0		Ttpal	tocopherol (alpha) transfer protein-like
-3.2		Niacr1	niacin receptor 1
-2.9		Gas6	growth arrest specific 6
-2.9		Lrg1	leucine-rich alpha-2-glycoprotein 1
-2.8		Tnfaip3	tumor necrosis factor, alpha-induced protein 3
-2.9		Atp10d	ATPase, class V, type 10D
-2.9		Junb	Jun-B oncogene
-2.9		Reg3b	regenerating islet-derived 3 beta
-2.8		Lgals3	lectin, galactose binding, soluble 3
-2.8		Fos	FBJ osteosarcoma oncogene
-2.7		Fas	Fas (TNF receptor superfamily member 6)
-2.8		Sgms1	sphingomyelin synthase 1
-2.9		Ptpn1	protein tyrosine phosphatase, non-receptor type 1
-3.0		Ch25h	cholesterol 25-hydroxylase
-2.8		Ung	uracil DNA glycosylase
-2.7		Zc3h12a	zinc finger CCCH type containing 12A
-2.8		Il17ra	interleukin 17 receptor A
-4.3		Apoc2	apolipoprotein C-II
-2.8		Gpnmb	glycoprotein nmb
-2.7		Tnfrsf12a	tumor necrosis factor receptor superfamily, member 12a
-2.7		Ier3	immediate early response 3
-2.6		Litaf	LPS-induced TN factor
-2.8		Serpina3f	serine (or cysteine) peptidase inhibitor, clade A, member 3F
-2.7		Irak3	interleukin-1 receptor-associated kinase 3
-2.8		Ms4a6d	membrane-spanning 4-domains, subfamily A, member 6D
-2.6		Itih4	inter alpha-trypsin inhibitor, heavy chain 4
-2.8		Zbtb7c	zinc finger and BTB domain containing 7C
-2.7		Efna1	ephrin A1
-3.5		Serpina4-ps1	serine (or cysteine) peptidase inhibitor, clade A, member 4, pseudogene 1
-2.7		Dpep1	dipeptidase 1
-2.6		Piga	phosphatidylinositol glycan anchor biosynthesis, class A
-2.9		Egfr	epidermal growth factor receptor
-2.6		Lpgat1	lysophosphatidylglycerol acyltransferase 1
-2.5		Myd88	myeloid differentiation primary response gene 88
-2.7		Tgm1	transglutaminase 1, K polypeptide
-2.6		Tsku	tsukushi
-2.6		Nedd4l	neural precursor cell expressed, developmentally down-regulated gene 4-like
-2.5		Nop58	NOP58 ribonucleoprotein
-2.8		Ttc39a	tetratricopeptide repeat domain 39A
-2.5		Serpina10	serine (or cysteine) peptidase inhibitor, clade A, member 10
-2.7		Chac1	ChaC, cation transport regulator 1
-2.4		Saa4	serum amyloid A 4
-2.4		Stk19	serine/threonine kinase 19
-2.5		Ifi27l2a	interferon, alpha-inducible protein 27 like 2A
-2.6		Dnajb9	DnaJ (Hsp40) homolog, subfamily B, member 9
-2.5		Acnat1	acyl-coenzyme A amino acid N-acyltransferase 1
-2.6		Retnlg	resistin like gamma
-2.5		H2afx	H2A histone family, member X
-2.5		Gm136	
-2.7		Ankhd1	ankyrin repeat and KH domain containing 1
-2.5		Serpina3g	serine (or cysteine) peptidase inhibitor, clade A, member 3G
-2.4		DL205570	
-2.4		Stk19	serine/threonine kinase 19
-2.5		Alg9	asparagine-linked glycosylation 9
-2.4		Fkbp5	FK506 binding protein 5
-2.5		Stx18	syntaxin 18
-2.4		1700028N14Rik	
-2.4		Slc11a2	solute carrier family 11, member 2
-2.5		Gvin1	GTPase, very large interferon inducible 1

-2.4	Il1r1	interleukin 1 receptor, type I
-2.5	Hdc	histidine decarboxylase
-2.4	Hmox1	heme oxygenase (decycling) 1
-2.5	Arntl	aryl hydrocarbon receptor nuclear translocator-like
-2.3	Timp1	tissue inhibitor of metalloproteinase 1
-2.3	Tom1l2	target of myb1-like 2
-2.4	Bhlha15	basic helix-loop-helix family, member a15
-2.4	9530077C05Rik	
-2.4	Capzb	capping protein muscle Z-line, beta
-2.3	Crem	cAMP responsive element modulator
-2.4	Srrm4	serine/arginine repetitive matrix 4
-2.4	Bag3	BCL2-associated athanogene 3
-2.3	Clp1	CLP1, cleavage and polyadenylation factor I subunit
-2.3	Hspb1	heat shock protein 1
-2.3	Crem	cAMP responsive element modulator
-2.4	Lnx1	ligand of numb-protein X 1
-2.3	Ppl	periplakin
-2.3	Hsp90aa1	heat shock protein 90, alpha (cytosolic), class A member 1
-2.3	Tmem176a	transmembrane protein 176A
-2.2	Caskin2	CASK-interacting protein 2
-3.7	Tpmt	thiopurine methyltransferase
-2.2	Slc30a5	solute carrier family 30 (zinc transporter), member 5
-2.3	Gdf9	growth differentiation factor 9
-2.2	D10Wsu102e	DNA segment, Chr 10, Wayne State University 102, expressed
-2.3	Map7d1	MAP7 domain containing 1
-2.3	Ctps	cytidine 5'-triphosphate synthase
-2.4	Egfr	epidermal growth factor receptor
-2.3	Hip1r	huntingtin interacting protein 1 related
-2.4	Timp1	tissue inhibitor of metalloproteinase 1
-2.3	Vcam1	vascular cell adhesion molecule 1
-2.3	Serpina7	serine (or cysteine) peptidase inhibitor, clade A, member 7
-2.3	Serpina3c	serine (or cysteine) peptidase inhibitor, clade A, member 3C
-2.3	C4b	complement component 4B (Chido blood group)
-2.3	Dnaja4	DnaJ (Hsp40) homolog, subfamily A, member 4
-2.2	Capzb	capping protein muscle Z-line, beta
-2.4	BC048546	
-2.2	Acpp	acid phosphatase, prostate
-2.2	Uhrf1	ubiquitin-like, containing PHD and RING finger domains, 1
-2.2	Hspb8	heat shock protein 8
-2.3	BC048546	
-2.2	Col1a1	collagen, type I, alpha 1
-2.4	Chrna4	cholinergic receptor, nicotinic, alpha polypeptide 4
-2.3	Tes	testis derived transcript
-2.3	Atf3	activating transcription factor 3
-2.2	Cebpb	CCAAT/enhancer binding protein (C/EBP), beta
-2.2	Slc30a5	solute carrier family 30 (zinc transporter), member 5
-2.2	Capzb	capping protein muscle Z-line, beta
-2.2	Col4a1	collagen, type IV, alpha 1
-2.4	Slc16a6	solute carrier family 16 (monocarboxylic acid transporters), member 6
-2.1	Itih3	inter-alpha trypsin inhibitor, heavy chain 3
-2.2	Gmds	GDP-mannose 4, 6-dehydratase
-2.2	Apol10b	apolipoprotein L 10B
-2.6	Tff3	trefoil factor 3, intestinal
-2.1	Nedd9	neural precursor cell expressed, developmentally down-regulated gene 9
-2.1	Pim3	proviral integration site 3
-2.1	Rpl12	ribosomal protein L12
-2.1	Chordc1	cysteine and histidine-rich domain (CHORD)-containing, zinc-binding protein 1
-2.2	Trmt61a	tRNA methyltransferase 61A
-2.2	Gja1	gap junction protein, alpha 1
-2.1	Mettl20	methyltransferase like 20
-2.1	Serpina3m	serine (or cysteine) peptidase inhibitor, clade A, member 3M
-3.8	Eqtn	equatorin, sperm acrosome associated
-2.1	Sema6b	sema domain, transmembrane domain (TM), and cytoplasmic domain, 6B
-2.2	Eif1a	eukaryotic translation initiation factor 1A
-2.4	Plk3	polo-like kinase 3
-2.1	Mvp	major vault protein

-2.2	Nfkbiz	nuclear factor of kappa light polypeptide gene enhancer in B cells inhibitor, z
-2.1	Gm8144	
-2.1	Cd68	CD68 antigen
-2.1	Stat3	signal transducer and activator of transcription 3
-2.1	B4galt1	UDP-Gal:betaGlcNAc beta 1,4- galactosyltransferase, polypeptide 1
-2.1	Akap12	A kinase anchor protein 12
-2.2	Fam25c	family with sequence similarity 25, member C
-2.1	Lyz2	lysozyme 2
-2.1	Tgm2	transglutaminase 2, C polypeptide
-2.0	Lgmn	legumain
-2.3	Selenbp2	selenium binding protein 2
-2.1	Rpp38	ribonuclease P/MRP 38 subunit
-2.1	Tmc5	transmembrane channel-like gene family 5
-2.2	Orm1	orosomucoid 1
-2.2	Chrna4	cholinergic receptor, nicotinic, alpha polypeptide 4
-2.1	Gm6305	
-2.1	Stat3	signal transducer and activator of transcription 3
-2.1	Rcan1	regulator of calcineurin 1
-2.2	Atf4	activating transcription factor 4
-2.1	Ly6e	lymphocyte antigen 6 complex, locus E
-2.1	Casp4	caspase 4, apoptosis-related cysteine peptidase
-2.0	Heatr1	HEAT repeat containing 1
-2.0	Relb	avian reticuloendotheliosis viral (v-rel) oncogene related B
-2.0	Tpd52	tumor protein D52
-2.0	Hp	haptoglobin
-2.0	Ets2	E26 avian leukemia oncogene 2, 3' domain
-2.0	Hist2h3b	histone cluster 2, H3b
-2.3	Il21r	interleukin 21 receptor
-2.1	Map7d1	MAP7 domain containing 1
-2.2	Srrm4	serine/arginine repetitive matrix 4
-2.0	Ifitm5	interferon induced transmembrane protein 5
-2.1	Gm6560	
-2.1	Sbno2	strawberry notch homolog 2
-2.1	Mtmr11	myotubularin related protein 11
-2.4	Mkks	McKusick-Kaufman syndrome
-2.1	Mcam	melanoma cell adhesion molecule
-2.1	Vsig4	V-set and immunoglobulin domain containing 4
-2.1	Atm	ataxia telangiectasia mutated homolog
-2.0	Tbl2	transducin (beta)-like 2
-2.0	Ddit4	DNA-damage-inducible transcript 4
-2.2	Pilrb1	paired immunoglobin-like type 2 receptor beta 1
-2.0	Nos3	nitric oxide synthase 3, endothelial cell
-2.0	Sla	src-like adaptor
-2.1	Slc39a14	solute carrier family 39 (zinc transporter), member 14
-2.0	Bhlha15	basic helix-loop-helix family, member a15
-2.0	Wfdc17	WAP four-disulfide core domain 17
-2.0	Ikbke	inhibitor of kappaB kinase epsilon
-1.9	Gm7665	
-2.1	Syvn1	synovial apoptosis inhibitor 1, synoviolin
-2.0	Stap2	signal transducing adaptor family member 2
-2.0	Slc13a3	solute carrier family 13, member 3
-2.0	Fmn2	formin 2
-2.0	Csf2rb2	colony stimulating factor 2 receptor, beta 2, low-affinity
-2.0	Trf	transferrin
-2.7	Psmd8	proteasome 26S subunit, non-ATPase, 8
-2.0	Spp1	secreted phosphoprotein 1
-2.1	Ttc39a	tetratricopeptide repeat domain 39A
-2.1	C1qc	complement component 1, q subcomponent, C chain
-3.5	Ctsll3	cathepsin L-like 3
-1.9	Hist2h3b	histone cluster 2, H3b
-1.9	Heatr1	HEAT repeat containing 1
-2.0	Ccp110	centriolar coiled coil protein 110
-2.1	Adam11	a disintegrin and metallopeptidase domain 11
-1.9	Nupr1	nuclear protein transcription regulator 1
-2.0	Stat3	signal transducer and activator of transcription 3
-2.0	Cd163	CD163 antigen

-1.9		Zdhhc13	zinc finger, DHHC domain containing 13
-2.0		C1qb	complement component 1, q subcomponent, beta polypeptide
-2.0		Creb3l2	cAMP responsive element binding protein 3-like 2
-2.2		Mup4	major urinary protein 4
-2.0		Ctps	cytidine 5'-triphosphate synthase
-1.9		Il33	interleukin 33
-1.9		Tnip2	TNFAIP3 interacting protein 2
-1.9		Abcb1b	ATP-binding cassette, sub-family B, member 1B
-2.1		Gm5697	
-2.0		Gm5697	
-2.0		Cyp2c70	cytochrome P450, family 2, subfamily c, polypeptide 70
-2.0		Adrb2	adrenergic receptor, beta 2
-2.0		Ly6d	lymphocyte antigen 6 complex, locus D
-1.9		Tnfsf14	tumor necrosis factor superfamily, member 14
-2.0		Hist2h3b	histone cluster 2, H3b
-2.2		Cxcl9	chemokine (C-X-C motif) ligand 9
-1.9		Map3k8	mitogen-activated protein kinase kinase kinase 8
-2.0		Lyz2	lysozyme 2
-2.0		Tmem39a	transmembrane protein 39a
-2.1		Dnaic1	dynein, axonemal, intermediate chain 1
-2.0		Id3	inhibitor of DNA binding 3
-1.9		Flot1	flotillin 1
-1.9		Adh7	alcohol dehydrogenase 7 (class IV), mu or sigma polypeptide
-2.0		Csrp1	cysteine and glycine-rich protein 1
-2.0		Cap1	CAP, adenylate cyclase-associated protein 1
-1.9		Jun	Jun oncogene
-1.9		Mphosph6	M phase phosphoprotein 6
-1.9		AK193661	
-2.0		Insc	inscuteable homolog
-2.0		Sowahb	sosondowah ankyrin repeat domain family member B
-1.9		Hist2h3b	histone cluster 2, H3b
-2.1		Pvrl2	poliovirus receptor-related 2
-1.9		Sybu	syntabulin (syntaxin-interacting)
-1.9		Slc25a19	solute carrier family 25, member 19
-2.0		Fam107a	family with sequence similarity 107, member A
-2.0		Dusp1	dual specificity phosphatase 1
-1.9		Crem	cAMP responsive element modulator
-1.9		Hp	haptoglobin
-1.9		Kcna5	potassium voltage-gated channel, shaker-related subfamily, member 5
-1.9		Il13ra1	interleukin 13 receptor, alpha 1
-2.1		Agpat9	1-acylglycerol-3-phosphate O-acyltransferase 9
-1.9		Zdhhc13	zinc finger, DHHC domain containing 13
-1.9		Wars	tryptophanyl-tRNA synthetase
-1.9		Nfkb2	nuclear factor of kappa light polypeptide gene enhancer in B cells 2
-2.0		Gdf15	growth differentiation factor 15
-1.9		Sept5	septin 5
-1.9		Mpg	N-methylpurine-DNA glycosylase
-1.9		Egfr	epidermal growth factor receptor
-1.9		Ddhd1	DDHD domain containing 1
-1.9		Alg9	asparagine-linked glycosylation 9
-1.9		Xbp1	X-box binding protein 1
-1.9		Trem2	triggering receptor expressed on myeloid cells 2
-1.9		Slc51b	solute carrier family 51, beta subunit
-2.0		Zfp426	zinc finger protein 426
-2.0		Syn1	synapsin I
-1.9		Il1b	interleukin 1 beta
-1.9		Cd207	CD207 antigen
-1.9		Ifnlr1	interferon lambda receptor 1
-1.9		Bach1	BTB and CNC homology 1
-1.9		Fkbp11	FK506 binding protein 11
-1.9		Mthfd2	methylenetetrahydrofolate dehydrogenase 2
-1.9		Wars	tryptophanyl-tRNA synthetase
-1.9		Jak3	Janus kinase 3
-1.9		Mcm6	minichromosome maintenance deficient 6
-1.9		Arfgap3	ADP-ribosylation factor GTPase activating protein 3
-1.9		Tubb4b	tubulin, beta 4B class IVB

-1.9		Sfxn3	sideroflexin 3
-1.9		Tmed3	transmembrane emp24 domain containing 3
-1.9		Tuba1c	tubulin, alpha 1C
-2.0		Cdh3	cadherin 3
-1.9		Tmed3	transmembrane emp24 domain containing 3
-1.9		Fam26f	family with sequence similarity 26, member F
-1.9		Derl3	Der1-like domain family, member 3
-1.9		Zfp235	zinc finger protein 235
-2.0		Krt6a	keratin 6A
-2.0		Gnat1	guanine nucleotide binding protein, alpha transducing 1

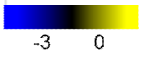

Supplementary Table S5: Heat map brain.

mean linear fold change	Pts-ki/ki A B C	Gene ID	Gene name
-121.7		Tmem25	transmembrane protein 25
-31.2		Lcn2	lipocalin 2
-6.4		S100a8	S100 calcium binding protein A8
-3.9		Retnlg	resistin like gamma
-4.1		Plin4	perilipin 4
-4.4		S100a9	S100 calcium binding protein A9
-4.0		Ch25h	cholesterol 25-hydroxylase
-3.0		Cd14	CD14 antigen
-3.4		Lrg1	leucine-rich alpha-2-glycoprotein 1
-3.3		Ccl12	chemokine (C-C motif) ligand 12
-2.3		Tmem66	transmembrane protein 66
-2.3		Tnnc2	troponin C2, fast
-2.5		Alg9	asparagine-linked glycosylation 9
-2.3		Plac8	placenta-specific 8
-2.0		Ms4a6d	membrane-spanning 4-domains, subfamily A, member 6D
-2.5		Atm	ataxia telangiectasia mutated homolog
-1.9		Hspb1	heat shock protein 1
-2.4		Serpina3f	serine (or cysteine) peptidase inhibitor, clade A, member 3F
-2.0		Xdh	xanthine dehydrogenase
-2.0		Cryab	crystallin, alpha B
-2.1		Socs3	suppressor of cytokine signaling 3
-2.1		Serpina3g	serine (or cysteine) peptidase inhibitor, clade A, member 3G
-2.0		Osmr	oncostatin M receptor
-2.1		Gm6522	
-2.2		Ccl9	chemokine (C-C motif) ligand 9
-2.4		Ccl12	chemokine (C-C motif) ligand 12
-2.7		Srpr	signal recognition particle receptor
-2.8		Hp	haptoglobin
-2.0		Cd207	CD207 antigen
-2.2		Mkks	McKusick-Kaufman syndrome
-2.1		Niacr1	niacin receptor 1
-2.1		Fcgr4	Fc receptor, IgG, low affinity IV
-1.9		Atm	ataxia telangiectasia mutated homolog
-2.2		Zfp235	zinc finger protein 235
-2.0		Mds1	MDS1 and EVI1 complex locus
-2.2		Gh	growth hormone
-2.2		Olfr1132	olfactory receptor 1132
-2.2		Xlr4a	X-linked lymphocyte-regulated 4A

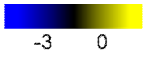

Heat map of regulated genes in liver (Table S4) and brain (Table S5) of *Pts*-ki/ki mice compared to wild type animals. Fold changes were calculated as ratios of signal intensities of single mutant samples and the mean of the respective wild type controls. Log2 fold changes were color coded according the scale bar at the bottom of the heat maps. Blue represents the down-regulation and yellow the up-regulation in the mutant tissue.

Supplementary Table S6: Over-represented gene ontology categories for genes regulated in brain and liver of *Pts*-ki/ki mice. *The *p*-values (right-tailed Fisher Exact Test) for a given process annotation is calculated by considering the number of genes that participate in that process and the total number of genes known to be associated with that process.

A) Brain

Functions annotation	p-value*	# genes
leukocyte migration	2.11E-09	14
vascular disease	3.80E-06	11
differentiation of cells	6.60E-04	12
proliferation of cells	9.70E-03	15

B) Liver

Functions annotation	p-value	# genes
leukocyte migration	1.25E-23	71
vascular disease	2.43E-21	70
quantity of immunoglobulin	8.53E-21	37
morphology of body cavity	1.77E-16	66
lipid metabolism	3.19E-15	57
cell death	1.13E-14	133
protein synthesis	1.08E-13	39
glucose metabolism	9.29E-13	61
differentiation of cells	2.09E-12	86
weight loss	8.02E-12	24
inflammatory response	2.48E-10	11
hepatic steatosis	8.82E-09	21
metabolism of reactive oxygen species	2.70E-08	34
morphology of liver	3.65E-08	18
hypertrophy	4.09E-08	29
obesity	5.32E-08	27
insulin sensitivity	1.10E-07	13
i-kappab kinase/nf-kappab cascade	6.98E-07	13

Supplementary Table S7: e*Nos*/*Nos3*-gene expression and PTPS protein in liver and brain.

Genotype	Liver e*Nos*/*Nos*3-mRNA[a]	Brain e*Nos*/*Nos*3-mRNA[a]
***Pts*-wt/wt (n=5)**	1.00 (0.78-1.28)	1.00 (0.71-1.41)
***Pts*-ki/wt (n=4-5)**	1.04 (0.85-1.27)	1.18 (0.86-1.64)
***Pts*-ki/ki (n=5)**	0.85 (0.67-1.06)	1.24 (0.93-1.64)
***Pts*-ko/wt (n=4-5)**	1.41 (0.88-2.23)	1.23 (0.77-1.96)
***Pts*-ki/ko (n=5)**	0.67 (0.43-1.03)	1.19 (1.00-1.41)

[a]Normalized relative to *Gapdh*-mRNA, *Gapdh*, glyceraldehyde 3-phosphate dehydrogenase; e*Nos*/*Nos*3, Endothelial nitric oxide synthase/ nitric oxide synthase 3

REFERENCES

1. Werner ER, Blau N, Thony B. Tetrahydrobiopterin: biochemistry and pathophysiology. *Biochem J* 2011; **438**(3)**:** 397-414.

2. Blau N, van Spronsen FJ, Levy HL. Phenylketonuria. *Lancet* 2010; **376**(9750)**:** 1417-27.

3. McNeill E, Channon KM. The role of tetrahydrobiopterin in inflammation and cardiovascular disease. *Thromb Haemost* 2012; **108**(5)**:** 832-9.

4. Shi W, Meininger CJ, Haynes TE, Hatakeyama K, Wu G. Regulation of tetrahydrobiopterin synthesis and bioavailability in endothelial cells. *Cell Biochem Biophys* 2004; **41**(3)**:** 415-34.

5. Forstermann U, Munzel T. Endothelial nitric oxide synthase in vascular disease: from marvel to menace. *Circulation* 2006; **113**(13)**:** 1708-14.

6. Wu G, Meininger CJ. Regulation of nitric oxide synthesis by dietary factors. *Annu Rev Nutr* 2002; **22:** 61-86.

7. Duplain H, Burcelin R, Sartori C, Cook S, Egli M, Lepori M *et al.* Insulin resistance, hyperlipidemia, and hypertension in mice lacking endothelial nitric oxide synthase. *Circulation* 2001; **104**(3)**:** 342-5.

8. Wyss CA, Koepfli P, Namdar M, Siegrist PT, Luscher TF, Camici PG *et al.* Tetrahydrobiopterin restores impaired coronary microvascular dysfunction in hypercholesterolaemia. *Eur J Nucl Med Mol Imaging* 2005; **32**(1)**:** 84-91.

9. Meininger CJ, Marinos RS, Hatakeyama K, Martinez-Zaguilan R, Rojas JD, Kelly KA *et al.* Impaired nitric oxide production in coronary endothelial cells of the spontaneously diabetic BB rat is due to tetrahydrobiopterin deficiency. *Biochem J* 2000; **349**(Pt 1)**:** 353-6.

10. Alp NJ, Mussa S, Khoo J, Cai S, Guzik T, Jefferson A *et al.* Tetrahydrobiopterin-dependent preservation of nitric oxide-mediated endothelial function in diabetes by targeted transgenic GTP-cyclohydrolase I overexpression. *J Clin Invest* 2003; **112**(5)**:** 725-35.

11. Pannirselvam M, Simon V, Verma S, Anderson T, Triggle CR. Chronic oral supplementation with sepiapterin prevents endothelial dysfunction and oxidative stress in small mesenteric arteries from diabetic (db/db) mice. *Br J Pharmacol* 2003; **140**(4)**:** 701-6.

12. Ihlemann N, Rask-Madsen C, Perner A, Dominguez H, Hermann T, Kober L *et al.* Tetrahydrobiopterin restores endothelial dysfunction induced by an oral glucose challenge in healthy subjects. *Am J Physiol Heart Circ Physiol* 2003; **285**(2)**:** H875-82.

13. Nystrom T, Nygren A, Sjoholm A. Tetrahydrobiopterin increases insulin sensitivity in patients with type 2 diabetes and coronary heart disease. *Am J Physiol Endocrinol Metab* 2004; **287**(5)**:** E919-25.

14. Meininger CJ, Cai S, Parker JL, Channon KM, Kelly KA, Becker EJ *et al.* GTP cyclohydrolase I gene transfer reverses tetrahydrobiopterin deficiency and increases nitric oxide synthesis in endothelial cells and isolated vessels from diabetic rats. *Faseb J* 2004; **18**(15)**:** 1900-2.

15. Wang X, Hattori Y, Satoh H, Iwata C, Banba N, Monden T *et al.* Tetrahydrobiopterin prevents endothelial dysfunction and restores adiponectin levels in rats. *Eur J Pharmacol* 2007; **555**(1)**:** 48-53.

16. Fox CS, Massaro JM, Hoffmann U, Pou KM, Maurovich-Horvat P, Liu CY *et al.* Abdominal visceral and subcutaneous adipose tissue compartments: association with metabolic risk factors in the Framingham Heart Study. *Circulation* 2007; **116**(1)**:** 39-48.

17. Rader DJ. Effect of insulin resistance, dyslipidemia, and intra-abdominal adiposity on the development of cardiovascular disease and diabetes mellitus. *Am J Med* 2007; **120**(3 Suppl 1)**:** S12-8.

18. Despres JP, Lemieux I. Abdominal obesity and metabolic syndrome. *Nature* 2006; **444**(7121)**:** 881-7.

19. Elzaouk L, Leimbacher W, Turri M, Ledermann B, Bürki K, Blau N *et al.* Dwarfism and low insulin-like growth factor-1 due to dopamine depletion in Pts-/- mice rescued by feeding neurotransmitter precursors and H4-biopterin. *J Biol Chem* 2003; **278**(30)**:** 28303-11.

20. Sumi-Ichinose C, Urano F, Kuroda R, Ohye T, Kojima M, Tazawa M *et al.* Catecholamines and serotonin are differently regulated by tetrahydrobiopterin. A study from 6-pyruvoyltetrahydropterin synthase knockout mice. *J Biol Chem* 2001; **276**(44)**:** 41150-60.

21. Turri MO, Ilg EC, Thöny B, Blau N. Structure, genomic localization and recombinant expression of the mouse 6-pyruvoyl-tetrahydropterin synthase gene. *Biol Chem* 1998; **379**(12)**:** 1441-7.

22. DePeters EJ, Hovey RC. Methods for collecting milk from mice. *J Mammary Gland Biol Neoplasia* 2009; **14**(4)**:** 397-400.

23. Haberman BH. Mechanical milk collection from mice for Bittner virus isolation. *Lab Anim Sci* 1974; **24**(6)**:** 935-7.

24. Rashed MS, Ozand PT, Bucknall MP, Little D. Diagnosis of inborn errors of metabolism from blood spots by acylcarnitines and amino acids profiling using automated electrospray tandem mass spectrometry. *Pediatr Res* 1995; **38**(3)**:** 324-31.

25. Livak KJ, Schmittgen TD. Analysis of relative gene expression data using real-time quantitative PCR and the 2(-Delta Delta C(T)) Method. *Methods* 2001; **25**(4)**:** 402-8.

26. Bucolo G, David H. Quantitative determination of serum triglycerides by the use of enzymes. *Clin Chem* 1973; **19**(5)**:** 476-82.

27. Oppliger T, Thöny B, Nar H, Burgisser D, Huber R, Heizmann CW *et al.* Structural and functional consequences of mutations in 6-pyruvoyltetrahydropterin synthase causing hyperphenylalaninemia in humans. Phosphorylation is a requirement for in vivo activity. *J Biol Chem* 1995; **270**(49)**:** 29498-506.

28. Fuchs H, Gailus-Durner V, Adler T, Aguilar-Pimentel JA, Becker L, Calzada-Wack J *et al.* Mouse phenotyping. *Methods* 2011; **53**(2)**:** 120-35.

29. Beckers J, Wurst W, de Angelis MH. Towards better mouse models: enhanced genotypes, systemic phenotyping and envirotype modelling. *Nat Rev Genet* 2009; **10**(6)**:** 371-80.

30. Frayn KN. Calculation of substrate oxidation rates in vivo from gaseous exchange. *J Appl Physiol Respir Environ Exerc Physiol* 1983; **55**(2)**:** 628-34.

31. Rathkolb B, al. e. Clinical Chemistry and Other Laboratory Tests on Mouse Plasma or Serum. *in: Birgit Rathkolb, Wolfgang Hans, Cornelia Prehn, Helmut Fuchs, Valérie Gailus-Durner, Bernhard Aigner, Jerzy Adamski, Eckhard Wolf, Martin Hrabě de Angelis* 2013.

32. Horsch M, Schadler S, Gailus-Durner V, Fuchs H, Meyer H, de Angelis MH *et al.* Systematic gene expression profiling of mouse model series reveals coexpressed genes. *Proteomics* 2008; **8**(6)**:** 1248-56.

33. Kugler JE, Horsch M, Huang D, Furusawa T, Rochman M, Garrett L *et al.* High mobility group N proteins modulate the fidelity of the cellular transcriptional profile in a tissue- and variant-specific manner. *J Biol Chem* 2013; **288**(23)**:** 16690-703.

34. Saeed AI, Bhagabati NK, Braisted JC, Liang W, Sharov V, Howe EA *et al.* TM4 microarray software suite. *Methods in enzymology* 2006; **411:** 134-93.

35. Tusher VG, Tibshirani R, Chu G. Significance analysis of microarrays applied to the ionizing radiation response. *Proc Natl Acad Sci U S A* 2001; **98**(9)**:** 5116-21.

36. Edgar R, Domrachev M, Lash AE. Gene Expression Omnibus: NCBI gene expression and hybridization array data repository. *Nucleic Acids Res* 2002; **30**(1)**:** 207-10.

37. Thöny B, Leimbacher W, Blau N, Harvie A, Heizmann CW. Hyperphenylalaninemia due to defects in tetrahydrobiopterin metabolism: molecular characterization of mutations in 6-pyruvoyl-tetrahydropterin synthase. *Am J Hum Genet* 1994; **54**(5)**:** 782-92.

38. Thöny B, Ding Z, Martinez A. Tetrahydrobiopterin protects phenylalanine hydroxylase activity in vivo: Implications for tetrahydrobiopterin-responsive hyperphenylalaninemia. *FEBS Lett* 2004; **577**(3)**:** 507-11.

39. Matsubara Y, Gaull GE. Biopterin and neopterin in various milks and infant formulas. *Am J Clin Nutr* 1985; **41**(1)**:** 110-2.

40. Leeming RJ, Blair JA, Melikian V, O'Gorman DJ. Biopterin derivatives in human body fluids and tissues. *J Clin Pathol* 1976; **29**(5)**:** 444-51.

41. Joseph B, Dyer CA. Relationship between myelin production and dopamine synthesis in the PKU mouse brain. *J Neurochem* 2003; **86**(3)**:** 615-26.

42. Embury JE, Charron CE, Martynyuk A, Zori AG, Liu B, Ali SF *et al.* PKU is a reversible neurodegenerative process within the nigrostriatum that begins as early as 4 weeks of age in Pah(enu2) mice. *Brain Res* 2007; **1127**(1)**:** 136-50.

43. Gailus-Durner V, Fuchs H, Adler T, Aguilar Pimentel A, Becker L, Bolle I *et al.* Systemic First-Line Phenotyping. *Methods Mol Biol* 2009; **530:** 1-47.

44. Gailus-Durner V, Fuchs H, Becker L, Bolle I, Brielmeier M, Calzada-Wack J *et al.* Introducing the German Mouse Clinic: open access platform for standardized phenotyping. *Nat Methods* 2005; **2**(6)**:** 403-4.

45. Wang XA, Deng S, Jiang D, Zhang R, Zhang S, Zhong J *et al.* CARD3 deficiency exacerbates diet-induced obesity, hepatosteatosis, and insulin resistance in male mice. *Endocrinology* 2013; **154**(2)**:** 685-97.

46. Ghosh PM, Shu ZJ, Zhu B, Lu Z, Ikeno Y, Barnes JL *et al.* Role of beta-adrenergic receptors in regulation of hepatic fat accumulation during aging. *J Endocrinol* 2012; **213**(3)**:** 251-61.

47. Daugherity EK, Balmus G, Al Saei A, Moore ES, Abi Abdallah D, Rogers AB *et al.* The DNA damage checkpoint protein ATM promotes hepatocellular apoptosis and fibrosis in a mouse model of non-alcoholic fatty liver disease. *Cell Cycle* 2012; **11**(10)**:** 1918-28.

48. VerHague MA, Cheng D, Weinberg RB, Shelness GS. Apolipoprotein A-IV expression in mouse liver enhances triglyceride secretion and reduces hepatic lipid content by promoting very low density lipoprotein particle expansion. *Arterioscler Thromb Vasc Biol* 2013; **33**(11)**:** 2501-8.

49. Yang P, Wang Z, Zhan Y, Wang T, Zhou M, Xia L *et al.* Endogenous A1 adenosine receptor protects mice from acute ethanol-induced hepatotoxicity. *Toxicology* 2013; **309:** 100-6.

50. Park HJ, Kang YM, Kim CH, Jung MH. ATF3 negatively regulates adiponectin receptor 1 expression. *Biochem Biophys Res Commun* 2010; **400**(1)**:** 72-7.

51. Burke SJ, Goff MR, Updegraff BL, Lu D, Brown PL, Minkin SC, Jr. *et al.* Regulation of the CCL2 gene in pancreatic beta-cells by IL-1beta and glucocorticoids: role of MKP-1. *PLoS One* 2012; **7**(10)**:** e46986.

52. Babaev VR, Runner RP, Fan D, Ding L, Zhang Y, Tao H *et al.* Macrophage Mal1 deficiency suppresses atherosclerosis in low-density lipoprotein receptor-null mice by activating peroxisome proliferator-activated receptor-gamma-regulated genes. *Arterioscler Thromb Vasc Biol* 2011; **31**(6)**:** 1283-90.

53. Wang L, Xu S, Lee JE, Baldridge A, Grullon S, Peng W *et al.* Histone H3K9 methyltransferase G9a represses PPARgamma expression and adipogenesis. *EMBO J* 2013; **32**(1)**:** 45-59.

54. Guenard F, Bouchard L, Tchernof A, Deshaies Y, Hould FS, Lebel S *et al.* DUSP1 Gene Polymorphisms Are Associated with Obesity-Related Metabolic Complications among Severely Obese Patients and Impact on Gene Methylation and Expression. *Int J Genomics* 2013; **2013:** 609748.

55. Sheng L, Zhou Y, Chen Z, Ren D, Cho KW, Jiang L *et al.* NF-kappaB-inducing kinase (NIK) promotes hyperglycemia and glucose intolerance in obesity by augmenting glucagon action. *Nat Med* 2012; **18**(6)**:** 943-9.

56. Tsuchiya K, Accili D. Liver sinusoidal endothelial cells link hyperinsulinemia to hepatic insulin resistance. *Diabetes* 2013; **62**(5)**:** 1478-89.

57. Tai SC, Robb GB, Marsden PA. Endothelial nitric oxide synthase: a new paradigm for gene regulation in the injured blood vessel. *Arterioscler Thromb Vasc Biol* 2004; **24**(3)**:** 405-12.

58. De Rosa S, Cirillo P, Pacileo M, Petrillo G, D'Ascoli GL, Maresca F *et al.* Neopterin: from forgotten biomarker to leading actor in cardiovascular pathophysiology. *Curr Vasc Pharmacol* 2011; **9**(2)**:** 188-99.

59. Yan JQ, Tan CZ, Wu JH, Zhang DC, Chen JL, Zeng BY *et al.* Neopterin negatively regulates expression of ABCA1 and ABCG1 by the LXRalpha signaling pathway in THP-1 macrophage-derived foam cells. *Mol Cell Biochem* 2013; **379**(1-2)**:** 123-31.

60. Farooqi IS, O'Rahilly S. Monogenic obesity in humans. *Annu Rev Med* 2005; **56:** 443-58.

3.2 CHALLENGING THE OBSERVATION OF ñUNAFFECTEDò AND ñAFFECTEDò *PTS*-KI/KO MICE FROM DIFFERENT BREEDING COMBINATIONS OF *PTS*-KI AND *PTS*-KO PARENTS

3.2.1 ABSTRACT

Dea Adamsen reported in her PhD thesis the existence of two different phenotypes in compound heterozygous *Pts*-ki/ko mice derived from homozygous *Pts*-ki/ki mothers: a severely ñaffectedò group that died around 3-4 days after birth, and a second ñunaffectedò group with normal survival (described in chapter 3.1). The analyzed liver and brain tissue in the ñaffectedò group showed low PTPS enzyme activity, reduced biopterin and increased neopterin levels (only in liver). Furthermore, they showed mild HPA and non detectable amounts of brain monoamine neurotransmitters. It should be emphasized that D. Adamsen also reported that *Pts*-ki/wt or *Pts*-ko/wt mothers did not generate ñaffectedò *Pts*-ki/ko mice, indicating that genotype of the parents, especially of the mother, lead to phenotypical variations in the offspring. Therefore, it was the objectives to validate and eventually understand the cause for these two phenotypes and to deeper investigate potential difference in *Pts*-ki/ko mice derived from different breeding combinations, i.e. *Pts*-ki/ko offspring from *Pts*-ki/wt, *Pts*-ko/wt or *Pts*-ki/ki parents. In a first step, newborn mice, especially *Pts*-ki/ko newborns, derived from different breeding combinations of homozygous and heterozygous *Pts*-ki with heterozygous *Pts*-ko mice were investigated for potential differences. These analyses included potential mild variations in PTPS enzyme activity (liver and brain), biopterin (liver and brain), neopterin (liver) and serotonin (brain) levels. To confirm the appearance of the ñaffectedò versus ñunaffectedò *Pts*-ki/ko phenotype, *Pts*-ki/ko mice from homozygous *Pts*-ki/ki mouse mothers were investigated for up to 4 days after birth, which was the described time span when the ñaffectedò phenotype was noticed by D. Adamsen. At the age of 4 days, the pups were sacrificed and biochemically analyzed. Furthermore, D. Adamsen suggested in her PhD thesis that ñlitter sizeò may enhance the appearance of the ñaffectedò *Pts*-ki/ko phenotype. Therefore, it was examined whether there are more ñaffectedò *Pts*-ki/ko offsprings in big litters with 8-9 pups compared to small litters with 3-4 pups 4 days after birth. Surprisingly, the appearance of the ñaffectedò *Pts*-ki/ko mouse phenotype could not be confirmed.

3.2.2 INTRODUCTION

To generate a severe and central phenotype of BH_4 deficiency in a mouse model without having newborn lethality, the *Pts*-ko mouse strain (Sumi-Ichinose et al., 2001, Elzaouk et al., 2003) was crossed to the *Pts*-ki mouse strain (R. Scavelli, 2006, Univerity of Zurich, Thöny et al., 1994, Oppliger et al., 1995), generating the compound heterozygous *Pts*-ki/ko mouse model. Homozygous *Pts*-ko/ko showed a severe and central phenotype with newborn lethality, whereas the homozygous *Pts*-ki/ki mice had a mild and peripheral phenotype. The first phenotypical analysis of the compound heterozygous *Pts*-ki/ko mice was performed by D. Adamsen in 2011 (Adamsen, 2011). She reported in her dissertation that *Pts*-ki/ko mice from *Pts*-ki/ki mouse mothers showed two distinguishable phenotypes: the ñunaffectedò *Pts*-ki/ko mice with a slightly more severe BH_4 deficiency phenotype then *Pts*-ki/ki mice, and the ñaffectedò *Pts*-ki/ko mice, which showed a severe and central form of BH_4 deficiency with visible abnormalities at the age of 3-4 days, including reduced body size, altered milk-intake (no white belly), and behaviour and movement disorders (Fig. 18) (Adamsen, 2011). At birth, all *Pts*-ki/ko showed reduced PTPS activity in liver and brain, as well as elevated neopterin in liver. The ñaffectedò group worsened the following 3-4 days by having further reduced PTPS activity and low biopterin levels in liver and brain, increased neopterin levels in liver, mild HPA and non detectable amounts of brain monoamine neurotransmitters, and finally died or had to be sacrificed. In contrast, the so called ñunaffectedò group showed also reduced PTPS activity but normal levels of biopterin and neopterin in liver and brain, normal blood L-Phe and brain monoamine neurotransmitters. ñUnaffectedò *Pts*-ki/ko mice survived and had a normal lifespan. Heterozygous *Pts*-ki/wt or *Pts*-ko/wt mothers did not produced ñaffectedò *Pts*-ki/ko offsprings. A summary of D. Adamsenôs data is represented in table 4.

Figure 18: Pictures from D. Adamsen dissertation. A: 3-4 days after birth ñaffectedò *Pts*-ki/ko (right) mice stood out from their ñun-affectedò *Pts*-ki/ko (left) littermates.

Table 4: Summary of D. Adamsenös data (University of Zurich, 2011).

		♀ *Pts*-ki/ki x ♂ *Pts*-ko/wt			♀ *Pts*-ko/wt x ♂ *Pts*-ki/ki or ♂ *Pts*-ki/wt
		newborns	3-4 days		3 weeks
Parameter	**Tissue**		**"affected"**	**"unaffected"**	**"unaffected"**
PTPS activity	**Liver**	32 % of wt	10 % of wt	36 % of wt	no data
	Brain	25 % of wt	3 % of wt	53 % of wt	no data
L-Phe	**Blood**	normal	~900 µmol/l	normal	normal
Biopterin	**Liver**	normal	3 % of wt	normal	normal
	Brain	11 % of wt	4 % of wt	normal	normal
Neopterin	**Liver**	~2,300 % of wt	30,900 % of wt	normal	750 % of wt
	Brain	normal	normal	normal	normal
Neurotransmitters	**Brain**	normal	n.d.	normal	normal

Wt, wild-type; n.d., non detectable.

Overall, it was proposed that ñaffectedò *Pts*-ki/ko mice had the potential to be a suitable mouse model to study BH_4 deficiency as they mimic the biochemical hallmarks of the severe and central human BH_4 deficiency (Adamsen, 2011). It was discussed that this preliminary observation of two phenotypes could be explained by a ñmother effectò (*Pts*-ki/ki mothers) in combination with ñallelic effectò (homozygosity) (Adamsen, 2011). Furthermore, D. Adamasenös hypothesized that differences in biopterin amounts in mother milk and/or that the ñmother effectò (*Pts*-ki/ki females) in combination with ñallelic effectò (homozygosity) led to these two diverse phenotypes (D. Adamsen, 2011, Haberman, 1974).

The objective in this study was focused on the validation of D. Adamsenös preliminary observation of the two described phenotypes and the investigation on the possible causes. D. Adamsenös first hypothesis that different amounts of biopterin in mother milk could lead to the appearance of the two phenotypes could be excluded (see chapter 3.1). It was previously described in a creatine deficiency knock-out mouse model for guanidinoacetate N-methyltransferase (GAMT) that intercrosses of heterozygous mutant mice resulted in a deviation from the Mendelian inheritance pattern probably caused by newborn lethality (Schmidt et al., 2004). Heterozygous *Pts*-ki/wt or *Pts*-ko/wt mice are generated by breeding heterozygous *Pts*-ki/wt or *Pts*-ko/wt males with wild-type females, whereas homozygous *Pts*-ki/ki mice can only be produced by intercrosses. Therefore, a ñmother effectò (*Pts*-ki/ki mothers) in combination with ñallelic effectò (homozygosity) would be more likely to explain D. Adamsenös summarized observation that only *Pts*-ki/ki females produced ñaffectedò *Pts*-ki/ko offsprings.

To examine this thesis, *Pts*-ki/ko newborns and their siblings from all possible breeding combinations of *Pts*-ki/wt, *Pts*-ko/wt and *Pts*-ki/ki parents were compared for alterations in their PTPS activity, biopterin, neopterin, L-Phe, L-Tyr and monoamine neurotransmitter levels. In a next step, the ñaffectedò phenotype was reproduced by breeding homozygous *Pts*-ki/ki females to heterozygous Pts-ko/wt males and the offsprings are closely investigated the following 4 days to detect ñaffectedò animals. Furthermore, it was investigated if there are more ñaffectedò pups in big litters (8-9 pups) than in small litters (3-4 pups) due to decreased availability of mother milk (rich source of BH_4) in big litters due to increased competitions between the pups (Weinmann et al., 2011). All material and methods used in this study were described in chapter 3.1.

3.2.3 RESULTS

3.2.3.1 Characterisation of newborn mice from different breeding combinations of *Pts*-ki/wt, *Pts*-ko/wt and *Pts*-ki/ki parents

In a first step, the characterisation of *Pts*-ki/ko newborns was extended by breeding homozygous or heterozygous *Pts*-ki mice with heterozygous *Pts*-ko mice in all possible combination (Fig. 19), and newborns were collected for biochemical analysis. Breeding combinations with a *Pts*-ki/ki parent is abbreviated as ñhomozygousò breeding, whereas breeding combinations with a *Pts*-ki/wt parent is abbreviated as ñheterozygousò breeding (Fig. 19). Fig. 19 also summarizes the percentage of all pups born from each breeding combination showing that the pups were born at the expected Mendelian frequency.

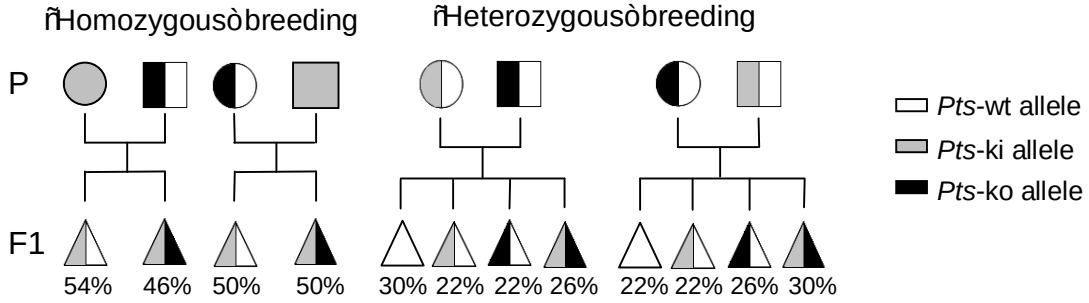

Figure 19: Schematic representation of all possible breeding combinations of *Pts*-ki/wt, *Pts*-ko/wt and *Pts*-ki/ki: ñHomozygousò *Pts*-ki/ki breedings pairs generate *Pts*-ki/wt and *Pts*-ki/ko offsprings; ñheterozygousò *Pts*-ki/wt breedings pairs generate *Pts*-wt/wt, *Pts*-ki/wt, *Pts*-ko/wt and *Pts*-ki/ko offsprings. Females are indicated by circles; males are indicated by squares; unknown sex is indicated by triangle; *Pts*-wt allele is indicated in white; *Pts*-ki allele is indicated in gray; *Pts*-ko allele is indicated in black.

A summary of the biochemical analysis of all offsprings from each breeding combination is listed in table 5. All newborn mice were investigated for their liver and brain PTPS activity, biopterin and neopterin, blood L-Phe and L-Tyr, and brain monoamine neurotransmitters (table 5).

Table 5: Summary of mouse newborns from different breedingcombinations.

Parameter		PTPS activity*		Biopterin**		Neopterin**		L-Phe***	L-Tyr***	Dopamine**	Norepinephrine**	Epinephrine**	Serotonin**
Tissue		Liver	Brain	Liver	Brain	Liver	Brain	Blood		Brain			
I *Pts*-ki/ki x II *Pts*-ko/wt	*Pts*-ki/wt (15)	26.9 ± 10.0[c]	29.1 ± 13.3[b]	21.8 ± 6.5[a]	14.2 ± 6.6	n.d.	1.0 ± 1.4	103.3 ± 27.5	140.5 ± 50.1[a]	24.1 ± 6.4	10.5 ± 8.3	6.5 ± 3.4	55.6 ± 13.4
	Pts-ki/ko (13)	2.9 ± 2.4[c]	4.2 ± 1.5[c]	19.7 ± 5.5[a]	11.4 ± 4.3	10.2 ± 5.8[c]	2.5 ± 1.0	89.8 ± 24.7[a]	130.9 ± 32.3[b]	23.6 ± 6.0	12.7 ± 6.1	8.6 ± 4.8	49.1 ± 8.8
I *Pts*-ki/wt x II *Pts*-ko/wt	*Pts*-wt/wt (7)	60.8 ± 25.4	69.4 ± 38.0	30.6 ± 12.5	13.8 ± 4.0	n.d.	1.4 ± 1.8	138.0 ± 11.5	192.5 ± 58.6	25.9 ± 12.1	21.2 ± 6.0	5.2 ± 5.4	61.0 ± 28.8
	Pts-ki/wt (5)	35.4 ± 8.8[a]	44.0 ± 18.7	27.2 ± 6.5	16.3 ± 5.8	0.6 ± 1.4	2.1 ± 2.3	129.9 ± 9.0	156.7 ± 24.1	27.2 ±6.4	20.5 ± 9.1	7.2 ± 4.6	63.9 ± 15.4
	Pts-ko/wt (5)	29.9 ± 11.5[a]	32.7 ± 14.2	44.4 ± 23.6	16.8 ± 2.4	n.d.	1.2 ± 1.8	157.4 ± 47.9	229.7 ± 76.2	28.4 ± 12.1	19.8 ± 9.4	9.3 ± 6.0	66.7 ±18.9
	Pts-ki/ko (6)	9.6 ± 5.2[c]	5.8 ± 1.4[c]	33.5 ± 11.2	14.4 ± 2.6	21.7 ± 10.1[c]	3.2 ± 3.1	126.7± 21.4a	142.5 ± 40.0	23.1 ± 4.6	18.1 ± 11.2	6.9 ± 3.3	58.8 ± 9.4
I *Pts*-ko/wt x II *Pts*-ki/ki	*Pts*-ki/wt (8)	33.0 ± 5.8b	38.4 ± 16.0	24.6 ± 3.3	13.8 ± 4.8	1.5 ± 3.6	1.6 ± 1.5	112.0 ± 20.4	182.4 ± 24.0	31.7 ± 10.1	10.9 ± 10.9	10.2 ± 2.9	66.9 ±30.2
	Pts-ki/ko (8)	3.8 ± 1.9[c]	3.3 ± 2.0[c]	23.7 ± 5.3	11.2 ± 2.2	12.1 ± 4.0[c]	1.7 ± 2.0	93.0 ± 17.2[a]	142.0 ± 53.5	32.0 ± 18.5	13.8 ± 9.9	10.6 ± 10.0	76.9 ± 27.5
I *Pts*-ko/wt x II *Pts*-ki/wt	*Pts*-wt/wt (6)	56.6 ± 8.9	57.1 ± 23.1	28.3 ± 9.7	13.5 ± 2.4	n.d.	1.1 ± 1.2	133.0 ± 32.8	203.9 ± 57.1	24.3 ± 4.3	15.7 ± 5.9	10.7 ± 2.6	54.8 ± 10.9
	Pts-ki/wt (7)	30.8 ± 9.6[a]	39.2 ± 17.7	25.1 ± 11.9	15.0 ± 4.0	n.d.	2.2 ± 2.3	118.5 ± 22.5	220.5 ± 71.1	21.3 ± 5.9	10.1 ± 4.5	7.8 ± 4.1	57.8 ± 11.8
	Pts-ko/wt (8)	22.5 ± 5.9[b]	21.1 ± 4.5[b]	26.8 ± 8.1	13.3 ± 4.1	n.d.	1.5 ± 2.2	148.4 ± 25.5	217.9 ± 43.8	34.6 ± 15.3	22.8 ± 13.8	7.8 ± 3.9	76.7 ± 29.9
	Pts-ki/ko (6)	5.3 ± 1.2[c]	5.6 ± 2.3[c]	31.6 ± 9.1	10.4 ± 1.5	13.4 ± 5.9[c]	3.7 ± 2.3	161.9 ± 40.3	244.2 ± 76.4	20.6 ± 3.4	19.0 ± 12.9	8.6 ± 6.4	65.4 ± 15.0

n.d., not detectable; * µU/mg protein; ** pmol/mg protein; *** µmol/l; Significant difference from the corresponding wild-type values: [a]p < 0.05, [b]p <0.01, [c]p < 0.001 (two-tailed Student's *t*-test).

Newborns were counted as ñaffectedò, when detected with mild HPA (L-Phe 360-600 µmol), low biopterin (< 5 pmol/mg protein) and/or low monoamine neurotransmitters, which are hallmarks for the described ñaffectedò animals. None of the analyzed *Pts*-ki/ko newborns fulfilled these criteria. Overall, PTPS activity in liver from *Pts*-ki/wt, *Pts*-ko/wt and *Pts*-ki/ko newborns from all breeding combinations was significantly lower than in both *Pts*-wt/wt offspring groups. On average, *Pts*-ki/ko mice had 9% ($p < 0.001$), *Pts*-ki/wt mice had 54% ($p < 0.05$), and *Pts*-ko/wt mice 45% ($p < 0.05$) of PTPS activity in comparison to *Pts*-wt/wt animals (table 5). PTPS activity in brain, was significantly different from *Pts*-wt/wt offsprings in all *Pts*-ki/ko mouse groups (average: 7% of wt; $p < 0.001$), in *Pts*-ki/wt pups (46% of wt; $p < 0.01$) derived *Pts*-ki/ki mothers, and *Pts*-ko/wt offsprings (33% of wt; $p < 0.01$) animals derived from *Pts*-ko/wt mothers (table 5). Biopterin levels in liver from *Pts*-ki/ko (67% of wt; $p<0.05$) and *Pts*-ki/wt (74% of wt; $p<0.05$) derived from *Pts*-ki/ki mothers were significantly lower in comparison to the *Pts*-wt/wt mouse groups (table 5). In contrast, there was no difference in biopterin amounts in brain in any of the newborn groups (table 5). All *Pts*-ki/ko newborns had significantly increased neopterin levels in liver (average: 14 times higher; $p<001$), but not in brain (table 5). Blood L-Phe levels of *Pts*-ki/ko offsprings from *Pts*-ki/ki mothers (66% of wt; $p<0.05$) or fathers (69% of wt; $p<0.05$) were significantly lower in comparison to the *Pts*-wt/wt mouse groups (table 5). Blood L-Tyr levels from *Pts*-ki/ko (66% of wt; $p<0.05$) and *Pts*-ki/wt (71% of wt; $p<0.05$) derived from *Pts*-ki/ki mothers were significantly lower in comparison to the *Pts*-wt/wt mouse groups (table 5). In the measurement of brain monoamine neurotransmitters dopamine, norepinephrine, epinephrine and serotonin, no significant difference between *Pts*-ki/ko, *Pts*-ki/wt and *Pts*-ko/wt newborns to *Pts*-wt/wt offsprings was detected (table 5).

In summary, *Pts*-ki/ko mice had significantly lower liver and brain PTPS activity, increased neopterin levels in liver, and mainly normal biopterin levels, except for *Pts*-ki/ko and *Pts*-ki/wt newborns derived from *Pts*-ki/ki mothers, which showed significantly lower biopterin levels in their liver. None of the newborns had mild HPA or altered brain monoamine neurotransmitter levels. Therefore, no affected *Pts*-ki/ko newborn could be detected.

3.2.3.2 Direct comparison of newborn *Pts*-ki/ko mice derived from different breeding combinations of *Pts*-ki/wt, *Pts*-ko/wt and *Pts*-ki/ki parents

Since we found slight differences in blood L-Phe and L-Tyr, and liver biopterin levels in-between same genotypes from different breeding combinations, *Pts*-ki/ko newborns from different breeding groups were directly compared (Fig. 20 A-E).

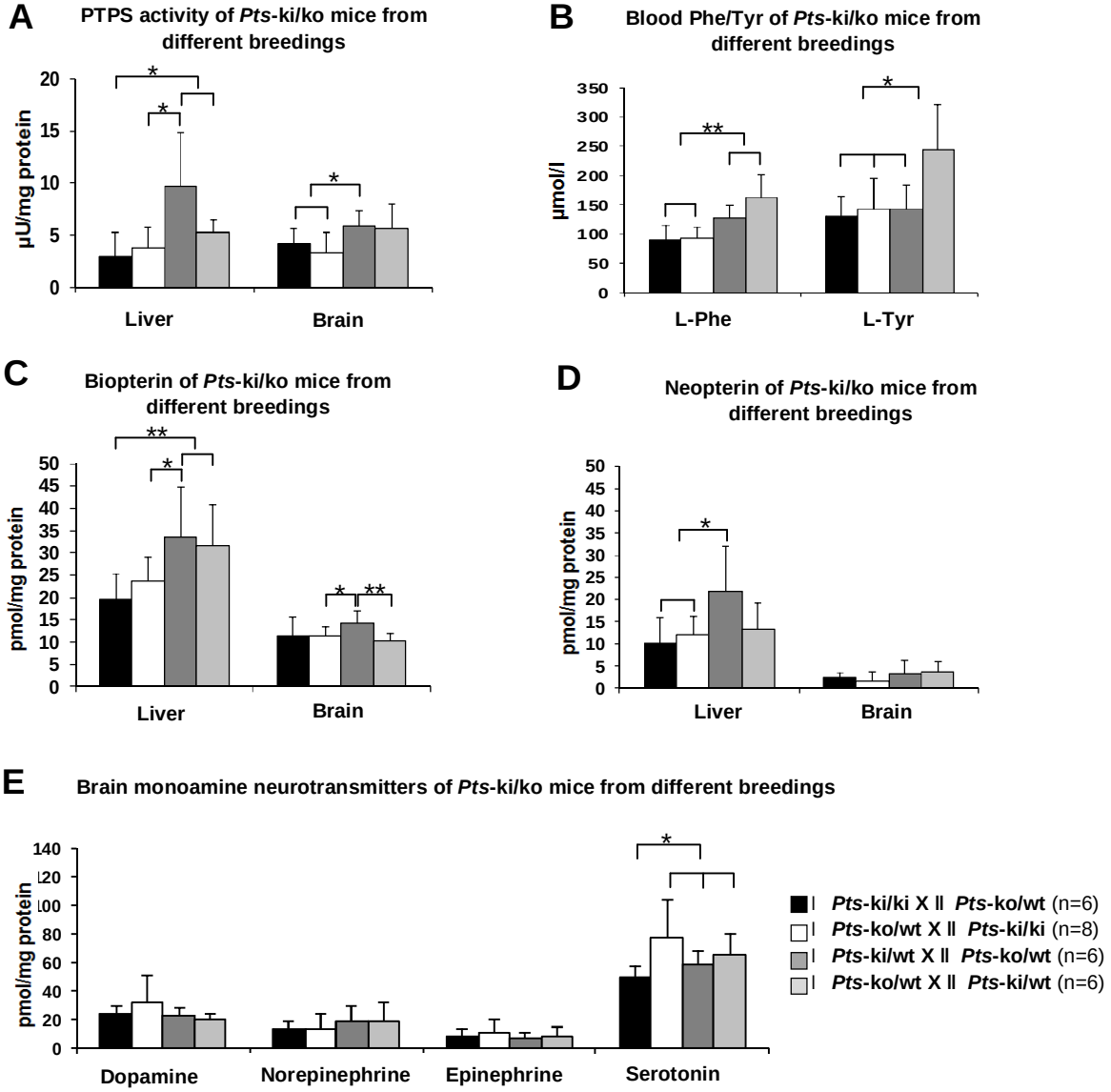

Figure 20: Comparison between *Pts*-ki/ko mice from different breeding combinations of *Pts*-ki and *Pts*-ko parents by biochemical analysis of blood, liver and brain tissue. **(A)** PTPS enzyme activity in liver and brain (µU/mg protein). **(B)** Blood L-Phe and L-Tyr concentrations (µmol/l). **(C)** Biopterin levels in liver and brain (pmol/mg protein). **(D)** Neopterin levels in liver and brain (pmol/mg protein). **(E)** Brain monoamine neurotransmitters dopamine, norepinephrine, epinephrine and serotonin levels (pmol/mg protein). Breeding combination indicated by bar colour: ñomozygous breedingò pairs: Ⅰ *Pts*-ki/ki x Ⅱ *Pts*-ko/wt (black), and Ⅰ *Pts*-ko/wt x Ⅱ *Pts*-ki/ki (white); ñeterozygous breedingò pairs: **Ⅰ** *Pts*-ki/wt *x* **Ⅱ** *Pts*-ko/wt (dark gray), and **Ⅰ** *Pts*-ko/wt *x* **Ⅱ** *Pts*-ki/wt (light gray). Significant difference is indicated by asterisks: * $p < 0.05$, ** $p < 0.01$ (two-tailed Studentõs *t*-test).

In liver, *Pts*-ki/ko offspring from *Pts*-ki/ki (5% of wt) mothers or fathers (6% of wt) showed the lowest PTPS activity and were significantly different from *Pts*-ki/ko animals from *Pts*-ki/wt mothers ($p < 0.05$), which showed the highest PTPS activity (16% of wt) (Fig. 20 A). In brain, *Pts*-ki/ko mice from ñheterozygousò breeding pairs had the highest PTPS activity (9% of wt), and especially *Pts*-ki/ko mice from *Pts*-ki/wt mothers had significantly higher PTPS activity then *Pts*-ki/ko mice derived *Pts*-ki/ki mothers (7% of wt; $p < 0.05$) or fathers (5% of wt; $p < 0.05$) (Fig. 20 A). *Pts*-ki/ko mice from *Pts*-ki/ki mothers (66% of wt) or fathers (69% of wt) had significantly lower L-Phe levels than *Pts*-ki/ko mice derived from a ñheterozygousò *Pts* parents ($p < 0.01$) (Fig. 20 B). In contrast, *Pts*-ki/ko offspring from *Pts*-ko/wt mothers and *Pts*-ki/wt fathers had the highest blood L-Tyr levels and significantly differed from other *Pts*-ki/ko animal groups ($p < 0.05$) (Fig. 20 B). In liver, *Pts*-ki/ko mice from *Pts*-ki/ki mothers (67% of wt) or fathers (80% of wt) had significantly lower liver biopterin levels than *Pts*-ki/ko mice from *Pts*-ki/wt mothers ($p < 0.05$) (Fig. 20 C). In brain, *Pts*-ki/ko mice from *Pts*-ki/wt mothers had the highest biopterin amount (105% of wt), and were significantly higher then *Pts*-ki/ko mice from *Pts*-ko/wt mothers ($p < 0.05$) (Fig. 20 C). In liver, *Pts*-ki/ko mice derived *Pts*-ki/wt mothers had the highest neopterin amount (22 times higher than wt), and were significantly higher than *Pts*-ki/ko mice from *Pts*-ko/wt mothers (Fig. 20 D). There was no difference for neopterin levels in brain between the different *Pts*-ki/ko mouse groups (Fig. 20 D). No differences were observed in brain catecholamines between the different *Pts*-ki/ko mouse groups (Fig. 20 E), but *Pts*-ki/ko mice from *Pts*-ki/ki mothers (85% of wt) had significantly lower serotonins levels than *Pts*-ki/ko mice from other breeding combinations ($p < 0.05$; Fig. 20 E). In summary, *Pts*-ki/ko newborns from ñhomozygousò breedings, especially from *Pts*-ki/ki mothers, showed lower PTPS activity in liver and brain, blood L-Phe and L-Tyr, biopterin levels in liver, and serotonin levels in brain, in comparison to *Pts*-ki/ko newborns from ñheterozygousò breedings.

3.2.3.3 Breeding of ñaffectedò *Pts*-ki/ko mice: Comparison of 3-4 days old *Pts*-ki/ko mice derived from small and large litters

To study, if ñaffectedò animals are present in 3-4 days old animals, *Pts*-ki/ki females were bred with *Pts*-ko/wt males. Furthermore, it was investigated, if there are more ñaffectedò animals in big litters with at least 8 pups then in small litters containing maximum 4 pups. It is hypothesized that newborns are depending on the BH_4 received from the mother milk to develop normal and prevent them to get ñaffectedò (Adamsen, 2011). In a big litter there are more struggles between the siblings to get mother milk, which could lead to more ñaffectedò animals. Animals were phenotypically defined as ñaffectedò when they appeared smaller then other litter mice, located out side the nest, showed movement disorders and/or had no visible white belly from drinking mother milk. Biochemically, *Pts*-ki/ko mice were counted as affected when they had HPA (L-Phe >360 µmol/l), low biopterin in liver and brain and/or low brain neurotransmitters (Adamsen, 2011). Two big litters and five small litters were phenotypically investigated with totally 12 *Pts*-ki/ko and 24 *Pts*-ki/wt pups. A summary of all animals is listed in table 6.

Table 6: Summary of 3-4 days old mice from small and large litters from *Pts*-ki/ki females bred with *Pts*-ko/wt males.

Litter size	*Pts*-ki/wt	"unaffected" *Pts*-ki/ko	"affected" *Pts*-ki/ko
Total big litters (2 litters; 8-9 pups)	**11**	**6**	**0**
Total small litters (5 litters; 3-4 pups)	**13**	**6**	**0**

None of the total 12 *Pts*-ki/ko showed signs to have an ñaffectedò phenotype. All animals were investigated for their PTPS activity in liver and brain (Fig. 21 A), blood L-Phe and L-Tyr (Fig. 21 B), biopterin in liver and brain (Fig. 21 C), neopterin in liver and brain (Fig. 21 D), and brain monoamine neurotransmitters dopamine, norepinephrine, epinephrine and serotonin (Fig. 21 E). *Pts*-ki/wt siblings were used as control comparison, where no differences were expected between small and large litters.

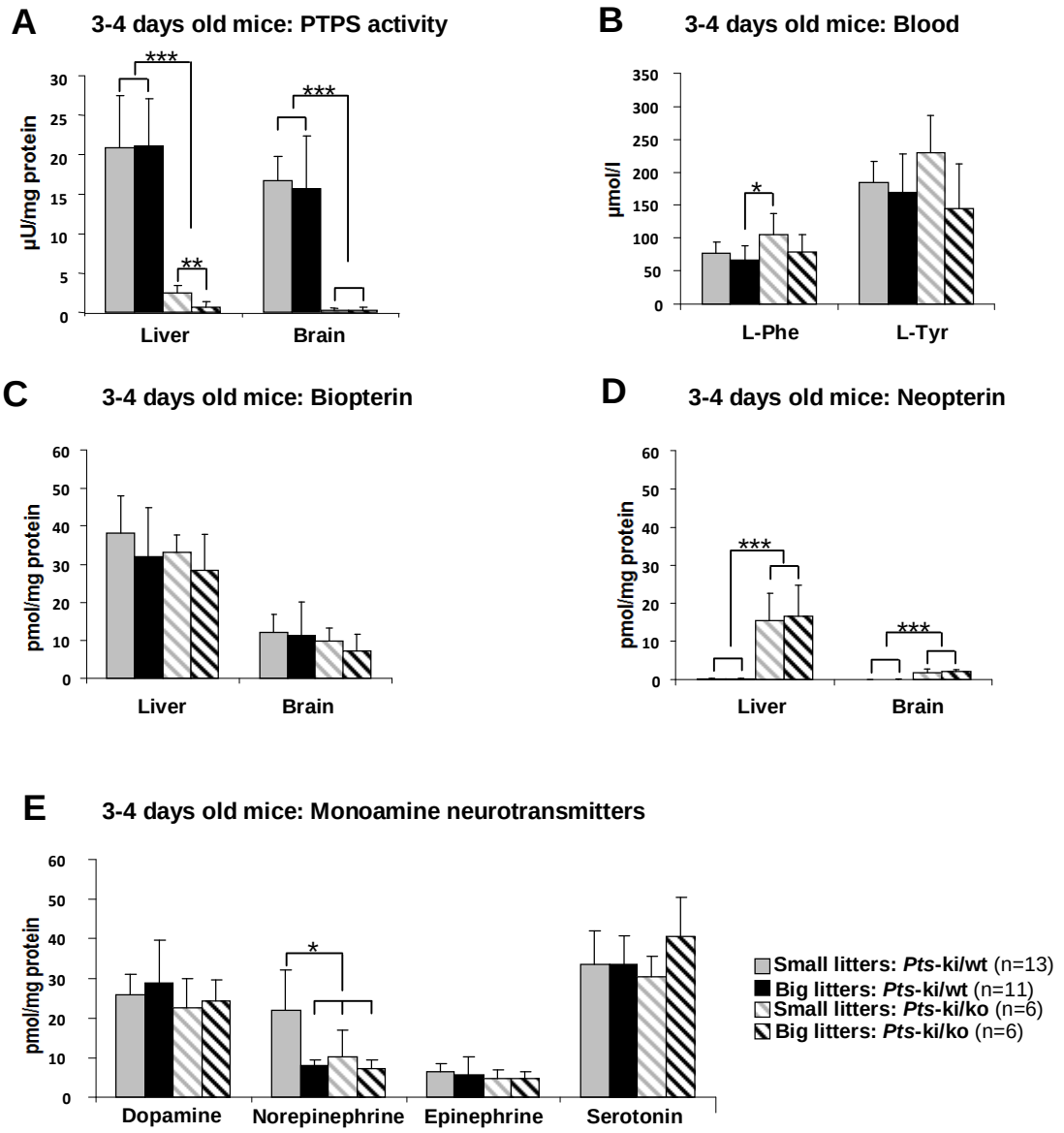

Figure 21: Comparison between *Pts*-ki/ko mice from big litters (8-9 pups) and small litters (3-4 pups) of *Pts*-ki/ki mothers and *Pts*-ko/wt fathers by biochemical analysis of blood, liver and brain tissue. **(A)** Blood L-Phe and L-Tyr concentrations (µmol/l). **(B)** PTPS enzyme activity in liver and brain (µU/mg protein). **(C)** Biopterin levels in liver and brain (pmol/mg protein). **(D)** Neopterin levels in liver and brain (pmol/mg protein). **(E)** Brain monoamine neurotransmitters dopamine, norepinephrine, epinephrine and serotonin levels (pmol/mg protein). Genotypes are indicated by bar colour: *Pts*-ki/wt mice from small litters are shown in gray, *Pts*-ki/ko mice from small litters are shown in gray striped, *Pts*-ki/wt mice from large litters are shown in black, and *Pts*-ki/ko mice from large litters are shown in black striped. Significant difference is indicated by asterisks: * $p < 0.05$, ** $p < 0.01$, *** $p < 0.001$ (two-tailed Student's *t*-test).

Pts-ki/ko mice from big litters had significantly reduced PTPS activity in liver in comparison to *Pts*-ki/ko mice from small litters (3.6 times less; $p < 0.01$; Fig. 21 A). There was no difference in liver PTPS activity in *Pts*-ki/wt siblings derived from different litter sizes. There was no significantly difference in brain PTPS activity for *Pts*-ki/ko (or *Pts*-ki/wt) derived from small or big litters (Fig. 21 A). *Pts*-ki/ko mice from small litters had the highest blood L-Phe levels and were significantly different from *Pts*-ki/wt from big litters ($p < 0.05$; Fig. 21 B). There was no significant difference in blood L-Tyr levels (Fig. 21 B) or biopterin amounts in liver and brain (Fig. 21 C) for *Pts*-ki/ko and *Pts*-ki/wt derived from small or big litters. In general, *Pts*-ki/ko mice had increased neopterin levels in liver and brain in comparison to *Pts*-ki/wt ($p < 0.001$), but there were no significant differences between *Pts*-ki/ko mice or *Pts*-ki/wt derived from small or big litters (Fig. 21 D). *Pts*-ki/wt mice from small litters had significant higher norepinephrine levels then *Pts*-ki/wt and *Pts*-ki/ko mice from big litters or *Pts*-ki/ko from small litters ($p < 0.05$; Fig. 21 E). There was no difference for the brain catecholamines dopamine or epinephrine, or the brain monoamine neurotransmitter serotonin for *Pts*-ki/ko and *Pts*-ki/wt derived from small or big litters (Fig. 21 E). In summary, *Pts*-ki/ko mice from big litters had significantly reduced PTPS activity in liver in comparison to *Pts*-ki/ko mice from small litters, but not for the other parameters measured. Furthermore, none of the investigated *Pts*-ki/ko mice had an ñaffectedò phenotype.

3.2.4 DISCUSSION

The observation in the dissertation of D. Adamsen (2011) that *Pts*-ki/ki mothers produce ñaffectedò *Pts*-ki/ko mice, which reflect the severe and central form of BH_4 deficiency, was not supported in the presented study. It is unknown what led to the description of ñaffectedò *Pts*-ki/ko mouse phenotype. A possible explanation could be found in the different breeding conditions for D. Adamsenôs and the present study. In the present study, female mice were separated from other mice to raise their pups in order to decrease stress and stress induced cannibalism of pups reported to frequently appear in C57BL/6 derived mouse strains, and to increase the chances of newborn survival (Burds Connor, 2007). In D. Adamsen breeding, several females were kept with a male mouse in a cage, which led to high litters when the mouse mothers gave birth and therefore, it increased the ñstruggle stressò for mother milk between the newborns, which also increased the newborn lethality rate. This effect of increased newborn ñstruggle stressò is even bigger when litters were born at different time points, given the younger and weaker mice decreased chances of getting mother care. Probably due to mixed aged litters and in consequence increased lethality rate in newborns, the wrong impression of ñaffectedò and ñunaffectedò *Pts*-ki/ko mice could have been raised. Indications for this assumption can be found on Fig. 18 shown in chapter 3.2.1, which shows a picture from D. Adamsenôs dissertation, showing a so called ñunaffectedò (left) and an ñaffectedò (right) *Pts*-ki/ko mouse (Adamsen, 2011). Since genotyping of mice at this age was not possible, it would be not possible to distinguish *Pts*-ki/wt from *Pts*-ki/ko siblings, and therefore, it is unclear if the mouse pups on Fig. 18, actually shows *Pts*-ki/ko or *Pts*-ki/wt mice. Nevertheless, the right pup does not show unhealthy sings such as starvation or dehydration, which would lead to a shrunken and skinny body due to negligence from the mother as described in D. Adamsenôs dissertation to happen at day 3-4 after birth. In comparison, the skin color of the left animal on Fig. 18 looks rather gray due to changes of the skin color from pink to gray during day 3-4, whereas the skin colour of the right animal is still quite pink (Schertzer and Lynch, 2008; Burds Connor, 2007). Therefore, Fig. 18 rather shows two pups with different ages, then a healthy and an under developed animal. Nevertheless, there is still the open question of the biochemical analysis of the so called ñaffectedò *Pts*-ki/ko mice, which showed depletion of biopterin and brain monoamine neurotransmitters, and mild HPA. It can be only speculated that maybe dying or dead newborns were collected and

compared with 3-4 days old healthy mice, which could lead to not comparable and/or not reliable results. Nevertheless, in my own biochemical comparison I found in *Pts*-ki/ko newborns from different breeding combination of homozygous or heterozygous *Pts*-ki bred with heterozygous *Pts*-ko mice slightly differences in PTPS activity (liver and brain), biopterin (liver and brain), neopterin (liver), blood L-Phe and L-Tyr, and brain serotonin levels. Therefore, it might be of interest in potential further and future studies to investigate whether such differences could also be found in adult mice.

4.

STUDY OF A MUSCLE-DIRECTED NON-VIRAL GENE THERAPEUTIC APPROACH FOR PKU

AND

ATTEMPT TO GENERATE A MOUSE MODEL EXPRESSING BH_4 IN MUSCLE

CHAPTERS:

- 4.1 EXPERIMENTAL STUDY ON A NON-VIRAL GENE THERAPY APPROACH BY INTRA-MUSCULAR EXPRESSION OF A COMPLETE PHENYLALANINE HYDROXYLATING SYSTEM

- 4.2 ATTEMPT TO GENERATE A PKU MOUSE MODEL SYNTHESISING BH_4 IN MUSCLE BY EXPRESSING THE *GCH*1 AND *PTS* GENES USING AAV

4.1 EXPERIMENTAL STUDY ON A NON-VIRAL GENE THERAPY APPROACH BY INTRAMUSCULAR EXPRESSION OF A COMPLETE PHENYLALANINE HYDROXYLATING SYSTEM

4.1.1 ABSTRACT

Complete correction of cPKU with rAAV in the *Pah*$^{enu2/2}$ mouse model system was shown by targeting skeletal muscle to express the complete L-Phe hydroxylating system by coordinate expression of the three murine genes *Pah*, *Gch*1 and *Pts* to produce PAH and its cofactor BH_4 that are both naturally not present in muscle. Nevertheless, AAV gene therapy in human patients would need very high amount of virus, which is technically difficult and related with high costs. Furthermore, rAAV can trigger immunogenicity, inflammatory response, severe malignancy and eventually complete shutdown of transgene expression in humans. Recently, the first non-viral gene therapy was reported that corrected cPKU in *Pah*$^{enu2/2}$ mice by liver-targeting with naked DNA vectors named MC (Viecelli et al., 2014). The goal of this study is to achieve a non-viral muscle-directed gene therapy to correct cPKU in the *Pah*$^{enu2/2}$ mouse model system. Besides applying the original triple-cystronic cassette used in the viral approach, various additional modifications to potentially enhance expression, including codon-optimization, insertion of intronic sequences, transcription or gene expression latency elements like WPRE and/or the scaffold/matrix attachment region (S/MAR) were generated, resulting in up to 12 potential therapeutic MC vectors for *in vivo* testing. All vectors were validated under cell culture conditions for enzyme activity and biopterin biosynthesis. MCs were delivered to skeletal muscles of *Pah*$^{enu2/2}$ mice by hydrodynamic limb vein (HLV) injection or electroporation. To assess extension and distribution of MCs in muscle tissue, a MC expressing the *firefly* luciferase (*Luc*) was electroporated into *Pah*$^{enu2/2}$ mice and analyzed thereafter by using an *in vivo* imaging system (IVIS) (Ding et al., 2008, Lim et al., 2009). Although high concentrations of triple-cistronic MCs were applied, there was no correction of blood L-Phe levels in the *Pah*$^{enu2/2}$ mice.

4.1.2 INTRODUCTION

Although cPKU is a treatable metabolic disease by life-long restricted diet of the amino acid L-Phe, a permanent cure that would eliminate sole dependence upon dietary therapy would be a big improvement in life quality for all individuals with cPKU, their families, and health care providers. Therefore, gene therapy is an attractive approach to treat cPKU. Several experimental gene therapies reported the complete and life-long gender-independent correction of blood L-Phe levels in *Pah*$^{enu2/2}$ mice, by targeting the liver using high viral doses of AAV2 pseudo-typed with serotypes 1, 2 or 8 expressing the m*Pah* transgene (Ding et al., 2006, McDonnald, 2006, Rebuffat et al., 2010, Thöny, 2010). The pathophysiology of many inborn errors of metabolism like in e.g. cPKU is mediated by circulating toxic metabolites, rather than a local effect of enzyme deficiency in a specific tissue (Meyburg and Hoffmann, 2008, Alfadhel et al., 2013). Therefore, expression of a L-Phe metabolizing system in tissues other than liver should also lead to correction of HPA and its attendant phenotypic features. The complete correction of cPKU in *Pah*$^{enu2/2}$ mice by AAV2 serotype 1 mediated intramuscular expression of a complete L-Phe hydroxylating system, which required the coordinate expression of the three murine genes m*Pah*-m*Gch*1-m*Pts* (vector AAV2-PKU3) in skeletal muscle was successfully achieved (see Fig. 22) (Ding et al., 2008). Skeletal muscle is an attractive target tissue because it is a not essential vital organ with readily accessibility through direct injection or intravascular delivery methods, it is supported by a vigorous blood supply, and it makes up as much as 20-30% of the human body weight and 35% of mouse body weight (Arora and Rochester, 1982, Stratikopoulos et al., 2008).

Despite the worldwide success with AAV-based gene transfer in small and large animal disease models, AAV can trigger immunogenicity, inflammatory response, severe malignancy like e.g. that neonatal injection of an AAV vector led to hepatocellular carcinoma in mice, and eventually complete shutdown of transgene expression in humans (Donsante et al., 2007, Hasbrouck and High, 2008). Furthermore, it was reported that the transduction efficacy and transgene expression after liver-targeted delivery of AAV in female mice was significantly decreased in comparison to male mice, whereas sex did not have a significant effect on AAV gene transfer into non-hepatic tissues (Davidoff et al., 2003). In this context, non-viral

vectors for gene therapy have recently gained considerable momentum, and are becoming very attractive in combination with the MC technology (Viola et al., Donsante et al., 2001, Al-Dosari and Gao, 2009; see also chapter 1.3.6.2). Moreover, it was shown that MCs express their transgenes longer and at higher levels in the liver in comparison to their PP, which still includes the bacterial backbone, upon a single hydrodynamic tail vein injection (Hutchins, 2000, Gorecki, 2006, Viecelli et al., 2014). Recently, complete correction of HPA in *Pah*$^{enu2/2}$ mice was achieved by liver-directed MC naked DNA gene therapy (Viecelli et al., 2014).

The goal of this study was to evaluate a non-viral triple-cystronic expression of a complete L-Phe metabolizing system in skeletal muscle for the normalization of L-Phe and correction of the cPKU phenotype in *Pah*$^{enu2/2}$ mice, analog to the approved viral muscle gene therapy (see Fig. 22). Therefore, the triple-cistronic m*Pah*-m*Gch*1-m*Pts* expression cassette was used in a MC vector to target the skeletal muscles of *Pah*$^{enu2/2}$ mice (Fig. 22).

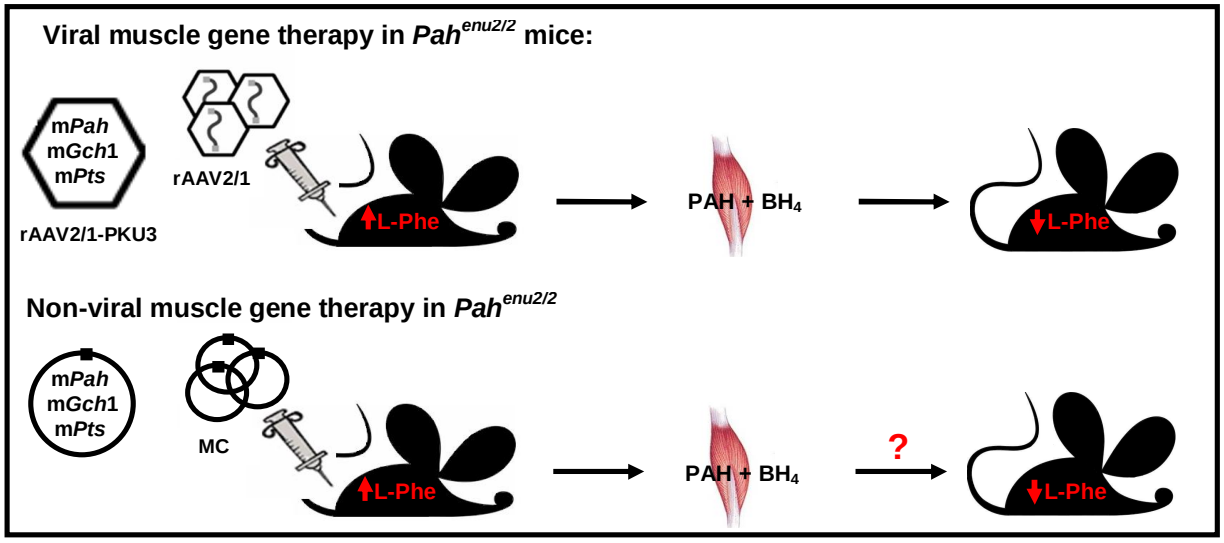

Figure 22: Schematic representation of viral and non-viral vector gene therapy. m*Pah*, murine phenylalanine hydroxylase gene; m*Gch*1, murine guanosine triphosphate cyclohydrolase 1 gene; m*Pts*, murine 6-pyruvoyl-tetrahydropterin synthase gene; MC, minicircle; BH_4, tetrahydrobiopterin; L-Phe, L-phenylalanine, rAAV2/1-PKU3, recombinant AAV2 serotype 1-mediated vector expressing the genes m*Pah*-m*Gch*1-m*Pts*.

Since naked DNA has a low transfection efficacy and transient expression *in vivo*, the triple-cistronic vector was modified by codon optimization, and insertion of intronic sequence, woodchuck hepatitis WPRE and/or the scaffold/matrix attachment region (S/MAR) elements (Hagstrom et al., 2004). The codon optimization refers to the 20 so-called biogenic amino acids, which are encoded by 61 codons (three nucleotides

encoding for a specific amino acid) and therefore many amino acids are encoded by more than one codon (õcodon degenerationö). There can be preferences for one of the synonymous codons that encode for the same amino acid (codon usage bias), and this preference could influence e.g. gene expression level (Gustafsson et al., 2004). There are several statistical methods to predict gene expression levels based on codon usage bias, which differs from organism to organism and can be even cell or tissue specific (Comeron and Aguade, 1998, Fox and Erill, 2010). Furthermore, codon optimization algorithms include avoidance of CpG islands, secondary structures, cryptic splice sites splice suppressors and restriction enzyme recognition sites (Satya et al., 2003, Gustafsson et al., 2004). Modifications of genes according to such statistical methods showed that these codon-optimized genes had positive effects at transcriptional, translational, and mRNA stability levels (Grosjean and Fiers, 1982, Fath et al., 2011). Furthermore, it has been shown that the insertion of intronic sequence into a transgene increases expression in mice which can lead to 400-time more RNA, depending on the position of insertion (Buchman and Berg, 1988, Palmiter et al., 1991). Therefore, a minimized version of m*Pah* intron 1 was inserted in some MC constructs. The minimized intron 1 version consists of only 819 bp out of 6,222 bp of the total intron 1 sequence, including 299 bp downstream of exon 1 and 520 bp upstream of exon 2. To further enhance gene expression, WPRE was inserted in some of the MC vectors (Klein et al., 2006). Furthermore, it was described that the addition of a S/MAR sequence in MC increases stability of expression and latency *in vivo* (Argyros et al., 2011). For a first validation of the different modified MC vectors, *in vitro* (cell culture) studies were used to elucidate the MCs with the highest enzyme activity and biopterin biosynthesis, which were then tested in a second step *in vivo* in *Pah*$^{enu2/2}$ mice for therapeutic efficacy. Two *in vivo* application techniques to target skeletal muscle cells were used: HLV injection or electroporation (Schertzer and Lynch, 2008, Zhang et al., 2010). Furthermore, to assess the extension of distribution of MC in the muscle *in vivo*, a MC expressing the *Luc* was used to perform IVIS (Ding et al., 2008, Lim et al., 2009).

4.1.3 MATERIALS AND METHODS

4.1.3.1 Vector plasmids

Sequencing analysis of AAV2-PKU3 plasmid revealed two missense mutations, one located in the m*Pah* (c.1126G>A, p.E376K) and one in the m*Pts* gene (c.230A>G; p.E77G) and the disruption of one of the two inverted terminal repeat (ITR) sites, necessary to generate rAAV. Therefore, the AAV2-PKU3.3 was cloned with the correction of the two mutations and the replacement of the disrupted ITR site (see chapter 5.1). The m*Pts* and m*Gch*1 cDNA were codon optimized and synthesized by GenScript USA Inc. (Piscataway, USA). The m*Pah* were codon optimized and synthesized by GeneArt® Life technology (Regensburg, Germany). Detailed descriptions of all plasmids are listed in chapter 5.1.

4.1.3.2 Transfection of COS-1 cells with PP or MC vectors

MC or PP vectors were transfected in combination with a ɓ-galactosidase-expressing plasmid in COS-1 cells as described in a published method (Heintz et al., 2012).

4.1.3.3 Enzyme activity assays *in vitro*

ɓ-galactosidase expression assay was performed according to the protocol of the ß-galactosidase enzyme assay system by Promega (Ref. nr. E2000, Dübendorf, Switzerland). The optical density (OD) at 420 nm was measured with an Ultrospec 3100 Pro UV/visible spectrophotometer (linear range OD 0.2-0.8; Ref. nr. 80-2112-31; Amersham Bioscience, Glattbrugg, Switzerland). The amount of biopterin and PAH, GTPCH and PTPS enzyme activities of the PP or MC transfected COS-1 cells were measured according to published methods (Bonafe et al., 2001, Blau, 2008b, Heintz et al., 2012). Enzyme activity and biopterin levels were normalized to the ɓ-galactosidase expression and the plasmid size using the AAV2-PKU3 plasmid as reference.

4.1.3.4 Hydrodynamic limb vein injection of MC into *Pah*$^{enu2/2}$ mice

Both hind limbs of *Pah*$^{enu2/2}$ mice were used for hydrodynamic limb vein injection with total of 1 mg MC DNA per injection. This was done in a collaborative approach in the laboratory of C. O. Harding and S. Winn at the Department of Molecular and Medical Genetics at the Oregon Health & Science University (Portland, Oregon, USA) (Zhang et al., 2010). *Pah*$^{enu2/2}$ mice are fed with standard mouse chow leading to high blood L-Phe levels in the *Pah*$^{enu2/2}$ mice.

4.1.3.5 Electroporation of MC into *Pah*$^{enu2/2}$ mice

120 µg MC DNA was electroporated into the musculus (m.) gastrocnemius (left leg) or m. vastus (right leg) of the hind limbs of *Pah*$^{enu2/2}$ mice in collaboration with Lars Aagaard and Hanne Gissel Hyldkrog from the Department of Biomedicine at the University of Aarhus (Denmark). All *Pah*$^{enu2/2}$ mice were fed with L-Phe deficient diet with 1.5% tyrosine from Harlan Teklad custom research diets (https://www.harlan.com), and 0.625 mg/ml L-Phe is added in the drinking water. Under these housing conditions *Pah*$^{enu2/2}$ mice show low L-Phe levels (<360 µmol/l). After electroporation, the drinking L-Phe levels were elevated to 2.5 mg/ml during the length of the experiment, which increases the blood L-Phe (>360 µmol/l) levels in PKU mice (Schertzer and Lynch, 2008).

4.1.3.6 In vivo imaging system

Mice were anaesthetized with 2-3% isoflurane and 150 mg/kg body weight D-luciferin (Ref. nr. LUCNA-1G; Gold Biotechnology, St. Louis, USA) was subcutaneously injected. After 10 min, mice were screened for *Luc* expression with the bioluminescence by the Xenogen IVIS Imaging 200 Series (Ref. nr. IVIS200; Perkin Elmer, Santa Clara, USA). Data are analyzed by using LIVINGIMAGE 3.20 software from Xenogen. Background levels of bioluminescence for mice should be around 3 x 10^5 photons/sec (p/s).

4.1.3.7 Blood L-Phe measurements

Blood L-Phe was measured in dried blood spots by tandem MS/MS according to a published method (Guthrie and Susi, 1963; Rashed et al., 1995).

4.1.4 RESULTS

4.1.4.1 MC vectors and *in vitro* expression

Table 7 lists all MC vectors generated for this study. All MC vectors contained the human cytomegalovirus promoter (CMV) for coordinately expression in combination with internal ribosomal entry site (IRES) elements between the three genes m*Pah*, m*Gch*1 and m*Pts*. In this study, control vector AAV2-PKU3.3 was used instead of the published triple-cystronic AAV2-PKU3 vector because of the found disruptions in the AAV2-PKU3 vector described in chapter 4.1.3.1 and 5.1. Analogous to the therapeutic viral vector AAV2-PKU3.3, the MC vector MC.PKU104 was generated. In a next step, the viral element WPRE was excluded from the MC vector to avoid potential immune reaction against the WPRE, generating the MC.PKU105 vector. To increase stability of expression and latency *in vivo*, S/MAR was added to the triple-cystronic vector, named MC.PKU106. Furthermore, the *Luc* was added for potential IVIS recording (MC.PKU102). In a next step, the MC vectors were stepwise codon optimized. First, m*Pah* was converted to murine codon optimized (mco) *Pah* with (MC.PKU108) or without (MC.PKU109) WPRE. The mco*Pah* has all exons codon optimized except of exon 1, which remained wild-type. A shorted version of m*Pah* intron 1 (819 bp) was introduced in the mco*Pah* with (pMC.PKU114) or without (MC.PKU115) WPRE. In a second step, all three genes were codon optimized, again with (MC.PKU116) or without (MC.PKU117) WPRE. In a last step, MC vectors with mco*Pah* containing the short intron 1, mco*Gch*1 and mco*Pts* genes were generated with (MC.PKU118) or without (MC.PKU119) WPRE. For IVIS studies, MC.PKU121 was generated containing only *Luc*.

Table 7. List of MC vectors.

Vector	Vector type	Promoter	m*Pah*	m*Gch*1	m*Pts*	*Luc*	Enhancing elements	PP size (bp)	MC size (bp)
AAV2-PKU3.3	viral	CMV	wt	wt	wt	-	WPRE	9,376	-
MC.PKU104	non-viral	CMV	wt	wt	wt	-	WPRE	9,382	5,382
MC.PKU105	non-viral	CMV	wt	wt	wt	-	-	8,798	4,798
MC.PKU106	non-viral	CMV	wt	wt	wt	-	S/MAR	11,040	7,040
MC.PKU102	non-viral	CMV	wt	wt	wt	wt	S/MAR	13,065	9,065
MC.PKU108	non-viral	CMV	mco	wt	wt	-	WPRE	9,434	5,434
MC.PKU109	non-viral	CMV	mco	wt	wt	-	-	8,850	4,850
MC.PKU114	non-viral	CMV	mco + intron	wt	wt	-	WPRE	10,092	6,092
MC.PKU115	non-viral	CMV	mco + intron	wt	wt	-	-	9,508	5,508
MC.PKU116	non-viral	CMV	mco	mco	mco	-	WPRE	9,443	5,443
MC.PKU117	non-viral	CMV	mco	mco	mco	-		8,859	4,859
MC.PKU118	non-viral	CMV	mco + intron	mco	mco	-	WPRE	10,101	6,101
MC.PKU119	non-viral	CMV	mco + intron	mco	mco	-	-	9,517	5,517
MC.PKU121	non-viral	CMV	-	-	-	wt	-	7,390	3,390

CMV, human cytomegalovirus promoter; m*Pah*, murine phenylalanine hydroxylase gene; m*Gch*1, murine GTP cyclohydroxylase 1 gene; m*Pts*, murine 6-pyruvoyl-tetrahydropterin synthase gene; *Luc*, *firefly* luciferase gene; WPRE, woodchuck hepatitis post-transcriptional regulatory element; S/MAR, scaffold/matrix attachment region; wt, wild-type; mco, mouse codon optimized; PP, parental plasmid; MC, minicircle.

To compare the enzyme activity of the non-viral vectors, the MC and PP vectors were tested in transiently transduced COS-1 cells for their biopterin biosynthesis and for their PAH, PTPS and GTPCH enzyme activity (summarized in Fig. 23 A-D).

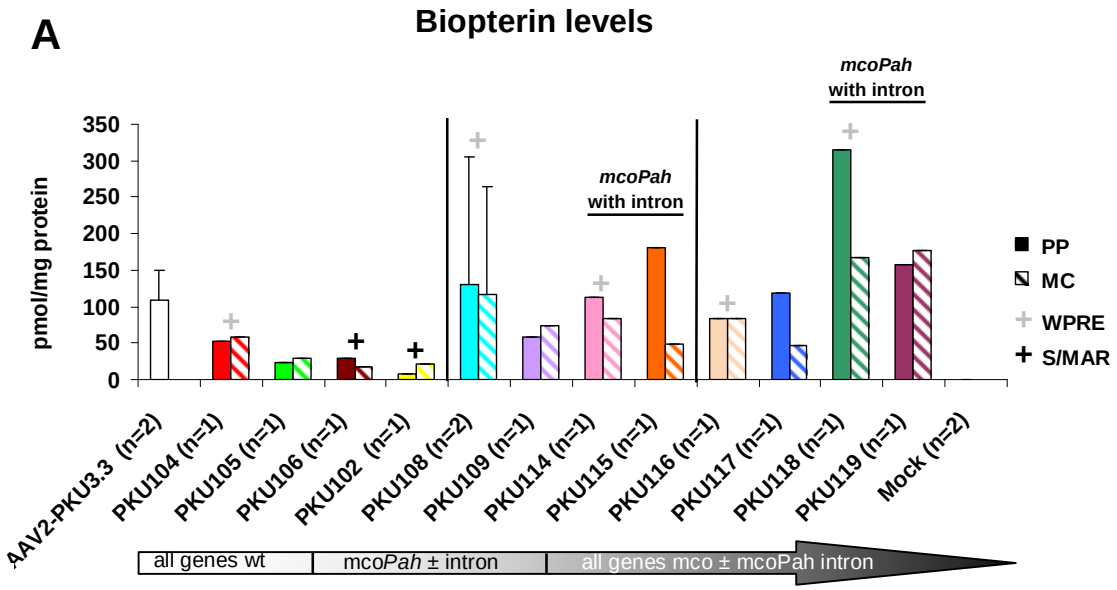

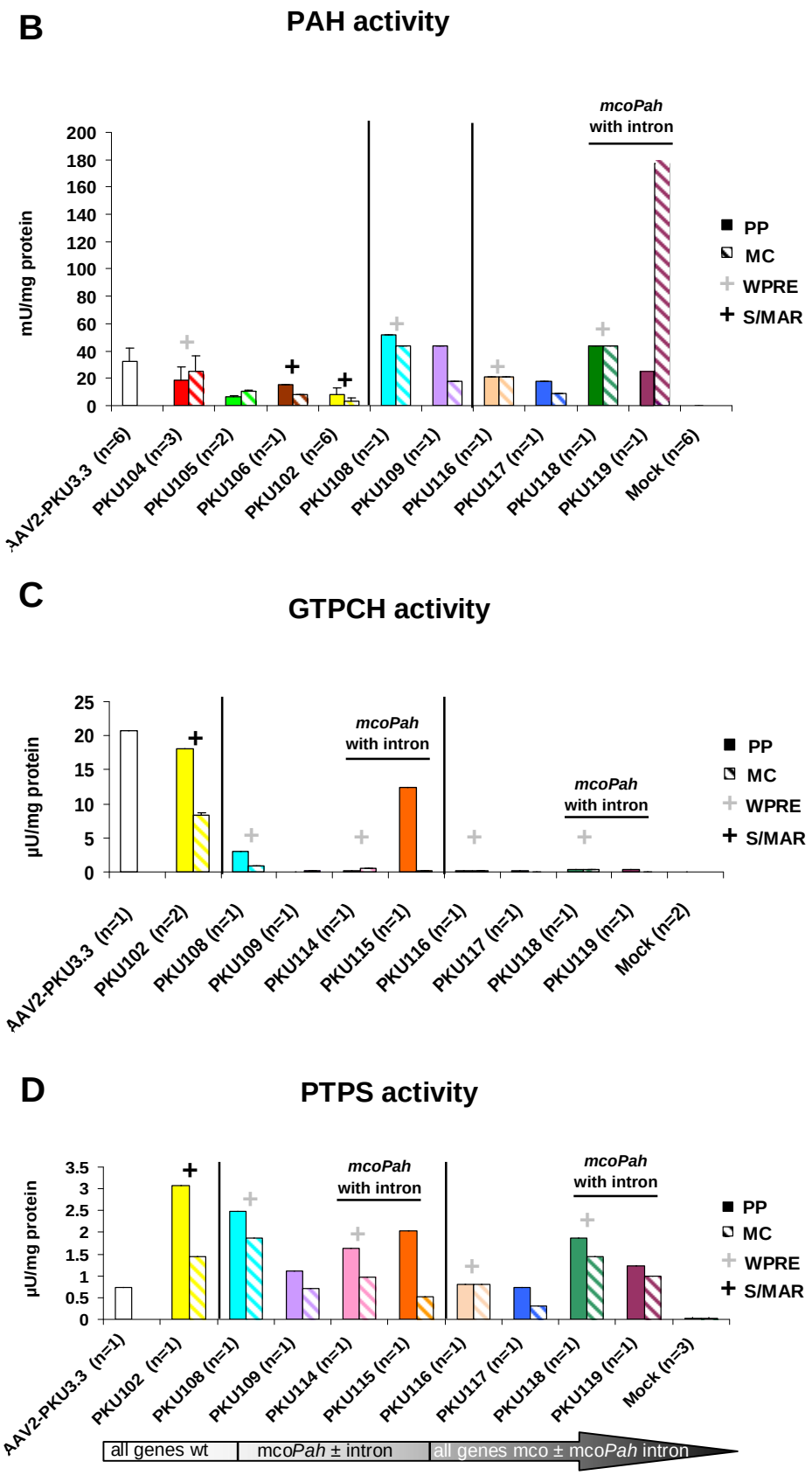

Figure 23: Biopterin amount or enzyme activities (PAH, GTPCH and PTPS) of PP and MC vectors. **(A)** Biopterin levels (pmol/mg protein). **(B)** PAH activity (mU/mg protein). **(C)** GTPCH activity (µU/mg protein). **(D)** PTPS activity (µU/mg protein). PPs are shown by filled out bars; MCs are shown by striped bars; insertion of WPRE is indicated with a gray plus; insertion of S/MAR is indicated with a black plus.

All tested PP and MC vectors showed enzyme activity and biopterin biosynthesis *in vitro*. MC vectors showed not much more enzyme activity or higher biopterin levels then PP plasmids *in vitro*. Furthermore, codon optimization and/or the insertion of an intron did not lead to much higher enzyme activity or increased biopterin levels *in vitro*. MC vectors containing the WPRE showed in general slightly elevated enzyme activity and/or biopterin levels in comparison to equivalent vectors without WPRE.

4.1.4.2 *In vivo* application of MCs by HLV injection

To investigate the therapeutic efficacy *in vivo* of the triple-cystronic MCs, namely MC.PKU102, 104, 105, 108, 109, 117, 118 or 119, 1 mg DNA of each of the MC vectors was HLV-injected into both hind legs of *Pah*$^{enu2/2}$ mice. An overview of the type and amount of HLV injected MCs is summarized in table 8.

Table 8: List of HLV injected MCs into the hind limbs of *Pah*$^{enu2/2}$ mice.

Vector	Size	Amount (µg)	Amount (pmol)	Vector particles (vp)
MC.PKU102	9065	1000	167.1	1.0 x10^{14}
MC.PKU104	5382	1000	281.5	1.7 x10^{14}
MC.PKU105	4798	1000	315.7	1.9 x10^{14}
MC.PKU108	5434	1000	278.8	1.7 x10^{14}
MC.PKU109	4850	1000	312.4	1.9 x10^{14}
MC.PKU117	4859	1000	311.8	1.9 x10^{14}
MC.PKU118	6101	1000 (x4)	248.3 (x4)	1.5 x10^{14} (x4)
MC.PKU119	5517	1000 (x4)	274.6 (x4)	1.7 x10^{14} (x4)

Injection efficacy was between 30-60% (personal communication with S. Winn). To calculate the injection efficacy, the amount of muscle expansion was observed during the HLV injection as well as the leakage of the injection fluid. In an optimal injection procedure, the m. gastrocnemius expanded 2x-3x with less than 10% fluid "leakage" or loss leading to approximately 70% of the muscle cells to take-up and express the genetic material (shown by GFP expression system; personal communication with S. Winn). Blood L-Phe was measured at different time points as depicted in Fig. 24. *Pah*$^{enu2/2}$ mice injected with MC.PKU118 or 119 were re-injected at day 18, 45 and 60 with 1 mg of MC DNA.

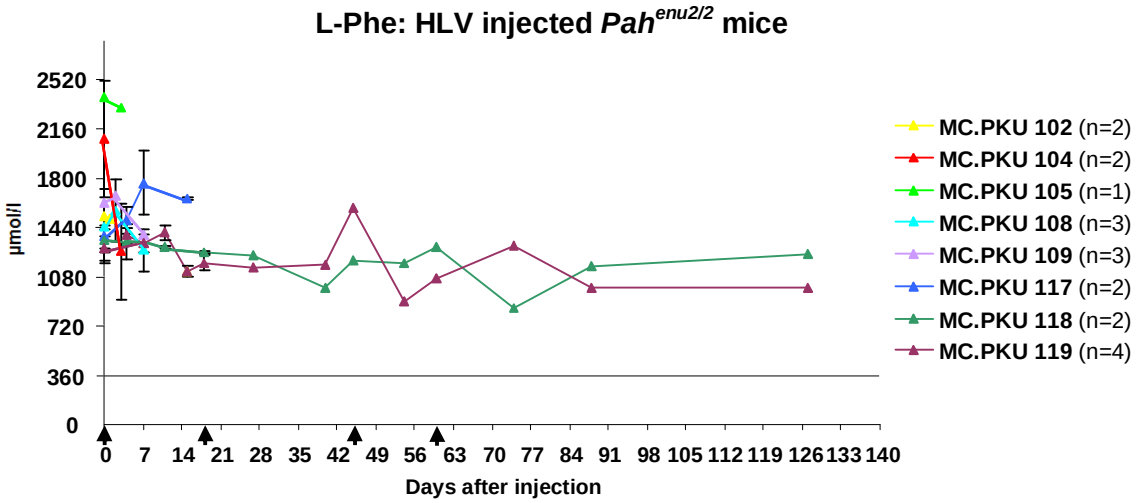

Figure 24: Blood L-Phe levels of MC HLV injected *Pah*$^{enu2/2}$ mice (µmol/l). Arrows are indicating (re)injection; MC.PKU102 is shown in yellow; MC.PKU104 is shown in red; MC.PKU105 is shown in light green; MC.PKU108 is shown in turquoise; MC.PKU109 is shown in purple; MC.PKU117 is shown in blue; MC.PKU118 is shown in dark green; MC.PKU119 is shown in violet. Therapeutic range is indicated below 360 µmol/l L-Phe.

Unfortunately, none of the MC injected into *Pah*$^{enu2/2}$ mice showed normalization L-Phe levels (<360 µmol/l). Further measurements are needed to elucidate the vector copy number, PAH, GTPCH and PTPS activities, and/or BH_4 content in the MC treated muscle tissue.

4.1.4.3 *In vivo* application of MCs by electroporation

The HLV injection method showed high variation in transfection efficacy. Therefore, a potentially more precise application method, namely electroporation, was used to transfer the MCs into muscle cells in a next approach. For the electroporation, MCs with the wild-type versions of three genes with (MC.PKU104) or without (MC.PKU105) WPRE or mco*Pah* including an intron in combination with the wild-type m*Gch*1 and m*Pts* genes with WPRE (MC.PKU114) were chosen. MC.PKU105 was chosen to exclude the probability that any immune reaction against WPRE would eliminate the MC DNA *in vivo*. MC.PKU121, which expresses the *Luc* gene, was used to visualize the expression and distribution of the electroporated MCs *in vivo* by using IVIS. 120 µg DNA was electroporated for each vector into either m. vastus (right hind leg) or m. gastrocnemius (left hind leg) of *Pah*$^{enu2/2}$ mice (total 240 µg) by H. G. Hyldkrog (see table 9).

Table 9: List of electroporated MCs into the hind limbs of *Pah*$^{enu2/2}$ mice.

Vector	Size	Amount (µg)	Amount (pmol)	Vector particles (vp)
MC.PKU104	5382	240	67.6	4.1 x10^{13}
MC.PKU105	4798	240	75.8	4.6 x10^{13}
pMC.PKU114	6092	240	59.7	3.6 x10^{13}
pMC.PKU121	3390	240	107.3	6.5 x10^{13}

The *Pah*$^{enu2/2}$ mice were housed on a low L-Phe diet leading to low blood L-Phe levels (<360 µmol/l). After electroporation, their diet was supplemented with an increased dose of L-Phe, which leads to HPA in untreated PAH deficient mice. Theoretically, the MC.PKU 104, 105 or 114 treatments should prevent *Pah*$^{enu2/2}$ mice to develop HPA when supplied with high dose of L-Phe. The L-Phe increased diet was continued until mice were sacrificed at day 56. PKU mice electroporated with vector MC.PKU121 (expressing only the *Luc* gene) were used as negative control. For positive control, a *Pah*$^{enu2/2}$ mouse was hydrodynamic tail vein (HTV) injected with a liver directed lentivirus expressing m*Pah*. *Luc* expression was investigated by IVIS at day 3, 6, 14, and 29 (Fig. 25 A-B) as well as blood L-Phe until day 56 (Fig. 25 C).

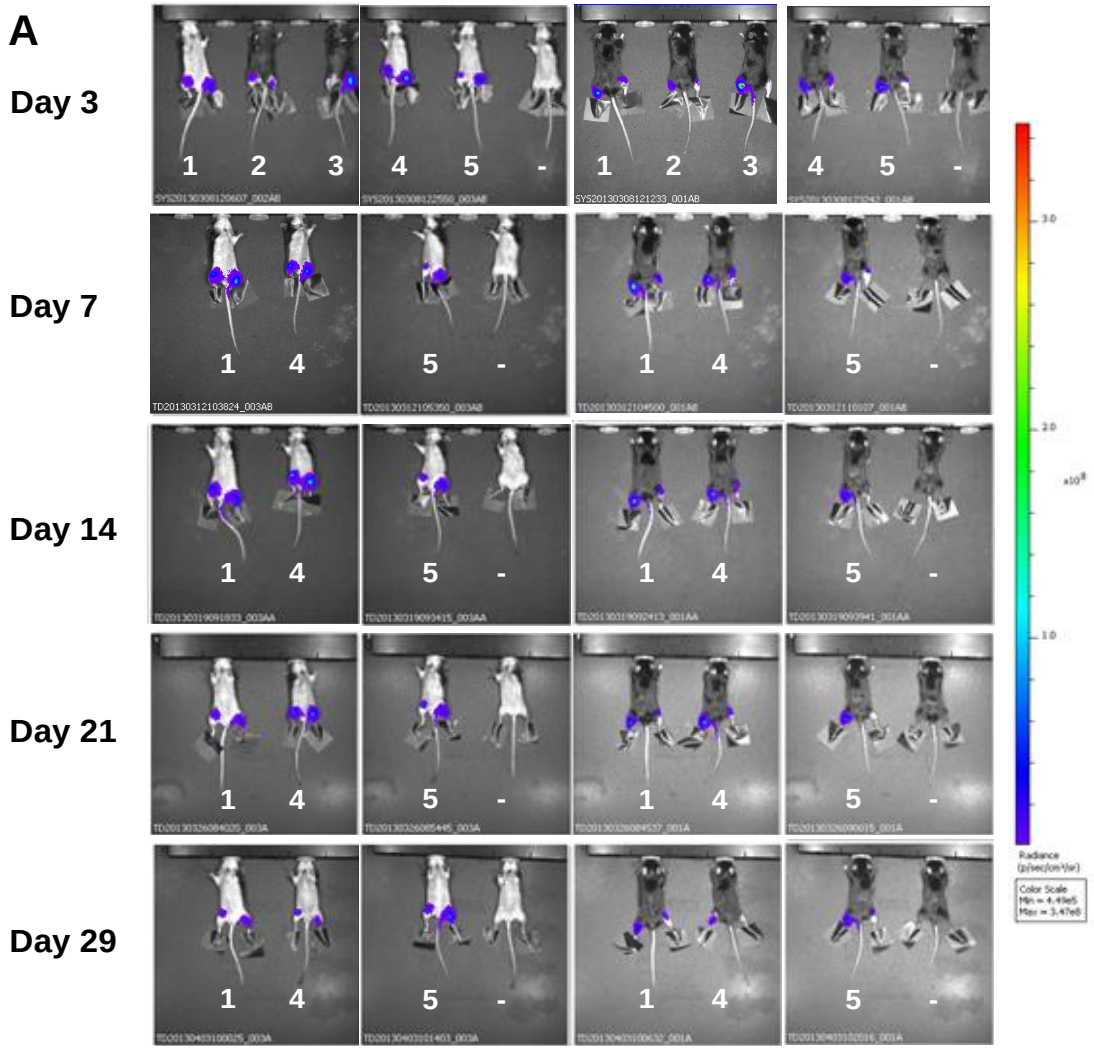

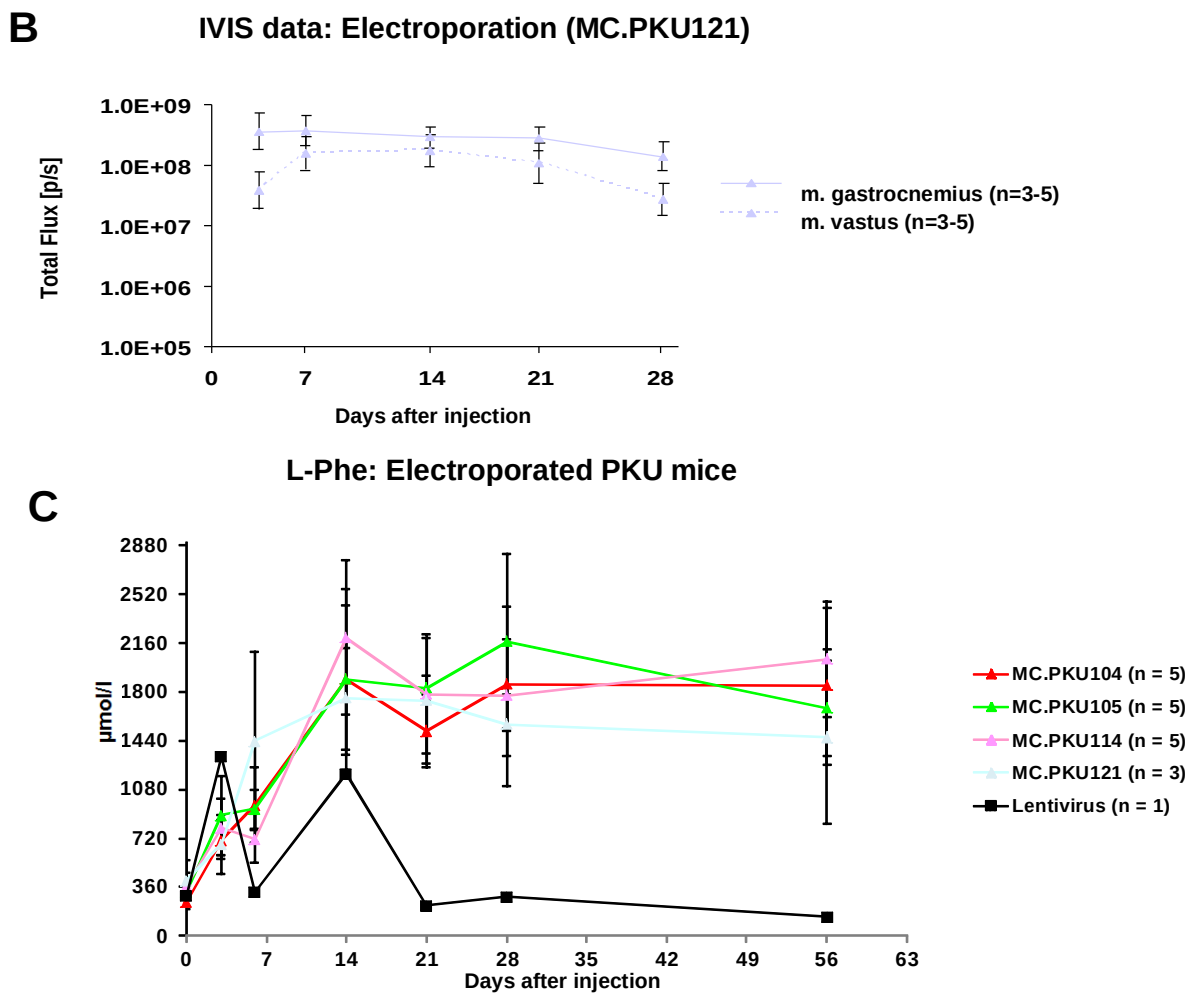

Figure 25: IVIS and blood L-Phe levels of MC electroporated *Pah*$^{enu2/2}$ mice. **(A)** IVIS pictures of MC.PKU121 application. **(B)** IVIS data of MC.PKU121 application (p/s). **(C)** Blood L-Phe levels (µmol/l). MC.PKU104 shown in red; MC.PKU105 shown in light green; MC.PKU114 shown in pink; MC.PKU121 shown in light blue; lentivirus black; therapeutic range is indicated below 360 µmol/l L-Phe.

Pah$^{enu2/2}$ mice electroporated with MC.PKU121 showed stable *Luc* expression up to 29 days (Fig. 25 A-B). None of the MCs electroporated *Pah*$^{enu2/2}$ mice showed low L-Phe levels (< 360 µmol/l) until day 56 (Fig. 25 C). It seems that at day 6 the blood L-Phe levels of the PKU mice electroplated with MC.PKU104, 105 or 114 had slightly lower L-Phe levels than *Pah*$^{enu2/2}$ mice electroplated with the negative control vector, although it was not a significant different ($p > 0.053$). At day 6 the positive control *Pah*$^{enu2/2}$ mouse, which was HTV injected with the lentivirus, showed low blood L-Phe levels (< 360 µmol/l). Surprisingly, at day 14 the blood L-Phe level of this mouse was high and dropped again at day 21 and stayed low until day 56. In general, there were high fluctuations in blood L-Phe levels because the *Pah*$^{enu2/2}$ mice were not starved. Again, further analyses need to be done with muscle tissue of MCs treated mice to reveal the vector copy number, PAH, GTPCH and PTPS activities, and/or BH_4 content.

4.1.5 DISCUSSION

In this study, 12 potential therapeutic MC vectors were generated, and in a first step, the different vectors with various modifications (codon-optimization, insertion of intron, WPRE and S/MAR) were compared *in vitro*: PAH, GTPCH and PTPS enzyme activity as well as the biosynthesis of biopterin was quantified in comparison the control vector AAV2-PKU3.3. All PP and MC constructs showed PAH, GTPCH and PTPS enzyme activity, despite that the GTPCH enzyme activity was rather low and all transfected cells showed detectable levels of biopterin. The results of enzyme activity and biopterin production from cells transfected with PP compared to MC showed that transgene expression from MC vectors was not advantageous over the PP. The *in vivo* study of PP versus MC treated *Pah*$^{enu2/2}$ mice showed that *Pah*$^{enu2/2}$ mice injected with the same amount of PP and MC had indeed similar relative m*Pah*-mRNA gene expressions and DNA copy numbers per diploid genome, but PP injected *Pah*$^{enu2/2}$ mice had only little to no PAH enzyme activity and therefore, no therapeutic efficacy, whereas MC treaded *Pah*$^{enu2/2}$ mice lowered blood L-Phe levels for a period of up to 180 days (Viecelli et al., 2014). It was hypothesized that PP were either transcriptionally blocked or very rapidly suppressed due to the phenomenon of plasmid-derived transcription blocking or silencing in liver and other organs due to the bacterial backbone (Viecelli et al., 2014). Vectors (PPs or MCs) carrying the WPRE had somewhat higher enzyme expression and produced more biopterin *in vitro*.

Although all vectors were shown to be functional *in vitro*, none of the MCs vectors lead to lower blood L-Phe levels in *Pah*$^{enu2/2}$ mice independent whether they were infused by HLV injection or electroporation, even at very high doses of up to 4 mg of MC DNA (total 6-6.8 x 10^{14} vp). For HLV injected *Pah*$^{enu2/2}$ mice, the transfection varied from 30-60% efficacy. In liver, 3 x 10^{12} vp (7.7 µg) of MC DNA still showed blood L-Phe lowering to less than 600 µmol/l up to 180 days. Personal communication with Hiu Man Viecelli (Division of Metabolism, University Childrenôs Hospital Zurich, Switzerland) revealed that MC expressing the mco*Pah* version used in this study did not let to therapeutic efficacy when HTL injected into the liver for unknown reasons. In contrast, MC vector expressing the mco*Pah* including the short version of intron 1 (same as used in this study) showed up to 10 times better efficacy then MC containing the wild-type *Pah* cDNA version. Therefore, it would be not surprising if MCs carrying a codon optimized version of m*Pah* or even m*Gch*1 and

m*Pts* are inefficient *in vivo*, which concerns the vectors MC.PKU108, 109 and 116-119. This would also theoretically explain why multiple injection of MC.PKU118 or 119 did not lead to blood L-Phe lowering in the *Pah*$^{enu2/2}$ mice.

The HLV injection method showed apparently high variations based on the amount of muscle expansion during the HLV injection as well as the leakage of the injection fluid (was between 30-60%; personal communication by S. Winn, see chapter 4.1.4.2). Analysis of treated mice still needs to be done to validate the efficacy of the HVL technique. Validation includes measuring vector genome copy numbers or immunohistology to show the number of PAH expressing transduced myocytes. In parallel, another established method, namely electroporation, was used to transfer MC DNA into skeletal muscle tissue. Electroporation has the advantage that different muscle parties can be targeted independent from each other. In this study, *Pah*$^{enu2/2}$ mice were electroporated into the m. vastus and m. gastrocnemius. For electroporation, MCs only carrying a wild-type m*Pah* or a mco*Pah* including an intron were chosen. Studies with MC.PKU121 expressing *Luc* showed relative stable transcription in the m. gastrocnemius and m. vastus. In general, the electroporated m. gastrocnemius showed slightly higher *Luc* expression than m. vastus, although there was no significant difference between the two muscles (Studentôs t-test). Unfortunately, also the electroporated PKU mice had not lowered blood L-Phe levels when treated with MCs. In this study approach, *Pah*$^{enu2/2}$ mice were fed with a L-Phe poor diet and L-Phe is added in the drinking water. Before blood collection, mice were not starved which might lead to higher variations in blood L-Phe levels. On day 6, the *Pah*$^{enu2/2}$ mice electroporated with the theoretically expected best treatment vector MC.PKU114 had almost significant lower blood L-Phe levels then the negative control group injected with MC.PKU121. Very unusual is the behavior of the blood L-Phe levels of positive control mouse that was HTV injected with the lentivirus expressing m*Pah* in liver. As expected, this mouse showed low blood L-Phe levels at day 7, but surprisingly and for unknown reasons high levels at day 14, which declined again at day 21 and stayed low the rest of the experiment.

Overall, it is unknown, why none of the injected/electroporated MCs showed not even transient therapeutic efficacy. As mentioned, one parameter could be that codon optimized genes are not therapeutic, although the reason for this phenomenon is unknown. Furthermore, it was shown that liver targeting MCs including S/MAR or *Luc*

had no therapeutic efficacy in *Pah*$^{enu2/2}$ mice (personal communication H. M. Viecelli). Also in this study, MCs including *Luc* and/or S/MAR showed generally lower enzyme activities and biopterin production *in vitro*. It is not known if these elements alter the gene expression of m*Pah* or if the increased size of these MCs has a reduced injection and/or cell integration efficacy. Although there is theoretically no size limitation in MCs, it has been shown for electroporated muscle cells that smaller DNA molecules have a higher transfection efficacy (Molnar et al., 2004). Even the smallest therapeutic MC for muscle gene therapy is more then double the size of the used therapeutic MC for liver non-viral gene therapy (Viecelli et al., 2014). Therefore, it would be interesting to test if larger MCs also lead to therapeutic efficacy in liver, to exclude that larger vectors reduce therapeutic efficacy. There is also the probability of too low injected/electroporated dose of MCs. It was shown in MC liver gene therapy for PKU mice that 3 x 10^{12} vp were still sufficient for blood L-Phe lowering (Viecelli et al., 2014). In this study, doses between 4.1 ï 68 x 10^{13} vp were used still leading to no therapeutic efficacy. Open questions like silencing/methylation of the MCs or degradation could be answered by further analysis of the injected/electroporated tissue.

In the future, it should be focused on the application of non-viral vector analogous to the therapeutic vectors AAV-PKU3.3, i.e. MC.PKU105 or MC.PKU104. Also MCs including an intron in the mco*Pah* transgene but no codon-optimization like MC.PKU114 and 115 are very promising vectors for muscle gene therapy. Since HLV injection showed high variations in transfection efficiency, electroporation is the preferable method for MC delivery. Furthermore, it is necessary to figure out if therapeutic efficacy of MCs that can be altered by vector size, which could lead to a reduced cell transfection rate. Future analysis for enzyme activity and transgene expression studies for the injected/electroporated muscle tissues need to be done.

4.2 ATTEMPT TO GENERATE A PKU MOUSE MODEL SYNTHESISING BH_4 IN MUSCLE BY EXPRESSING THE *GCH*1 AND *PTS* GENES USING AAV

4.2.1 ABSTRACT

As reported in the precedent chapter, attempts to correct cPKU by coordinate expression of three genes in skeletal muscle from a non-viral MC vector were not successful. Although the reason for this was not clear, it was speculated that a PKU mouse with stable expression of m*Gch*1 and m*Pts* and thus biosynthesis of BH_4 in skeletal muscle might be a helpful tool for further studies. With such a PKU mouse, MC delivery and testing for muscle gene expression would be limited to one gene vector, i.e. *Pah*, instead of three genes, to eventually correct cPKU in muscle of the *Pah*$^{enu2/2}$ mice. Stable expression of m*Gch*1 and m*Pts* in PKU mice was attempted by using an AAV2 serotype 1 vector. Therefore, in a first step, it was tested if m*Pah* can be separated from m*Gch*1 and m*Pts* and still has therapeutic efficiency when co-expressed. Furthermore, to assess the required expression level and extension of distribution of PAH in muscle for therapeutic efficacy *in vivo*, an AAV2/1-vector expressing *Luc* downstream of the m*Pah* transgene was used to perform IVIS. Although, therapeutic doses of the all rAAV2/1ĉs were applied, not even the published viral therapeutic control vector AAV2/1-PKU5 showed cPKU correction in the *Pah*$^{enu2/2}$ mice for unknown reasons.

4.2.2 INTRODUCTION

So far, a triple-cystronic gene therapy approach to treat cPKU in muscle of *Pah*$^{enu2/2}$ mice by using non-viral vectors was negative (described in chapter 4.1). In general, a triple-cystronic gene therapy approach is challenging to establish because too low expression of one out of three genes can be the reason for no efficacy. In comparison to viral vectors, non-viral vectors have generally low transfection efficacy, which worsens with increasing vector size (Molnar et al., 2004). A transgenic mouse model (Tg/*Pah*^{enu2}), which expressed m*Pah* and m*Gch*1 in skeletal muscle was already reported (Ding et al., 2008). This mouse showed transient lowering of L-Phe levels in blood after a single intraperitoneal (i.p.) injection of BH_4. Unfortunately, this mouse model is not longer available (personal communication with C. Harding). However, the laboratory of C. Harding attempted to generate a new transgenic PKU mouse, which expresses h*Gch*1 and h*Pts* for BH_4 production in skeletal muscle. With such a mouse model, a non-viral gene therapy could be attempted by injecting a MC vector that expresses only one gene (m*Pah*). It is speculated that optimization of MC delivery and PAH expression in skeletal muscle would be easier than a triple-cystronic approach. Unfortunately, such a PKU mouse that expresses the BH_4-biosynthetic genes and produces the cofactor in skeletal muscle tissue was not available because after two series of embryo injections, no founder mice could be isolated due to unknown reasons (C. Harding, personal communication). Thus an alternative possibility was investigated by transducing skeletal muscles of PKU mice with an AAV2/1 vector that expresses m*Gch*1 and m*Pts*. Thus an alternative possibility was investigated by transducing skeletal muscles of PKU mice with an AAV2/1 vector that expresses m*Gch*1 and m*Pts*. Such a virally pre-injected PKU mouse could be used to test for HLV injection of a MC vector that expresses the m*Pah* gene in order to test for correction of HPA (Fig. 26).

To validate the potential benefit of such a variant PKU mouse model, it first had to be investigated if the separation of the triple-cystronic viral vector AAV2-PKU3 into a vector expressing m*Pah* and a second vector expressing m*Gch*1 and m*Pts* for cofactor production still lead to therapeutic efficiency when co-injected (Fig. 26). To test this, AAV2/1 vectors were used as they showed stable and long-term expression in mice. The triple-cistronic expression cassette from vector AAV2-PKU3.3 was separated into two viral vectors, AAV2-PKU16 expressing m*Pah* and AAV2-PKU12

expressing m*Gch*1 and m*Pts*. Furthermore, it was planned to assess the distribution and therapeutic expression of PAH in muscle by adding the *Luc* downstream of the m*Pah* transgene (AAV2-PKU11.2) for IVIS application. With this gain of knowledge, therapeutic doses of MC vector can be easier assessed by generating an MC vector, which also expresses *Luc* downstream of the m*Pah* transgene.

In summary, it was investigated if the separation of the therapeutic triple-cystronic setting is still therapeutic (needed to generated the BH_4 muscle expressing PKU mouse model) and if so, how much AAV2/1 m*Pah* expression leads to therapeutic efficacy *in vivo* (needed to determine the dose for the non-viral one gene MC approach). Therefore, PKU mice were rAAV injected into the m. gastrocnemius, the same method used in the therapeutic triple-cystronic AAV-PKU3 setting (Ding et al, 2009).

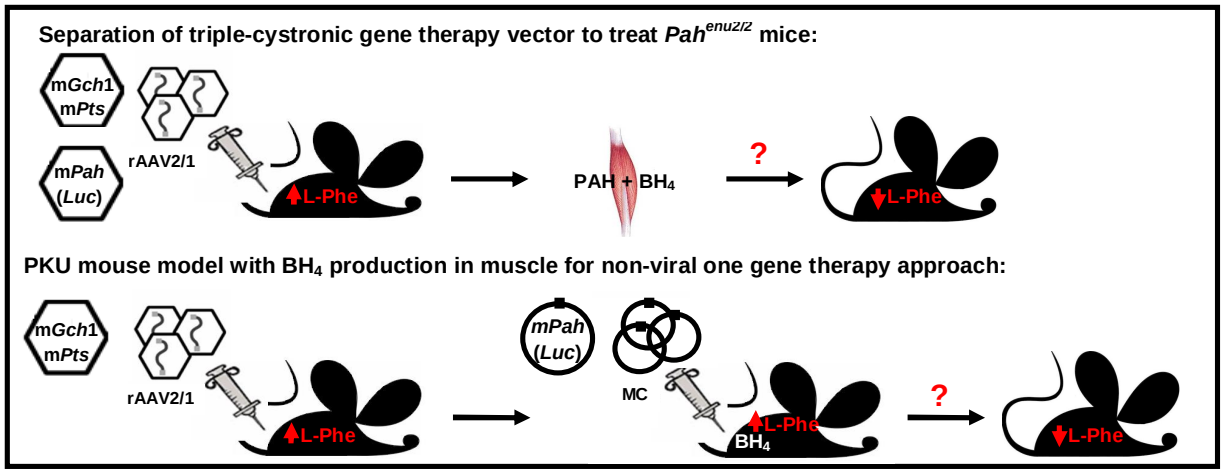

Figure 26: Schematic representation of generating a BH_4 muscle expressing PKU mouse model for non-viral one gene therapy. m*Gch*1, murine guanosine triphosphate cyclohydrolase 1 gene; m*Pts*, murine 6-pyruvoyl-tetrahydropterin synthase gene; *Luc*, *firefly* luciferase gene; BH_4, tetrahydrobiopterin; L-Phe, L-phenylalanine; MC, minicircle.

4.2.3 MATERIALS AND METHODS

4.2.3.1 Viral vector plasmids

In chapter 4.1.3.1 the correction of the two missense mutations in m*Pah* (c.1126G>A, p.E376K) and m*Pts* (c.230A>G; p.E77G) in the AAV2-PKU3 plasmid as well as the correction of the disrupted ITR site was described. Furthermore, the published vector AAV2-PKU5 showed also the m*Pah* p.E376K mutation, which was corrected and the AAV2-PKU56 plasmid was generated (received from H. M. Viecelli). Therefore, instead of AAV2-PKU3 and AAV2-PKU5, AAV2-PKU3.3 and AAV2-PKU56 were used as positive controls, respectively. Detailed summary of all viral plasmids is listed in chapter 5.1.

4.2.3.2 rAAV production

4.2.3.2.1 Transfection, purification and titer determination

Confluent 293T cells in a 15 cm plate were split into 1:3, and incubated over night at 37°C and 5% CO_2. The next day, cells had a confluence of 50-60%, and the Dulbecco's modified eagle medium (Thermo Scientific, Reinach, Basel, Switzerland) with 1% L-glutamine (Thermo Scientific) was changed. A transfection mixture for one plate containing 25 µg of viral plasmid, 37.5 µg helper plasmid and 20 µg of the AAV1-capsid plasmid were mixed in up to 1100 µl ddH_2O. 150 µl of 2.5 M $CaCl_2$ pH 7.13 (ref. nr. 21097, Fluka Chemie GmBH) followed by 1250 µl 2x HeBS pH 7, including 0.28 M NaCl, 0.05 M HEPES and 1.5 mM Na_2HPO_4, were added, mixed and incubated at room temperature for 5 min. The transfection reaction was added drop wise to the cells (total 20 plates per virus). The cells were incubated for 72 h at 37°C and 5% CO_2. Cells were collected, washed with 1x phosphate buffered saline, shock frozen with liquid nitrogen and stored at -80°C. rAAV purification and titer determination were performed as described in the published methods (Haberman RP, 1999, Ding et al., 2006).

4.2.3.2.2 Enzyme activity

To confirm that the generated rAAV are vital and infectious, 50-60% confluent 293T cells on a 15 cm plate were transduced with 25 µl AAV2/1-PKU3.3, 11.2, 12 or 16 for 48 h at 37°C and 5 % CO_2. PAH or PTPS activity was measured as described in chapter 4.1.3.3.

4.2.3.2.3 Application of AAV vectors to *Pah*$^{enu2/2}$ mice

Pah$^{enu2/2}$ mice were anaesthetized with 2-3% isoflurane. Hind limbs were shaved and disinfected with 70% ethanol. Both hind limbs were injected with a maximum volume of 100 µl rAAV2/1 per hind limb. Injection was done directly into m. gastrocnemius using a U-100 insulin syringe with a 28 G needle.

4.2.3.3 In vivo imaging system

Was performed as described in chapter 4.1.3.6 but D-luciferin was i.p. injected.

4.2.4 RESULTS

4.2.4.1 AAV vectors and *in vitro* expression

In a first step, the published triple-cystronic expression cassette from vector AAV2-PKU3, containing the genes m*Pah,* m*Gch*1 *and* m*Pts* expressed from the human CMV promoter, was separated into one vector expressing m*Pah* with *Luc* for analyzing expression level and distribution *in vivo* (AAV2-PKU11.2) and one expressing m*Gch*1 and m*Pts* (AAV2-PKU12) (Ding et al., 2006). In addition, an AAV expressing only m*Pah* (AAV2-PKU16) was generated. Theoretically, the co-injection of AAV2/1-PKU12 and AAV2/1-PKU11.2 or 16 into the m. gastrocnemius muscle should clear the high L-Phe levels in *Pah*$^{enu2/2}$ mice. The already published vectors AAV2-PKU3 and AAV2-PKU5, which is liver directed gene therapy vectors expressing m*Pah* under the liver expressing chicken ß-actin (CBA) promoter, was planned to use as positive control (Rebuffat et al., 2010). Due to sequence alteration found in control AAV2-PKU3 and AAV2-PKU5 vectors described in chapter 4.2.3.1, AAV2-PKU3.3 and AAV2-PKU56 were used as positive controls, respectively. All rAAV vectors were generated with serotype 1 capsid that had tropism for skeletal muscle. A summary of all viral plasmids is listed in table 10.

Table 10: Viral plasmid list.

Vector	Promoter	m*Pah*	m*Gch*1	m*Pts*	*Luc*	Enhancing elements	Vector size (bp)	Vector size ITR to ITR (bp)
AAV2-PKU3.3	CMV	wt	wt	wt	-	WPRE	9,361	5,628
AAV2-PKU11.2	CMV	wt	-	-	wt	WPRE	9,320	5,587
AAV2-PKU16	CMV	wt	-	-	-	WPRE	7,227	3,494
AAV2-PKU12	CMV	-	wt	wt	-	WPRE	7,419	3,777
AAV2-PKU56	CBA	wt	-	-	-	WPRE	7,973	4,292

CMV, human cytomegalovirus promoter; CBA, chicken ß-actin promoter; m*Pah*, murine phenylalanine hydroxylase gene; m*Gch*1, murine GTP cyclohydrolase 1 gene; m*Pts*, murine 6-pyruvoyl-tetrahydropterin synthase gene; Luc, *firefly* luciferase; WPRE, woodchuck hepatitis post-transcriptional regulatory element; wt, wild-type.

To validate that AAV2/1-PKU3.3, AAV2/1-PKU11.2, AAV2/1-PKU12 and AAV2/1-PKU16 are infectious, 293T cells were transduced with 25 µl of the AAV2/1 for 48h and enzyme activity was analyzed. PAH enzyme activity was measured for AAV2/1-PKU3.3, AAV2/1-PKU11.2 and AAV2/1-PKU16. PTPS activity was evaluated for AAV2/1-PKU12 (Fig. 27).

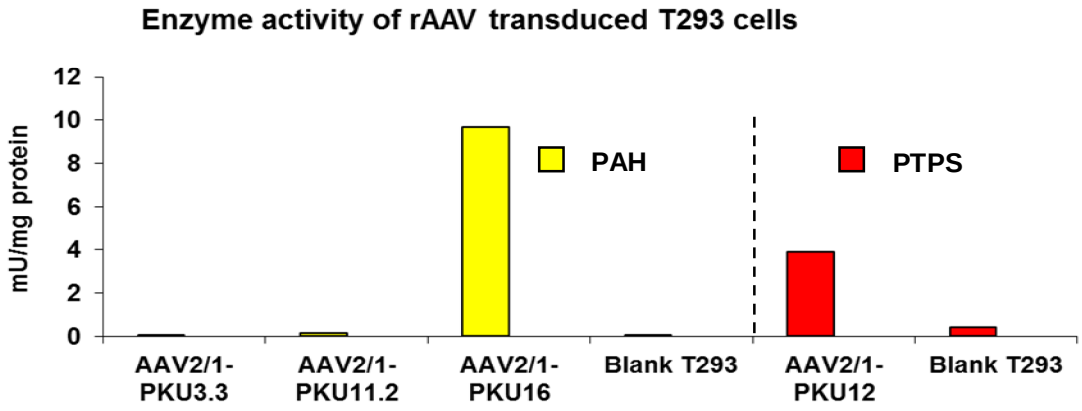

Figure 27: PAH or PTPS activity of AAV2/1-PKU3.3, AAV2/1-PKU11.2 and AAV2/1-PKU16 or AAV2/1-PKU12 transduced 293T cells, respectively (mU/mg protein).

In general, viral plasmid inserts with more than 5,500 bp (AAV2-PKU3.3 and AAV2-PKU11.2) had relative low titers. Unfortunately, the titer of viral vector AAV2/1-PKU3.3 was too low to reach therapeutic efficacy in mice (therapeutic dose of AAV2/1-PKU3: 3.5×10^{12} vp), and therefore, it could not be used as positive control (Ding et al., 2008). Because of the low titer of AAV2/1-PKU11.2, the viral vector was used to investigate the distribution in muscle but not to evaluate the therapeutic dose. Overall, all rAAV2/1 vectors showed PAH or PTPS enzyme activity, although viral rAAV2/1 with relative low titers, like e.g. AAV2/1-PKU3.3 and AAV2/1-PKU11.2, showed very low enzyme activity (Fig. 27).

4.2.4.2 *In vivo* evaluation of potential therapeutic efficacy of the separated rAAV2/1 triple-cystronic vector

Next, it was to evaluate if co-expression in muscle of AAV2/1-PKU12 expressing m*Gch*1-m*Pts* and rAAV2/1-PKU16 expressing m*Pah* would lead to L-Phe clearance in *Pah*$^{enu2/2}$ mice. 1.5 x 10^{13} vp (low dose) or 6.0 x 10^{13} vp (high dose) of vector AAV2/1-PKU12 was co-injected with 1.3 x 10^{14} vp of rAAV2/1-PKU16 into m. gastrocnemius of female *Pah*$^{enu2/2}$ mice. Since the titer of vector AAV2/1-PKU3.3 was too low to reach therapeutic dose (as described above), vector AAV2/1-PKU56 was used as control instead (therapeutic dose: 1.2 x 10^{12}, Rebuffat et al., 2010). Two doses of AAV2/1-PKU56 were applied, 1.7 x 10^{12} (low dose) to a male mouse and 2.2 x 10^{12} (high dose) to a female mouse. The control female mouse was injected with a slightly higher concentration of AAV2/1-PKU56 because of the known sexual

dimorphism of hepatic AAV transduction in *Pah*$^{enu2/2}$ mice probably caused by an androgen-dependent pathway. A summary of blood L-Phe levels are shown in Fig. 28.

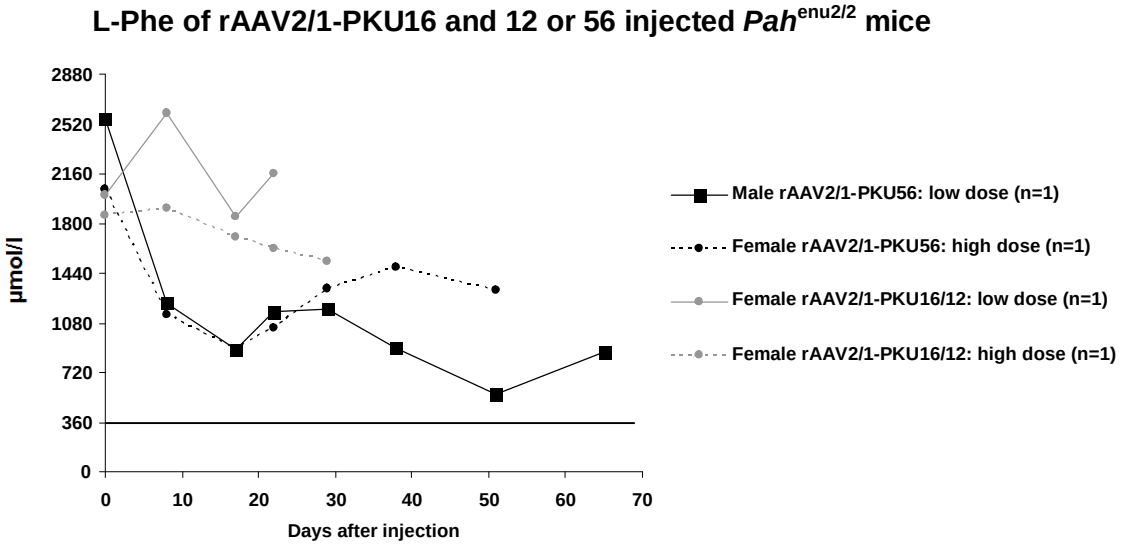

Figure 28: Blood L-Phe levels of *Pah*$^{enu2/2}$ mice co-injected with AAV2/1-PKU12 and AAV2/1-PKU16 or the therapeutic AAV2/1-PKU56 (µmol/l). AAV2/1-PKU56 injected *Pah*$^{enu2/2}$ mice are indicated by black lines; co-injected AAV2/1-PKU16 and AAV2/1-PKU12 injected *Pah*$^{enu2/2}$ mice are indicated by gray lines; Low dose are indicated by straight lines; High dose are indicated by dotted lines. Therapeutic range is indicated below 360 µmol/l L-Phe.

Surprisingly, none of injected *Pah*$^{enu2/2}$ mice showed clearance of blood L-Phe to therapeutic levels (<360 µmol/l), not even the control injected PKU mice (AAV2/1-PKU56). Nevertheless, the male mouse showed lowered L-Phe levels and the fur colour of the AAV2/1-PKU56 injected *Pah*$^{enu2/2}$ mice changed and revealed dark patches, which was more prominent in the male mouse then in the female mouse indicating a transient expression and/or mild efficacy of the virus (Fig. 29 A-D).

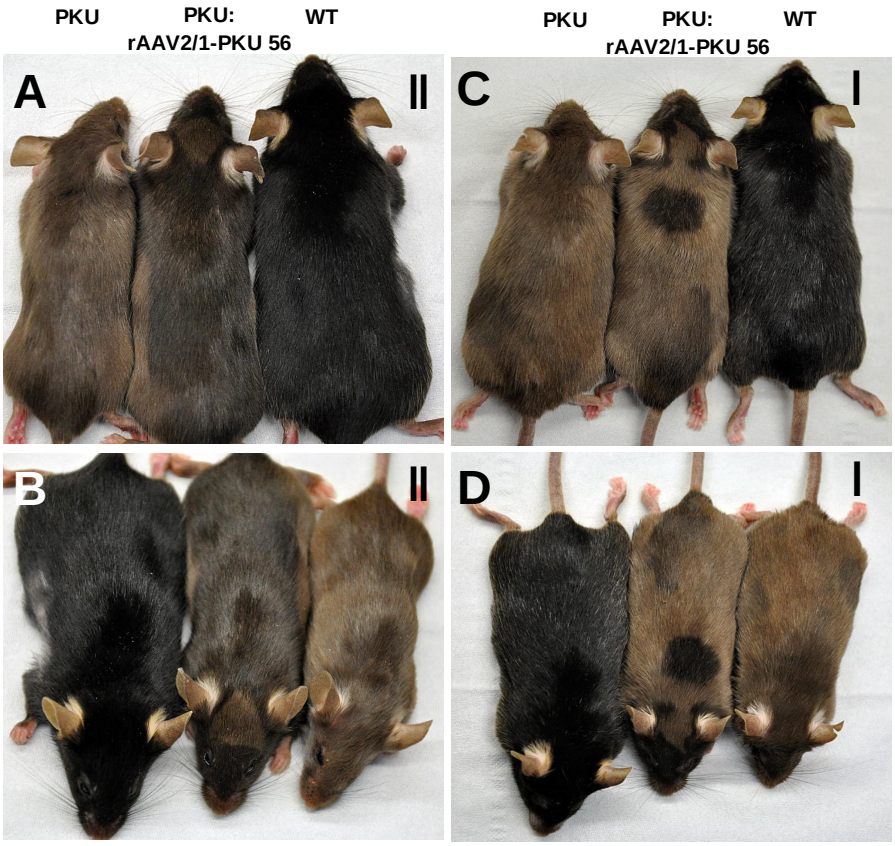

Figure 29: Pictures of AAV2/1-PKU56-injected *Pah*$^{enu2/2}$ mice 50 days after injection. **(A-B)** Males. **(C-D)** Females.

Although potential therapeutic doses of AAV2/1-PKU56 were injected into the *Pah*$^{enu2/2}$ mice, there was no therapeutic effect leading to the assumption that either the titer was incorrect calculated or the transfection efficacy of the AAV2/1 vectors were not high enough. Although, almost 10 to 100 times more then the reported therapeutic dose of AAV2/1-PKU5 was injected for AAV2/1-PKU12 and AAV2/1-PKU16 into *Pah*$^{enu2/2}$ mice, there was no lowering of L-Phe below 360 µmol/l. It was described that i.p. injection of 1.0 ε mol BH_4/g body weight into a transgenic Tg/*Pah*^{enu2} mouse, which expresses m*Gch*1 and m*Pah* in muscle, showed transient lowering of blood L-Phe 6 h after injection (<360 µmol/l), which was reversed after 24 h (Ding et al., 2008). Since the injected amount of AAV2/1-PKU16 was very high, it was investigated if at least i.p. injection of BH_4 would lead to correction of blood L-Phe levels after 6 h similar to the Tg/*Pah*^{enu2} mouse. Therefore, two male mice, one pre-injected with 1.3 x 10^{14} vp AAV2/1-PKU16 14 days before, and one not-injected *Pah*$^{enu2/2}$ control mouse received an i.p. injection of 1.0 ε mol BH_4/g body weight. Blood L-Phe was measured after 6, 28 and 76 h after injection shown in Fig. 30.

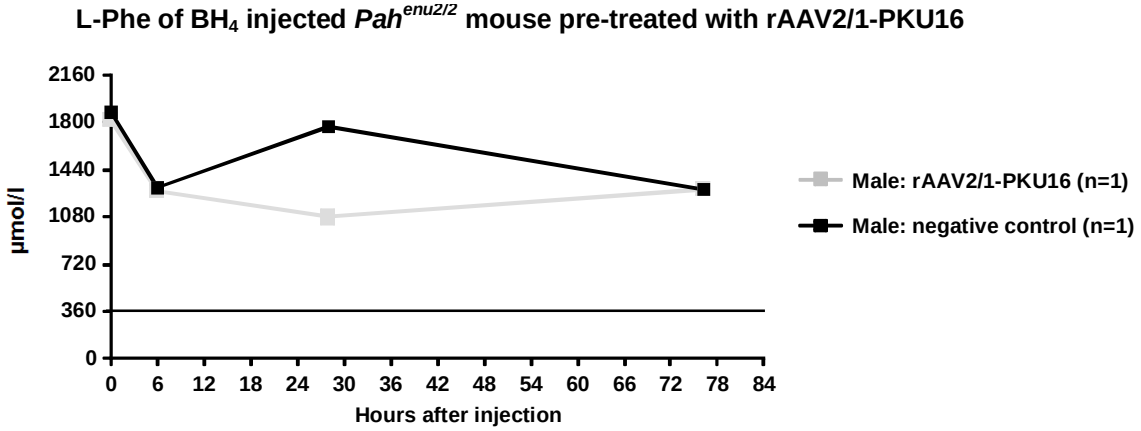

Figure 30: Blood L-Phe levels of 1.0 εmol BH_4/g body weight i.p. injected *Pah*$^{enu2/2}$ mice (µmol/l). AAV2/1-PKU16 pre-injected *Pah*$^{enu2/2}$ mouse is indicated by a black line; not pre-injected *Pah*$^{enu2/2}$ mouse is indicated by a gray line. Therapeutic range is indicated below 360 µmol/l L-Phe.

Unexpectedly, blood L-Phe levels were not lowered below 360 µmol/l after 6 h of BH_4 injection in the AAV2/1-PKU16 pre-injected *Pah*$^{enu2/2}$ mouse, indicating either that the potential therapeutic dose of AAV2/1-PKU16 was not reached or that the time point of potentially transient low L-Phe was missed. No further investigations were performed. Therefore, it is still unclear if m*Pah* can be separated from m*Gch*1 and m*Pts* and lead to therapeutic efficacy. In summary, the original plan to generate PKU mouse model by using rAAV2/1 expressing m*Gch*1 and m*Pts* for BH_4 production in muscle failed.

4.2.4.3 Evaluation of distribution and expression of PAH in muscle in combination with *Luc*

To investigate the distribution of PAH in muscle, 7.2 x 10^{10} vp (low dose) or 1.2 x 10^{11} vp (high dose) of AAV2/1-PKU11.2 was injected into the m. gastrocnemius muscle of both legs in a *Pah*$^{enu2/2}$ mouse. With this experiment it should be also verified that the rAAV2/1 is restricted to the injected hind limb muscles and not spreading to other muscle areas of the body. IVIS results and blood L-Phe levels are represented in Fig. 31 A-C showing the restricted expression and distribution of AAV2/1-PKU11.2 in m. gastrocnemius of the injected hind limbs up to 71 days.

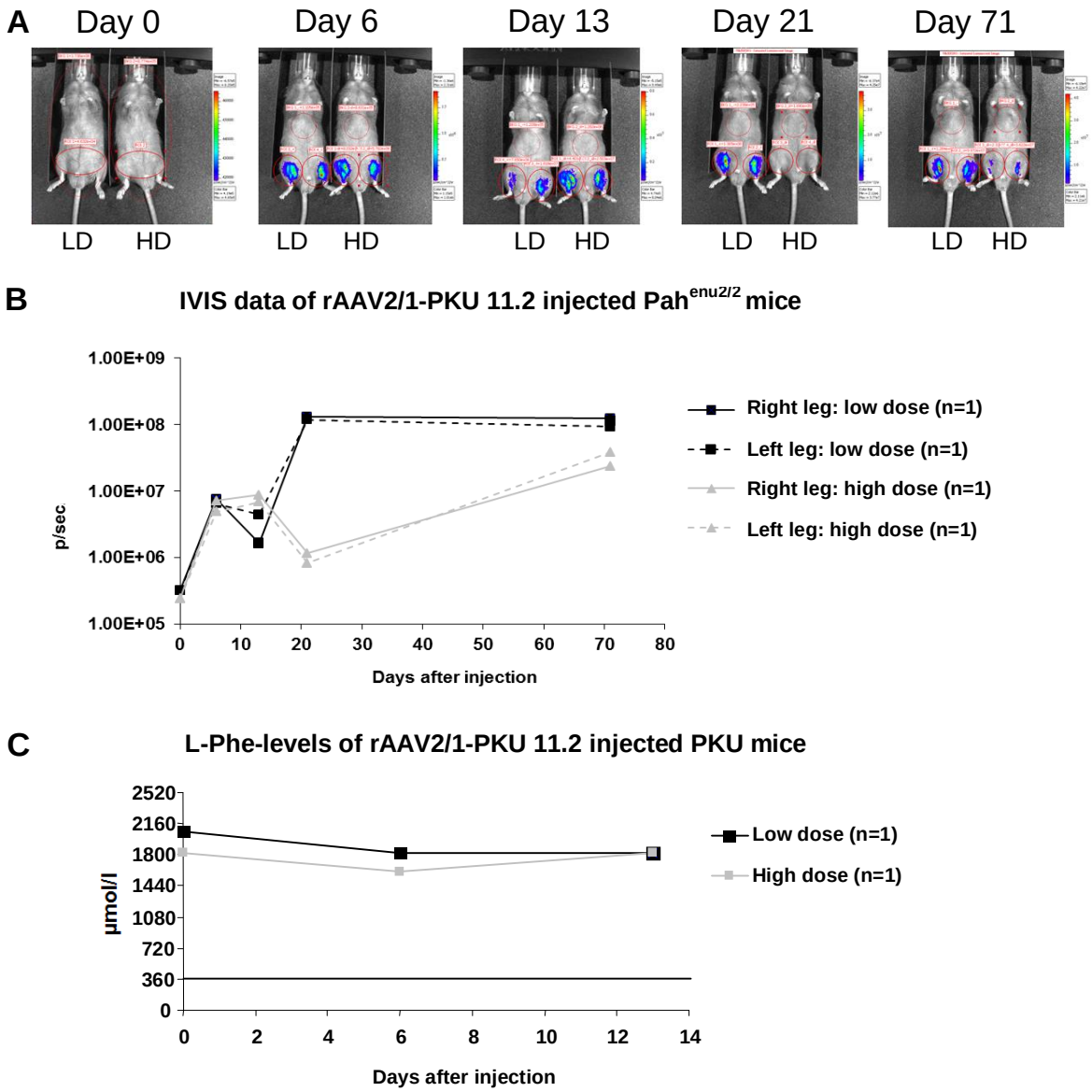

Figure 31: IVIS and blood L-Phe level results of AAV2/1-PKU11.2 injected limb muscles of *Pah*$^{enu2/2}$ mice with low and high dose before (day 0) and after injection (day 6, 13 and 71). **(A)** IVIS pictures of *Luc* expression. **(B)** IVIS graph of *Luc* expression (p/sec). **(C)** Blood L-Phe (µmol/l). Low dose injected mouse is indicated by black line; high dose injected mouse is indicated by gray line; right leg is indicated by straight lines; left leg is indicated by dotted lines; LD, low dose; HD, high dose. Therapeutic range is indicated below 360 µmol/l L-Phe.

Although, vector AAV2/1-PKU11.2 showed low PAH expression *in vitro*, there was clearly detectable *Luc* signaling *in vivo*. At the beginning, both doses showed equally *Luc* expression up to 13 days (Fig. 31 A-B). In contrast, at day 21 the higher dose injected mouse showed almost no *Luc* expression, which recovered at day 71, whereas the low dose injected mouse showed high and stable *Luc* expression up to 71 days after injection (Fig. 31 A-B). As expected, the blood L-Phe levels was not influenced by rAAV2/1 treatment (Fig. 31 C).

4.2.5 DISCUSSION

Unfortunately, generation of a PKU mouse which produces BH_4 in muscle by injecting rAAV2/1 expressing the two genes m*Gch*1 and m*Pts*, could not be achieved. With such a mouse model, non-viral gene therapy could have been optimized by only injecting a MC vector containing m*Pah,* which is easier to monitor in comparison to the triple-cystronic approach. So far, it is still unknown if the triple-cistronic m*Pah*-m*Gch*1-m*Pts* genes lead to correction of cPKU when separated and co-expressed i*n vivo* due to the fact that not even the control therapeutic AAV2/1-PKU56 injected *Pah*$^{enu2/2}$ mice showed lowered L-Phe levels (<360 µmol/l). One possibility would be that the titer was not calculated correctly. Titer recalculation of a rAAV2/1 aliquot with a known titer led to similar results. Therefore, it seems unlikely that miscalculation is the reason for the non-therapeutic efficacy. Another potential cause could be that the produced rAAV2/1 had too low transfection efficacy. All *in vitro* tested rAAV2/1 showed enzyme activity according to the virus titer either low (AAV2-PKU3.3 or 11.2) or high (AAV2-PKU16 or 12). Although the measured *in vitro* enzyme activity of AAV2/1-PKU11.2 was very low, there was stable *Luc* expressed up to 71 days *in vivo*. In contrast, AAV2/1-PKU16 or 12 showed higher virus titer and enzyme activity *in vitro* but surprisingly their co-expression did not lead to L-Phe lowering *in vivo*. Even i.p. injection of BH_4 did not lead to blood L-Phe lowering after 6 h in a 14 days pre-injected AAV2/1-PKU16 *Pah*$^{enu2/2}$ mouse. Perhaps it is necessary to increase the doses of BH_4 and measure blood L-Phe levels in shorter time intervals. Another mysterious phenomenon was that the control vector AAV2/1-PKU56 did not show blood L-Phe lowering *in vivo*, although it seemed that blood L-Phe was halved especially for the male mouse indicating some effect, which was also indicated by the changes of their fur coat by revealing dark patches, which was more prominent in the male mouse. Unfortunately, PAH enzyme activity of the control virus AAV2/1-PKU56 was not measured *in vitro* (cell culture), which would validate expression. Overall, it is rather unclear why the AAV2/1 vectors were not therapeutic. Probably it is a combination of too low titer and limited transgene expression. Determination of vector genome copy numbers in the treated mouse muscle tissues and/or the transduction frequency as judged from immunohistology against GTPCH or PTPS are definitively needed to better understand the limitations and to continue with future analyses. Furthermore, it is unclear in how far the two found but not yet described mutations in AAV2-PKU3 (m*Pah* p.E376K and m*Pts* p.E77G) and AAV2-PKU5 (m*Pah* p.E376K),

influenced the gene expression. Therefore, a mutation analysis for their enzyme activity would be interesting. Furthermore, analysis of the injected muscle tissue for the mRNA expression, vector copy number, and enzyme activity can be performed.

The second goal of showing m*Pah* expression and distribution in muscle was achieved although the therapeutic dose of m*Pah* in muscle could not be elucidated. Injection of AAV-PKU11.2 into m. gastrocnemius of *Pah*$^{enu2/2}$ mice showed that the *Luc* was only expressed in the injected hind limbs up to 71 days. Surprisingly, the mouse with the lower injected dose had higher and more stable expression than the mouse injected with the higher dose. It could be hypothesized from these preliminary results that too high *Luc* expression levels could be inhibitory. Further studies need to be done with larger animal groups to confirm these preliminary results.

5. SUPPLEMTARY INORMATION

5.1 Cloning of plasmids

AAV2-PKU3: CMV-m*Pah* (c.230A>G; p.E77G)-EMCV-IRES-m*Gch*1-FMDV-IRES-m*Pts* (c.1126G>A, p.E376K)-WPRE-pA (one disrupted ITR site)

AAV2-PKU3.1: CMV-m*Pah* (c.230A>G; p.E77G)-EMCV-IRES-m*Gch*1-FMDV-IRES-m*Pts*-WPRE-pA (one disrupted ITR site)

AAV2-PKU3.3: CMV-m*Pah*-EMCV-IRES-m*Gch*1-FMDV-IRES-m*Pts*-WPRE-pA (one disrupted ITR site)

AAV2-PKU3.3: CMV-m*Pah*-EMCV-IRES-m*Gch*1-FMDV-IRES-m*Pts*-WPRE-pA (corrected ITR site)

AAV2-PKU11.1: CMV-m*Pah*-EMCV-IRES-*Luc*-WPRE-pA (one disrupted ITR site)

AAV2-PKU11.2: CMV-m*Pah*-EMCV-IRES-*Luc*-WPRE-pA (corrected ITR site)

AAV2-PKU12: CMV-m*Gch*1-FMDV-IRES-m*Pts*-WPRE-pA

AAV2/8-PKU13: CBA-m*Pts*-EMCV-IRES-*Luc*-pA

AAV2-PKU16: CMV-m*Pah*-WPRE-pA

MC.PKU100: CMV-m*Pah* (c.230A>G; p.E77G)-EMCV-IRES-m*Gch*1-FMDV-IRES-m*Pts* (c.1126G>A, p.E376K)-EMCV-IRES-S/MAR-BGHpA

MC.PKU101: CMV-m*Pah* (c.230A>G; p.E77G)-EMCV-IRES-m*Gch*1-FMDV-IRES-m*Pts*-EMCV-IRES-S/MAR-BGHpA

pMC.PKU102: CMV-m*Pah*-EMCV-IRES-m*Gch*1-FMDV-IRES-m*Pts*-EMCV-IRES-*Luc*-S/MAR-BGHpA

MC.PKU104: CMV-m*Pah*-EMCV-IRES-m*Gch*1-FMDV-IRES-m*Pts*-WPRE-pA

MC.PKU105: CMV-m*Pah*-EMCV-IRES-m*Gch*1-FMDV-IRES-m*Pts*-BGHpA

MC.PKU106: CMV-m*Pah*-EMCV-IRES-m*Gch*1-FMDV-IRES-m*Pts*-S/MAR-BGHpA

MC.PKU108: CMV-mco*Pah*-EMCV-IRES-m*Gch*1-FMDV-IRES-m*Pts*-WPRE-pA

MC.PKU109: CMV-mco*Pah*-EMCV-IRES-m*Gch*1-FMDV-IRES-m*Pts*-pBGHA

MC.PKU114: CMV-mco*Pah*-IVS1B-EMCV-IRES-m*Gch*1-FMDV-IRES-m*Pts*-WPRE-pA

MC.PKU115: CMV-mco*Pah*-IVS1B-EMCV-IRES-m*Gch*1-FMDV-IRES-m*Pts*-pA

MC.PKU116: CMV-mco*Pah*-EMCV-IRES-mco*Gch*1-FMDV-IRES-mco*Pts*-WPRE-pA

MC.PKU117: CMV-mco*Pah*-EMCV-IRES-mco*Gch*1-FMDV-IRES-mco*Pts*-pA

MC.PKU118: CMV-mco*Pah*-IVS1B-EMCV-IRES-mco*Gch*1-FMDV-IRES-mco*Pts*-WPRE-pA

MC.PKU119: CMV-mco*Pah*-IVS1B-EMCV-IRES-mco*Gch*1-FMDV-IRES-mco*Pts*-pA

MC.PKU121: CMV-*Luc*-BGHpA

PLASMID: mco*Gch*1-FMDV-IRES-mco*Pts*

The m*Pts* and m*Gch*1 genes were codon optimized and synthesized by GenScript USA Inc. (Piscataway, USA) in the pUC57 vector.

PLASMID: CBA-m*Pts*-EMCV-IRES-m*Th*-FMDV-IRES-m*Tph*2

Synthesized by GeneArt® Life technology (Regensburg, Germany) in the pMA vector.

6. REVERENCES

Adamsen D (2011) Tetrahydrobiopterin and Monoamine Neurotransmitter Deficiency in Mouse Models and Human Disease. Dissertation; University of Zurich.

Al-Dosari MS, Gao X (2009) Nonviral gene delivery: principle, limitations, and recent progress. The AAPS journal 11:671-681.

Alfadhel M, Al-Thihli K, Moubayed H, Eyaid W, Al-Jeraisy M (2013) Drug treatment of inborn errors of metabolism: a systematic review. Archives of disease in childhood 98:454-461.

Alterio J, Ravassard P, Haavik J, Le Caer JP, Biguet NF, WaksmanG, Mallet J (1998) Human tyrosine hydroxylase isoforms. Inhibition by excess tetrahydropterin and unusual behavior of isoform 3 after camp-dependent protein kinase phosphorylation. 273: 10196-201

Anjema K, van Rijn M, Hofstede FC, Bosch AM, Hollak CE, Rubio-Gozalbo E, de Vries MC, Janssen MC, Boelen CC, Burgerhof JG, Blau N, Heiner-Fokkema MR, van Spronsen FJ (2013) Tetrahydrobiopterin responsiveness in phenylketonuria: prediction with the 48-hour loading test and genotype. Orphanet journal of rare diseases 8:103.

Argyros O, Wong SP, Fedonidis C, Tolmachov O, Waddington SN, Howe SJ, Niceta M, Coutelle C, Harbottle RP (2011) Development of S/MAR minicircles for enhanced and persistent transgene expression in the mouse liver. Journal of molecular medicine 89:515-529.

Argyros OaWS (2012) Gene Therapy for Phenylketonuria. Gene Therapy Review.

Arora NS, Rochester DF (1982) Effect of body weight and muscularity on human diaphragm muscle mass, thickness, and area. Journal of applied physiology: respiratory, environmental and exercise physiology 52:64-70.

Azzouz M, Martin-Rendon E, Barber RD, Mitrophanous KA, Carter EE, Rohll JB, Kingsman SM, Kingsman AJ, Mazarakis ND (2002) Multicistronic lentiviral vector-mediated striatal gene transfer of aromatic L-amino acid decarboxylase, tyrosine hydroxylase, and GTP cyclohydrolase I induces sustained transgene expression, dopamine production, and functional improvement in a rat model of Parkinson's disease. The Journal of neuroscience : the official journal of the Society for Neuroscience 22:10302-10312.

Bach-Mizrachi H, Underwood MD, Tin A, Ellis SP, Mann JJ, Arango V (2008) Elevated expression of tryptophan hydroxylase-2 mRNA at the neuronal level in the dorsal and median raphe nuclei of depressed suicides. Molecular psychiatry 13:507-513, 465.

Banta-Wright SA, Steiner RD (2004) Tandem mass spectrometry in newborn screening: a primer for neonatal and perinatal nurses. The Journal of perinatal & neonatal nursing 18:41-58; quiz 59-60.

Bayle JH, Randazzo F, Johnen G, Kaufman S, Nagy A, Rossant J, Crabtree GR (2002) Hyperphenylalaninemia and impaired glucose tolerance in mice lacking the bifunctional DCoH gene. The Journal of biological chemistry 277:28884-28891.

Bell P, Moscioni AD, McCarter RJ, Wu D, Gao G, Hoang A, Sanmiguel JC, Sun X, Wivel NA, Raper SE, Furth EE, Batshaw ML, Wilson JM (2006) Analysis of tumors arising in male B6C3F1 mice with and without AAV vector delivery to liver. Molecular therapy : the journal of the American Society of Gene Therapy 14:34-44.

Bickel H (1987) Early diagnosis and treatment of inborn errors of metabolism. Enzyme 38:14-26.

Bik-Multanowski M, Pietrzyk JJ (2006) LAT1 gene variants--potential factors influencing the clinical course of phenylketonuria. Journal of inherited metabolic disease 29:684.

Blau N (1988) Inborn errors of pterin metabolism. Annual review of nutrition 8:185-209.

Blau N (2008a) Defining tetrahydrobiopterin (BH4)-responsiveness in PKU. Journal of inherited metabolic disease 31:2-3.

Blau N, Bonafe L, Thöny B (2001) Tetrahydrobiopterin deficiencies without hyperphenylalaninemia: diagnosis and genetics of dopa-responsive dystonia and sepiapterin reductase deficiency. Molecular genetics and metabolism 74:172-185.

Blau N, Duran, M., and Gibson K. M. (2008b) Laboratory Guide to the Methods in Biochemical Genetics. Springer Verlag Berlin 2. Edition.

Blau N, Kierat L, Heizmann CW, Endres W, Giudici T, Wang M (1992) Screening for tetrahydrobiopterin deficiency in newborns using dried urine on filter paper. Journal of inherited metabolic disease 15:402-404.

Blau N, MacDonald A, van Spronsen F (2011) There is no doubt that the early identification of PKU and prompt and continuous intervention prevents mental retardation in most patients. Molecular genetics and metabolism 104 Suppl:S1.

Blau N, Thöny, B., Heizmann, C. W., Dhondt JL. (2013) Tetrahydrobiopterin Deficiency: From Phenotype to Genotype. Pteridines Volume 4:1ï 10.

Blau N, van Spronsen FJ, Levy HL (2010) Phenylketonuria. Lancet 376:1417-1427.

Blumenfeld CM, Wallace MJ, Anderson R (1966) Phenylketonuria-the guthrie screening test-a method of quantitation, observations on reliability and suggestions for improvement. California medicine 105:429-434.

Bode VC, McDonald JD, Guenet JL, Simon D (1988) hph-1: a mouse mutant with hereditary hyperphenylalaninemia induced by ethylnitrosourea mutagenesis. Genetics 118:299-305.

Bonafe L, Thöny B, Leimbacher W, Kierat L, Blau N (2001) Diagnosis of dopa-responsive dystonia and other tetrahydrobiopterin disorders by the study of biopterin metabolism in fibroblasts. Clinical chemistry 47:477-485.

Bondy CA (1991) Transient IGF-I gene expression during the maturation of functionally related central projection neurons. The Journal of neuroscience : the official journal of the Society for Neuroscience 11:3442-3455.

Bourget L, Chang TM (1986) Phenylalanine ammonia-lyase immobilized in microcapsules for the depletion of phenylalanine in plasma in phenylketonuric rat model. Biochimica et biophysica acta 883:432-438.

Bove J, Prou D, Perier C, Przedborski S (2005) Toxin-induced models of Parkinson's disease. NeuroRx : the journal of the American Society for Experimental NeuroTherapeutics 2:484-494.

Brautigam C, Wevers RA, Jansen RJ, Smeitink JA, de Rijk-van Andel JF, Gabreels FJ, Hoffmann GF (1998) Biochemical hallmarks of tyrosine hydroxylase deficiency. Clinical chemistry 44:1897-1904.

Broekman M, Costa, F., Laryssa, C., Stan L. and Miquel, S.E. (2005) Adeno-Associated Virus Vector Serotype 8 (AAV8) Achieves a Higher Level of Gene Transfer to the Central Nervous System

(CNS) upon Intraventricular Injection in Neonatal Mice Compared to AAV1 and AAV2. Molecular Therapy 11.

Buchman AR, Berg P (1988) Comparison of intron-dependent and intron-independent gene expression. Molecular and cellular biology 8:4395-4405.

Burds Connor A (2007) Auroraôs Guide to Mouse Colony Management at MIT. http://kimitedu/files/ki/cfile/sbc/escell/mouseManagementpdf.

Burton BK, Adams DJ, Grange DK, Malone JI, Jurecki E, Bausell H, Marra KD, Sprietsma L, Swan KT (2011) Tetrahydrobiopterin therapy for phenylketonuria in infants and young children. The Journal of pediatrics 158:410-415.

Butler IJ, O'Flynn ME, Seifert WE, Jr., Howell RR (1981) Neurotransmitter defects and treatment of disorders of hyperphenylalaninemia. The Journal of pediatrics 98:729-733.

Calikoglu A, Karayal A, D'Ercole A (2001) Nutritional regulation of IGF-I expression during brain development in mice. Pediatric research 49:197-202.

Calvo AC, Scherer T, Pey AL, Ying M, Winge I, McKinney J, Haavik J, Thöny B, Martinez A (2010) Effect of pharmacological chaperones on brain tyrosine hydroxylase and tryptophan hydroxylase 2. Journal of neurochemistry 114:853-863.

Camp KM, Lloyd-Puryear MA, Huntington KL (2012) Nutritional treatment for inborn errors of metabolism: indications, regulations, and availability of medical foods and dietary supplements using phenylketonuria as an example. Molecular genetics and metabolism 107:3-9.

Carbery ID, Ji D, Harrington A, Brown V, Weinstein EJ, Liaw L, Cui X (2010) Targeted genome modification in mice using zinc-finger nucleases. Genetics 186:451-459.

Carlson CM, Largaespada DA (2005) Insertional mutagenesis in mice: new perspectives and tools. Nature reviews Genetics 6:568-580.

Carlson DF, Tan W, Lillico SG, Stverakova D, Proudfoot C, Christian M, Voytas DF, Long CR, Whitelaw CB, Fahrenkrug SC (2012) Efficient TALEN-mediated gene knockout in livestock. Proceedings of the National Academy of Sciences of the United States of America 109:17382-17387.

Castaigne P, Rondot P, Ribadeau-Dumas JL, Said G (1971) [Progressive extra-pyramidal disorder in 2 young brothers. Remarkable effects of treatment with L-dopa]. Revue neurologique 124:162-166.

Centerwall SA, Centerwall WR (2000) The discovery of phenylketonuria: the story of a young couple, two retarded children, and a scientist. Pediatrics 105:89-103.

Cerone R, Schiaffino MC, Fantasia AR, Perfumo M, Birk Moller L, Blau N (2004) Long-term follow-up of a patient with mild tetrahydrobiopterin-responsive phenylketonuria. Molecular genetics and metabolism 81:137-139.

Chakrabarty P, Rosario A, Cruz P, Siemienski Z, Ceballos-Diaz C, Crosby K, Jansen K, Borchelt DR, Kim JY, Jankowsky JL, Golde TE, Levites Y (2013) Capsid serotype and timing of injection determines AAV transduction in the neonatal mice brain. PloS one 8:e67680.

Chang TM, Prakash S (1998) Therapeutic uses of microencapsulated genetically engineered cells. Molecular medicine today 4:221-227.

Chen L, Woo SL (2005) Complete and persistent phenotypic correction of phenylketonuria in mice by site-specific genome integration of murine phenylalanine hydroxylase cDNA. Proceedings of the National Academy of Sciences of the United States of America 102:15581-15586.

Chen L, Woo SL (2007) Correction in female PKU mice by repeated administration of mPAH cDNA using phiBT1 integration system. Molecular therapy : the journal of the American Society of Gene Therapy 15:1789-1795.

Chen ZY, He CY, Kay MA (2005) Improved production and purification of minicircle DNA vector free of plasmid bacterial sequences and capable of persistent transgene expression in vivo. Human gene therapy 16:126-131.

Cho A, Haruyama N, Kulkarni AB (2009) Generation of transgenic mice. Current protocols in cell biology / editorial board, Juan S Bonifacino [et al] Chapter 19:Unit 19 11.

Cho A, Haruyama N, Kulkarni AB (2009) Generation of transgenic mice. Current protocols in cell biology / editorial board, Juan S Bonifacino [et al] Chapter 19:Unit 19 11.

Cho S, McDonald JD (2001) Effect of maternal blood phenylalanine level on mouse maternal phenylketonuria offspring. Molecular genetics and metabolism 74:420-425.

Choi JH, Yu NK, Baek GC, Bakes J, Seo D, Nam HJ, Baek SH, Lim CS, Lee YS, Kaang BK (2014) Optimization of AAV expression cassettes to improve packaging capacity and transgene expression in neurons. Molecular brain 7:17.

Christ SE, Moffitt AJ, Peck D, White DA (2013) The effects of tetrahydrobiopterin (BH4) treatment on brain function in individuals with phenylketonuria. NeuroImage Clinical 3:539-547.

Christensen HN (1990) Role of amino acid transport and countertransport in nutrition and metabolism. Physiological reviews 70:43-77.

Chrysis D, Calikoglu AS, Ye P, D'Ercole AJ (2001) Insulin-like growth factor-I overexpression attenuates cerebellar apoptosis by altering the expression of Bcl family proteins in a developmentally specific manner. The Journal of neuroscience : the official journal of the Society for Neuroscience 21:1481-1489.

Cohen FE, Kelly JW (2003) Therapeutic approaches to protein-misfolding diseases. Nature 426:905-909.

Comeron JM, Aguade M (1998) An evaluation of measures of synonymous codon usage bias. Journal of molecular evolution 47:268-274.

Cote F, Thevenot E, Fligny C, Fromes Y, Darmon M, Ripoche MA, Bayard E, Hanoun N, Saurini F, Lechat P, Dandolo L, Hamon M, Mallet J, Vodjdani G (2003) Disruption of the nonneuronal tph1 gene demonstrates the importance of peripheral serotonin in cardiac function. Proceedings of the National Academy of Sciences of the United States of America 100:13525-13530.

Cui X, Ji D, Fisher DA, Wu Y, Briner DM, Weinstein EJ (2011) Targeted integration in rat and mouse embryos with zinc-finger nucleases. Nature biotechnology 29:64-67.

Dane AP, Wowro SJ, Cunningham SC, Alexander IE (2013) Comparison of gene transfer to the murine liver following intraperitoneal and intraportal delivery of hepatotropic AAV pseudo-serotypes. Gene therapy 20:460-464.

Davidoff AM, Ng CY, Zhou J, Spence Y, Nathwani AC (2003) Sex significantly influences transduction of murine liver by recombinant adeno-associated viral vectors through an androgen-dependent pathway. Blood 102:480-488.

de Baulny HO, Abadie V, Feillet F, de Parscau L (2007) Management of phenylketonuria and hyperphenylalaninemia. The Journal of nutrition 137:1561S-1563S; discussion 1573S-1575S.

de Rijk-Van Andel JF, Gabreels FJ, Geurtz B, Steenbergen-Spanjers GC, van Den Heuvel LP, Smeitink JA, Wevers RA (2000) L-dopa-responsive infantile hypokinetic rigid parkinsonism due to tyrosine hydroxylase deficiency. Neurology 55:1926-1928.

De Vry J, Martinez-Martinez P, Losen M, Temel Y, Steckler T, Steinbusch HW, De Baets MH, Prickaerts J (2010) In vivo electroporation of the central nervous system: a non-viral approach for targeted gene delivery. Progress in neurobiology 92:227-244.

Delafontaine P, Song YH, Li Y (2004) Expression, regulation, and function of IGF-1, IGF-1R, and IGF-1 binding proteins in blood vessels. Arteriosclerosis, thrombosis, and vascular biology 24:435-444.

DE Lonlay P, Nassogne MC, van Gennip AH, van Cruchten AC, Billatte de Villemeur T, Cretz M, Stoll C, Launay JM, Steenberger-Spante GC, van den Heuvel LP, Wevers RA, Saudubray JM, Abeling NG (2000) Tyrosine hydroxylase deficiency unresponsive to L-dopa treatment with unusual clinical and biochemical presentation. Journal of inherited metabolic disease 23:819-825.

Desviat LR, Perez B, Belanger-Quintana A, Castro M, Aguado C, Sanchez A, Garcia MJ, Martinez-Pardo M, Ugarte M (2004) Tetrahydrobiopterin responsiveness: results of the BH4 loading test in 31 Spanish PKU patients and correlation with their genotype. Molecular genetics and metabolism 83:157-162.

Ding Z, Georgiev P, Thöny B (2006) Administration-route and gender-independent long-term therapeutic correction of phenylketonuria (PKU) in a mouse model by recombinant adeno-associated virus 8 pseudotyped vector-mediated gene transfer. Gene therapy 13:587-593.

Ding Z, Harding CO, Rebuffat A, Elzaouk L, Wolff JA, Thöny B (2008) Correction of murine PKU following AAV-mediated intramuscular expression of a complete phenylalanine hydroxylating system. Molecular therapy : the journal of the American Society of Gene Therapy 16:673-681.

Donsante A, Miller DG, Li Y, Vogler C, Brunt EM, Russell DW, Sands MS (2007) AAV vector integration sites in mouse hepatocellular carcinoma. Science 317:477.

Donsante A, Vogler C, Muzyczka N, Crawford JM, Barker J, Flotte T, Campbell-Thompson M, Daly T, Sands MS (2001) Observed incidence of tumorigenesis in long-term rodent studies of rAAV vectors. Gene therapy 8:1343-1346.

Drago J, Gerfen CR, Lachowicz JE, Steiner H, Hollon TR, Love PE, Ooi GT, Grinberg A, Lee EJ, Huang SP, et al. (1994) Altered striatal function in a mutant mouse lacking D1A dopamine receptors. Proceedings of the National Academy of Sciences of the United States of America 91:12564-12568.

Dunkley PR, Bobrovskaya L, Graham ME, von Nagy-Felsobuki EI, Dickson PW (2004) Tyrosine hydroxylase phosphorylation: regulation and consequences. Journal of neurochemistry 91:1025-1043.

During MJ, Naegele JR, O'Malley KL, Geller AI (1994) Long-term behavioral recovery in parkinsonian rats by an HSV vector expressing tyrosine hydroxylase. Science 266:1399-1403.

Dymecki SM (1996) Flp recombinase promotes site-specific DNA recombination in embryonic stem cells and transgenic mice. Proceedings of the National Academy of Sciences of the United States of America 93:6191-6196.

Eisensmith RC, Woo SL (1996) Somatic gene therapy for phenylketonuria and other hepatic deficiencies. Journal of inherited metabolic disease 19:412-423.

Elzaouk L, Leimbacher W, Turri M, Ledermann B, Burki K, Blau N, Thöny B (2003) Dwarfism and low insulin-like growth factor-1 due to dopamine depletion in Pts-/- mice rescued by feeding neurotransmitter precursors and H4-biopterin. The Journal of biological chemistry 278:28303-28311.

Erlandsen H, Patch MG, Gamez A, Straub M, Stevens RC (2003) Structural studies on phenylalanine hydroxylase and implications toward understanding and treating phenylketonuria. Pediatrics 112:1557-1565.

Fan DS, Ogawa M, Fujimoto KI, Ikeguchi K, Ogasawara Y, Urabe M, Nishizawa M, Nakano I, Yoshida M, Nagatsu I, Ichinose H, Nagatsu T, Kurtzman GJ, Ozawa K (1998) Behavioral recovery in 6-hydroxydopamine-lesioned rats by cotransduction of striatum with tyrosine hydroxylase and aromatic L-amino acid decarboxylase genes using two separate adeno-associated virus vectors. Human gene therapy 9:2527-2535.

Fang B, Eisensmith RC, Li XH, Finegold MJ, Shedlovsky A, Dove W, Woo SL (1994) Gene therapy for phenylketonuria: phenotypic correction in a genetically deficient mouse model by adenovirus-mediated hepatic gene transfer. Gene therapy 1:247-254.

Fath S, Bauer AP, Liss M, Spriestersbach A, Maertens B, Hahn P, Ludwig C, Schafer F, Graf M, Wagner R (2011) Multiparameter RNA and codon optimization: a standardized tool to assess and enhance autologous mammalian gene expression. PloS one 6:e17596.

Feng G, Lu J, Gross J (2004) Generation of transgenic mice. Methods in molecular medicine 99:255-267.

Ferre S, de Baaij JH, Ferreira P, Germann R, de Klerk JB, Lavrijsen M, van Zeeland F, Venselaar H, Kluijtmans LA, Hoenderop JG, Bindels RJ (2014) Mutations in PCBD1 cause hypomagnesemia and renal magnesium wasting. Journal of the American Society of Nephrology : JASN 25:574-586.

Fitzpatrick PF (2012) Allosteric regulation of phenylalanine hydroxylase. Archives of biochemistry and biophysics 519:194-201.

Flatmark T, Stevens RC (1999) Structural Insight into the Aromatic Amino Acid Hydroxylases and Their Disease-Related Mutant Forms. Chemical reviews 99:2137-2160.

Folling AaC, K. (1938) The appearance of l-phenylalanine in urine and blood during imbecillitas phenylpyrouvica. Hoppe-Seylers Zeitschrift Fur Physiologische Chemie 254: p. 115-116.

Fox JM, Erill I (2010) Relative codon adaptation: a generic codon bias index for prediction of gene expression. DNA research : an international journal for rapid publication of reports on genes and genomes 17:185-196.

Furukawa Y (2003) Genetics and biochemistry of dopa-responsive dystonia: significance of striatal tyrosine hydroxylase protein loss. Advances in neurology 91:401-410.

Furukawa Y, Kish SJ, Fahn S (2004) Dopa-responsive dystonia due to mild tyrosine hydroxylase deficiency. Annals of neurology 55:147-148.

Furukawa Y, Shimadzu M, Rajput AH, Shimizu Y, Tagawa T, Mori H, Yokochi M, Narabayashi H, Hornykiewicz O, Mizuno Y, Kish SJ (1996) GTP-cyclohydrolase I gene mutations in hereditary progressive amd dopa-responsive dystonia. Annals of neurology 39:609-617.

Gamez A, Wang L, Straub M, Patch MG, Stevens RC (2004) Toward PKU enzyme replacement therapy: PEGylation with activity retention for three forms of recombinant phenylalanine hydroxylase. Molecular therapy : the journal of the American Society of Gene Therapy 9:124-129.

Goldstein DS, Eisenhofer G, Kopin IJ (2006) Clinical catecholamine neurochemistry: a legacy of Julius Axelrod. Cellular and molecular neurobiology 26:695-702.

Gordon SL, Bobrovskaya L, Dunkley PR, Dickson PW (2009) Differential regulation of human tyrosine hydroxylase isoforms 1 and 2 in situ: Isoform 2 is not phosphorylated at Ser35. Biochimica et biophysica acta 1793:1860-1867.

Gorecki DC (2006) "Dressed-up" naked plasmids: emerging vectors for non-viral gene therapy. Discovery medicine 6:191-197.

Grieger JC, Choi VW, Samulski RJ (2006) Production and characterization of adeno-associated viral vectors. Nature protocols 1:1412-1428.

Grosjean H, Fiers W (1982) Preferential codon usage in prokaryotic genes: the optimal codon-anticodon interaction energy and the selective codon usage in efficiently expressed genes. Gene 18:199-209.

Gustafsson C, Govindarajan S, Minshull J (2004) Codon bias and heterologous protein expression. Trends in biotechnology 22:346-353.

Guthrie R, Susi A (1963) A Simple Phenylalanine Method for Detecting Phenylketonuria in Large Populations of Newborn Infants. Pediatrics 32:338-343.

Haavik J, Toska K (1998) Tyrosine hydroxylase and Parkinson's disease. Molecular neurobiology 16:285-309.

Haberman BH (1974) Mechanical milk collection from mice for Bittner virus isolation. Laboratory animal science 24:935-937.

Haberman RP K-LG, Samulski RJ (1999) Production of adenoassociated viral vectors. Current Protocols in Human Genetics 12.19.11ï 12.19.17.

Hagstrom JE, Hegge J, Zhang G, Noble M, Budker V, Lewis DL, Herweijer H, Wolff JA (2004) A facile nonviral method for delivering genes and siRNAs to skeletal muscle of mammalian limbs. Molecular therapy : the journal of the American Society of Gene Therapy 10:386-398.

Harding CO, Gillingham MB, Hamman K, Clark H, Goebel-Daghighi E, Bird A, Koeberl DD (2006) Complete correction of hyperphenylalaninemia following liver-directed, recombinant AAV2/8 vector-mediated gene therapy in murine phenylketonuria. Gene therapy 13:457-462.

Hasbrouck NC, High KA (2008) AAV-mediated gene transfer for the treatment of hemophilia B: problems and prospects. Gene therapy 15:870-875.

He X, Lee, K. Y., Li, Lh., Meller, E.,Goldstein, M. (1996) Relationship between enzymatic activity and oligomerization state oftyrosine hydroxylase. J Biomed Sci 3:332-337.

Heintz C, Troxler H, Martinez A, Thöny B, Blau N (2012) Quantification of phenylalanine hydroxylase activity by isotope-dilution liquid chromatography-electrospray ionization tandem mass spectrometry. Molecular genetics and metabolism 105:559-565.

Hennermann JB, Buhrer C, Blau N, Vetter B, Monch E (2005) Long-term treatment with tetrahydrobiopterin increases phenylalanine tolerance in children with severe phenotype of phenylketonuria. Molecular genetics and metabolism 86 Suppl 1:S86-90.

Herschkowitz N (1982) Inborn Errors of Metabolism in Humans: Inborn errors of metabolism affecting brain development ð Introduction. Springer Verlag pp 157-160.

Hiroi R, McDevitt RA, Neumaier JF (2006) Estrogen selectively increases tryptophan hydroxylase-2 mRNA expression in distinct subregions of rat midbrain raphe nucleus: association between gene expression and anxiety behavior in the open field. Biological psychiatry 60:288-295.

Ho G, Reichardt J, Christodoulou J (2013) In vitro read-through of phenylalanine hydroxylase (PAH) nonsense mutations using aminoglycosides: a potential therapy for phenylketonuria. Journal of inherited metabolic disease 36:955-959.

Hoffmann GF, Assmann B, Brautigam C, Dionisi-Vici C, Haussler M, de Klerk JB, Naumann M, Steenbergen-Spanjers GC, Strassburg HM, Wevers RA (2003) Tyrosine hydroxylase deficiency causes progressive encephalopathy and dopa-nonresponsive dystonia. Annals of neurology 54 Suppl 6:S56-65.

Hofker MH, Breuer M (1998) Generation of transgenic mice. Methods in molecular biology 110:63-78.

Hollon TR, Bek MJ, Lachowicz JE, Ariano MA, Mezey E, Ramachandran R, Wersinger SR, Soares-da-Silva P, Liu ZF, Grinberg A, Drago J, Young WS, 3rd, Westphal H, Jose PA, Sibley DR (2002) Mice lacking D5 dopamine receptors have increased sympathetic tone and are hypertensive. The Journal of neuroscience : the official journal of the Society for Neuroscience 22:10801-10810.

Horellou P, Vigne E, Castel MN, Barneoud P, Colin P, Perricaudet M, Delaere P, Mallet J (1994) Direct intracerebral gene transfer of an adenoviral vector expressing tyrosine hydroxylase in a rat model of Parkinson's disease. Neuroreport 6:49-53.

Horellou P, Vigne E, Castel MN, Barneoud P, Perricaudet M, Delaere P, Mallet J (1995) Transplantation of cells genetically modified and direct intracerebral gene transfer with an adenoviral vector expressing tyrosine hydroxylase in a rat model of Parkinson's disease. Restorative neurology and neuroscience 8:63.

Hoskins JA, Holliday SB, Greenway AM (1984) The metabolism of cinnamic acid by healthy and phenylketonuric adults: a kinetic study. Biomedical mass spectrometry 11:296-300.

Hoskins JA, Jack G, Wade HE, Peiris RJ, Wright EC, Starr DJ, Stern J (1980) Enzymatic control of phenylalanine intake in phenylketonuria. Lancet 1:392-394.

Houdebine LM (2002) The methods to generate transgenic animals and to control transgene expression. Journal of biotechnology 98:145-160.

Hutchins B (2000) Characterization of plasmids and formulations for non-viral gene therapy. Current opinion in molecular therapeutics 2:131-135.

Hyland K (1999) Presentation, diagnosis, and treatment of the disorders of monoamine neurotransmitter metabolism. Seminars in perinatology 23:194-203.

Hyland K, Gunasekara RS, Munk-Martin TL, Arnold LA, Engle T (2003) The hph-1 mouse: a model for dominantly inherited GTP-cyclohydrolase deficiency. Annals of neurology 54 Suppl 6:S46-48.

Ievers-Landis CE, Hoff AL, Brez C, Cancilliere MK, McConnell J, Kerr D (2005) Situational analysis of dietary challenges of the treatment regimen for children and adolescents with phenylketonuria and their primary caregivers. Journal of developmental and behavioral pediatrics : JDBP 26:186-193.

Ittner LM, Gotz J (2007) Pronuclear injection for the production of transgenic mice. Nature protocols 2:1206-1215.

Iwata N, Sekiguchi M, Hattori Y, Takahashi A, Asai M, Ji B, Higuchi M, Staufenbiel M, Muramatsu S, Saido TC (2013) Global brain delivery of neprilysin gene by intravascular administration of AAV vector in mice. Scientific reports 3:1472.

Jaber M, Robinson SW, Missale C, Caron MG (1996) Dopamine receptors and brain function. Neuropharmacology 35:1503-1519.

Jaenisch R, Mintz B (1974) Simian virus 40 DNA sequences in DNA of healthy adult mice derived from preimplantation blastocysts injected with viral DNA. Proceedings of the National Academy of Sciences of the United States of America 71:1250-1254.

Jang YC, Sinha M, Cerletti M, Dall'Osso C, Wagers AJ (2011) Skeletal muscle stem cells: effects of aging and metabolism on muscle regenerative function. Cold Spring Harbor symposia on quantitative biology 76:101-111.

Jervis GA (1953) Phenylpyruvic oligophrenia deficiency of phenylalanine-oxidizing system. Proceedings of the Society for Experimental Biology and Medicine Society for Experimental Biology and Medicine 82:514-515.

Kato T, Miyata K, Sonobe M, Yamashita S, Tamano M, Miura K, Kanai Y, Miyamoto S, Sakuma T, Yamamoto T, Inui M, Kikusui T, Asahara H, Takada S (2013) Production of Sry knockout mouse using TALEN via oocyte injection. Scientific reports 3:3136.

Kaufman S (1958) A new cofactor required for the enzymatic conversion of phenylalanine to tyrosine. The Journal of biological chemistry 230:931-939.

Kay MA, He CY, Chen ZY (2010) A robust system for production of minicircle DNA vectors. Nature biotechnology 28:1287-1289.

Kim DS, Szczypka MS, Palmiter RD (2000) Dopamine-deficient mice are hypersensitive to dopamine receptor agonists. The Journal of neuroscience : the official journal of the Society for Neuroscience 20:4405-4413.

Kim JY, Ash RT, Ceballos-Diaz C, Levites Y, Golde TE, Smirnakis SM, Jankowsky JL (2013) Viral transduction of the neonatal brain delivers controllable genetic mosaicism for visualising and manipulating neuronal circuits in vivo. The European journal of neuroscience 37:1203-1220.

Klein R, Ruttkowski B, Knapp E, Salmons B, Gunzburg WH, Hohenadl C (2006) WPRE-mediated enhancement of gene expression is promoter and cell line specific. Gene 372:153-161.

Kobayashi K, Morita S, Sawada H, Mizuguchi T, Yamada K, Nagatsu I, Hata T, Watanabe Y, Fujita K, Nagatsu T (1995) Targeted disruption of the tyrosine hydroxylase locus results in severe

catecholamine depletion and perinatal lethality in mice. The Journal of biological chemistry 270:27235-27243.

Korner GaS, T., Rozman, J., , Adamsen, D., Rassi, A. , Scavelli, R., Homma, D. , Ledermann, B., Konrad, D., Ichinose, H. , Wolfrum, C. , Blau, N. and Thöny B. (2014) Mildly compromised tetrahydrobiopterin biosynthesis mouse mutants exhibit abnormal body fat distribution and abdominal obesity (in preparation).

Kure S, Hou DC, Ohura T, Iwamoto H, Suzuki S, Sugiyama N, Sakamoto O, Fujii K, Matsubara Y, Narisawa K (1999) Tetrahydrobiopterin-responsive phenylalanine hydroxylase deficiency. The Journal of pediatrics 135:375-378.

Lagler FB, Gersting SW, Zsifkovits C, Steinbacher A, Eichinger A, Danecka MK, Staudigl M, Fingerhut R, Glossmann H, Muntau AC (2010) New insights into tetrahydrobiopterin pharmacodynamics from Pah enu1/2, a mouse model for compound heterozygous tetrahydrobiopterin-responsive phenylalanine hydroxylase deficiency. Biochemical pharmacology 80:1563-1571.

Lang F (2009) Encyclopedia of Molecular Mechanisms of Disease. Springer-Verlag GmbH Berlin Heidelberg Band 3:925.

Lee YW, Lee DH, Kim ND, Lee ST, Ahn JY, Choi TY, Lee YK, Kim SH, Kim JW, Ki CS (2008) Mutation analysis of PAH gene and characterization of a recurrent deletion mutation in Korean patients with phenylketonuria. Experimental & molecular medicine 40:533-540.

Lenzi G, Pistone D, Zammarchi E, Benini MP, La Torre A, Matteoni D (1989) DHPR activity decrease in dried blood spots stored at 4 degrees C. Enzyme 41:43-46.

Lewis DA, Melchitzky DS, Haycock JW (1993) Four isoforms of tyrosine hydroxylase are expressed in human brain. Neuroscience 54:477-492.

Lim E, Modi KD, Kim J (2009) In vivo bioluminescent imaging of mammary tumors using IVIS spectrum. Journal of visualized experiments : JoVE.

Livak KJ, Schmittgen TD (2001) Analysis of relative gene expression data using real-time quantitative PCR and the 2(-Delta Delta C(T)) Method. Methods 25:402-408.

Lowry CA, Hale MW, Evans AK, Heerkens J, Staub DR, Gasser PJ, Shekhar A (2008) Serotonergic systems, anxiety, and affective disorder: focus on the dorsomedial part of the dorsal raphe nucleus. Annals of the New York Academy of Sciences 1148:86-94.

Lu J, Zhang F, Xu S, Fire AZ, Kay MA (2012) The extragenic spacer length between the 5' and 3' ends of the transgene expression cassette affects transgene silencing from plasmid-based vectors. Molecular therapy : the journal of the American Society of Gene Therapy 20:2111-2119.

Madathil SK, Carlson SW, Brelsfoard JM, Ye P, D'Ercole AJ, Saatman KE (2013) Astrocyte-Specific Overexpression of Insulin-Like Growth Factor-1 Protects Hippocampal Neurons and Reduces Behavioral Deficits following Traumatic Brain Injury in Mice. PloS one 8:e67204.

Martynyuk AE, Ucar DA, Yang DD, Norman WM, Carney PR, Dennis DM, Laipis PJ (2007) Epilepsy in phenylketonuria: a complex dependence on serum phenylalanine levels. Epilepsia 48:1143-1150.

Matalon R, Michals K (1991) Phenylketonuria: screening, treatment and maternal PKU. Clinical biochemistry 24:337-342.

McDonald JD, Andriolo M, Cali F, Mirisola M, Puglisi-Allegra S, Romano V, Sarkissian CN, Smith CB (2002) The phenylketonuria mouse model: a meeting review. Molecular genetics and metabolism 76:256-261.

McDonald JD, Bode VC, Dove WF, Shedlovsky A (1990) The use of N-ethyl-N-nitrosourea to produce mouse models for human phenylketonuria and hyperphenylalaninemia. Progress in clinical and biological research 340C:407-413.

McDonnald D (2006) The genetic mouse model for PKU. PKU and BH4: Advances in Phenylketonuria and Tetrahydrobiopterin Nenad Blau (Ed):SHS Publications, Heilbronn, Germany.

Mendel DB, Khavari PA, Conley PB, Graves MK, Hansen LP, Admon A, Crabtree GR (1991) Characterization of a cofactor that regulates dimerization of a mammalian homeodomain protein. Science 254:1762-1767.

Metzger D, Chambon P (2001) Site- and time-specific gene targeting in the mouse. Methods 24:71-80.

Metzger D, Pezier TF, Veraguth D (2013) Evaluation of universal newborn hearing screening in Switzerland 2012 and follow-up data for Zurich. Swiss medical weekly 143:w13905.

Meyburg J, Hoffmann GF (2008) Liver cell transplantation for the treatment of inborn errors of metabolism. Journal of inherited metabolic disease 31:164-172.

Mochizuki S, Mizukami H, Ogura T, Kure S, Ichinohe A, Kojima K, Matsubara Y, Kobayahi E, Okada T, Hoshika A, Ozawa K, Kume A (2004) Long-term correction of hyperphenylalaninemia by AAV-mediated gene transfer leads to behavioral recovery in phenylketonuria mice. Gene therapy 11:1081-1086.

Molnar MJ, Gilbert R, Lu Y, Liu AB, Guo A, Larochelle N, Orlopp K, Lochmuller H, Petrof BJ, Nalbantoglu J, Karpati G (2004) Factors influencing the efficacy, longevity, and safety of electroporation-assisted plasmid-based gene transfer into mouse muscles. Molecular therapy : the journal of the American Society of Gene Therapy 10:447-455.

Morello JP, Petaja-Repo UE, Bichet DG, Bouvier M (2000) Pharmacological chaperones: a new twist on receptor folding. Trends in pharmacological sciences 21:466-469.

Mosharov EV, Larsen KE, Kanter E, Phillips KA, Wilson K, Schmitz Y, Krantz DE, Kobayashi K, Edwards RH, Sulzer D (2009) Interplay between cytosolic dopamine, calcium, and alpha-synuclein causes selective death of substantia nigra neurons. Neuron 62:218-229.

Nagasaki Y, Matsubara Y, Takano H, Fujii K, Senoo M, Akanuma J, Takahashi K, Kure S, Hara M, Kanegae Y, Saito I, Narisawa K (1999) Reversal of hypopigmentation in phenylketonuria mice by adenovirus-mediated gene transfer. Pediatric research 45:465-473.

Nagatsu T (1995) Tyrosine hydroxylase: human isoforms, structure and regulation in physiology and pathology. Essays in biochemistry 30:15-35.

Netchine I, Azzi S, Houang M, Seurin D, Perin L, Ricort JM, Daubas C, Legay C, Mester J, Herich R, Godeau F, Le Bouc Y (2009) Partial primary deficiency of insulin-like growth factor (IGF)-I activity associated with IGF1 mutation demonstrates its critical role in growth and brain development. The Journal of clinical endocrinology and metabolism 94:3913-3921.

Oppliger T, Thöny B, Nar H, Burgisser D, Huber R, Heizmann CW, Blau N (1995) Structural and functional consequences of mutations in 6-pyruvoyltetrahydropterin synthase causing

hyperphenylalaninemia in humans. Phosphorylation is a requirement for in vivo activity. The Journal of biological chemistry 270:29498-29506.

Palmiter RD, Sandgren EP, Avarbock MR, Allen DD, Brinster RL (1991) Heterologous introns can enhance expression of transgenes in mice. Proceedings of the National Academy of Sciences of the United States of America 88:478-482.

Passini MA, Watson DJ, Vite CH, Landsburg DJ, Feigenbaum AL, Wolfe JH (2003) Intraventricular brain injection of adeno-associated virus type 1 (AAV1) in neonatal mice results in complementary patterns of neuronal transduction to AAV2 and total long-term correction of storage lesions in the brains of beta-glucuronidase-deficient mice. Journal of virology 77:7034-7040.

Patel PD, Pontrello C, Burke S (2004) Robust and tissue-specific expression of TPH2 versus TPH1 in rat raphe and pineal gland. Biological psychiatry 55:428-433.

Penrose L (1935) Inheritance of phenylpyruvic amentia (phenylketonuria. Lancet Volume 2:pp 192-194.

Pinkert CA (2014) Transgenic Animal Technology: A Laboratory Handbook. Elsevier third edition.

Rahim AA, Wong AM, Hoefer K, Buckley SM, Mattar CN, Cheng SH, Chan JK, Cooper JD, Waddington SN (2011) Intravenous administration of AAV2/9 to the fetal and neonatal mouse leads to differential targeting of CNS cell types and extensive transduction of the nervous system. FASEB journal : official publication of the Federation of American Societies for Experimental Biology 25:3505-3518.

Rashed MS, Ozand PT, Bucknall MP, Little D. Diagnosis of inborn errors of metabolism from blood spots by acylcarnitines and amino acids profiling using automated electrospray tandem mass spectrometry. *Pediatr Res* 1995; **38**(3)**:** 324-31.

Rebuffat A, Harding CO, Ding Z, Thöny B (2010) Comparison of adeno-associated virus pseudotype 1, 2, and 8 vectors administered by intramuscular injection in the treatment of murine phenylketonuria. Human gene therapy 21:463-477.

Saito T (2006) In vivo electroporation in the embryonic mouse central nervous system. Nature protocols 1:1552-1558.

Sarkissian CN, Gamez A (2005) Phenylalanine ammonia lyase, enzyme substitution therapy for phenylketonuria, where are we now? Molecular genetics and metabolism 86 Suppl 1:S22-26.

Sarkissian CN, Shao Z, Blain F, Peevers R, Su H, Heft R, Chang TM, Scriver CR (1999) A different approach to treatment of phenylketonuria: phenylalanine degradation with recombinant phenylalanine ammonia lyase. Proceedings of the National Academy of Sciences of the United States of America 96:2339-2344.

Satya RV, Mukherjee A, Ranga U (2003) A pattern matching algorithm for codon optimization and CpG motif-engineering in DNA expression vectors. Proceedings / IEEE Computer Society Bioinformatics Conference IEEE Computer Society Bioinformatics Conference 2:294-305.

Scavelli R (2006) Tetrahydrobiopterin Metabolism in the Mouse: Feeding Studies and Generation of a New Mutant Model. Dissertation; University of Zurich.

Schertzer JD, Lynch GS (2008) Plasmid-based gene transfer in mouse skeletal muscle by electroporation. Methods in molecular biology 433:115-125.

Schiller A, Wevers RA, Steenbergen GC, Blau N, Jung HH (2004) Long-term course of L-dopa-responsive dystonia caused by tyrosine hydroxylase deficiency. Neurology 63:1524-1526.

Schmidt A, Marescau B, Boehm EA, Renema WK, Peco R, Das A, Steinfeld R, Chan S, Wallis J, Davidoff M, Ullrich K, Waldschutz R, Heerschap A, De Deyn PP, Neubauer S, Isbrandt D (2004) Severely altered guanidino compound levels, disturbed body weight homeostasis and impaired fertility in a mouse model of guanidinoacetate N-methyltransferase (GAMT) deficiency. Human molecular genetics 13:905-921.

Segawa H, Fukasawa Y, Miyamoto K, Takeda E, Endou H, Kanai Y (1999) Identification and functional characterization of a Na+-independent neutral amino acid transporter with broad substrate selectivity. The Journal of biological chemistry 274:19745-19751.

Shedlovsky A, McDonald JD, Symula D, Dove WF (1993) Mouse models of human phenylketonuria. Genetics 134:1205-1210.

Shen Y, Muramatsu SI, Ikeguchi K, Fujimoto KI, Fan DS, Ogawa M, Mizukami H, Urabe M, Kume A, Nagatsu I, Urano F, Suzuki T, Ichinose H, Nagatsu T, Monahan J, Nakano I, Ozawa K (2000) Triple transduction with adeno-associated virus vectors expressing tyrosine hydroxylase, aromatic-L-amino-acid decarboxylase, and GTP cyclohydrolase I for gene therapy of Parkinson's disease. Human gene therapy 11:1509-1519.

Shih DQ, Screenan S, Munoz KN, Philipson L, Pontoglio M, Yaniv M, Polonsky KS, Stoffel M (2001) Loss of HNF-1alpha function in mice leads to abnormal expression of genes involved in pancreatic islet development and metabolism. Diabetes 50:2472-2480.

Shintaku H (2002) Disorders of tetrahydrobiopterin metabolism and their treatment. Current drug metabolism 3:123-131.

Stenler S, Wiklander OP, Badal-Tejedor M, Turunen J, Nordin JZ, Hallengard D, Wahren B, Andaloussi SE, Rutland MW, Smith CE, Lundin KE, Blomberg P (2014) Micro-minicircle Gene Therapy: Implications of Size on Fermentation, Complexation, Shearing Resistance, and Expression. Molecular therapy Nucleic acids 2:e140.

Stratikopoulos E, Szabolcs M, Dragatsis I, Klinakis A, Efstratiadis A (2008) The hormonal action of IGF1 in postnatal mouse growth. Proceedings of the National Academy of Sciences of the United States of America 105:19378-19383.

Sumi-Ichinose C, Urano F, Kuroda R, Ohye T, Kojima M, Tazawa M, Shiraishi H, Hagino Y, Nagatsu T, Nomura T, Ichinose H (2001) Catecholamines and serotonin are differently regulated by tetrahydrobiopterin. A study from 6-pyruvoyltetrahydropterin synthase knockout mice. The Journal of biological chemistry 276:41150-41160.

Swoboda KJ, Furukawa Y (1993) Tyrosine Hydroxylase Deficiency. In: GeneReviews(R) (Pagon, R. A. et al., eds) Seattle (WA).

Szentivanyi K, Hansikova H, Krijt J, Vinsova K, Tesarova M, Rozsypalova E, Klement P, Zeman J, Honzik T (2012) Novel mutations in the tyrosine hydroxylase gene in the first Czech patient with tyrosine hydroxylase deficiency. Prague medical report 113:136-146.

Templeton NS (2005) Gene and Cell Therapy: Therapeutic Mechanisms and Strategies. Taylor and Francis e-Library Second Edition.

Thöny B (2010) Long-term correction of murine phenylketonuria by viral gene transfer: liver versus muscle. Journal of inherited metabolic disease 33:677-680.

Thöny B, Auerbach G, Blau N (2000) Tetrahydrobiopterin biosynthesis, regeneration and functions. The Biochemical journal 347 Pt 1:1-16.

Thöny B, Auerbach G, Blau N (2000) Tetrahydrobiopterin biosynthesis, regeneration and functions. Biochem J 347 Pt 1:1-16.

Thöny B, Blau N (2006) Mutations in the BH4-metabolizing genes GTP cyclohydrolase I, 6-pyruvoyl-tetrahydropterin synthase, sepiapterin reductase, carbinolamine-4a-dehydratase, and dihydropteridine reductase. Human mutation 27:870-878.

Thöny B, Calvo AC, Scherer T, Svebak RM, Haavik J, Blau N, Martinez A (2008) Tetrahydrobiopterin shows chaperone activity for tyrosine hydroxylase. Journal of neurochemistry 106:672-681.

Thöny B, Heizmann CW, Mattei MG (1994) Chromosomal location of two human genes encoding tetrahydrobiopterin-metabolizing enzymes: 6-pyruvoyl-tetrahydropterin synthase maps to 11q22.3-q23.3, and pterin-4 alpha-carbinolamine dehydratase maps to 10q22. Genomics 19:365-368.

Trugman JM, James CL, Wooten GF (1991) D1/D2 dopamine receptor stimulation by L-dopa. A [14C]-2-deoxyglucose autoradiographic study. Brain : a journal of neurology 114 (Pt 3):1429-1440.

Tsai YS TP, Jiang MJ, Chang CS (2007) Designer mice for human disease - A close view of Nobel Laureate : Oliver Smithies. http://projnckuedutw/research/ commentary/e/ 20071116/2html Volume 2.

van Spronsen FJ, Hoeksma M, Reijngoud DJ (2009) Brain dysfunction in phenylketonuria: is phenylalanine toxicity the only possible cause? Journal of inherited metabolic disease 32:46-51.

Viecelli HM, Harbottle RP, Wong SP, Schlegel A, Chuah MK, Vandendriessche T, Harding CO, Thöny B (2014) Treatment of phenylketonuria using minicircle-based naked-DNA gene transfer to murine liver. Hepatology 60:1035-1043.

Viola JR, El-Andaloussi S, Oprea, II, Smith CI Non-viral nanovectors for gene delivery: factors that govern successful therapeutics. Expert Opin Drug Deliv 7:721-735.

von Jonquieres G, Mersmann N, Klugmann CB, Harasta AE, Lutz B, Teahan O, Housley GD, Frohlich D, Kramer-Albers EM, Klugmann M (2013) Glial promoter selectivity following AAV-delivery to the immature brain. PloS one 8:e65646.

Voytek B, Knight RT (2010) Prefrontal cortex and basal ganglia contributions to visual working memory. Proceedings of the National Academy of Sciences of the United States of America 107:18167-18172.

Waisbren S, White DA (2010) Screening for cognitive and social-emotional problems in individuals with PKU: tools for use in the metabolic clinic. Molecular genetics and metabolism 99 Suppl 1:S96-99.

Walther DJ, Bader M (2003) A unique central tryptophan hydroxylase isoform. Biochemical pharmacology 66:1673-1680.

Wang H, Yang H, Shivalila CS, Dawlaty MM, Cheng AW, Zhang F, Jaenisch R (2013) One-step generation of mice carrying mutations in multiple genes by CRISPR/Cas-mediated genome engineering. Cell 153:910-918.

Watschinger K, Keller MA, Golderer G, Hermann M, Maglione M, Sarg B, Lindner HH, Hermetter A, Werner-Felmayer G, Konrat R, Hulo N, Werner ER (2010) Identification of the gene encoding alkylglycerol monooxygenase defines a third class of tetrahydrobiopterin-dependent enzymes. Proceedings of the National Academy of Sciences of the United States of America 107:13672-13677.

Wei CC, Crane BR, Stuehr DJ (2003) Tetrahydrobiopterin radical enzymology. Chemical reviews 103:2365-2383.

Weinmann A, Post M, Pan J, Rafi M, O'Connor DL, Unger S, Pencharz P, Belik J (2011) Tetrahydrobiopterin is present in high quantity in human milk and has a vasorelaxing effect on newborn rat mesenteric arteries. Pediatric research 69:325-329.

Werner ER, Gorren AC, Heller R, Werner-Felmayer G, Mayer B (2003) Tetrahydrobiopterin and nitric oxide: mechanistic and pharmacological aspects. Experimental biology and medicine 228:1291-1302.

Wevers RA, de Rijk-van Andel JF, Brautigam C, Geurtz B, van den Heuvel LP, Steenbergen-Spanjers GC, Smeitink JA, Hoffmann GF, Gabreels FJ (1999) A review of biochemical and molecular genetic aspects of tyrosine hydroxylase deficiency including a novel mutation (291delC). Journal of inherited metabolic disease 22:364-373.

Willemsen MA, Verbeek MM, Kamsteeg EJ, de Rijk-van Andel JF, Aeby A, Blau N, Burlina A, Donati MA, Geurtz B, Grattan-Smith PJ, Haeussler M, Hoffmann GF, Jung H, de Klerk JB, van der Knaap MS, Kok F, Leuzzi V, de Lonlay P, Megarbane A, Monaghan H, Renier WO, Rondot P, Ryan MM, Seeger J, Smeitink JA, Steenbergen-Spanjers GC, Wassmer E, Weschke B, Wijburg FA, Wilcken B, Zafeiriou DI, Wevers RA (2010) Tyrosine hydroxylase deficiency: a treatable disorder of brain catecholamine biosynthesis. Brain : a journal of neurology 133:1810-1822.

Williams RA, Mamotte CD, Burnett JR (2008) Phenylketonuria: an inborn error of phenylalanine metabolism. The Clinical biochemist Reviews / Australian Association of Clinical Biochemists 29:31-41.

Woo SL (2010) Retraction for Chen et al., Complete and persistent phenotypic correction of phenylketonuria in mice by site-specific genome integration of murine phenylalanine hydroxylase cDNA. Proceedings of the National Academy of Sciences of the United States of America 107:14514.

Yagi H, Ogura T, Mizukami H, Urabe M, Hamada H, Yoshikawa H, Ozawa K, Kume A (2011) Complete restoration of phenylalanine oxidation in phenylketonuria mouse by a self-complementary adeno-associated virus vector. The journal of gene medicine 13:114-122.

Yanagida O, Kanai Y, Chairoungdua A, Kim DK, Segawa H, Nii T, Cha SH, Matsuo H, Fukushima J, Fukasawa Y, Tani Y, Taketani Y, Uchino H, Kim JY, Inatomi J, Okayasu I, Miyamoto K, Takeda E, Goya T, Endou H (2001) Human L-type amino acid transporter 1 (LAT1): characterization of function and expression in tumor cell lines. Biochimica et biophysica acta 1514:291-302.

Yang S, Lee YJ, Kim JM, Park S, Peris J, Laipis P, Park YS, Chung JH, Oh SP (2006) A murine model for human sepiapterin-reductase deficiency. American journal of human genetics 78:575-587.

Yang XJ, Kaufman S (1994) High-level expression and deletion mutagenesis of human tryptophan hydroxylase. Proceedings of the National Academy of Sciences of the United States of America 91:6659-6663.

Zhang G, Wooddell CI, Hegge JO, Griffin JB, Huss T, Braun S, Wolff JA (2010) Functional efficacy of dystrophin expression from plasmids delivered to mdx mice by hydrodynamic limb vein injection. Human gene therapy 21:221-237.

Zhang Y, Calon F, Zhu C, Boado RJ, Pardridge WM (2003) Intravenous nonviral gene therapy causes normalization of striatal tyrosine hydroxylase and reversal of motor impairment in experimental parkinsonism. Human gene therapy 14:1-12.

Zhang Y, Schlachetzki F, Zhang YF, Boado RJ, Pardridge WM (2004) Normalization of striatal tyrosine hydroxylase and reversal of motor impairment in experimental parkinsonism with intravenous nonviral gene therapy and a brain-specific promoter. Human gene therapy 15:339-350.

Zhou QY, Palmiter RD (1995) Dopamine-deficient mice are severely hypoactive, adipsic, and aphagic. Cell 83:1197-1209.

Zhou QY, Quaife CJ, Palmiter RD (1995) Targeted disruption of the tyrosine hydroxylase gene reveals that catecholamines are required for mouse fetal development. Nature 374:640-643.

7. Acknowledgments

My cordial thanks belong to my supervisor Prof. Dr. Beat Thöny, who offered me these interesting variegated projects. Thanks to him I could not only develop my technical skills but also grow as a person. Due to his encouragements, I also had the possibility to present my work to several international conferences. Thank you so much for four exciting years of research, for your trust in me and all your support.

My deepest thanks also go to my dear colleague and friend Dr. Tanja Scherer. She was not only always very supportive and encouraged me, but also inspired me in my research work. I appreciate the collaboration we had. Thank you so much for being there for me and for your friendship.

To my colleague Dr. Hiu Man Viecelli I like to thank for being a reliable colleague who provided me her knowledge and help whenever she could.

To Dr. Gabriella Allegri I would like to thank for the great team-work and all your support in this thesis.

Special thanks also to Anahita Rassi, who always spoke up for my projects and took her precious time to support me.

I also want to express my gratefulness to all my former lab colleagues who supported me during my PhD-thesis and gave me a good time in the lab: Dr. Caroline Heintz, Dr. Dea Adamsen, Merima Mustedanagic and Simona Schäfer.

Furthermore, I would like to thank all the people of the division of metabolism, the division of clinical chemistry and biochemistry, the protein hormone laboratory and newborns screening, and the animal facility of the UZH, Irchel and Frühlingsdorf for all their support.

I also thank the international collaborators, Prof. Dr. Aurora Martinez and Ming Ying, Prof. Dr. Cary O. Harding and Dr. Shelley Winn, and Prof. Dr. Lars Aagaard and his team.

Many thanks also to Prof. Dr. François Verrey and Prof. Dr. Isabelle Mansuy for being my committee members and taken their time for supervise my PhD thesis.

Finally, I want to thank my wonderful and supportive family.

Thanks to you all, I loved every single working day and I regret that this time went over so fast.

8. Curriculum vitae

Personal Information:

Name:	Germaine Korner
Address:	Stollberghalde 2, 6003 Lucerne
Tel:	+41 041 240 91 74
E-Mail:	germaine.korner@gmx.ch
Date of birth:	16.11.1986
Born:	Zurich, Switzerland
Nationality:	Swiss

Education:

06.2010-09.2014	**PhD in Genetics at the University of Zurich** PhD thesis: ñPhenotypical and Therapeutic Studies in Genetic Mouse Models for Inherited Neurotransmitter Disordersò performed at the University Childrenôs Hospital of Zurich (Switzerland), Division of Metabolism under supervision of Prof. Dr. Beat Thöny
PhD-program	ZNZ International Ph.D. Program in Neuroscience ZNZ fellowship
11.2008-01.2010	**M.Sc. in Genetics at the University of Zurich** Master thesis ñ*Studies on the Therapeutic Potential of U1 snRNA to Rescue Splice Defects*òperformed at the Institute of Medical Molecular Genetics in Schwerzenbach (Switzerland) under supervision of Dr. John Neidhardt and Prof. Dr. Wolfgang Berger
09.2005-11.2008	**Bachelor in Biology at the University of Zurich**
08.2001-06.2005	**Matura at the Kantonsschule Alpenquai in Lucerne** (Switzerland)

Papers:

- Korner and Scherer et al, Abnormal body fat distribution and abdominal obesity in mouse mutant with mildly compromised tetrahydrobiopterin cofactor biosynthesis (submitted).

- Korner et al, Progressive catecholamine depletion and severely impaired motor control in a hypomorphic tyrosine hydroxylase knock-in (*Th*-ki) mouse (in preparation).

Oral presentations:

- **15th International Symposium on Pteridines and Folates, Antalya, Turkey, May 2012**

ñNovel mouse models for BH_4 deficiency by targeting the 6-pyruvoyltetrahydropterin synthase gene *Pts*ò

- **International Conference on Tetrahydrobiopterin, Phenylketonuria, Monoamine Neurotransmitters and Nitric Oxide Synthase, St. Moritz - Champfèr, Switzerland, March 2013**

ñCharacterization and treatment studies of the *Th*-ki mouse: a model for TH deficiencyò

ñA murine *Pts* mouse model to study its role in BH_4 deficiency and monoamine neurotransmitter function and contribution to human diseaseò

- **12th International Congress of Inborn Errors of Metabolism, Barcelona, Spain, September 2013**

ñA novel tyrosine hydroxylase knock-in (*Th*-ki) mouse as a model for brain catecholamine deficiencyò

- **3rd Forschungszentrum für das Kind (FZK)/Childrenôs Research Center (CRC) Retreat, Halbinsel Au, Switzerland, October 2013**

ñTyrosine hydroxylase knock-in (*Th*-ki) mice show brain catecholamine depletion and impaired motor control, and replicate the severe form of L-Dopa non-responsive dystoniaò

- 10th Symposium of the Zurich Center for Integrative Human Physiology (ZIHP), Zurich, Switzerland, August 2014

ñA tyrosine hydroxylase (TH) knock-in mouse with catecholamine depletion and impaired motor control replicates a severe form of L-Dopa TH deficiencyò

Poster presentations:

- Zentrum für Neurowissenschaften Zürich (ZNZ) Symposium 2011, Zurich, Switzerland, September 2011

ñExperimental gene therapy to correct PTPS/BH_4-cofactor and brain neurotransmitter deficiency in Pts-ki/ko mice by targeting the liverò

- **Society for the Study of Inborn Errors of Metabolism (SSIEM) Annual Symposium, Geneva, Switzerland, August-September 2011**

"Experimental gene therapy to correct PTPS/BH_4-cofactor and brain neurotransmitter deficiency in Pts-ki/ko mice by targeting the liver"

- **1st FZK/CRC Retreat, Halbinsel Au, Switzerland, October 2011**

ñAAV2/8 to target the liver for correction of hepatic BH_4 and brain monoamine neurotransmitter deficiency in a *Pts*-ki/ko mouse modelò

- **European Society of Gene and Cell Therapy (ESGCT) Congress, Brighton, United Kingdom, October 2011**

"AAV2/8 to target the liver for correction of hepatic BH_4 and brain neurotransmitter deficiency in *Pts*-ki/ko mouse model"

- **ZNZ and NCCR NEURO JOINT SYMPOSIUM, Zurich, Switzerland, June 2012**

ñViral versus non-viral gene therapy to correct PKU in *Pah*^{enu2} mice by targeting skeletal muscleò

- **2nd FZK/CRC Retreat, Halbinsel Au, Switzerland, October 2012**

"A murine *Pts* mouse model to study its role in BH_4 deficiency and monoamine neurotransmitter function and contribution to human disease"

- **1st Rare Diseases Summer School-Rare Disease Initiative Zurich (RaDIZ), Halbinsel Au, Switzerland, July 2013**

ñA novel tyrosine hydroxylase knock-in (*Th*-ki/ki) mouse as a model for brain catecholamine deficiencyò

- **ZNZ Symposium 2013, Zurich, Switzerland, September 2013**

ñTyrosine-hydroxylase knock-in (*Th*-ki) mouse: A novel model for brain catecholamine deficiencyò

Achieved rewards:

- Travel grant of the 15th international symposium on pteridines and folates, Antalya (Turkey) 2012

- Travel grant of International Conference on Tetrahydrobiopterin, Phenylketonuria, Monoamine Neurotransmitters and Nitric Oxide Synthase, St. Moritz - Champfèr, Switzerland, March 2013